University at Buffalo
The State University of New York

Modeling Triple Friction Pendulum Bearings in Program OpenSees Including Frictional Heating Effects

by

Hyun-Myung Kim and Michael C. Constantinou

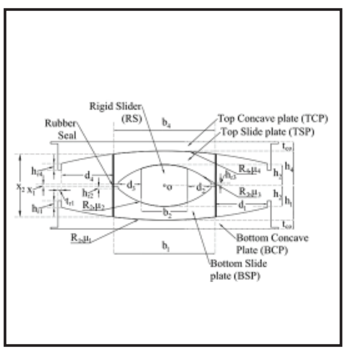

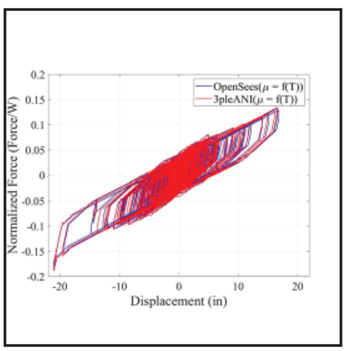

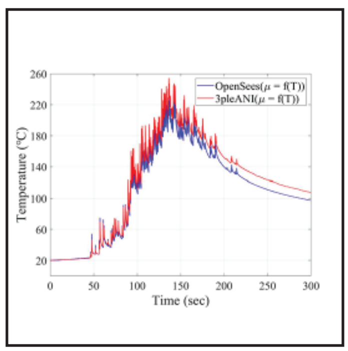

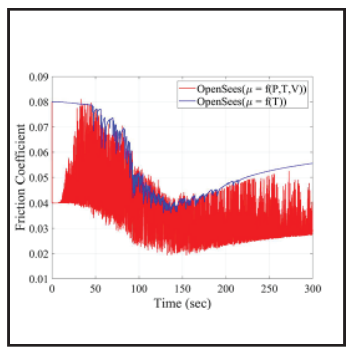

Technical Report MCEER-22-0001

April 18, 2022

MCEER: Earthquake Engineering to Extreme Events

NOTICE

Modeling Triple Friction Pendulum Bearings in Program OpenSees Including Frictional Heating Effects

by

Hyun-Myung Kim[1] and Michael C. Constantinou[2]

Publication Date: April 18, 2022
Submittal Date: December 24, 2021

Technical Report MCEER-22-0001

1. Graduate Student, Graduate Student, Department of Civil, Structural and Environmental Engineering, University at Buffalo, The State University of New York
2 Samuel P. Capen Professor and SUNY Distinguished Professor, Department of Civil, Structural and Environmental Engineering, University at Buffalo, The State University of New York

MCEER: Earthquake Engineering to Extreme Events
University at Buffalo, The State University of New York
212 Ketter Hall, Buffalo, NY 14260
buffalo.edu/mceer

Preface

MCEER is a national center of excellence dedicated to the discovery and development of new knowledge, tools and technologies that equip communities to become more disaster resilient in the face of earthquakes and other extreme events. MCEER accomplishes this through a system of multidisciplinary, multi-hazard research, in tandem with complimentary education and outreach initiatives.

Headquartered at the University at Buffalo, The State University of New York, MCEER was originally established by the National Science Foundation in 1986, as the first National Center for Earthquake Engineering Research (NCEER). In 1998, it became known as the Multidisciplinary Center for Earthquake Engineering Research (MCEER), from which the current name, MCEER, evolved.

Comprising a consortium of researchers and industry partners from numerous disciplines and institutions throughout the United States, MCEER's mission has expanded from its original focus on earthquake engineering to one which addresses the technical and socio-economic impacts of a variety of hazards, both natural and man-made, on critical infrastructure, facilities, and society.

The Center derives support from several Federal agencies, including the National Science Foundation, Federal Highway Administration, Department of Energy, Nuclear Regulatory Commission, and the State of New York, foreign governments and private industry.

This report presents and verifies a revised model of the behavior of triple friction pendulum bearings that explicitly computes the sliding displacements, sliding velocities and the rise in temperature at its four sliding interfaces. This permits consideration of the effects of velocity and temperature on the coefficients of friction. The model is based on the earlier model of Fenz and Constantinou, which did not explicitly compute the conditions at each sliding interface but correctly predicted the global force-displacement relationship of the bearing. The model was implemented in program OpenSees and interested users may obtain the source code from the authors.

ABSTRACT

A Triple FP bearing element currently available in program OpenSees is based on the series model, which consists of properly combined hysteretic/frictional and gap elements. The model can account for the dependency of the friction coefficient on axial pressure and on sliding velocity using modified parameters without explicitly calculating the velocity at each sliding surface. The model cannot be directly used to account for frictional heating effects since for those calculations, the histories of velocity and displacement on each sliding surface are needed.

This report presents a new triple FP element in OpenSees that is based on the existing element in program OpenSees but modified to account for the effect of frictional heating on the friction coefficient. To accomplish this, the displacement and velocity of the top of the bearing with respect to its bottom computed by the element are partitioned into components at each sliding surface. This partitioning is based on two different procedures: (a) modification of the histories of displacements and velocities computed in the three individual FP elements in the series model of the bearing, and (b) retracing the histories of displacements and velocities based on the force-displacement relationship of the theory of Fenz and Constantinou.

Verification of the modified Triple FP element is performed by computing force-displacement loops and histories of displacement, velocity, and temperature at each sliding surface for two configurations of the bearing under various imposed sinusoidal displacements of the top of the bearing and ground motions and comparing it with results obtained by the program 3pleANI.

ACKNOWLEDGEMENTS

The lead author has been supported by a University at Buffalo Presidential Scholarship and by funds provided by the Samuel P. Capen Professorship.

TABLE OF CONTENTS

TABLE OF CONTENTS (CONT'D)

LIST OF FIGURES

LIST OF FIGURES (CONT'D)

LIST OF FIGURES (CONT'D)

LIST OF FIGURES (CONT'D)

LIST OF FIGURES (CONT'D)

LIST OF FIGURES (CONT'D)

LIST OF FIGURES (CONT'D)

LIST OF FIGURES (CONT'D)

LIST OF TABLES

SECTION 1
INTRODUCTION

The behavior of Triple Friction Pendulum™ (FP) bearings has been previously described by many of which the works of Fenz and Constantinou (2008a to d, 2009), Dao et al. (2013), and Sarlis and Constantinou (2013, 2016) are most relevant to this report. Figure 1-1 shows the geometry of the Triple FP bearing and its parameters. R_1, R_2, R_3 and R_4 are radii of curvature; h_1, h_2, h_3 and h_4 are distances of the slide plate to the pivot point(O); d_1, d_2, d_3 and d_4 are the nominal displacement capacities; $b_1, b_2,$ and b_3 are diameters of the rigid slider and the two inner slide plates; and μ_1, μ_2, μ_3 and μ_4 are the friction coefficients of the four sliding interfaces. Figure 1-1 shows the Triple FP isolator with an inner ring (or displacement restrainer) which is not needed, and modern versions of the isolator do not have it. In those cases, the displacement capacities d_2 and d_3 are larger than the nominal capacities shown in Figure 1-1.

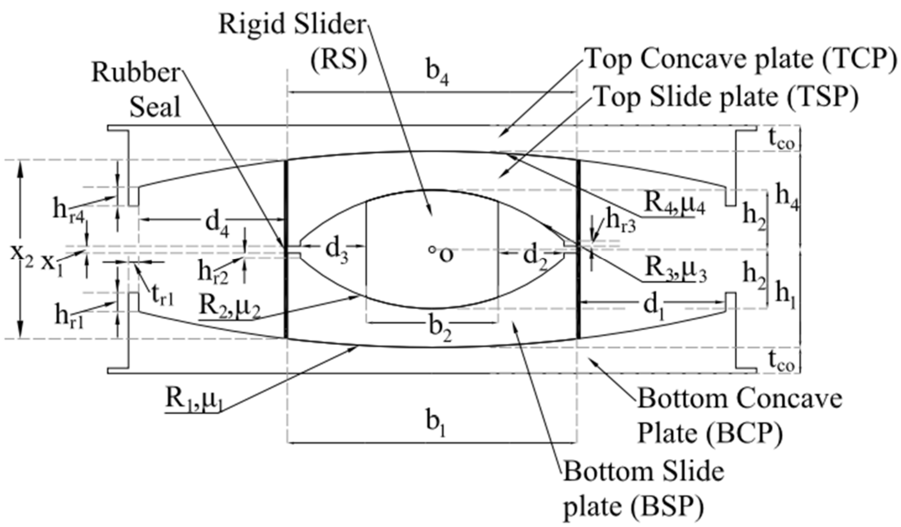

Figure 1-1 Geometry of the Triple FP Bearing (Sarlis and Constantinou, 2013)

The behavior of Triple FP bearing has been described in Fenz and Constantinou (2008a to 2008d, 2009) and summarized in Constantinou et al. (2011). The following parameters determine the response of Triple FP bearing: friction coefficients at its four sliding interfaces, μ_i, nominal displacement capacities, d_i, radii of curvature R_i, and heights h_i, where i = 1 to 4. The effective radii of curvature are defined as $R_{effi} = R_i - h_i$, and the actual displacement capacities are given by $d_i^* = \frac{R_{effi}}{R_i} d_i$. When the inner ring is absent, the actual total displacement is increased by $b_2/2$, at which point the isolator becomes unstable (Sarlis and Constantinou, 2013)

In the Fenz and Constantinou (2008a, c) model, the following conditions need to apply: 1) $R_{eff1} = R_{eff2} \gg R_{eff2} = R_{eff3}$, 2) $\mu_2 = \mu_3 < \mu_1 < \mu_4$, 3) $d_1^* > (\mu_4 - \mu_1)R_{eff1}$, 4) $d_2^* > (\mu_1 - \mu_2)R_{eff2}$, 5) $d_3^* > (\mu_4 - \mu_3)R_{eff3}$. These conditions typically apply for practical Triple FP bearings. The more complex theory of Sarlis and Constantinou (2013, 2016) is more general and is not restricted by these conditions. It can also explicitly calculate the state of motion at each of the four sliding surfaces of the bearing.

A computational model for the Triple FP element was developed initially by Fenz and Constantinou (2008d, 2009), and later Sarlis and Constantinou (2010) presented details of modeling the bearing in program SAP2000 (CSI, 2011) in a report to the engineering community. Dao et al. (2013) implemented the same model in the program OpenSees (McKenna et al., 2010), having improved on the use of multi-directional gap elements, whereas the model in SAP2000 required the use of several one-directional gap elements. Sarlis and Constantinou (2013) then developed many advanced theories for the behavior of the Triple FP bearing, which were not bound by the conditions of the Fenz and Constantinou (2008a) theory. They implemented these theories in computer program 3pleANI (Sarlis and Constantinou, 2013). These theories can produce histories of displacement, velocity and temperature at each of the sliding interfaces of the bearing, can account for pressure, velocity and temperature dependency of the friction coefficient of each sliding interface, and can model uplift and collapse of the bearing. Program 3pleANI was developed for motion in one horizontal and the vertical directions. It cannot be used for simulation of behavior or response history analysis under triaxial motion.

There is no element in any commercial or open-source software capable of simulation of the triaxial behavior of the Triple FP bearing with due consideration for the dependency of friction on the temperature at each sliding interface. Such a model is needed when performing simulations with significant heating effects, as in the case of long-duration ground motions. The only available element that can do is for the simpler Single FP bearing element FPBearingPTV in OpenSees (Kumar et al., 2015).

This work reports on a modification of the current Triple FP element in OpenSees (Dao et al., 2013) to account for the triaxial behavior of the Triple FP bearing with due consideration for the dependency of friction on the temperature, velocity, and pressure at each sliding interface. Program 3pleANI is used in this work for verification of the model implemented in program OpenSees.

SECTION 2
MODELING THE BEHAVIOR OF TRIPLE FRICTION PENDULUM BEARING

2.1 Model of Triple FP Bearing in Program OpenSees by Dao et al. (2013)

Figure 2-1 depicts the series model for the Triple FP bearing that was implemented by Dao et al. (2013) in the program OpenSees (McKenna et al., 2010). In the numerical model, k_{21}, k_{23} and k_{25} are normalized stiffnesses due to the curvature (inverse of pendulum length). Quantities k_{11}, k_{13} and k_{15} are high initial stiffnesses with small yield displacement to account for frictional behavior as shown in Figure 2-2. Also, k_2, k_4 and k_6 are stiffnesses, with large values, of circular gap elements which are needed to represent the behavior of the element when there is contact with any of restrainers of the bearing. The resulting backbone curve is shown in Figure 2-3. The model is identical to the series model of Fenz and Constantinou (2008d, 2009) but for the nomenclature used: L_1 for effective radii R_{eff2}=R_{eff3}, L_2 for effective radius R_{eff1}, and L_3 for effective radius R_{eff4}. This may be realized by comparing Figure 3-1 in Fenz and Constantinou (2008d) to Figure 2-1 below.

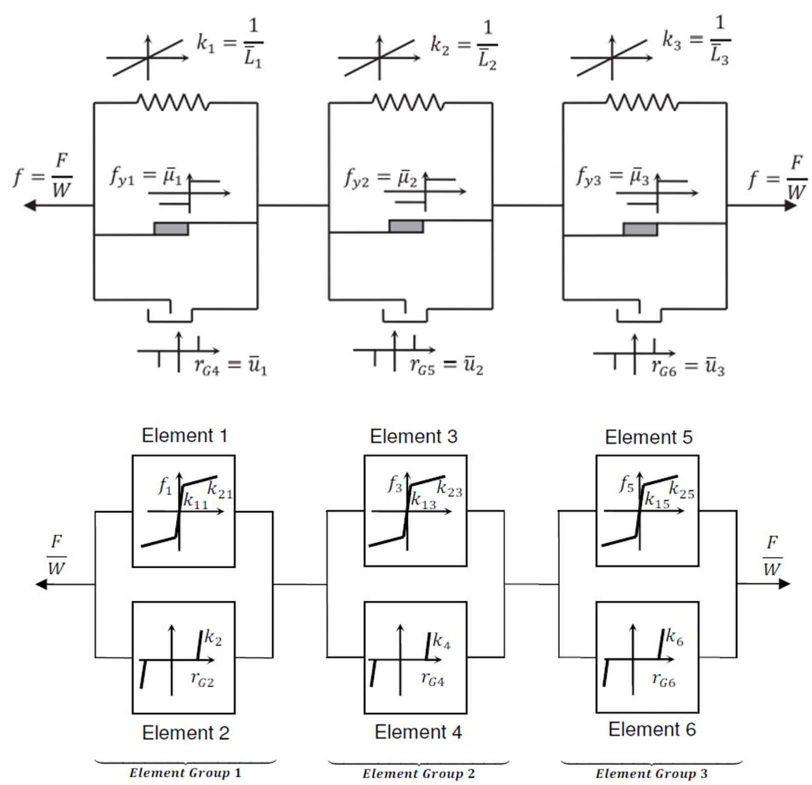

Figure 2-1 Series model and Numerical model for Triple FP bearing (Dao et al., 2013)

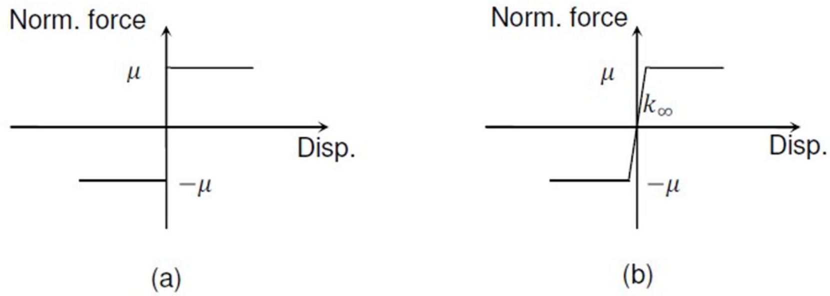

Figure 2-2 Modeling Friction Behavior (Dao et al., 2013)

(a) Theoretical “rigid-plastic" friction behavior

(b) “Elastoplastic” frictional behavior with very large initial stiffness in OpenSees

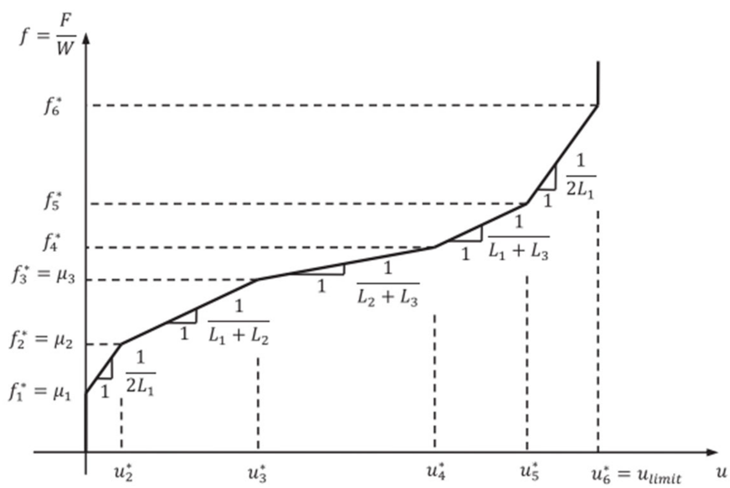

Figure 2-3 Normalized Backbone Curve (Dao et al., 2013)

However, in the implementation of the element in OpenSees by Dao et al. (2013), multidirectional circular gap elements were used, whereas the implementation of the element in program SAP2000 by Fenz and Constantinou (2009), several one-directional gap elements were used as they were the only gap elements available in the program.

Based on the nomenclature used in Figure 2-1, Table 2-1 presents the parameters in the series model in OpenSees. The parameters are identical to the Fenz and Constantinou (2009) model. Accordingly, the theory presented in Fenz and Constantinou, 2008c, d) is applicable to the Dao element in OpenSees.

Table 2-1 Parameters in Series Model

Bidirectional Plasticity Element	Friction Model	Actual Displacement limit (Gap Element)
$\bar{L}_1 = 2L_1$	$\bar{\mu}_1 = \mu_2 = \mu_3$	$\bar{u}_2 = u_{limit} - \bar{u}_2 - \bar{u}_3$
$\bar{L}_2 = L_2 - L_1$	$\bar{\mu}_2 = \mu_1$	$\bar{u}_2 = \left(1 - \frac{L_1}{L_2}\right) d_1^*$
$\bar{L}_3 = L_3 - L_1$	$\bar{\mu}_3 = \mu_4$	$\bar{u}_3 = \left(1 - \frac{L_1}{L_3}\right) d_4^*$
$u_{limit} = d_1^* + d_2^* + d_3^* + d_4^* + \frac{b_2}{2}$,	where $b_2 = diameter\ of\ rigid\ slider$	

The series model captures well the behavior of Triple FP bearings that satisfy the restrictions listed in the Introduction (Fenz and Constantinou, 2008a, c and Constantinou et al., 2011). It also captures acceptably well the velocity dependence of the coefficient of friction by use of adjusted friction model parameters as demonstrated in Fenz and Constantinou (2009). However, the model does not compute the actual histories of displacements and velocities at each of the four sliding interfaces. This topic will be addressed in Section 3.

2.2 Dependence of Friction Coefficient on Velocity, Pressure and Temperature

Constantinou et al. (2007) presented information on the dependency of the coefficient of friction at interfaces of sliding bearings on the velocity of sliding, apparent bearing pressure, and temperature. They also presented and validated by experimentation a theory on computing the change in temperature at a sliding interface as the result of frictional heating. In general, the coefficient of friction increases with increasing velocity, drops with increasing pressure and drops with increasing temperature, and reaches a somehow stable value at some large velocity, pressure and temperature. The behavior depends on the materials of the sliding interface and needs to be determined by testing, although some general rules apply and are discussed in Constantinou et al. (2007). Always one of the two sliding surfaces is stainless steel, and the other is a much softer material (plastic or fabric in woven form or several layers of these materials).

The computation of the temperature at the sliding interfaces requires knowledge of the instantaneous values of the coefficient of friction, the apparent bearing pressure (load divided by apparent contact area), and sliding velocity at each interface. The total temperature $T = T_0 + \Delta T$ at time t > 0, consists of the starting value T_0 at time zero and the rise ΔT at the sliding interface. The temperature rise ΔT at time t is given by (Constantinou et al., 2007):

$$\Delta T(t) = \frac{\sqrt{D}}{k\sqrt{\pi}} \int_0^t \frac{q(t-\tau)d\tau}{\sqrt{\tau}} \qquad (2-1)$$

where, *D* and *k* are the thermal diffusivity and conductivity of stainless steel, respectively, τ is a time parameter that varies between 0 and time *t*, and *q(t)* is the heat flux, which is calculated in accordance with the equation (2-2).

$$q(t) = \begin{cases} \mu(t)p(t)v(t), & d \leq rContact \\ 0, & otherwhise \end{cases} \qquad (2-2)$$

In equation (2-2), *μ(t)* is a friction coefficient, *p(t)* is the apparent bearing pressure at the sliding surface, and *v(t)* is the absolute value of the resultant velocity at the sliding surface. Also, *d* is the absolute value of the resultant displacement of the slider and *rContact* is the radius of the circular apparent contact area, which can be obtained by $b_{\mathrm{i}}/2$ (see Figure 1-1). Equation (2-2) computes the temperature at the center of the bearing. Note that the heat flux may be intermittent depending on the motion of the slider over the contact area (Constantinou et al., 2007). Typical values of the thermal properties of stainless are presented in Table 2-2.

Table 2-2 Thermal Properties of Stainless Steel

Parameter	Unit	Value
Thermal Diffusivity	m^2/sec	$0.444 * 10^{-5}$
Thermal Conductivity	$W/(m°\mathrm{C})$	18

A generally accepted relation for the velocity dependence of the friction coefficient is (Constantinou et al., 2007):

$$\mu(v) = \mu_{max}(1 - (1 - \widetilde{\mu_v})e^{-av}) \qquad (2-3)$$

In this equation, $\mu(v)$ is the friction coefficient at sliding velocity *v*, μ_{max} is friction coefficient at large sliding velocity, $\widetilde{\mu_v}$ is the ratio of the friction coefficient at very small velocity to μ_{max}, and a is the rate parameter, which has a value of about 100s/m for some of the materials used in sliding bearings (Constantinou et al., 2007). When $\widetilde{\mu_v}$ is assumed as 0.5, which is consistent with past studies (Constantinou et al., 2007), equation (2-3) reduces to the following form when the velocity is in units of meter/second:

$$\mu(v) = \mu_{max}(1 - 0.5e^{-100v}) \qquad (2-4)$$

Sarlis and Constantinou (2013) used the following relation to model the coefficient of friction as function of temperature:

$$\mu(T) = \mu_{min} + (\mu_{max} - \mu_{min})e^{-hT} \tag{2 – 5}$$

In equation (2-5), h is a heating rate parameter, μ_{max} is the value of the high velocity coefficient of friction at the start (t=0), and μ_{min} is the value of the high velocity coefficient of friction at some large temperature ($T \cong 1/h$) where it is assumed to be stable.

Tsopelas et al. (2005) implemented in program 3D-BASIS-ME-MB pressure dependency for the coefficient of friction based on the following relationship:

$$\mu_{max} = \mu_{max0} - (\mu_{max0} - \mu_{maxp})\tanh(\varepsilon p) \tag{2 – 6}$$

In this equation, μ_{max} is the value of the high velocity coefficient of friction at pressure p (axial load divided by apparent contact area), μ_{max0} is the value of the high velocity coefficient of friction at almost zero pressure, μ_{maxp} is the value of the high velocity coefficient of friction at some high value of pressure, tanh is the tangent hyperbolic function, and ε is a constant that controls the rate of change of the coefficient of friction with pressure. In this model it is assumed that the coefficient of friction at very low velocity is not dependent on pressure.

Kumar et al. (2015) combined and simplified these models into one composite model for the dependency of friction on velocity, pressure and temperature, and had the model implemented in program OpenSees for an element of the Single FP bearing (FPBearingPTV). The coefficient of friction is given by equations (2-7) to (2-10) in which μ_{ref} is the reference high speed coefficient of friction at the initial (time t=0) temperature $T_0 = 20°\text{C}$ and initial pressure p_0, a is velocity rate parameter, p is the apparent pressure, and v is the amplitude of the velocity.

$$\mu(p, v, T) = \mu_{ref} k_p k_v k_T \tag{2 – 7}$$

$$k_{\mathrm{p}} = 0.7^{0.02(p-p_0)} \tag{2 – 8}$$

$$k_v = (1 - 0.5e^{-av}) \tag{2 – 9}$$

$$k_T = 0.79 * (0.7^{0.02T} + 0.40) \tag{2 – 10}$$

Note that function k_T for the dependency of the coefficient of friction on the temperature and function k_{p} for the dependency of the coefficient of friction on instantaneous pressure have been calibrated using general data that apply for FP bearings. Also, function k_v for the dependency of the coefficient of friction on velocity is based on the assumption that the ratio of the very low speed to high-speed coefficient of friction equals to 0.5. The model of equations (2-7) to (2-10) has been used in the developed new Triple FP bearing in OpenSees.

SECTION 3
NEW TRIPLE FP ELEMENT TO ACCOUNT FOR HEATING EFFECTS

The new Triple FP element to be used in OpenSees is named “TripleFrictionPendulumX” to complement the “TripleFrictionPendulum” element of Dao et al. (2013) already implemented in OpneSees. The new element determines the state of motion (displacement and velocity) at each of the four sliding interfaces based on two different procedures. The user has the choice of selecting one of these for the execution. These procedures are: (1) Modification of the element displacement histories computed in the three elements of the series model (based on Fenz and Constantinou, 2008d, 2009) and (2) Retracing through the force-displacement relationship, which again is based on Fenz and Constantinou (2008a-d). The sliding velocities are computed from the displacement histories using numerical differentiation (Burden and Faires, 1989).

3.1 Approach 1: Modification of the displacement histories in the series elements

The series model of the Triple FP bearing employs three pendula with friction in order to represent the stiffnesses and strength that the bearing exhibits in its five regimes of operation. Figures 3-1 and 3-2 show the series model and its parameters and the force-displacement loop as determined by Fenz and Constantinou (2008d).

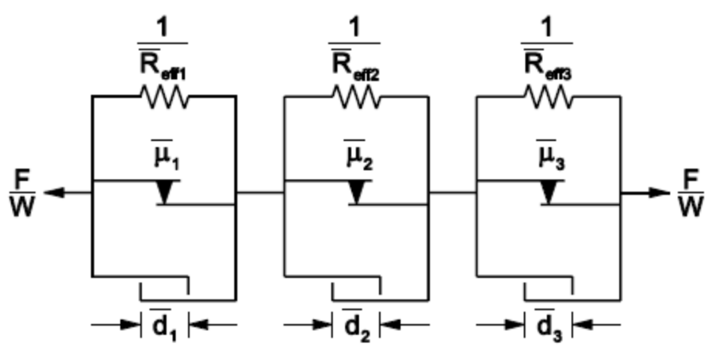

Figure 3-1 Series model for Triple FP bearing per Fenz and Constantinou (2008d)

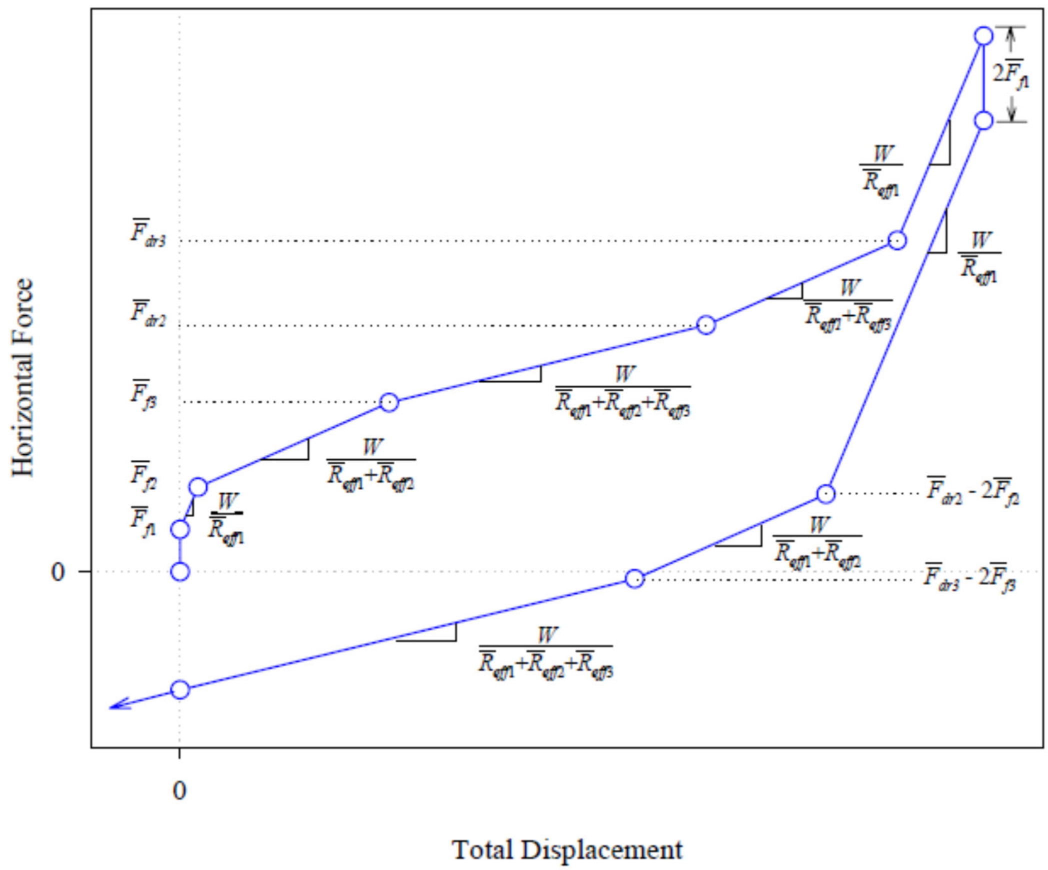

Figure 3-2 Force-displacement loop of Triple FP bearing as computed in the series model

Tables 3-1 and 3-2 depict the active ranges of motion in the four sliding interfaces and three pendula elements of the series model, in its five regimes of operation. Herein, u_i and v_i are the displacement and velocity on the four sliding interfaces (i=1 to 4), which comprise the bearing's top to bottom motion. From analyzing the information in Tables 3-1 and 3-2, some characteristics of the series model can be described: (a) the second and third pendulum elements in the series model match their active ranges well with actual motions in all five regimes, (b) the first pendulum element describes the actual motion of the inner slide plates u_2 and u_3 only within specific regimes but can represent the motion properly in an overall sense.$(\text{i.e.}, u_2 + u_3)$ From these characteristics, the motion of sliding interfaces can be approximately obtained using compatibility conditions between the actual motion of the pendula and the three representative motions in the series elements, and the methodology presented in Fenz and Constantinou (2008d, 2009) which has been used for accounting for the velocity dependence of friction by modification of the rate parameters in the three frictional elements of the series model.

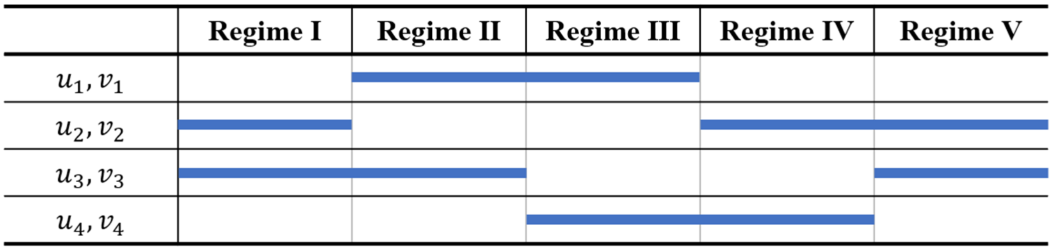

Table 3-1 Actual motion in each of four sliding interfaces in the five regimes of operation

Table 3-2 Activated elements in the series model in the five regimes of operation

In the sequel, there is a detailed presentation of the theory that leads to calculating the histories of displacement on the four sliding interfaces from the histories of displacement of three pendula. Velocity histories are then calculated numerically from the displacement histories.

1) Derivation for displacement history modification in Regime I

Initiation of motion occurs when the horizontal force exceeds the friction force on surfaces 2 and 3 (they are equal and less than the friction forces at surfaces 1 and 4). This is regime I per Fenz and Constantinou (2008a). During this regime, the force-displacement relationship for surfaces 2 and 3 can be expressed, respectively, as follows:

$$F = \frac{W}{R_{eff2}} u_2 + F_{f2} \tag{3 – 1}$$

$$F = \frac{W}{R_{eff3}} u_3 + F_{f3} \tag{3 – 2}$$

In these equations, F is the horizontal force, W is vertical load, R_{eff2} and R_{eff3} are effective radius of curvature, F_{f2} and F_{f3} are friction forces on surfaces 2 and 3, and u_2 and u_3 are displacement histories on surfaces 2 and 3, respectively.

In the series model, there is motion in element 1, and the corresponding force-displacement relationship can be written as follows:

$$F = \frac{W}{\overline{R_{eff1}}}\overline{u_1} + \overline{F_{f1}} \tag{3 – 3}$$

Where $\overline{R_{eff1}} = R_{eff2} + R_{eff3}$, $\overline{F_{f1}} = F_{f2} = F_{f3}$ and $\overline{u_1}$ is displacement in first series element. As $R_{eff2} = R_{eff3}$, the relationship between u_2, u_3 and $\overline{u_1}$ is expressed by combining equations (3-1) to (3-3).

$$u_2 = u_3 = 0.5\,\overline{u_1} \tag{3 – 4}$$

In this regime, the displacements on the outer sliding surfaces are zero, as there is no motion on surfaces 1 and 4.

$$u_1 = u_4 = 0 \tag{3 – 5}$$

2) Derivation for displacement history modification in Regime II

In regime II, motion occurs on surfaces 1 and 3, leading to the following relationship governing motion on the surface:

$$F = \frac{W}{R_{eff1}}u_1 + F_{f1} \tag{3 – 6}$$

Here, F_{f1} is friction force at surface 1. The equivalent motion in the second FP element in the series model initiates, and the relationship can be expressed as:

$$F = \frac{W}{\overline{R_{eff2}}}\overline{u_2} + \overline{F_{f2}} \tag{3 – 7}$$

Where $\overline{R_{eff2}} = R_{eff1} - R_{eff2}$, $\overline{F_{f2}} = F_{f1}$ and $\overline{u_2}$ is displacement in the second series element. By combining equation (3-6) and (3-7), the relation between u_1 and $\overline{u_2}$ is obtained as:

$$u_1 = \frac{R_{eff1}}{R_{eff1} - R_{eff2}}\overline{u_2} \tag{3 – 8}$$

The displacement history on surface 3 is still governed by the relation 3.4, with motion on surface 2 stopped and obtained by the following compatibility equation:

$$u_{total} = u_1 + u_2 + u_3 + u_4 = \overline{u_1} + \overline{u_2} + \overline{u_3} \tag{3 – 9}$$

This leads to

$$u_2 = u_{total} - (u_1 + u_3 + u_4) = u_{total} - (\frac{R_{eff1}}{R_{eff1} - R_{eff2}} \overline{u_2} + 0.5\, \overline{u_1}) \qquad (3-10)$$

Note that u_{total} is total displacement of the bearing, that is, the top to bottom relative displacement. Also, u_3 and u_1 are obtained by use of equations (3-4) and (3-8) with u_4 being zero. Note that $\overline{u_i}$ can be obtained directly from the series elements.

3) Derivation for displacement history modification in Regime III

In Regime III, motion occurs on surfaces, 1 and 4. Using equation (3-6) for surface 1, the governing relationship for motion on surface 4 can be expressed as:

$$F = \frac{W}{R_{eff4}} u_4 + F_{f4} \qquad (3-11)$$

Here, F_{f4} is friction force on surface 4. The onset of motion in the third FP element in Series occurs when applied horizontal force F exceeds $\overline{F_{f3}} = F_{f4}$ and corresponding force-displacement relationship is:

$$F = \frac{W}{\overline{R_{eff3}}} \overline{u_3} + \overline{F_{f3}} \qquad (3-12)$$

Where $\overline{R_{eff3}} = R_{eff4} - R_{eff3}$ and $\overline{u_3}$ is displacement in the third series element. Combining equations (3-11) and (3-12), results in:

$$u_4 = \frac{R_{eff4}}{R_{eff4} - R_{eff3}} \overline{u_3} \qquad (3-13)$$

Equation (3-8) still describes the motion on surface 1. Motion in inner two surfaces stops in Regime III, but the series model cannot capture these phenomena for surfaces 2 and 3 individually. Instead, the motion can be approximately captured based on the following compatibility equation:

$$u_2 + u_3 = u_{total} - (u_1 + u_4) = u_{total} - \left(\frac{R_{eff1}}{R_{eff1} - R_{eff2}} \overline{u_2} + \frac{R_{eff4}}{R_{eff4} - R_{eff3}} \overline{u_3}\right) \qquad (3-14)$$

Note that displacements u_2 and u_3 in Regime III have values equal to the last values recorded at the last time step in Regime I and II. Note that $\bar{u}_1$ varies during this regime, but it is very small and considered negligible.

4) Derivation for displacement history modification in Regime IV

Stiffening behavior occurs in Regime IV as motion stops on surface 1 and re-starts on surface 2, which has a smaller effective radius of curvature than surface 1. In the series model (Figures 2-1 and 3-1), the gap element in the second series element is activated with very high stiffness so that motion stops on surface 1. Displacements u_2 and u_4 are governed by equations (3-4) and (3-13), whereas u_3 has a constant value that is obtained by use of the following compatibility equation:

$$u_3 = u_{total} - (u_1 + u_2 + u_4) = u_{total} - \left(\frac{R_{eff1}}{R_{eff1} - R_{eff2}}\overline{u_2} + 0.5\overline{u_1} + \frac{R_{eff4}}{R_{eff4} - R_{eff3}}\overline{u_3}\right) \quad (3-15)$$

5) Derivation for displacement history modification in Regime V

Further stiffening behavior is achieved as motion on surface 4 stops and motion of surface 3 re-starts. The gap element in the third series element is activated and generates additional stiffness during this regime. Displacements = u_2 and u_3 are governed by equation (3-4).

6) Summary and considerations to account for heating effects

Table 3-3 summarizes the state of motion (displacement) at each of the four sliding interfaces.

Table 3-3 Displacement at each sliding interfaces (Approach 1)

Regime	Equations for Displacement
I	$u_1 = u_4 = 0$ $u_2 = u_3 = 0.5\overline{u_1}$ (based on $u_2 + u_3 = \overline{u_1}$)
II	$u_1 = \frac{R_{eff1}}{R_{eff1} - R_{eff2}}\overline{u_2}$ $u_2 = u_{total} - \left(\frac{R_{eff1}}{R_{eff1} - R_{eff2}}\overline{u_2} + 0.5\,\overline{u_1}\right) = u_{2\_regime\_I}$ $u_3 = 0.5\overline{u_1}$ $u_4 = 0$

	(based on $u_2 + u_3 = u_{total} - \frac{R_{eff1}}{R_{eff1}-R_{eff2}}\overline{u_2}$)
III	$$u_1 = \frac{R_{eff1}}{R_{eff1} - R_{eff2}}\overline{u_2}$$ $$u_2 + u_3 = u_{total} - \left(\frac{R_{eff1}}{R_{eff1} - R_{eff2}}\overline{u_2} + \frac{R_{eff4}}{R_{eff4} - R_{eff3}}\overline{u_3}\right) = u_{2\_regime\_I} + u_{3\_regime\_II}$$ $$u_4 = \frac{R_{eff4}}{R_{eff4} - R_{eff3}}\overline{u_3}$$ No explicit expressions for u_2 and u_3 (assumed to be constant)
IV	$$u_1 = \frac{R_{eff1}}{R_{eff1} - R_{eff2}}\overline{u_2} = u_{1\_regime\_III}\ (Gap\ element\ activated)$$ $$u_2 = 0.5\overline{u_1}\ (starting\ at\ u_{2\_regime\_I})$$ $$u_3 = u_{total} - \left(0.5\overline{u_1} + \frac{R_{eff1}}{R_{eff1} - R_{eff2}}\overline{u_2} + \frac{R_{eff4}}{R_{eff4} - R_{eff3}}\overline{u_3}\right) = u_{3\_regime\_II}$$ $$u_4 = \frac{R_{eff4}}{R_{eff4} - R_{eff3}}\overline{u_3}$$ (based on $u_2 + u_3 = u_{total} - \left(\frac{R_{eff1}}{R_{eff1}-R_{eff2}}\overline{u_2} + \frac{R_{eff4}}{R_{eff4}-R_{eff3}}\overline{u_3}\right)$
V	$$u_1 = \frac{R_{eff1}}{R_{eff1} - R_{eff2}}\overline{u_2} = u_{1\_regime\_III}\ (Gap\ element\ activated)$$ $$u_2 = 0.5\overline{u_1}$$ $$u_3 = 0.5\overline{u_1}\ (starting\ at\ u_{3\_regime\_II})$$ $$u_4 = \frac{R_{eff4}}{R_{eff4} - R_{eff3}}\overline{u_3} = u_{4\_regime\_IV}\ (Gap\ element\ activated)$$ (based on $u_2 + u_3 = u_{total} - \left(\frac{R_{eff1}}{R_{eff1}-R_{eff2}}\overline{u_2} + \frac{R_{eff4}}{R_{eff4}-R_{eff3}}\overline{u_3}\right)$

In Table 3-3, $u_{2\_regime\_I}$ is the value of displacement on surface 2 recorded at the last time step of Regime I, $u_{3\_regime\_II}$ is the value of displacement on surface 3 recorded at the last time step of Regime III, $u_{1\_regime\_III}$ is the value of displacement on surface 1 recorded at the last time step of Regime III, and $u_{4\_regime\_IV}$ is the value of displacement on surface 4 recorded at the last time step of Regime IV. The calculated histories of motion are then used for calculating the heat flux and updating values of the friction coefficients during analysis. The average value of u_2 and u_3 is used for updating the value of the friction coefficients $\mu_2 = \mu_3 = \overline{\mu_1}$.

Table 3-4 summarizes important equations used to calculate the displacement histories of individual surfaces in OpenSees element "TripleFrictionPendulumX".

Table 3-4 Equations to calculate surface displacements in element TripleFrictionPendulumX

Element	Equations
Element 1	$\overline{\overline{u_1}} = \dfrac{u_2 + u_3}{2} = 0.5\left\{u_{total} - \left(\dfrac{R_{eff1}}{R_{eff1} - R_{eff2}}\overline{u_2} + \dfrac{R_{eff4}}{R_{eff4} - R_{eff3}}\overline{u_3}\right)\right\}$
Element 2	$\overline{\overline{u_2}} = u_1 = \dfrac{R_{eff1}}{R_{eff1} - R_{eff2}}\overline{u_2}$
Element 3	$\overline{\overline{u_3}} = u_4 = \dfrac{R_{eff4}}{R_{eff4} - R_{eff3}}\overline{u_3}$

In Table 3-4, $\overline{\overline{u_1}}$, $\overline{\overline{u_2}}$, and $\overline{\overline{u_3}}$ are modified element displacements (modifications of displacements $\overline{u_1}$, $\overline{u_2}$ and $\overline{u_3}$) in order to obtain the actual displacement at each sliding surface. Note that $\overline{u_2} \cong 0$ in Regime I and $\overline{u_3} \cong 0$ during Regimes I and II. These displacements have very small but non-zero values. They occur due to the elasto-plastic representation of friction in the model (they are less than the "yield displacement").

3.2 Approach 2: Retracing Histories based on Force-displacement relationship

Approach 1 is incapable of capturing the start-stop-start behavior at all sliding surfaces so that it cannot provide the exact displacements of the inner surfaces 2 and 3 during the entire motion. However, with a small time increment in the analysis, the displacement and velocity histories on individual surfaces can be obtained based on the force obtained in the previous time step. Fenz and Constantinou (2008a) presented the force-displacement relationships for each sliding regime of the Triple FP bearing. In the modified Triple FP OpenSees element, forces and displacements are stored in each analysis step, and these are used for retracing displacement and velocity histories on the four sliding surfaces. The main purpose for developing Approach 2 is to verify the results of the simpler Approach 1.

In the sequel we present the steps needed for the calculations in Approach 2. Table 3-5 presents the force-displacement relationships in each regime and details of the computations for the initial (starting) loading phase.

1) Starting Loading Phase

Table 3-5 Force-displacement Relationships during Loading Phase

Regime	Force-Displacement Relationship
0	$u_1 = u_2 = u_3 = u_4 = 0$ Valid until: $f < F_{f2}$, Store sign of loading (say "sign")
I	$u_1 = u_4 = 0, u_2 = u_3 = \frac{f - \text{sign} * F_{f2}}{W} L_1$ Store u_1, u_2, u_3, u_4, f Valid until: $\text{sign} * f \le F_{f1}$
II	$u_1 = \frac{f - \text{sign} * F_{f1}}{W} * L_2, u_3 = \frac{f - \text{sign} * F_{f2}}{W} L_1$ $u_2 = u_{2\_stored}, u_4 = u_{4\_stored}$ Store u_1, u_2, u_3, u_4, f Valid until: $F_{f1} < \text{sign} * f \le F_{f4}$
III	$u_1 = \frac{f - \text{sign} * F_{f1}}{W} * L_2, \quad \mathrm{u}_4 = \frac{f - \text{sign} * F_{f4}}{W} * L_3$ $u_2 = u_{2\_stored}, u_3 = u_{3\_stored}$ Store u_1, u_2, u_3, u_4, f Valid until: $F_{f4} < \text{sign} * f \le F_{dr1}$
IV	$u_2 = \left(\frac{f - \text{sign} * F_{f2}}{W} - \frac{\text{sign} * d_2}{L_2}\right) L_1, \ \mathrm{u}_4 = \frac{f - \text{sign} * F_{f4}}{W} * L_3$ $u_1 = u_{1\_stored}, u_3 = u_{3\_stored}$ Store u_1, u_2, u_3, u_4, f Valid until: $F_{dr1} < \text{sign} * f \le F_{dr4}$
V	$u_2 = \left(\frac{f - \text{sign} * F_{f2}}{W} - \frac{\text{sign} * d_2}{L_2}\right) L_1, u_3 = \left(\frac{f - \text{sign} * F_{f2}}{W} - \frac{\text{sign} * d_3}{L_3}\right) L_1$ $u_1 = u_{1\_stored}, u_4 = u_{4\_stored}$ Store u_1, u_2, u_3, u_4, f Valid until: $F_{dr4} < \text{sign} * f$

- Note: See Tables 2-1 and 3-7 for nomenclature

In this table, L_1 is the effective radius $R_{eff2}=R_{eff3}$, L_2 is the effective radius R_{eff1}, L_3 is the effective radius R_{eff4}, F_{fi} are friction forces on surfaces i, F_{dri} are forces when the inner slide plates contact the restrainers on the outer surface i.

During the numerical analysis it is assumed that the bearing is in the loading phase until a change in the sign of the derivative of the force with respect to the displacement (slope of force-displacement curve) changes, in which case unloading occurs. The behavior during unloading depends on the regime in which the bearing is at the instant of change of sign of the slope. As an example, Table 3-6 presents details of one of the possible cases of behavior when the force is in Regime V during the unloading phase.

2) Unloading Phase, Force-displacement loop starts in Regime V

Table 3-6 Triple FP Element Behavior in Unloading Phase Starting in Regime V

Preparation	Call stored u_1, u_2, u_3, u_4 and f from previous loading phase and assign as reference points
Regime	**Force-Displacement Relationship**
0	$u_1 = u_{1\_stored}, u_2 = u_{2\_stored}, u_3 = u_{3\_stored}, u_4 = u_{4\_stored}$ Store u_1, u_2, u_3, u_4, f Valid until: $f_{ref} - 2F_{f2} < f$
I	$u_2 = \frac{f - f_{stored}}{W} L_1 + u_{2_{stored}} \leq sign(u_2) * d_1^*$ $u_3 = \frac{f - f_{stored}}{W} L_1 + u_{3_{stored}} \leq sign(u_3) * d_1^*$ $u_1 = u_{1\_stored}, u_4 = u_{4\_stored}$ Store u_1, u_2, u_3, u_4, f Valid until: $F_{dr1} - 2F_{f1} < f \leq f_{ref} - 2F_{f2}$
II	$u_1 = \frac{f - f\_stored}{W} L_2 + u_{1_{stored}} \leq sign(u_1) * d_2^*$ $u_3 = \frac{f - f_{stored}}{W} L_1 + u_{3_{stored}} \leq sign(u_3) * d_1^*$ $u_2 = u_{2\_stored}, u_4 = u_{4\_stored}$ Store u_1, u_2, u_3, u_4, f Valid until: $F_{dr4} - 2F_{f4} < f \leq F_{dr1} - 2F_{f1}$
III	$u_1 = \frac{f - f\_stored}{W} L_2 + u_{1_{stored}} \leq sign(u_1) * d_2^*$ $u_4 = \frac{f - f_{stored}}{W} L_3 + u_{4_{stored}} \leq sign(u_4) * d_3^*$ $u_2 = u_{2\_stored}, u_3 = u_{3\_stored}$ Store u_1, u_2, u_3, u_4, f Valid until: $-F_{dr1} < f \leq F_{dr4} - 2F_{f4}$
IV	$u_2 = \frac{f - f_{stored}}{W} L_1 + u_{2_{stored}} \leq sign(u_2) * d_1^*$

	$u_4 = \frac{f - f_{stored}}{W} L_3 + u_{4_{stored}} \leq sign(u_4) * d_3^*$ $u_1 = u_{1\_stored}, u_3 = u_{3\_stored}$ Store u_1, u_2, u_3, u_4, f Valid until: $-F_{dr4} < f \leq -F_{dr1}$
V	$u_2 = \frac{f - f_{stored}}{W} L_1 + u_{2_{stored}} \leq sign(u_2) * d_1^*$ $u_3 = \frac{f - f_{stored}}{W} L_1 + u_{3_{stored}} \leq sign(u_3) * d_1^*$ $u_1 = u_{1\_stored}, u_4 = u_{4\_stored}$ Store u_1, u_2, u_3, u_4, f Valid until: $f \leq -F_{dr4}$

. Note: See Tables 2-1 and 3-7 for nomenclature

In Table 3-6, d_i^* are the actual displacement capacities. Expressions for the force and corresponding displacement limits that define the boundaries of each regime are presented in Tables 3-7 and 3-8.

Table 3-7 Force and Displacement Limits in Each Regime

Force Limit		Displacement Limit	
F_{f1}	$\mu_1 W$	u^*	$2(\mu_1 - \mu_2)L_1$
F_{f4}	$\mu_4 W$	u^{**}	$u^* + (\mu_4 - \mu_1)(L_2 - L_1)$
F_{dr1}	$W\left(\frac{d_1^*}{L_2} + \mu_1\right)$	u_{dr1}	$u^{**} + d_1^*\left(1 + \frac{L_3}{L_2}\right) - (\mu_4 - \mu_1)(L_2 + L_3)$
F_{dr4}	$W\left(\frac{d_4^*}{L_3} + \mu_4\right)$	u_{dr4}	$u_{dr1} + \left(\left(\frac{d_4^*}{L_3} + \mu_4\right) - \left(\frac{d_1^*}{L_2} + \mu_1\right)\right)(L_1 + L_3)$

Table 3-8 Boundary Conditions in Each Regime (In Unloading Phase)

Regime	f_{ref} starts at regime 5	f_{ref} starts at regime 4	f_{ref} starts at regime 3,2,1
0 (START)	$f_{ref} - 2F_{f2} < f$	$f_{ref} - 2F_{f2} < f$	$f_{ref} - 2F_{f2} < f$
I	$F_{dr1} - 2F_{f1} < f \leq f_{ref} - 2F_{f2}$	$F_{dr1} - 2F_{f1} < f \leq f_{ref} - 2F_{f2}$	$f_{ref} - 2F_{f1} < f \leq f_{ref} - 2F_{f2}$
II	$F_{dr4} - 2F_{f4} < f \leq F_{dr1} - 2F_{f1}$	$f_{ref} - 2F_{f4} < f \leq F_{dr1} - 2F_{f1}$	$f_{ref} - 2F_{f4} < f \leq f_{ref} - 2F_{f1}$
III	$-F_{dr1} < f \leq F_{dr4} - 2F_{f4}$	$-F_{dr1} < f \leq f_{ref} - 2F_{f4}$	$-F_{dr1} < f \leq f_{ref} - 2F_{f4}$
IV	$-F_{dr4} < f \leq -F_{dr1}$	$-F_{dr4} < f \leq -F_{dr1}$	$-F_{dr4} < f \leq -F_{dr1}$
V	$f \leq -F_{dr4}$	$f \leq -F_{dr4}$	$f \leq -F_{dr4}$

Approach 2, like in Approach 1, makes use of the average value of u_2 and u_3 in accounting for the dependency of the friction coefficient on temperature in inner sliding interfaces.

3.3 Calculation of Velocities on Sliding Surfaces

The sliding velocities at each sliding surface are needed for the calculation of the coefficient of friction when velocity-dependent and for the calculation of the heat flux to be used in computing the temperature at each sliding surface. Following the calculation of the displacements at each sliding surface, the sliding velocities are calculated by numerical differentiation. The numerical scheme used is based on the three-point formula (Burden and Faires, 1989):

$$f'(x_0) = \frac{1}{2h}[(f(x_0 + h) - f(x_0 - h)] - \frac{h^2}{6}f'''(\xi) \qquad (3-16)$$

In this equation the first derivative of function f at point x_0 is computed as the slope of the function between points $x_0 + h$ and $x_0 - h$, where h is the step (or time-step). The error is order $O(h^2)$, which together with a small time-step results in an estimate of velocity with small error. Table 3-9 presents the equations used for each surface and for the two approaches used. In this table, subscript *i* denotes the current time.

Table 3-9 Calculation of Velocities

Surface	Approach 1	Approach 2
1	$\overline{\overline{v_2}}_i = \frac{1}{2h}(\overline{\overline{u_2}}_{,i} - \overline{\overline{u_2}}_{,i-2})$	$v_{1_i} = \frac{1}{2h}(u_{1_i} - u_{1_{i-2}})$
2	$\overline{\overline{v_1}}_i = \frac{1}{2h}(\overline{\overline{u_1}}_{,i} - \overline{\overline{u_1}}_{,i-2})$	$v_{2_i} = \frac{1}{2h}(u_{2_i} - u_{2_{i-2}})$
3	$\overline{\overline{v_1}}_i = \frac{1}{2h}(\overline{\overline{u_1}}_{,i} - \overline{\overline{u_1}}_{,i-2})$	$v_{3_i} = \frac{1}{2h}(u_{3_i} - u_{3_{i-2}})$
4	$\overline{\overline{v_3}}_i = \frac{1}{2h}(\overline{\overline{u_3}}_{,i} - \overline{\overline{u_3}}_{,i-2})$	$v_{4_i} = \frac{1}{2h}(u_{4_i} - u_{4_{i-2}})$

Equation (3-16) makes use of the displacement at a forward time, which is not known during analysis. Accordingly, the velocity is computed at one time-step backwards and used at the current time. This requires the use of a small time-step.

SECTION 4
VERIFICATION EXAMPLES FOR PRESCRIBED BEARING MOTION AND CONSTANT FRICTION

This section presents examples of verification of the modified Triple FP element (TripleFrictionPendulumX element) in OpenSees. Table 4-1 presents information on two configurations in a total of four different cases of Triple FP bearing used in the examples. The isolators have an inner displacement restrainer or ring. In this section the friction coefficient values are considered constant and independent of pressure, velocity and temperature. This assumption is relaxed in other examples presented in Section 5. Values of parameters used in the analysis in addition to those below are presented in Appendix A.

Table 4-1 Geometric and Frictional Properties used in Analysis (see Figure 1-1 for nomenclature)

Geometric and Frictional Properties	Configuration A		Configuration B	
R_1=R_4 (mm)	3962.4 (156”)		2235 (88”)	
R_2=R_3 (mm)	558.8 (22”)		305 (12”)	
h_1=h_4 (mm)	215.9 (8.5”)		114.5 (4.5”)	
h_2=h_3 (mm)	165.1 (6.5”)		76 (3”)	
R_{eff1}=R_{eff4} (mm)	3746.5 (147.5”)		2120.5 (83.5”)	
R_{eff2}=R_{eff3} (mm)	393.7 (15.5”)		229 (9”)	
b_1=b_4 (mm)	711.2 (28”)		279 (11”)	
b_2=b_3 (mm)	508 (20”)		196 (7.7”)	
d_1=d_4 (mm)	533.4 (21”)		267 (10.5”)	
d_2=d_3 (mm)	101.6 (4”)		40 (1.6”)	
d_1^*=d_4^* (mm)	504.3 (19.9”)		253.3 (10.0”)	
d_2^*=d_3^* (mm)	71.6 (2.8”)		30.0 (1.2”)	
Vertical Stiffness (MN/mm)	8.0 (45720 kip/in)		8.0 (45720 kip/in)	
Friction Case	Case 1	Case 2	Case 1	Case 2
$\boldsymbol{\mu_1}$	0.04	0.04	0.04	0.04
$\boldsymbol{\mu_4}$	0.08	0.04	0.08	0.04
$\boldsymbol{\mu_2 = \mu_3}$	0.01	0.01	0.01	0.01
Load W (kN)	13345 (3000kip)		6672 (1500kip)	

4.1 Examples of Displacement Control Analysis

This subsection presents the results of displacement control analysis in programs OpenSees and 3pleANI. In these analyses, a displacement history is imposed at the top of the bearing with respect to its bottom. The results include force-displacement loops, and displacement, velocity and temperature histories at the four sliding interfaces. In the figures that follow, results are presented with (a) color green and denoted as APP1 when Approach 1 is used in OpenSees, and (b) color blue and denoted as APP2 when Approach 2 is used.

4.1.1 Harmonic Motion: Amplitude of 20in and Period of 20sec

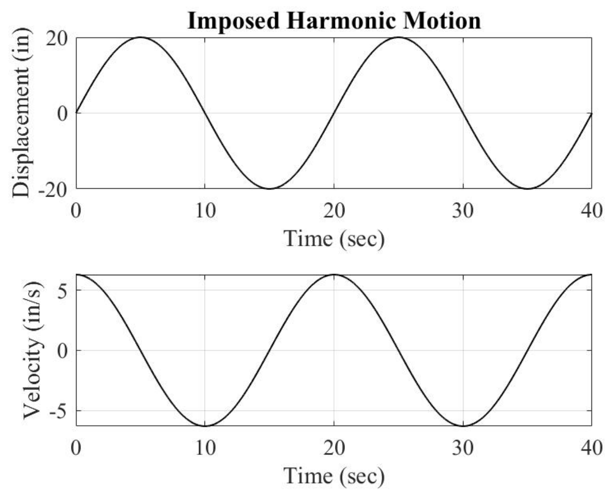

Figure 4-1 Imposed Harmonic Motion (Amplitude: 20in, Period: 20sec)

A) Configuration A

a. Case 1: Different Coefficient of Friction for Surfaces 1 and 4

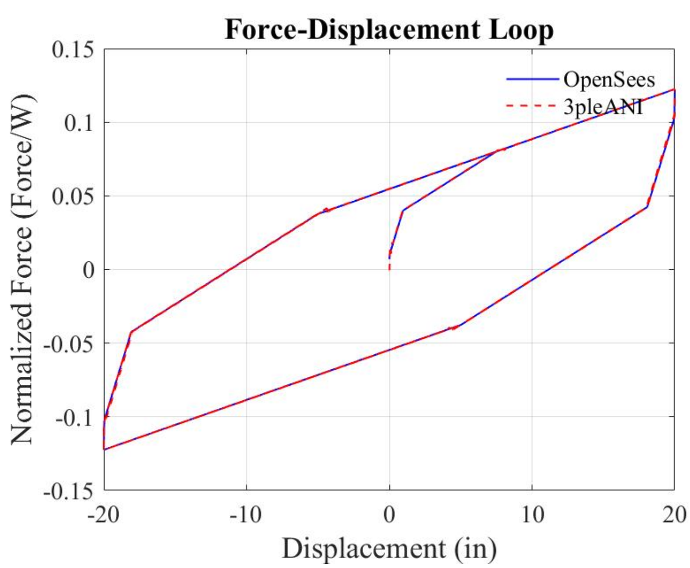

Figure 4-2 Comparison of Force-Displacement Loops

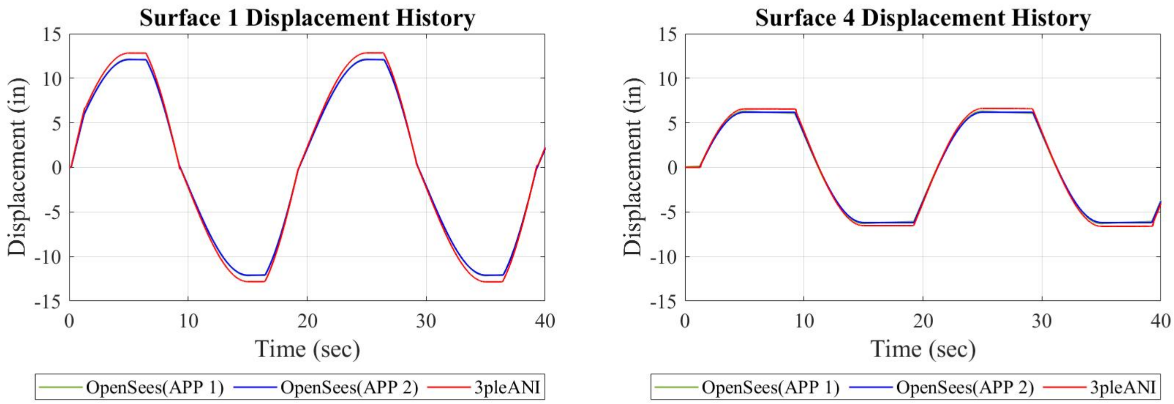

Figure 4-3 Comparison of Displacement Histories on Outer Surfaces (Surfaces 1 and 4)

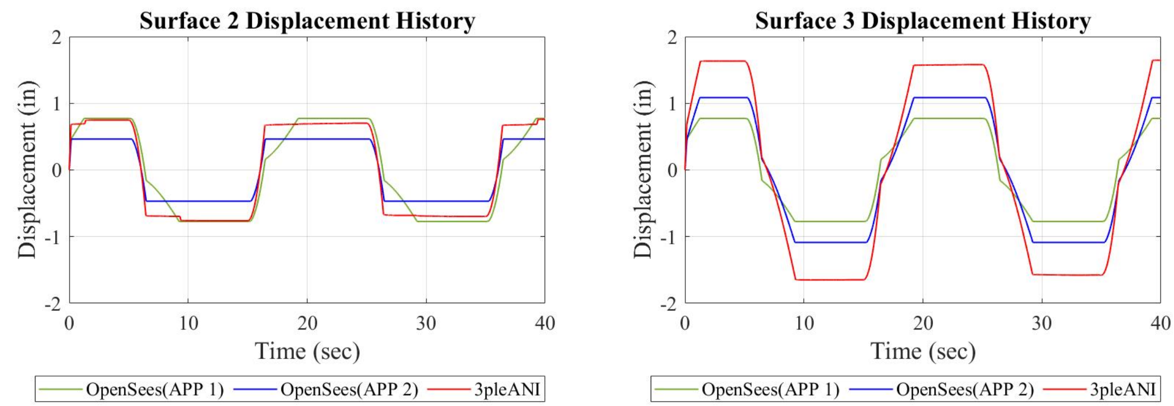

Figure 4-4 Comparison of Displacement Histories on Inner Surfaces (Surfaces 2 and 3)

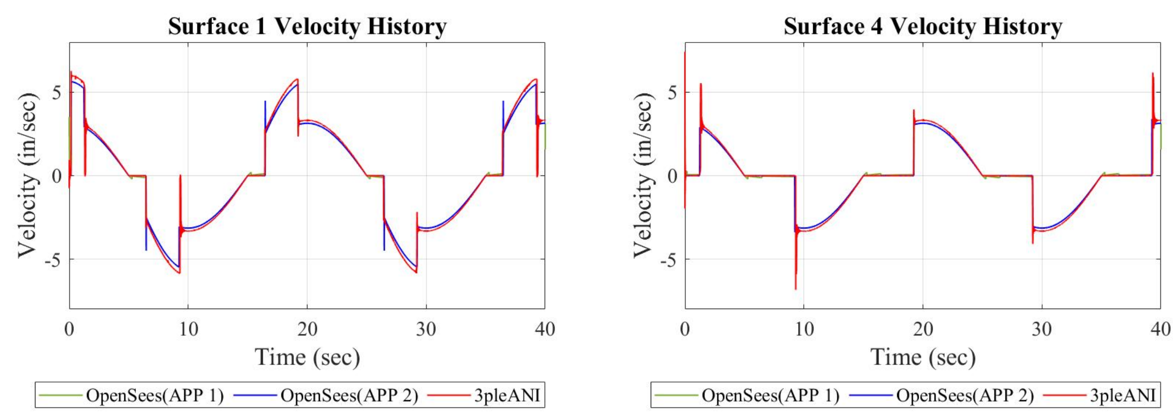

Figure 4-5 Comparison of Velocity Histories on Outer Surfaces (Surfaces 1 and 4)

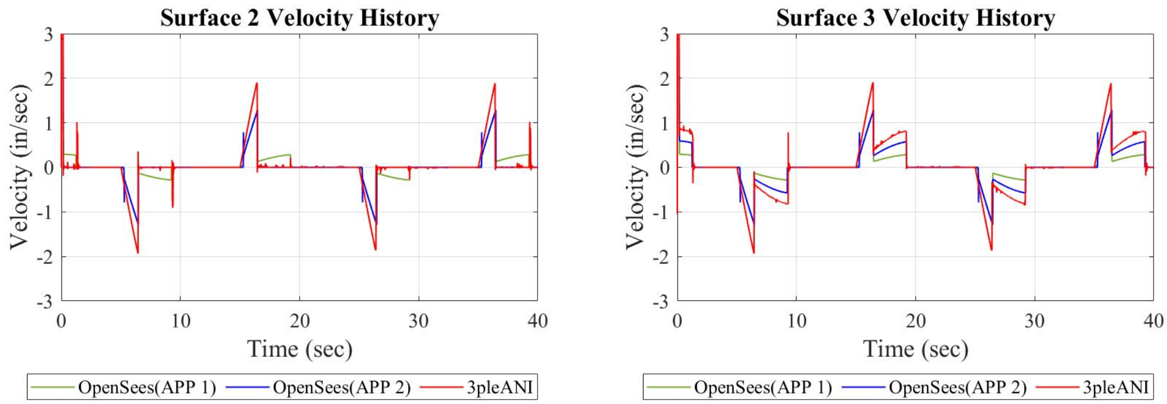

Figure 4-6 Comparison of Velocity Histories on Inner Surfaces (Surfaces 2 and 3)

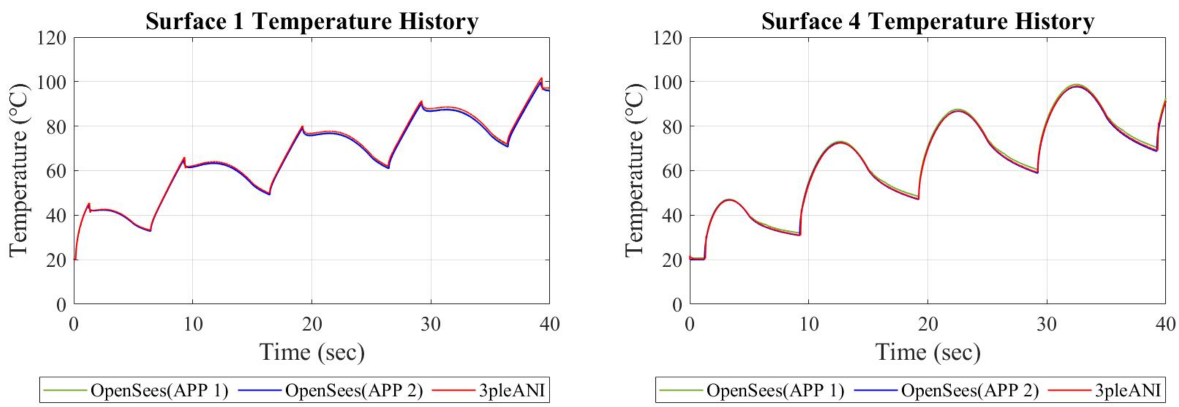

Figure 4-7 Comparison of Temperature Histories on Outer Surfaces (Surfaces 1 and 4)

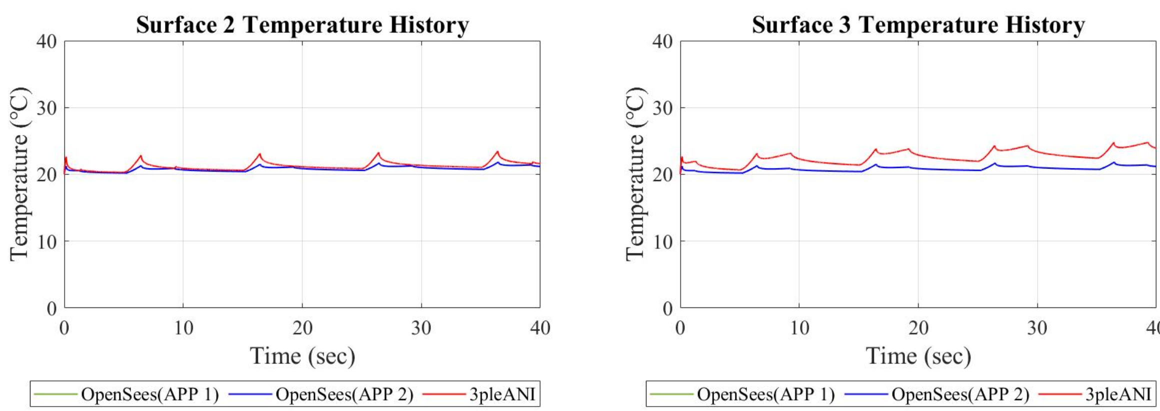

Figure 4-8 Comparison of Temperature Histories on Inner Surfaces (Surfaces 2 and 3)

b. Case 2: Same Coefficient of Friction for Surfaces 1 and 4

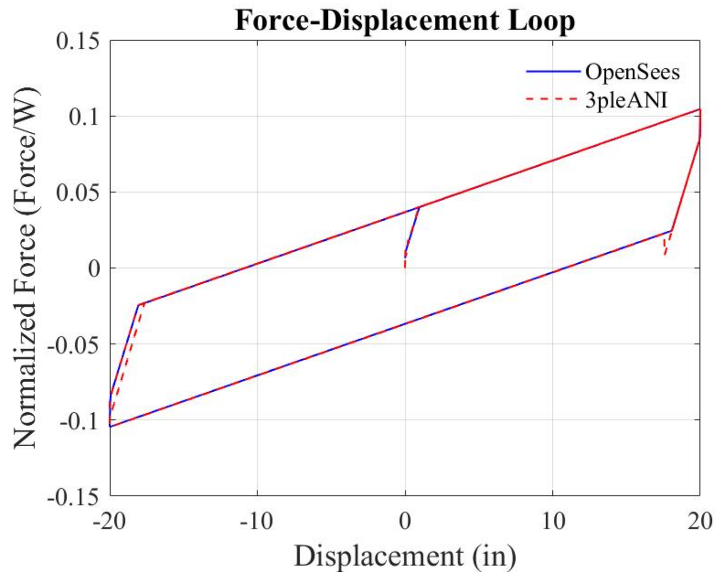

Figure 4-9 Comparison of Force-Displacement Loops

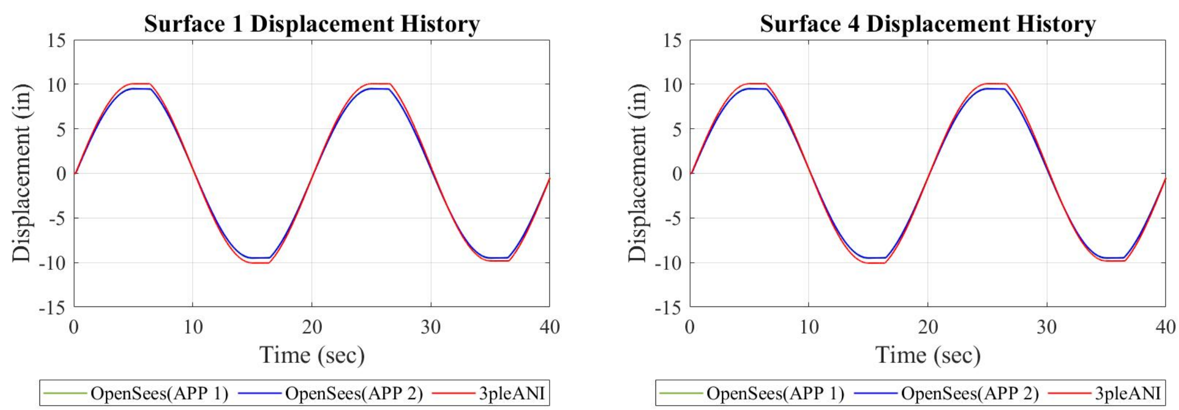

Figure 4-10 Comparison of Displacement Histories on Outer Surfaces (Surfaces 1 and 4)

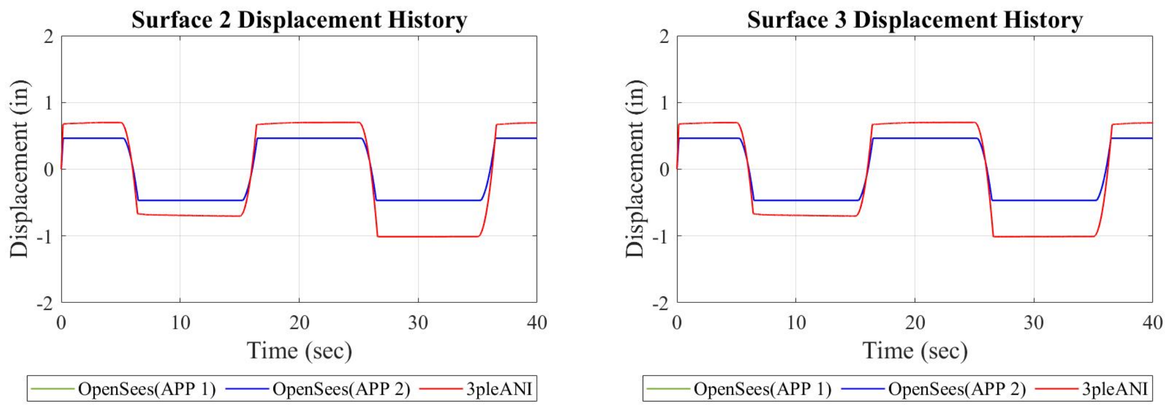

Figure 4-11 Comparison of Displacement Histories on Inner Surfaces (Surfaces 2 and 3)

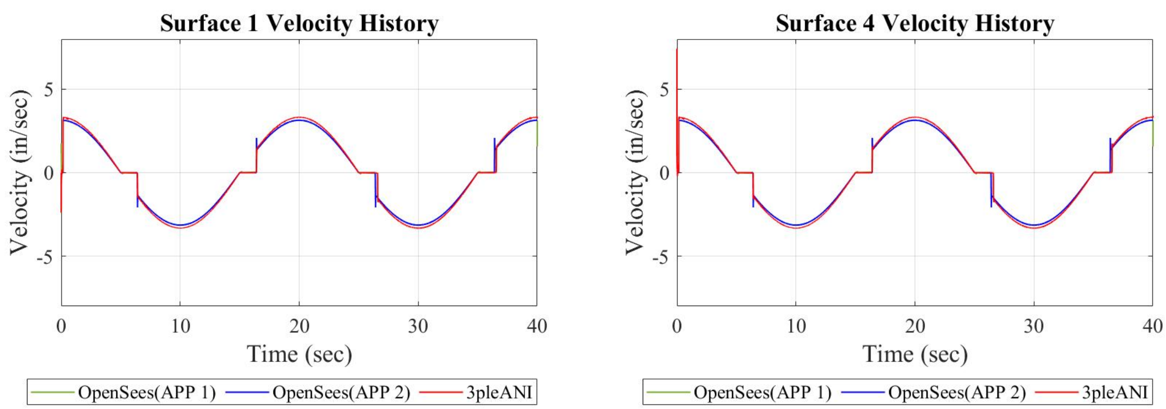

Figure 4-12 Comparison of Velocity Histories on Outer Surfaces (Surfaces 1 and 4)

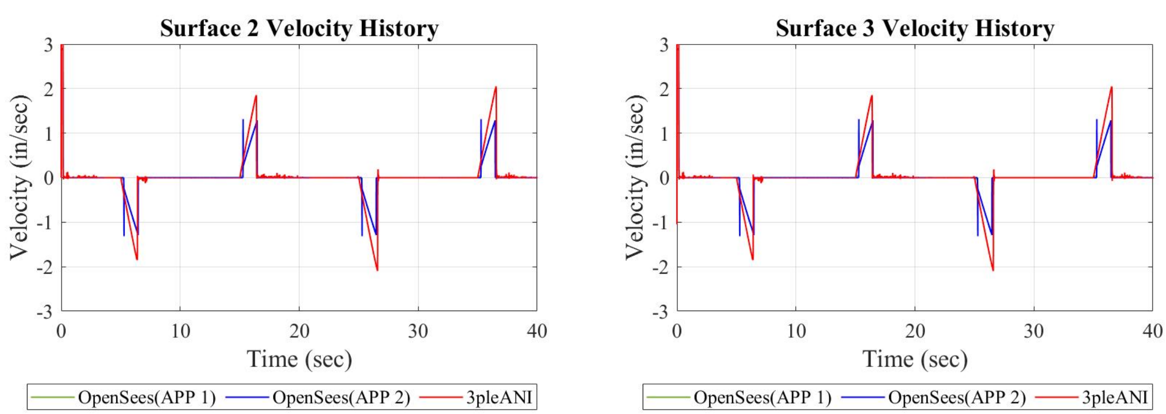

Figure 4-13 Comparison of Velocity Histories on Inner Surfaces (Surface 2 and 3)

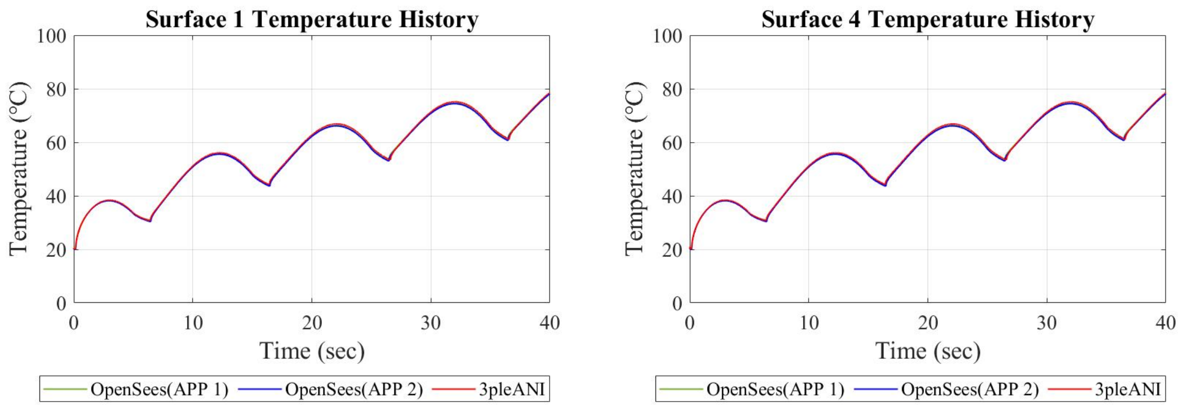

Figure 4-14 Comparison of Temperature Histories on Outer Surfaces (Surfaces 1 and 4)

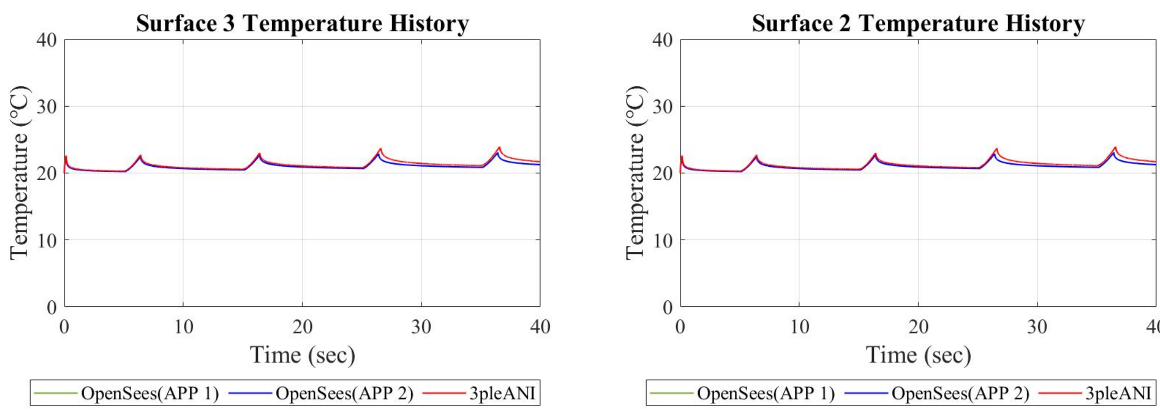

Figure 4-15 Comparison of Temperature Histories on Inner Surfaces (Surfaces 2 and 3)

B) Configuration B

a. Case 1: Different Coefficient of Friction for Surfaces 1 and 4

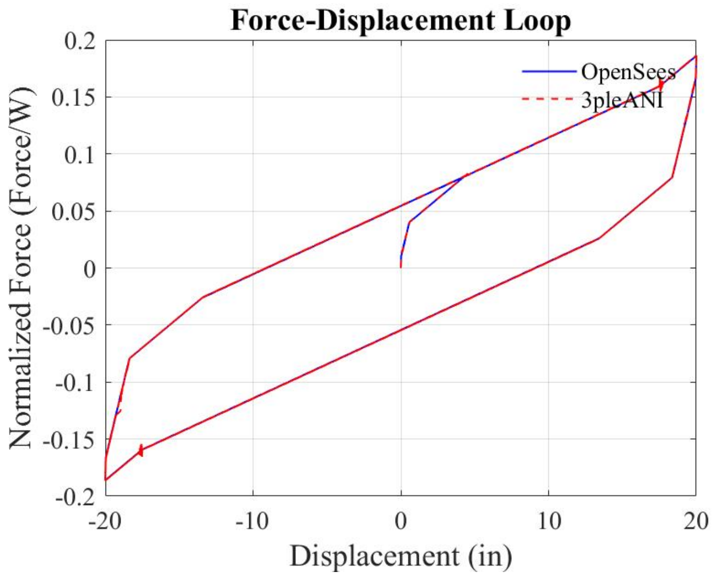

Figure 4-16 Comparison of Force-Displacement Loops

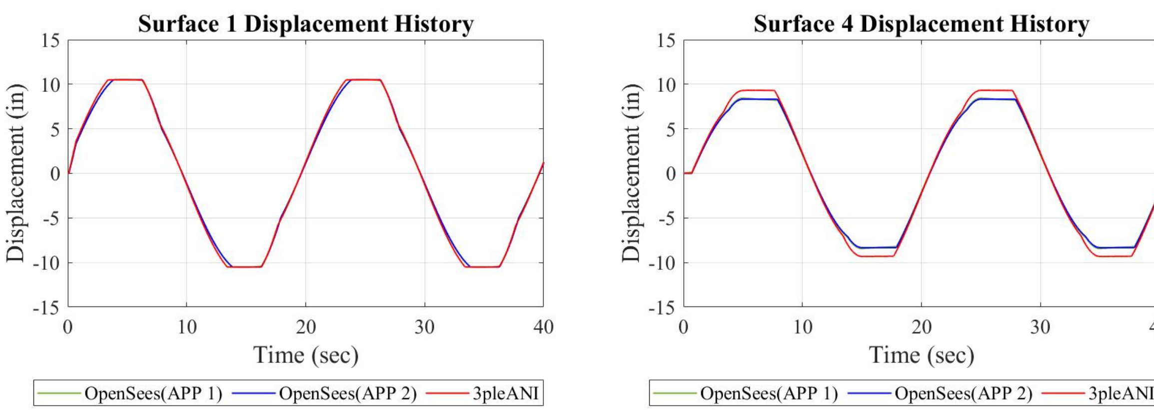

Figure 4-17 Comparison of Displacement Histories on Outer Surfaces (Surfaces 1 and 4)

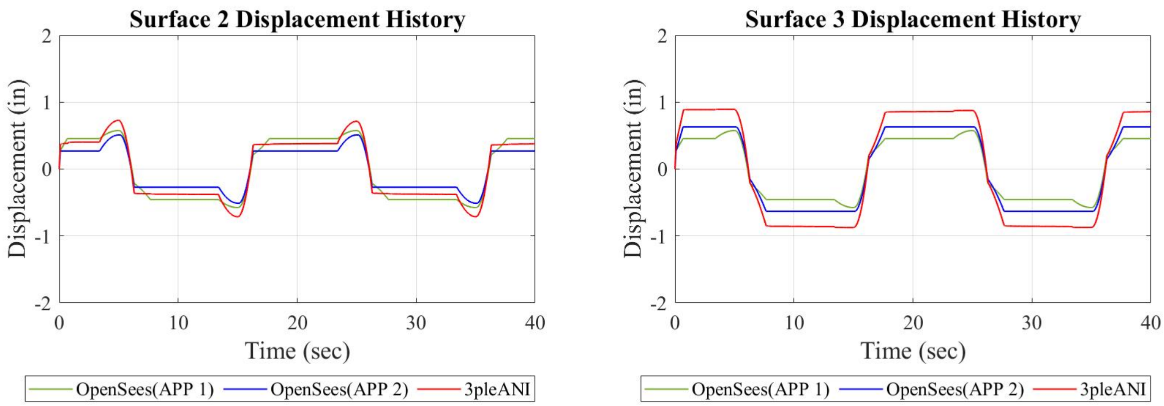

Figure 4-18 Comparison of Displacement Histories on Inner Surfaces (Surfaces 2 and 3)

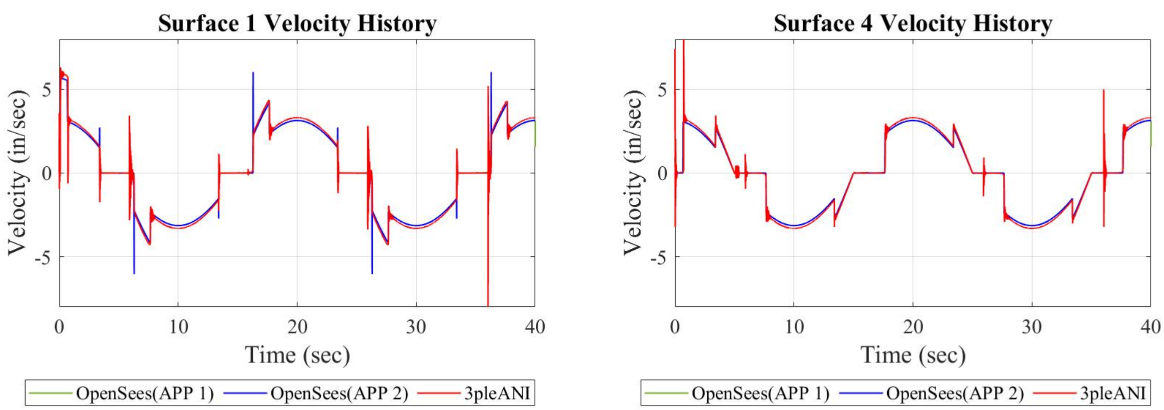

Figure 4-19 Comparison of Velocity Histories on Outer Surfaces (Surfaces 1 and 4)

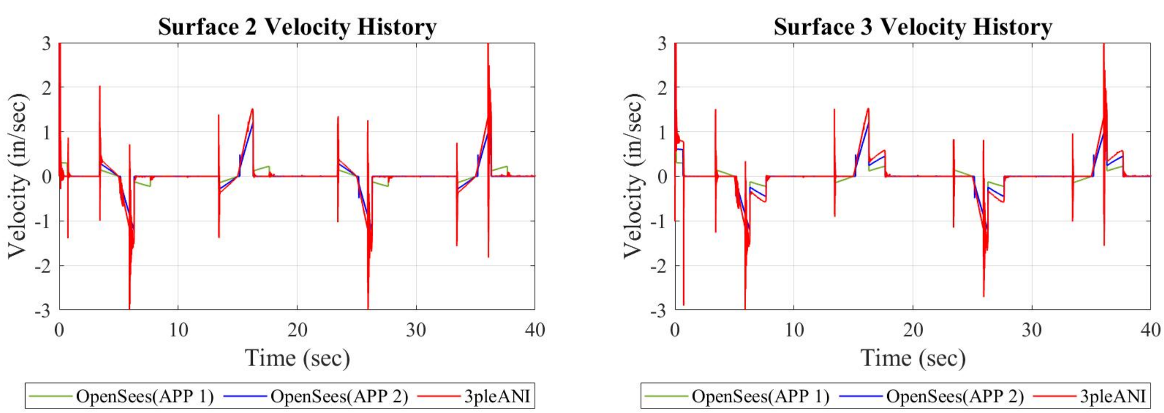

Figure 4-20 Comparison of Velocity Histories on Inner Surfaces (Surfaces 2 and 3)

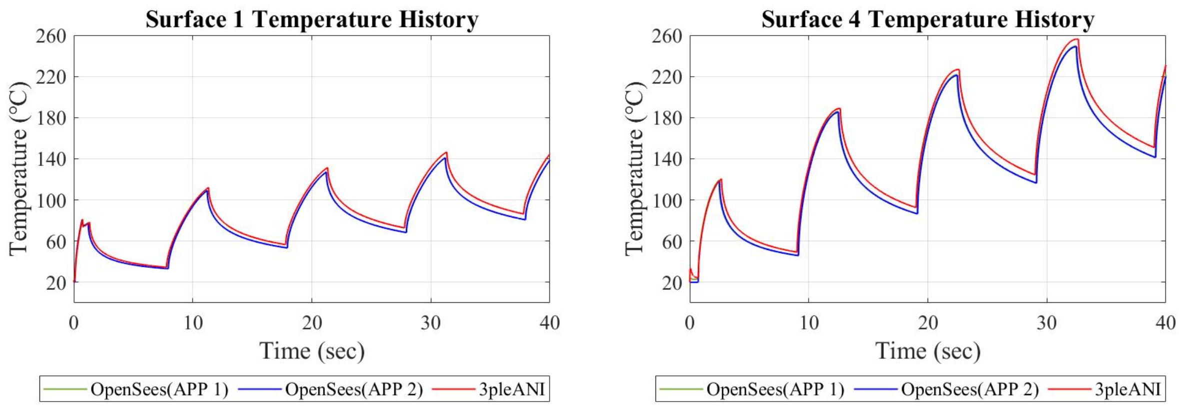

Figure 4-21 Comparison of Temperature Histories on Outer Surfaces (Surfaces 1 and 4)

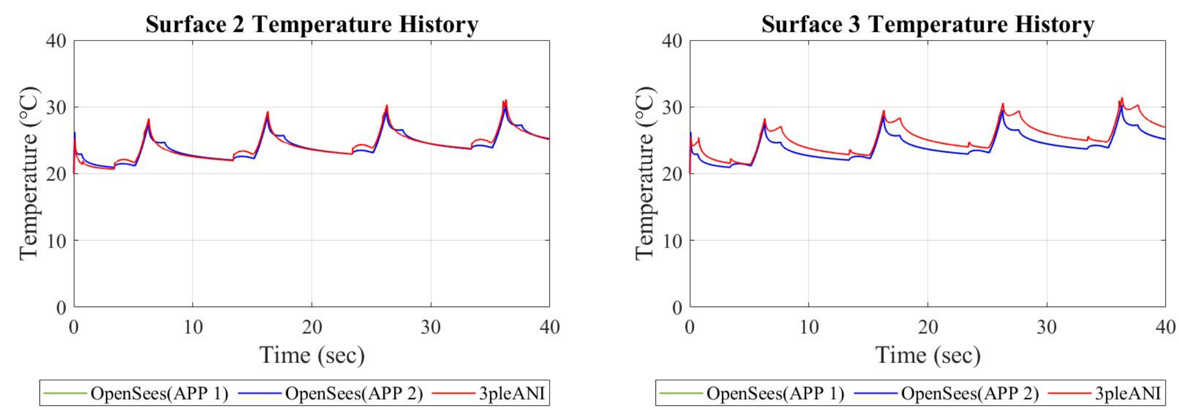

Figure 4-22 Comparison of Temperature Histories on Inner Surfaces (Surfaces 2 and 3)

b. Case 2: Same Coefficient of Friction for Surfaces 1 and 4

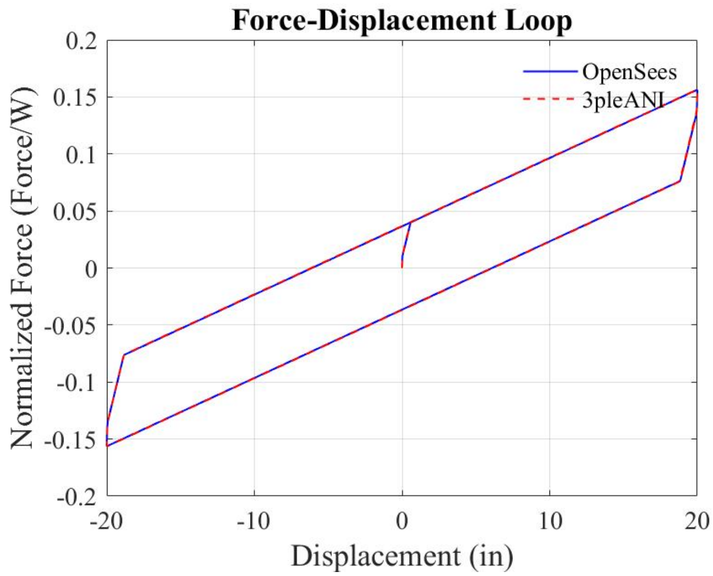

Figure 4-23 Comparison of Force-Displacement Loops

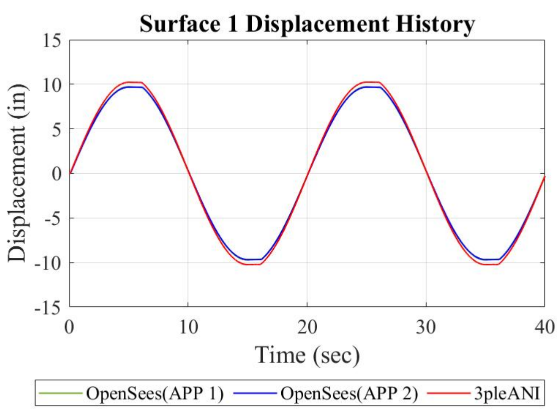

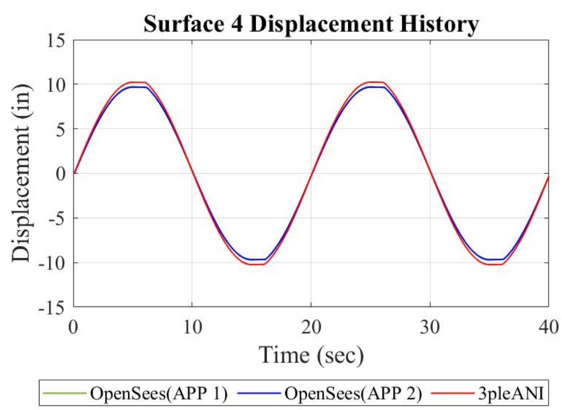

Figure 4-24 Comparison of Displacement Histories on Outer Surfaces (Surfaces 1 and 4)

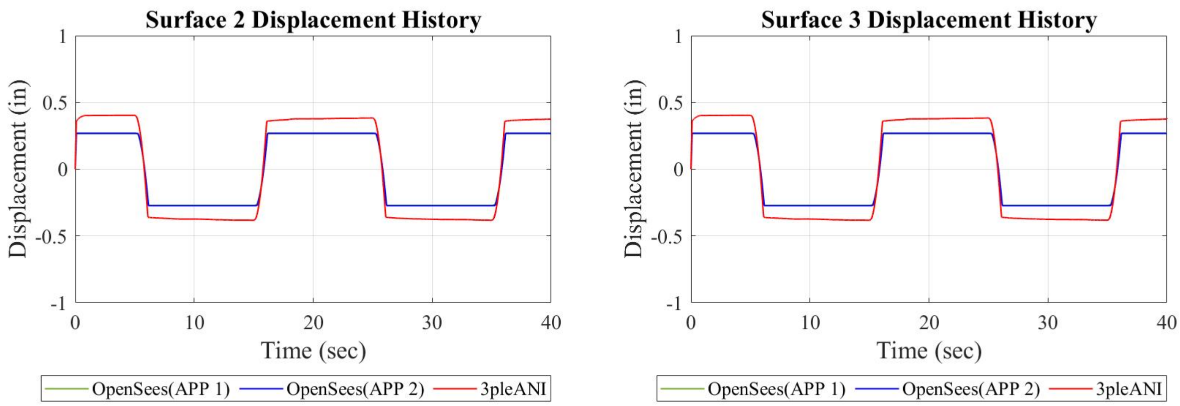

Figure 4-25 Comparison of Displacement Histories on Inner Surfaces (Surfaces 2 and 3)

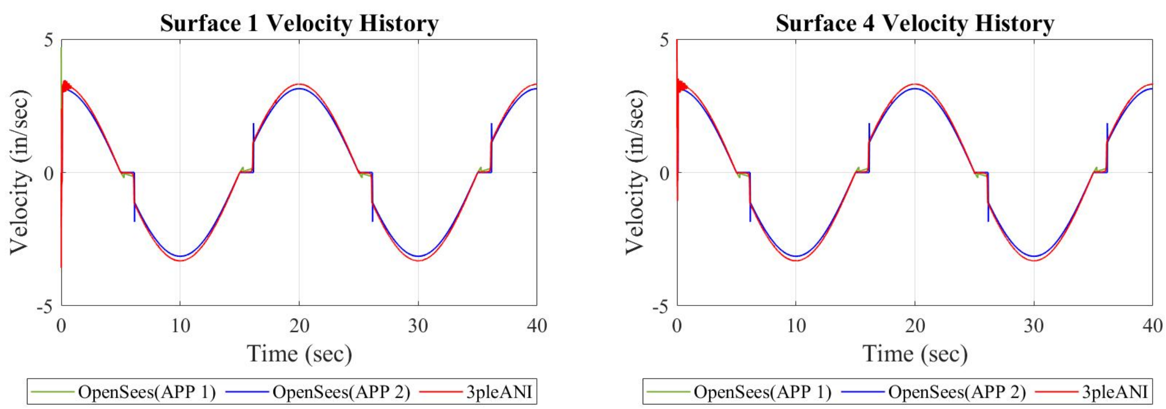

Figure 4-26 Comparison of Velocity Histories on Outer Surfaces (Surfaces 1 and 4)

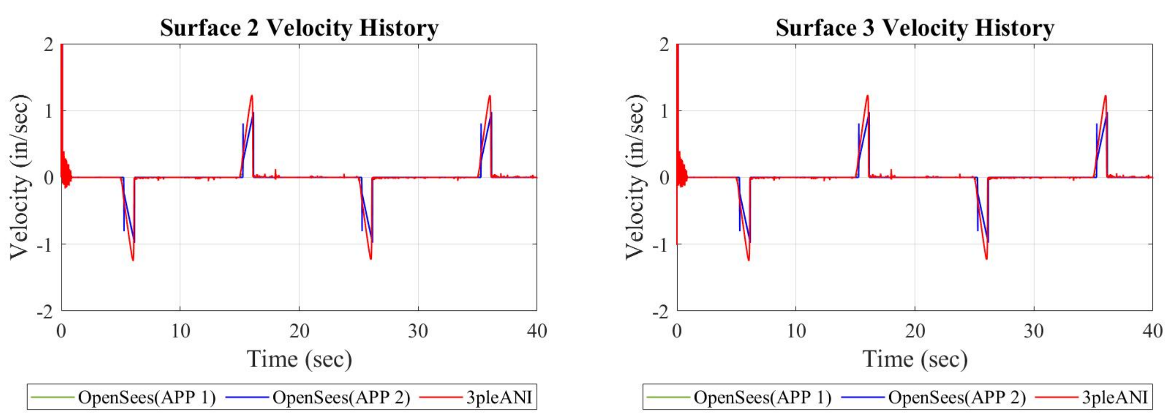

Figure 4-27 Comparison of Velocity Histories on Inner Surfaces (Surfaces 2 and 3)

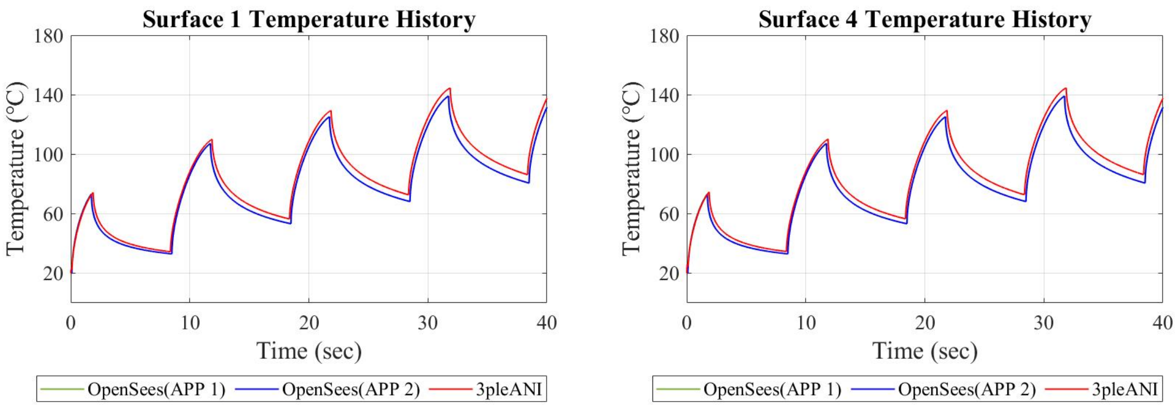

Figure 4-28 Comparison of Temperature Histories on Outer Surfaces (Surfaces 1 and 4)

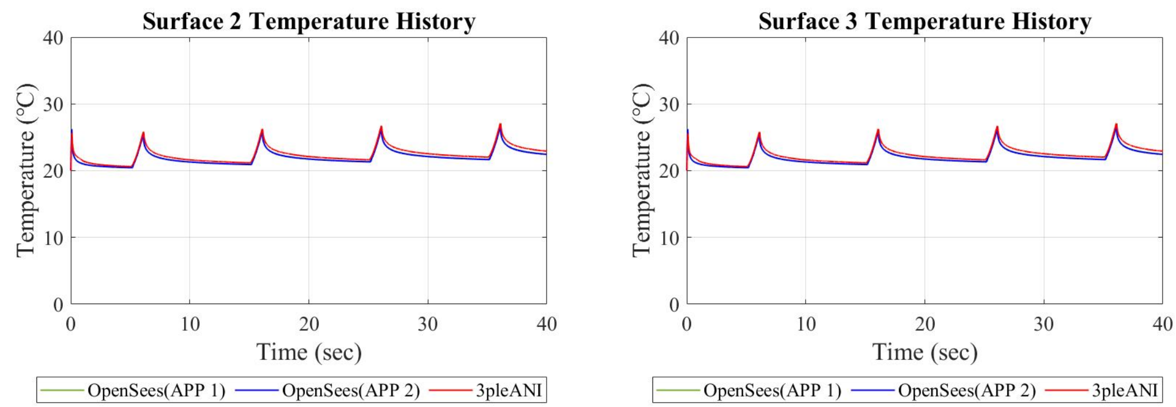

Figure 4-29 Comparison of Temperature Histories on Inner Surfaces (Surfaces 2 and 3)

4.1.2 Harmonic Motion: Amplitude of 22in and Period of 10sec

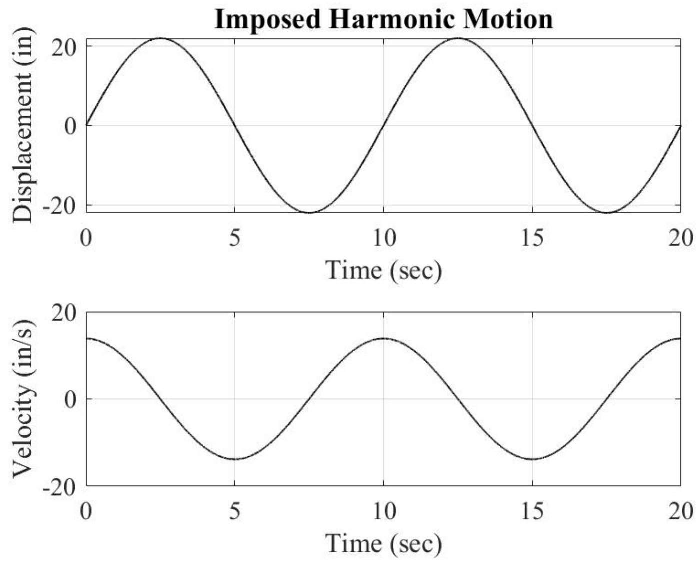

Figure 4-30 Imposed Harmonic Motion (Amplitude: 22in, Period: 10sec)

A) Configuration A

a. Case 1: Different Coefficient of Friction for Surfaces 1 and 4

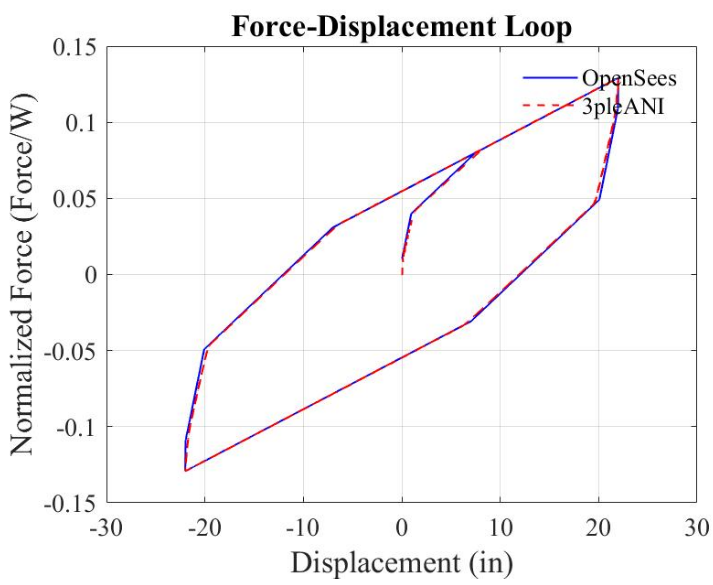

Figure 4-31 Comparison of Force-Displacement Loops

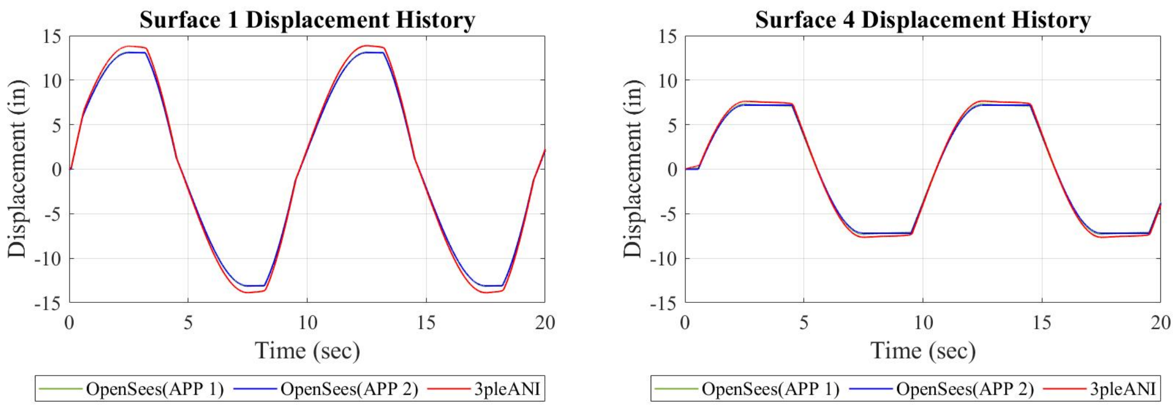

Figure 4-32 Comparison of Displacement Histories on Outer Surfaces (Surfaces 1 and 4)

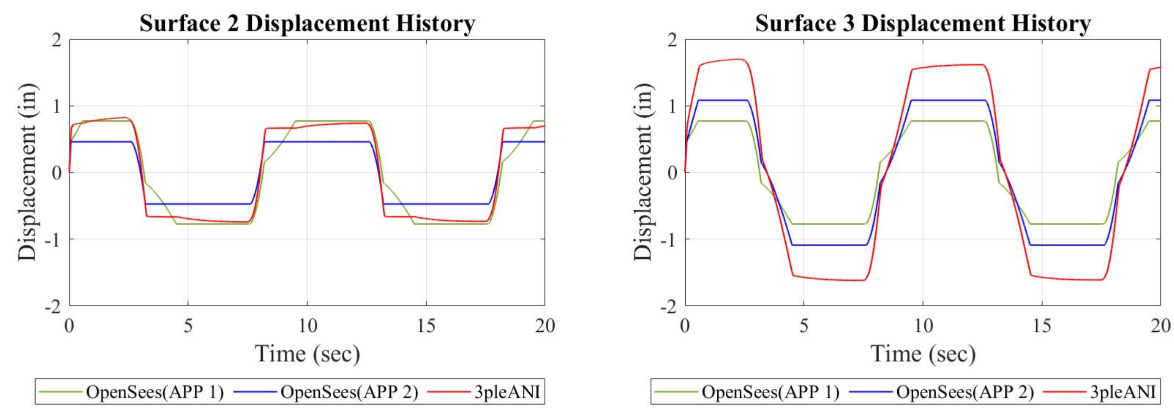

Figure 4-33 Comparison of Displacement Histories on Inner Surfaces (Surfaces 2 and 3)

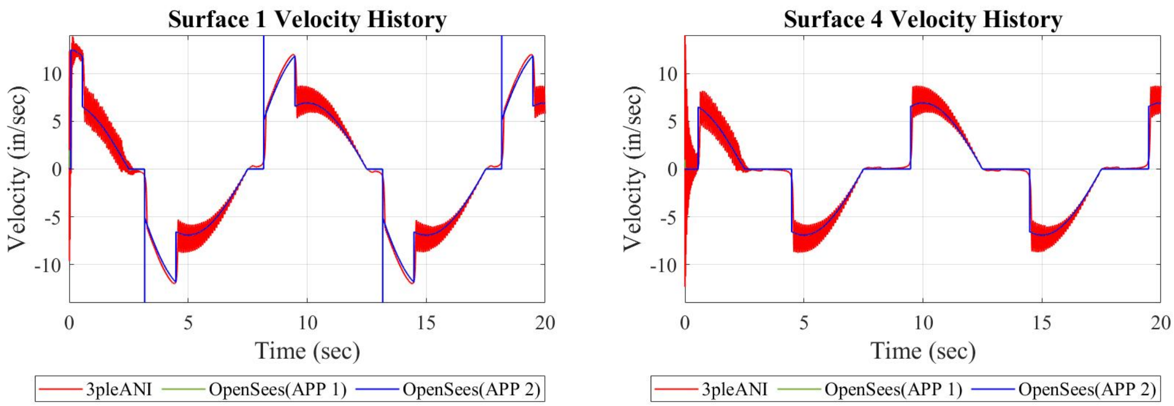

Figure 4-34 Comparison of Velocity Histories on Outer Surfaces (Surfaces 1 and 4)

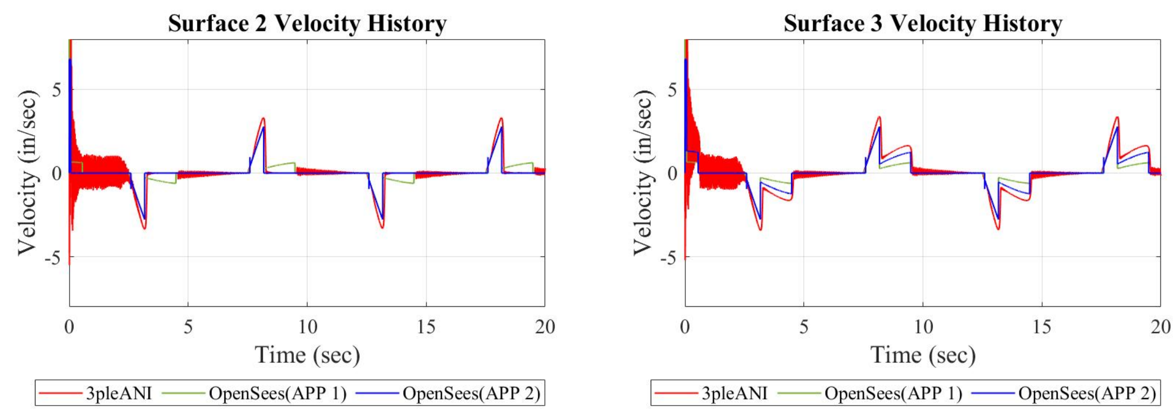

Figure 4-35 Comparison of Velocity Histories on Inner Surfaces (Surfaces 2 and 3)

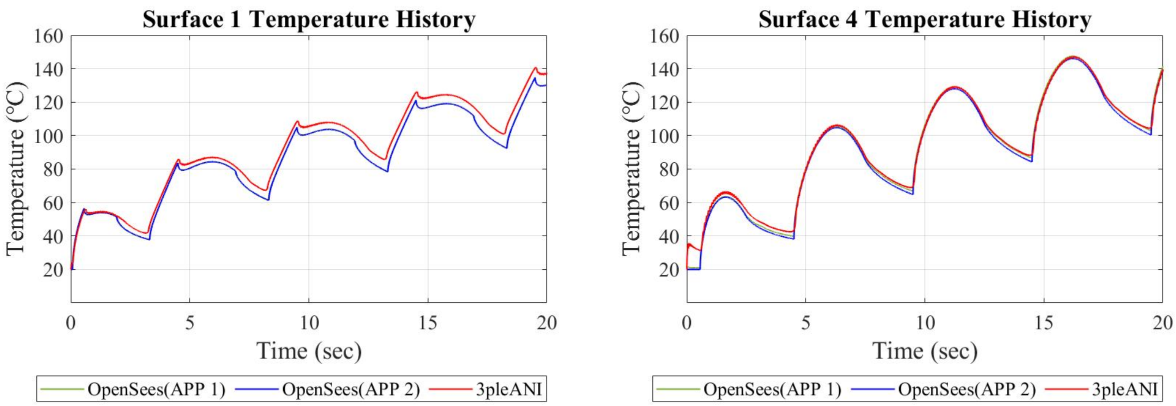

Figure 4-36 Comparison of Temperature Histories on Outer Surfaces (Surfaces 1 and 4)

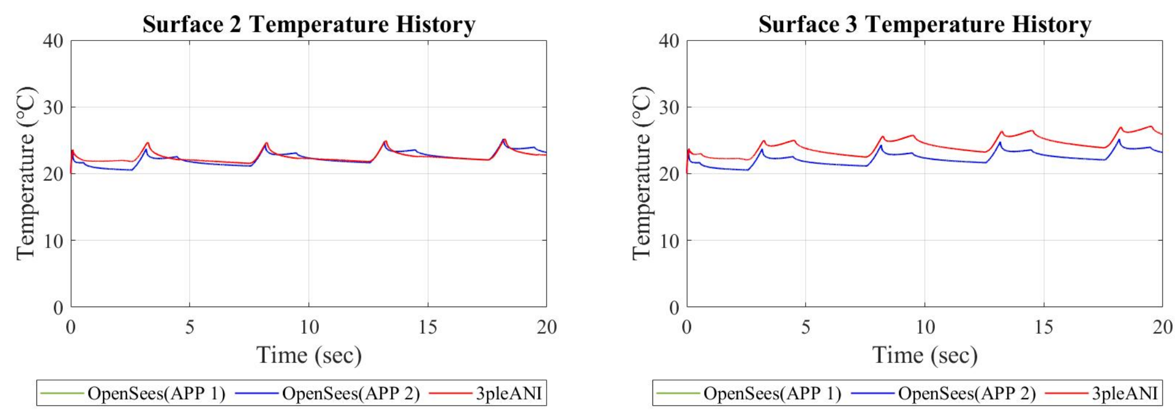

Figure 4-37 Comparison of Temperature Histories on Inner Surfaces (Surfaces 2 and 3)

b. **Case 2: Same Coefficient of Friction for Surfaces 1 and 4**

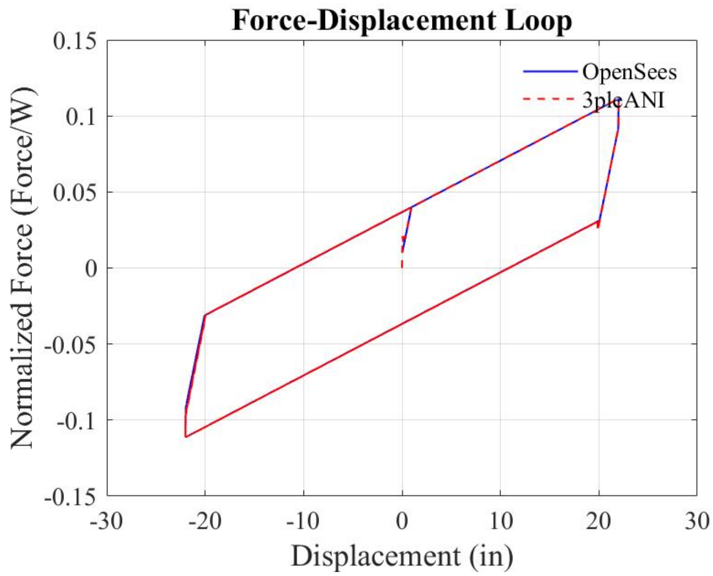

Figure 4-38 Comparison of Force-Displacement Loops

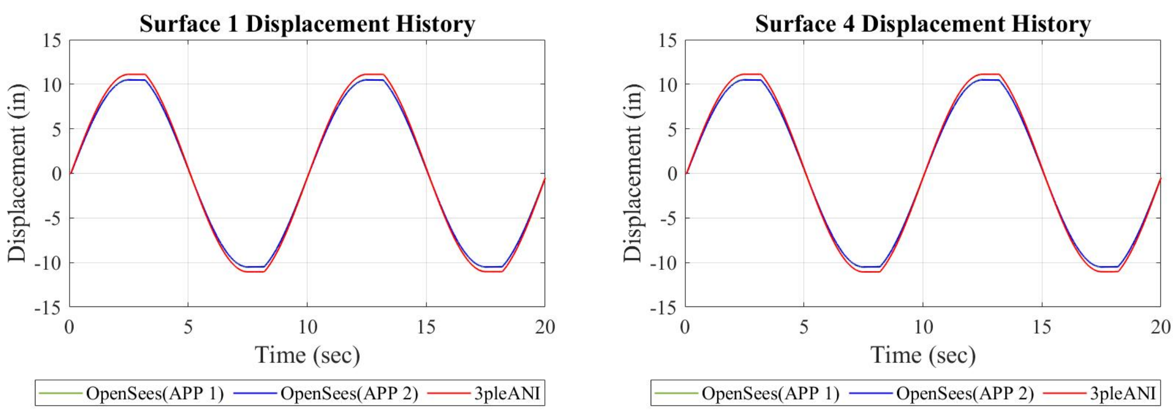

Figure 4-39 Comparison of Displacement Histories on Outer Surfaces (Surface 1 and 4)

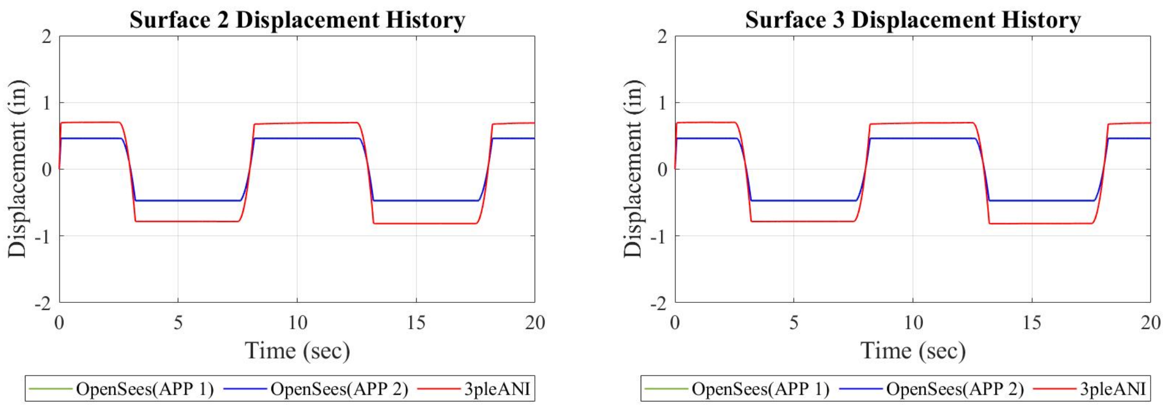

Figure 4-40 Comparison of Displacement Histories on Inner Surfaces (Surface 2 and 3)

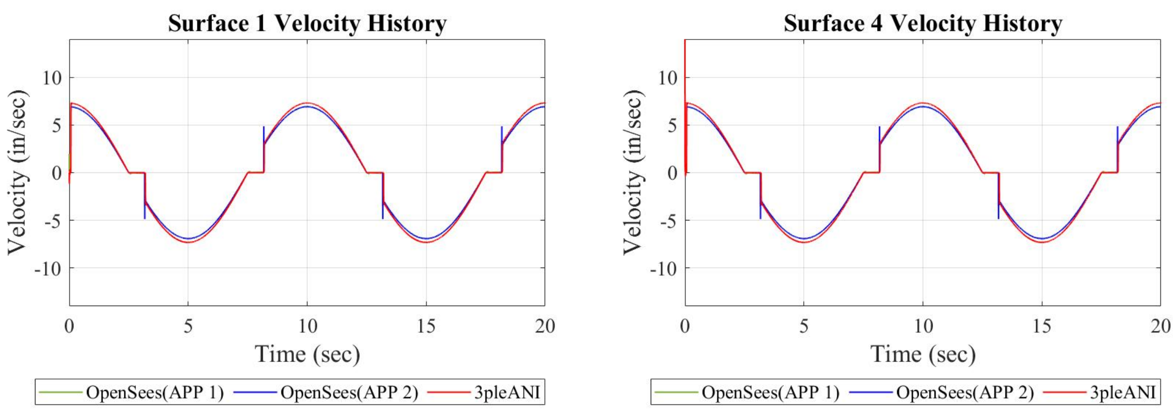

Figure 4-41 Comparison of Velocity Histories on Outer Surfaces (Surface 1 and 4)

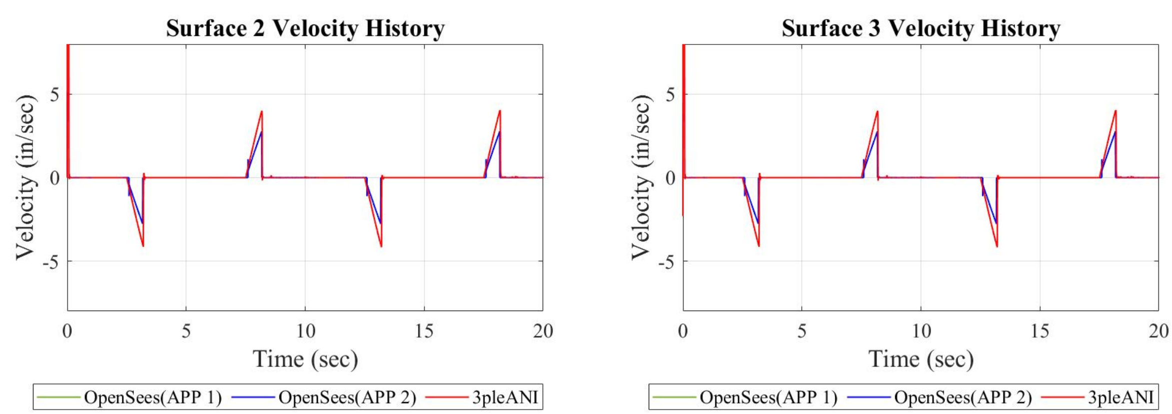

Figure 4-42 Comparison of Velocity Histories on Inner Surfaces (Surfaces 2 and 3)

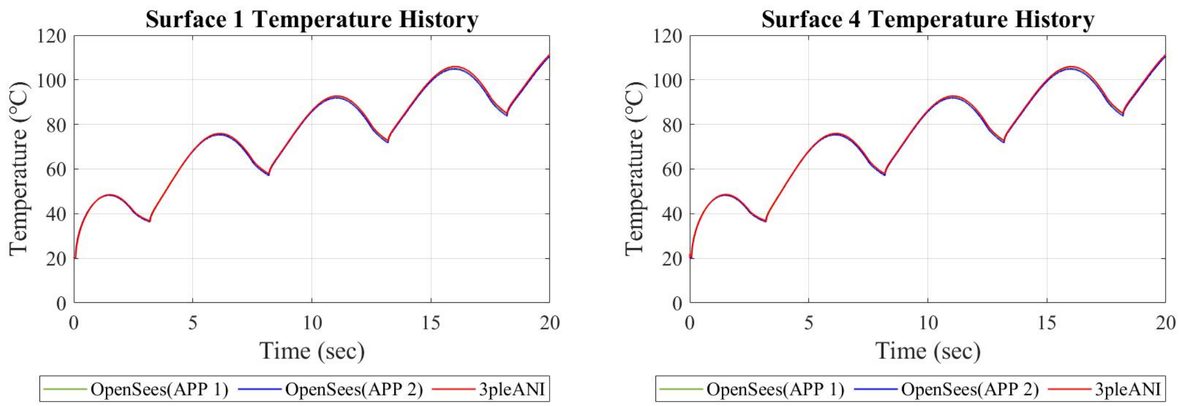

Figure 4-43 Comparison of Temperature Histories on Outer Surfaces (Surfaces 1 and 4)

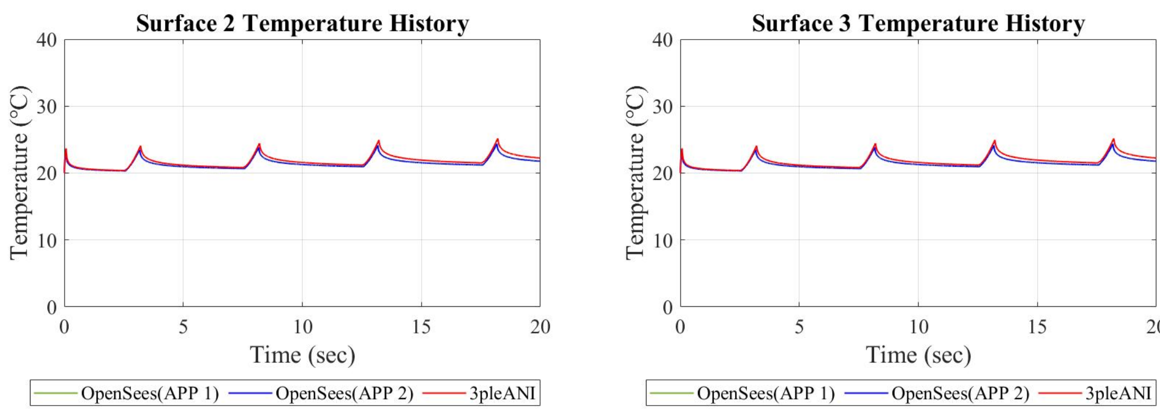

Figure 4-44 Comparison of Temperature Histories on Inner Surfaces (Surfaces 2 and 3)

B) Configuration B

a. Case 1: Different Coefficient of Friction for Surface 1 and 4

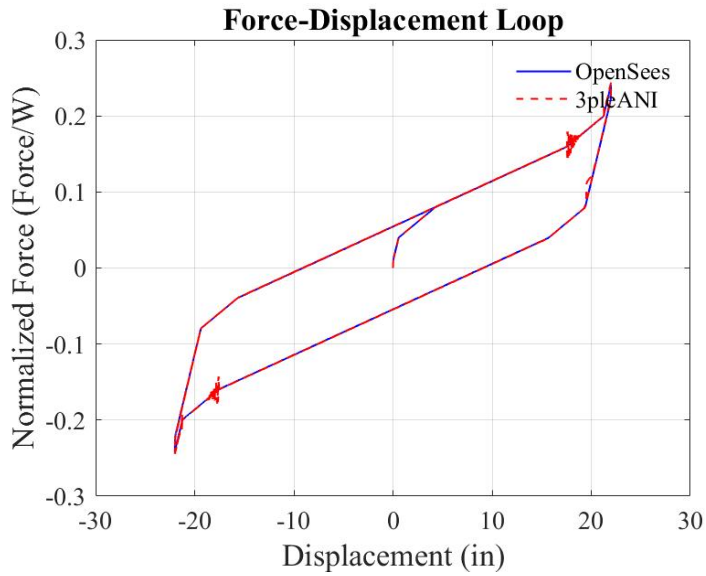

Figure 4-45 Comparison of Force-Displacement Loops

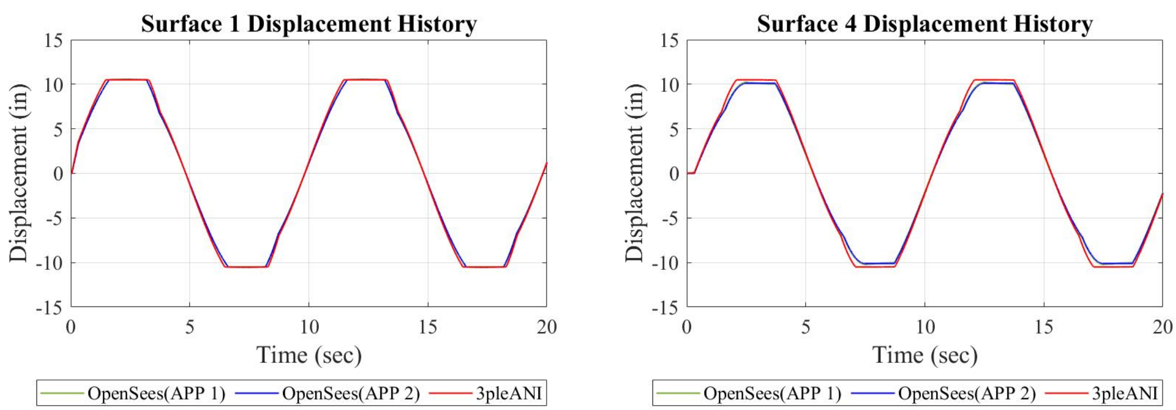

Figure 4-46 Comparison of Displacement Histories on Outer Surfaces (Surfaces 1 and 4)

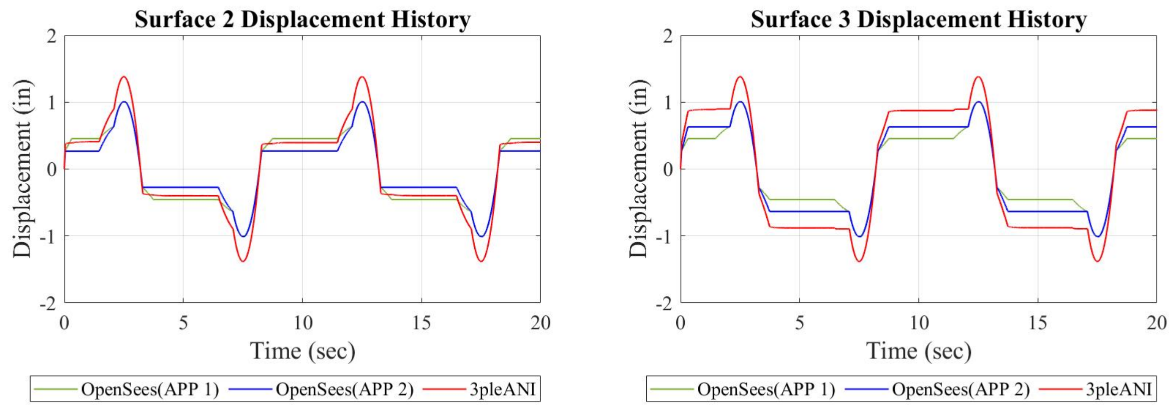

Figure 4-47 Comparison of Displacement Histories on Inner Surfaces (Surfaces 2 and 3)

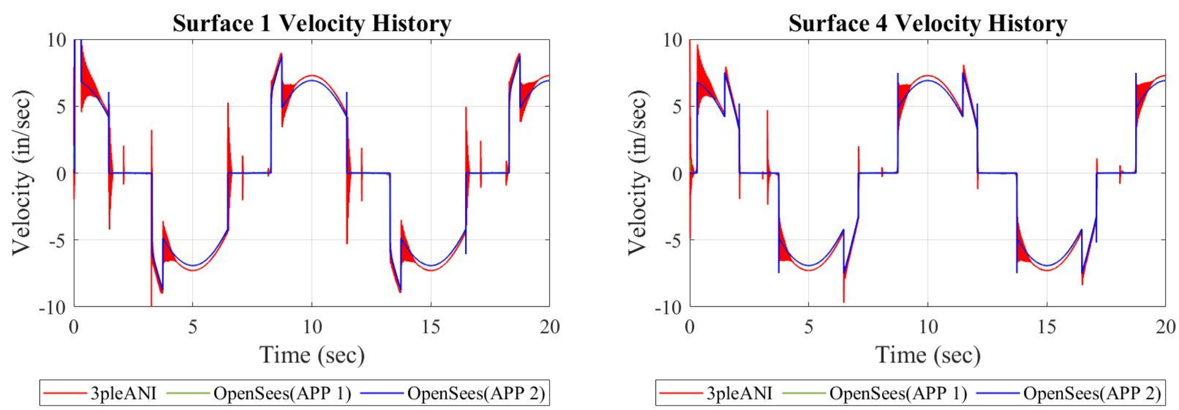

Figure 4-48 Comparison of Velocity Histories on Outer Surfaces (Surfaces 1 and 4)

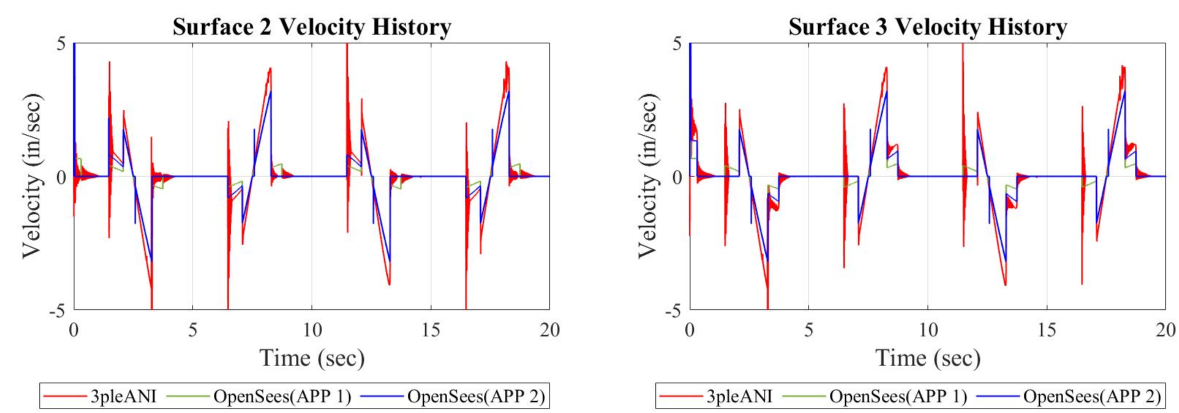

Figure 4-49 Comparison of Velocity Histories on Inner Surfaces (Surfaces 2 and 3)

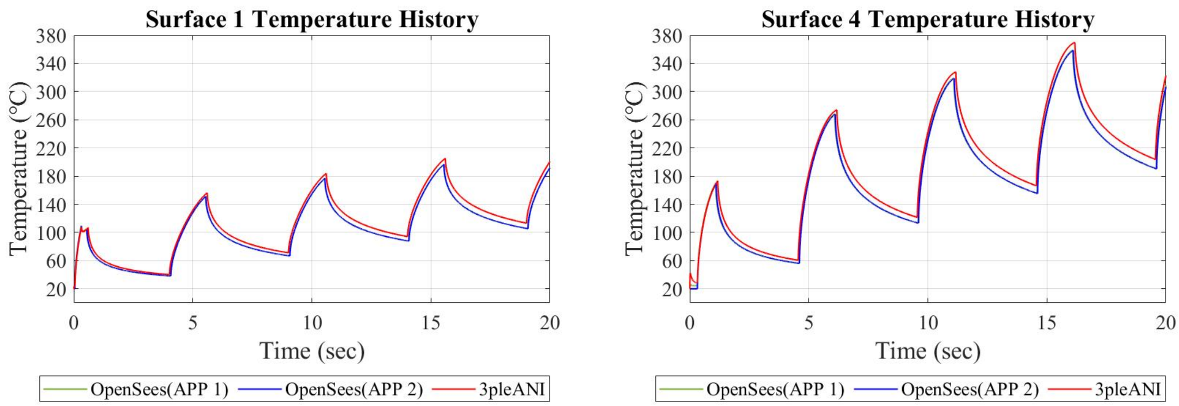

Figure 4-50 Comparison of Temperature Histories on Outer Surfaces (Surfaces 1 and 4)

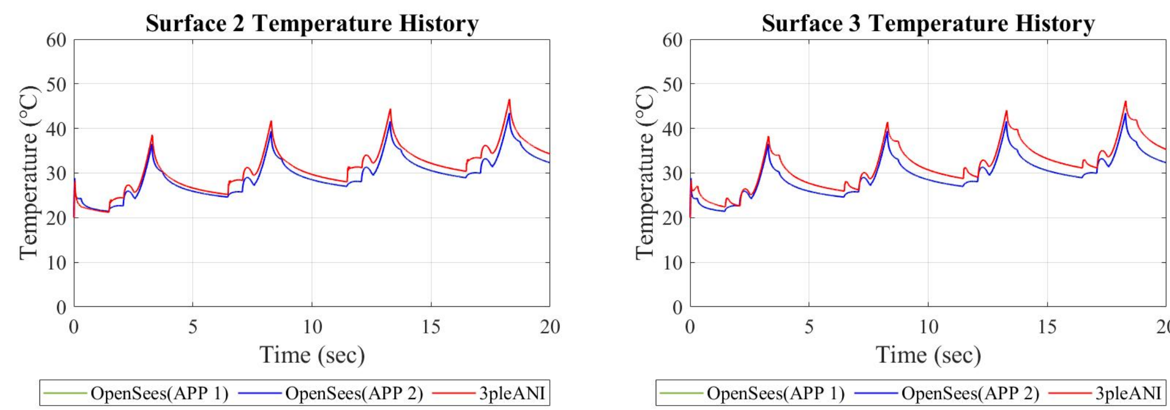

Figure 4-51 Comparison of Temperature Histories on Inner Surfaces (Surfaces 2 and 3)

b. Case 2: Same Coefficient of Friction for Surface 1 and 4

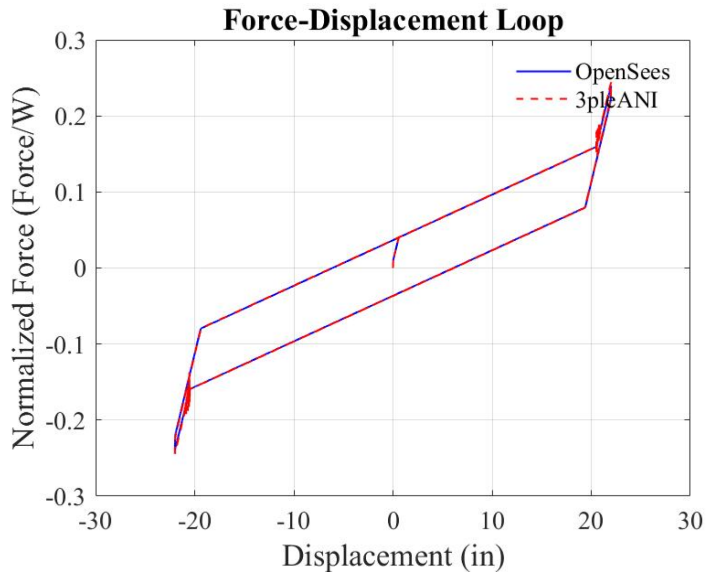

Figure 4-52 Comparison of Force-Displacement Loops

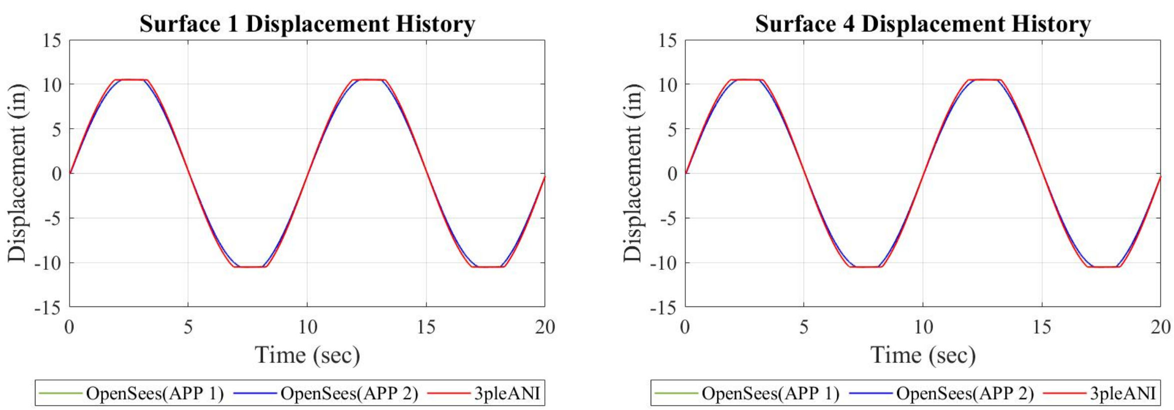

Figure 4-53 Comparison of Displacement Histories on Outer Surfaces (Surfaces 1 and 4)

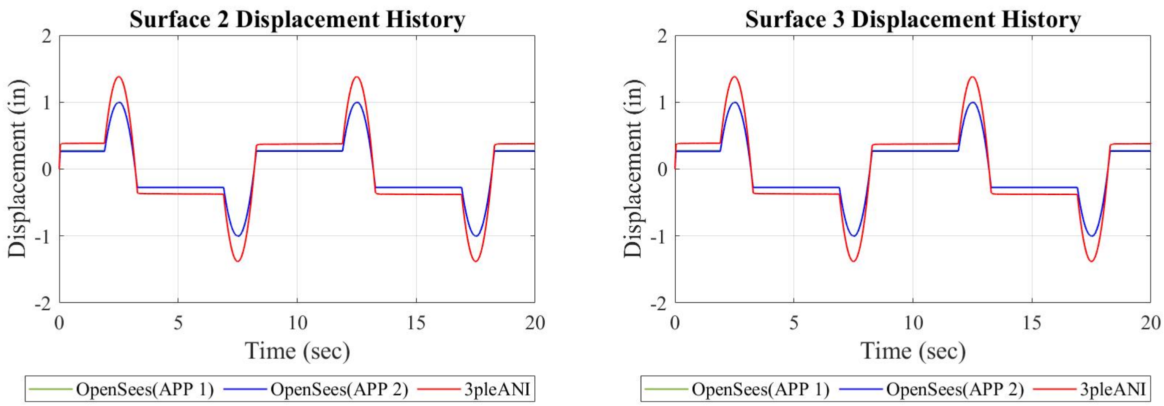

Figure 4-54 Comparison of Displacement Histories on Inner Surfaces (Surfaces 2 and 3)

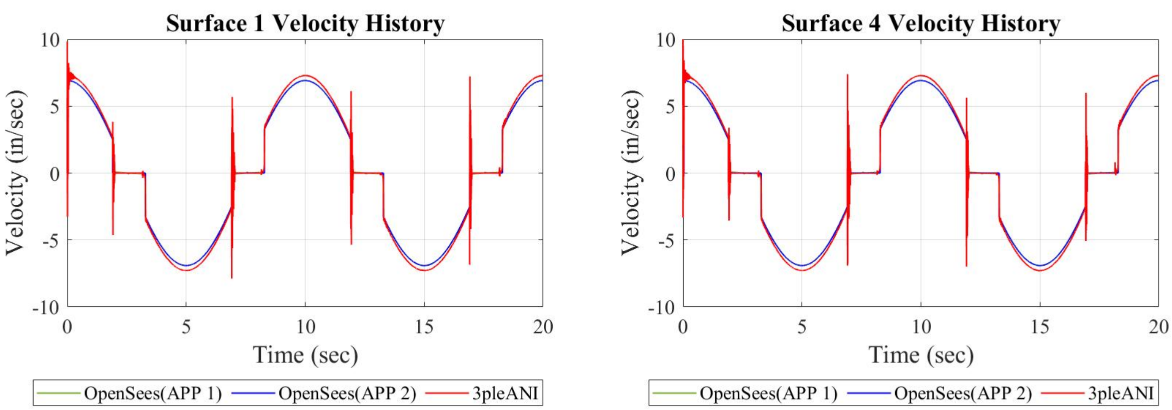

Figure 4-55 Comparison of Velocity Histories on Outer Surfaces (Surfaces 1 and 4)

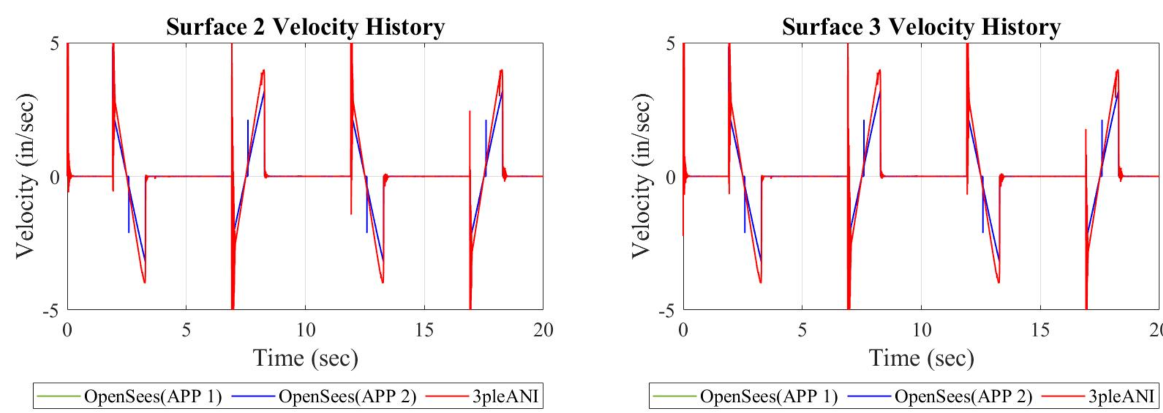

Figure 4-56 Comparison of Velocity Histories on Inner Surfaces (Surfaces 2 and 3)

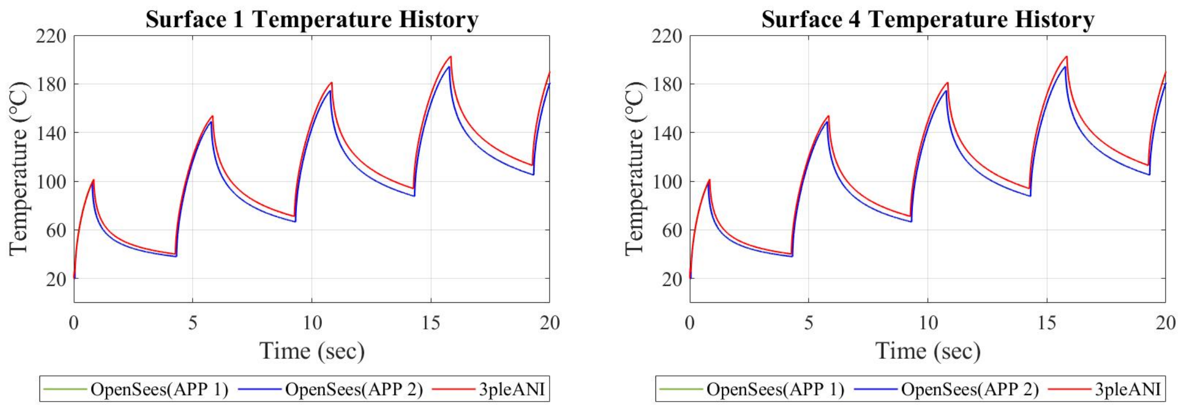

Figure 4-57 Comparison of Temperature Histories on Outer Surfaces (Surfaces 1 and 4)

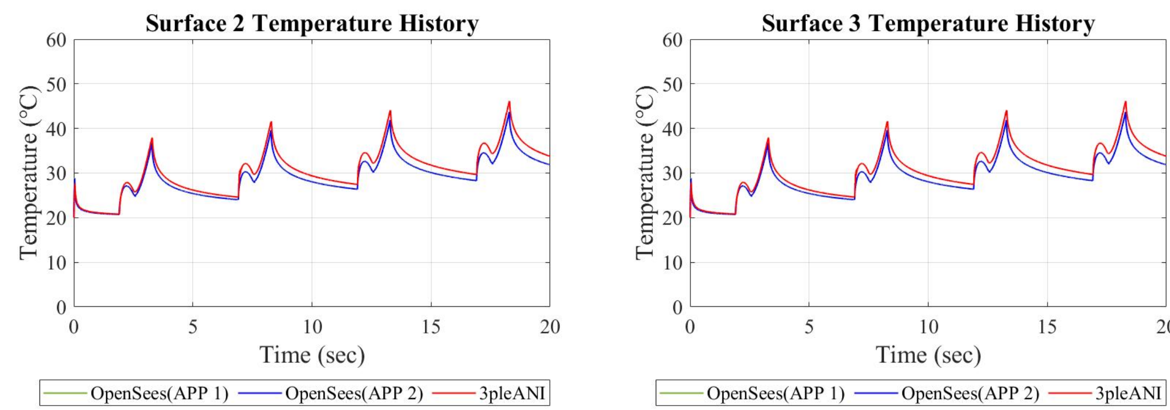

Figure 4-58 Comparison of Temperature Histories on Inner Surfaces (Surfaces 2 and 3)

4.1.3 Harmonic Motion: Amplitude of 20in and Period of 5sec

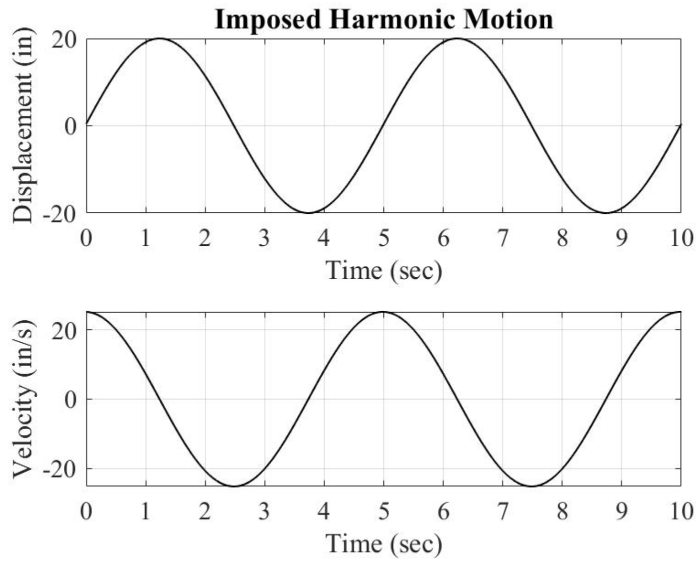

Figure 4-59 Imposed Harmonic Motion (Amplitude: 20in, Period: 5sec)

A) Configuration A

a. Case 1: Different Coefficient of Friction for Surfaces 1 and 4

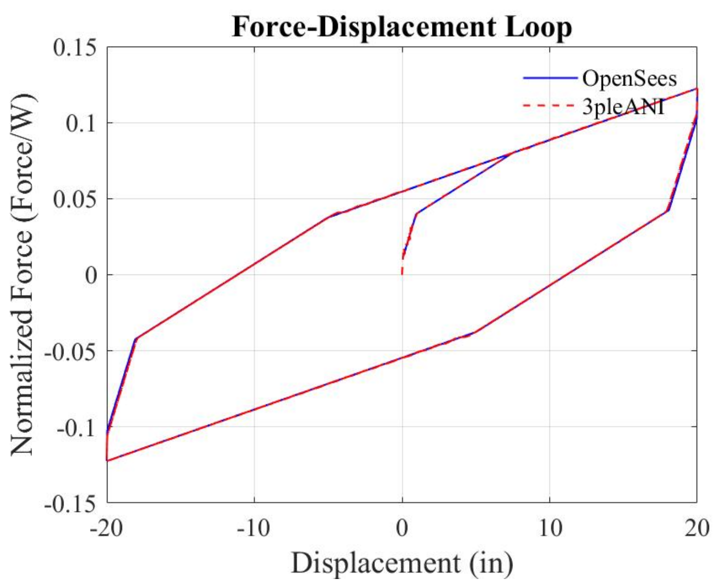

Figure 4-60 Comparison of Force-Displacement Loops

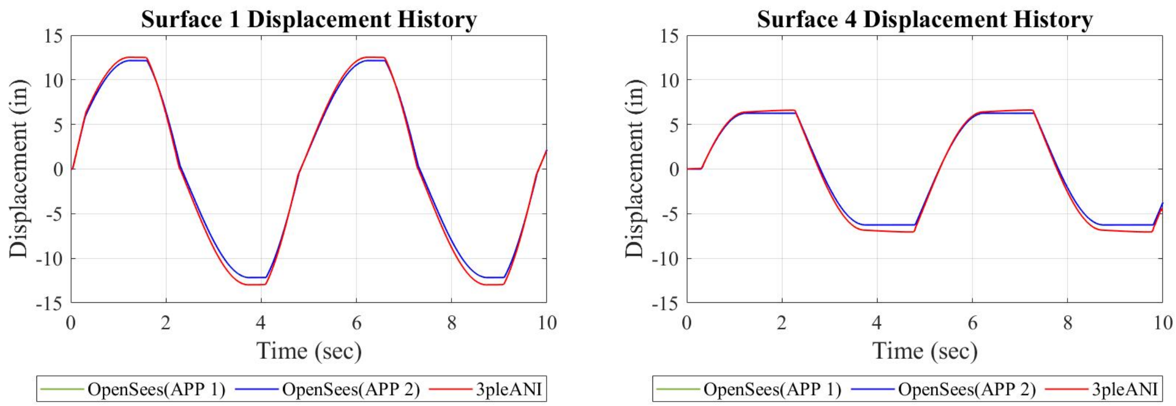

Figure 4-61 Comparison of Displacement Histories on Outer Surfaces (Surfaces 1 and 4)

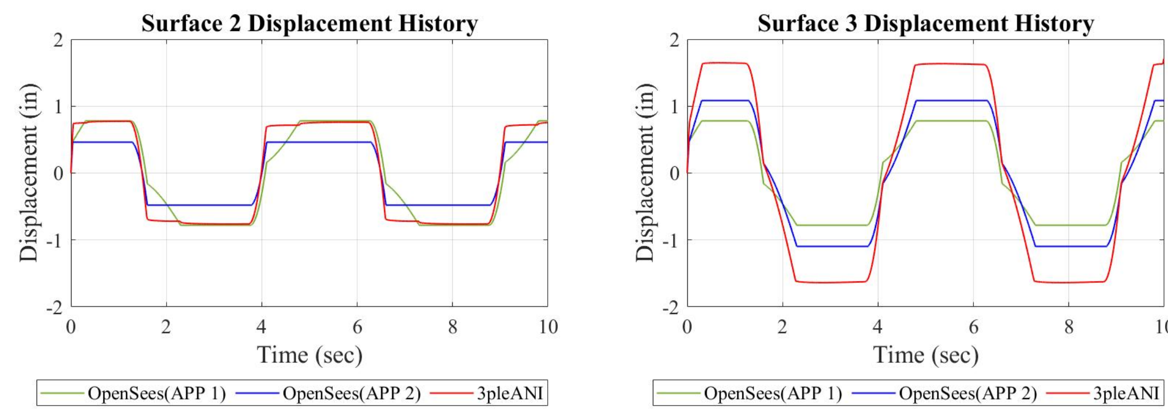

Figure 4-62 Comparison of Displacement Histories on Inner Surfaces (Surfaces 2 and 3)

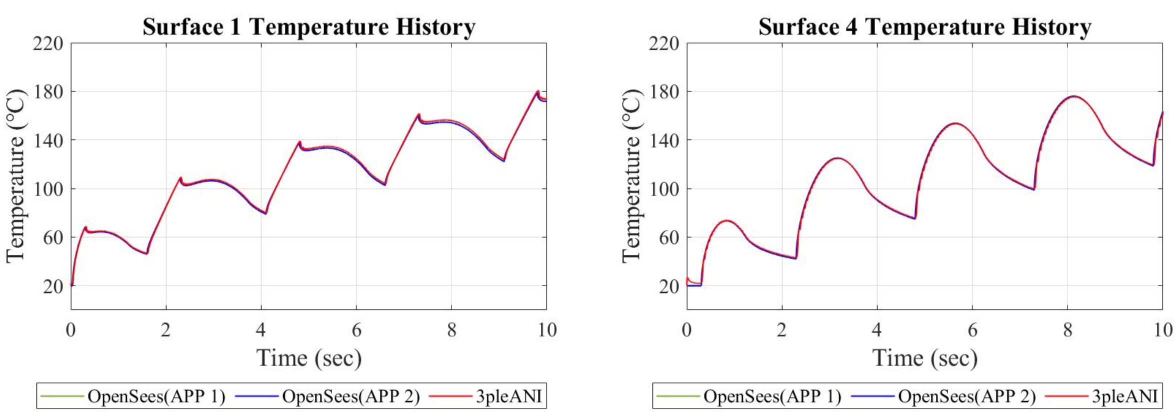

Figure 4-63 Comparison of Temperature Histories on Outer Surfaces (Surfaces 1 and 4)

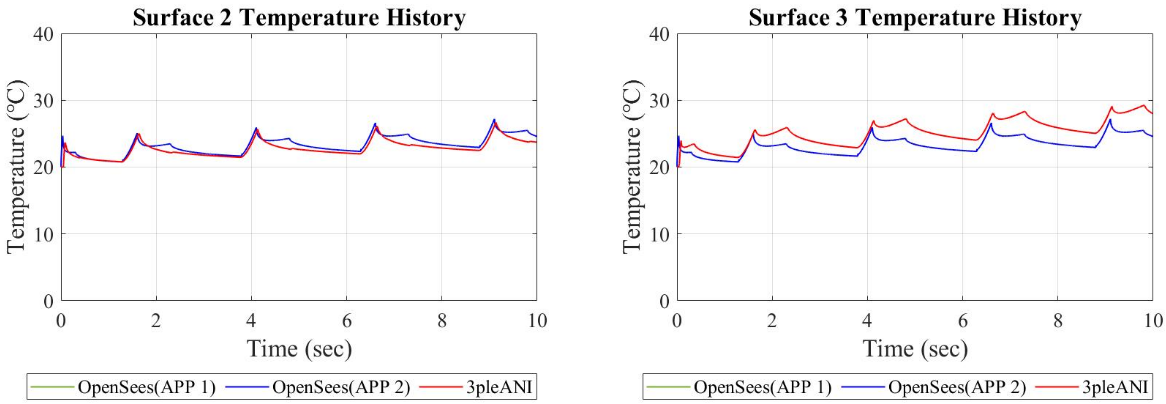

Figure 4-64 Comparison of Temperature Histories on Inner Surfaces (Surfaces 2 and 3)

b. **Case 2: Same Coefficient of Friction for Surfaces 1 and 4**

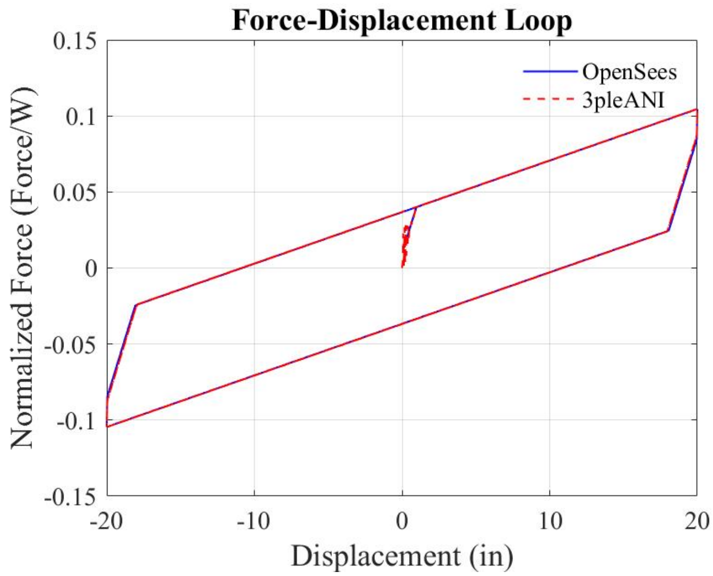

Figure 4-65 Comparison of Force-Displacement Loops

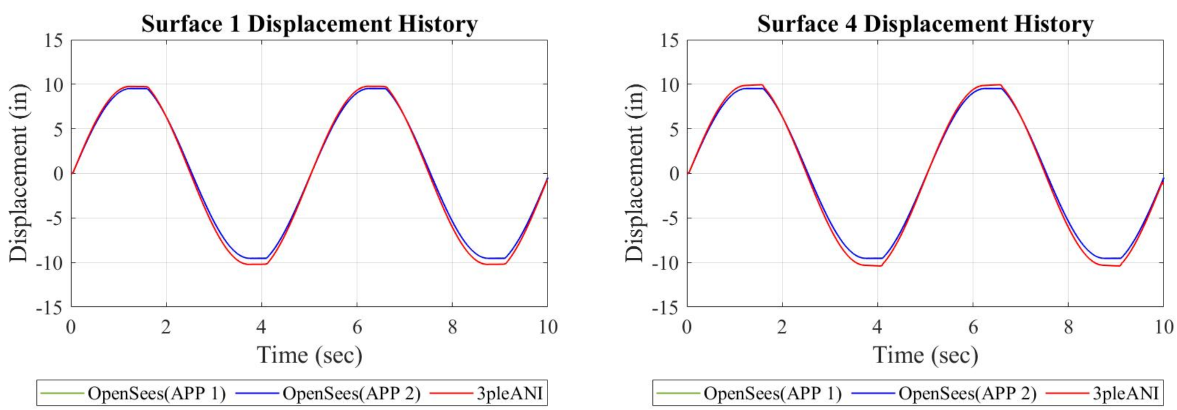

Figure 4-66 Comparison of Displacement Histories on Outer Surfaces (Surface 1 and 4)

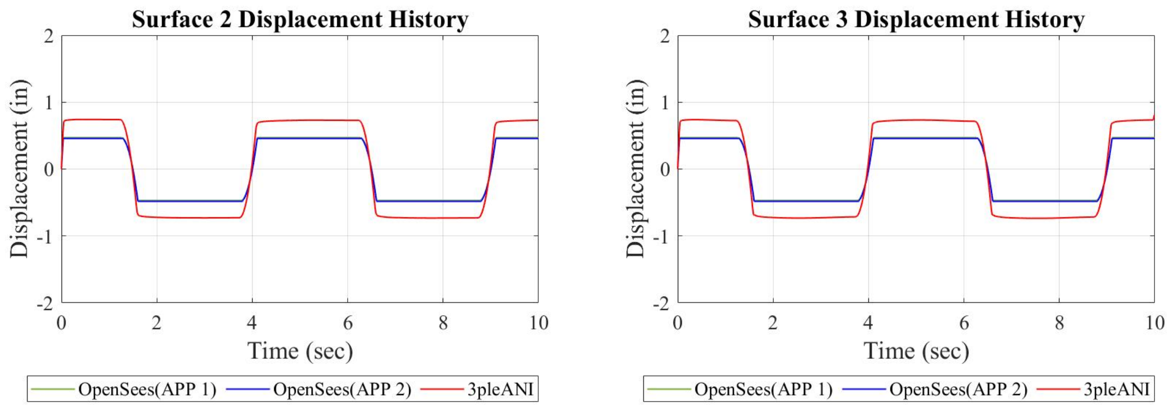

Figure 4-67 Comparison of Displacement Histories on Inner Surfaces (Surface 2 and 3)

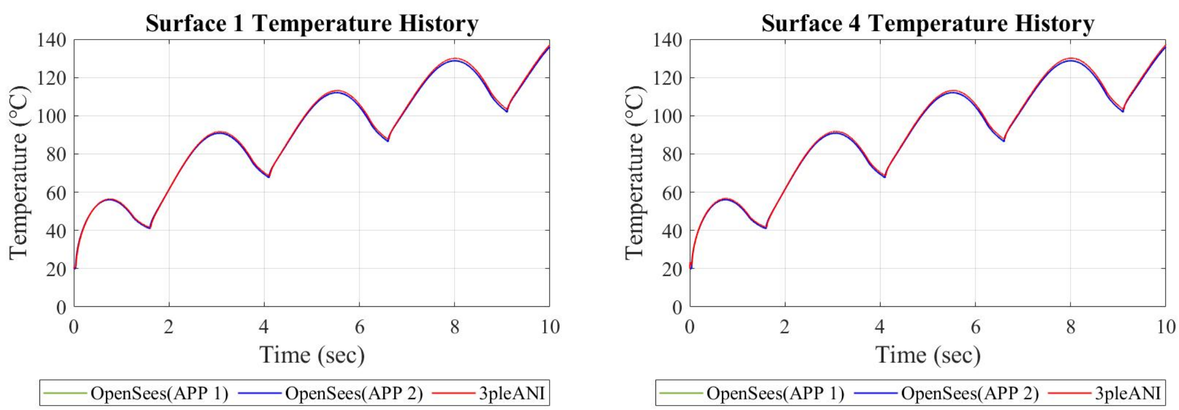

Figure 4-68 Comparison of Temperature Histories on Outer Surfaces (Surfaces 1 and 4)

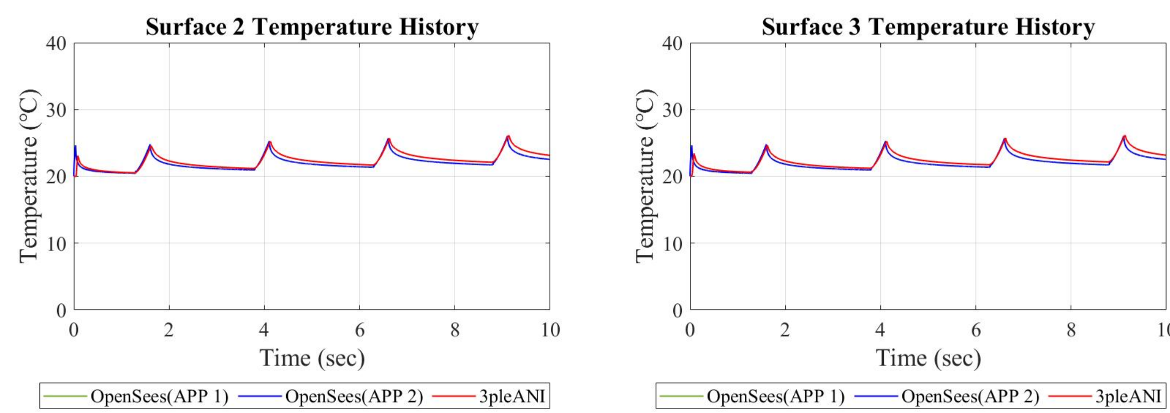

Figure 4-69 Comparison of Temperature Histories on Inner Surfaces (Surfaces 2 and 3)

B) Configuration B

a. Case 1: Different Coefficient of Friction for Surface 1 and 4

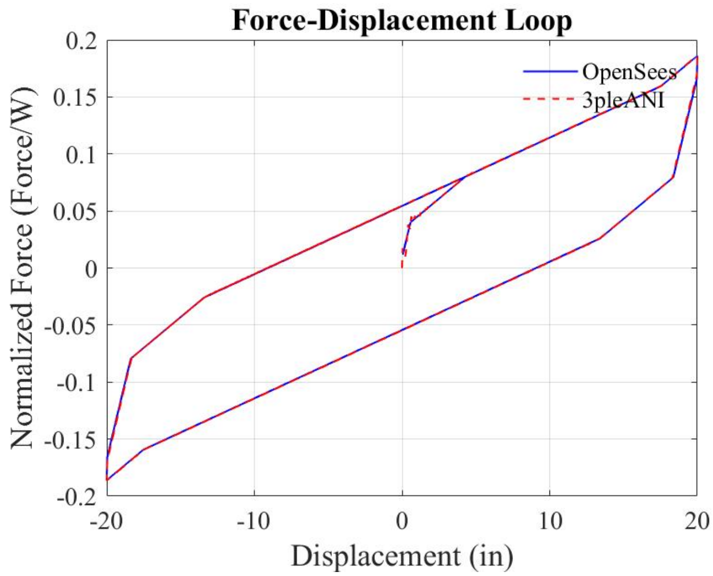

Figure 4-70 Comparison of Force-Displacement Loops

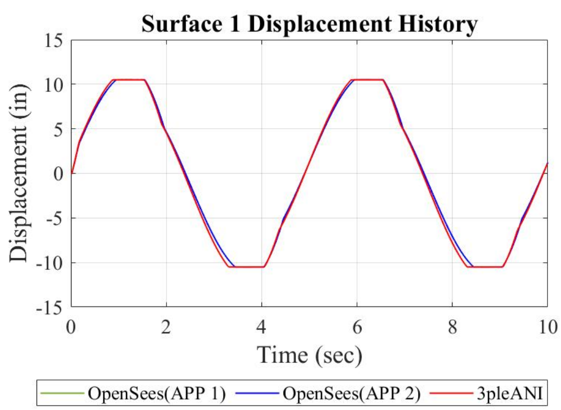

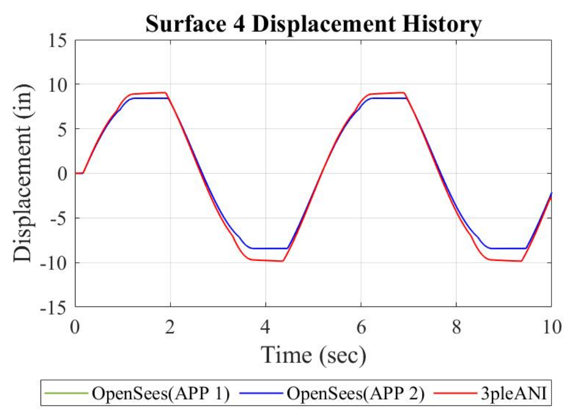

Figure 4-71 Comparison of Displacement Histories on Outer Surfaces (Surfaces 1 and 4)

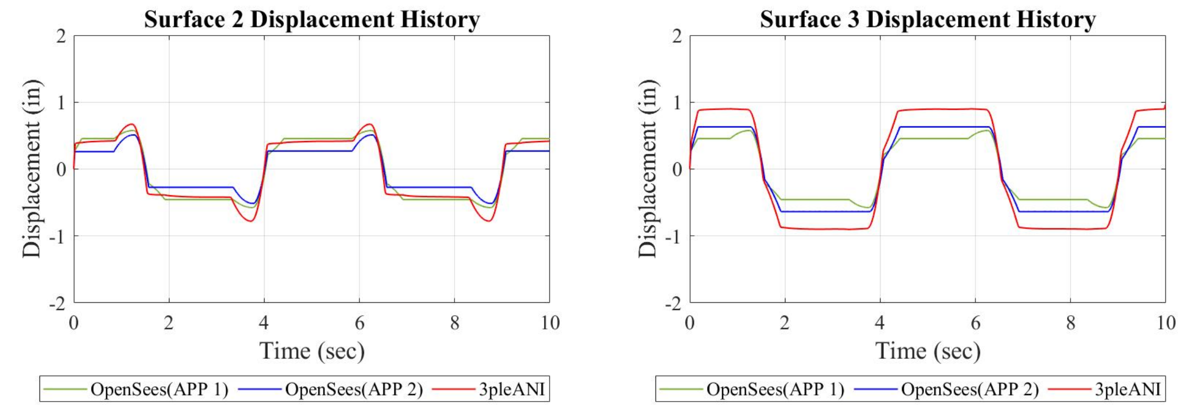

Figure 4-72 Comparison of Displacement Histories on Inner Surfaces (Surfaces 2 and 3)

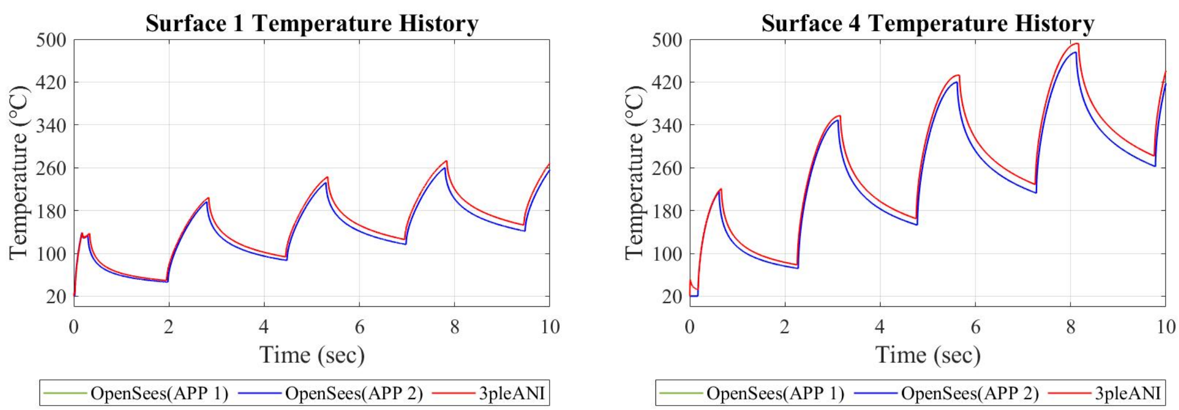

Figure 4-73 Comparison of Temperature Histories on Outer Surfaces (Surfaces 1 and 4)

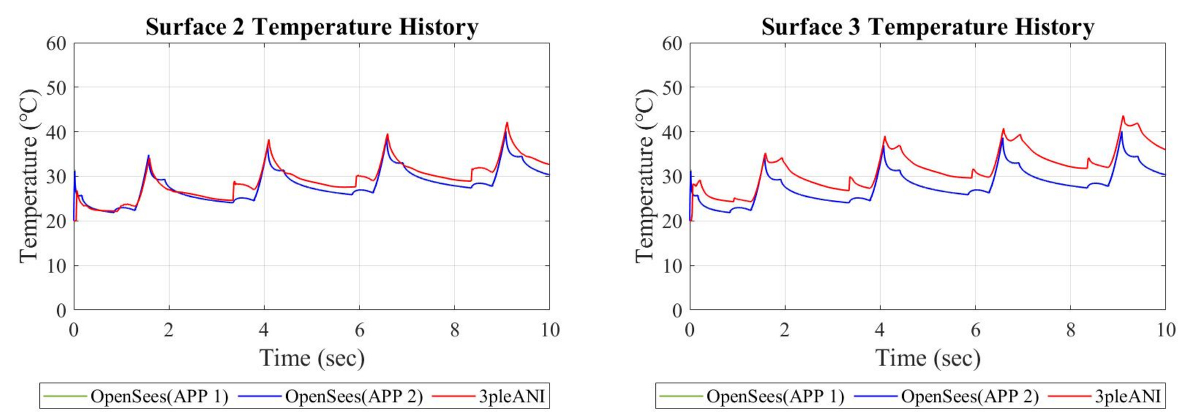

Figure 4-74 Comparison of Temperature Histories on Inner Surfaces (Surfaces 2 and 3)

b. Case 2: Same Coefficient of Friction for Surface 1 and 4

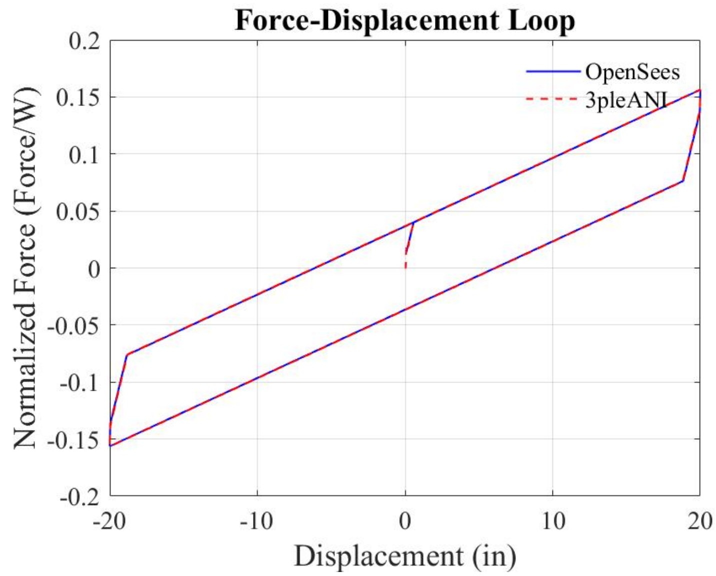

Figure 4-75 Comparison of Force-Displacement Loops

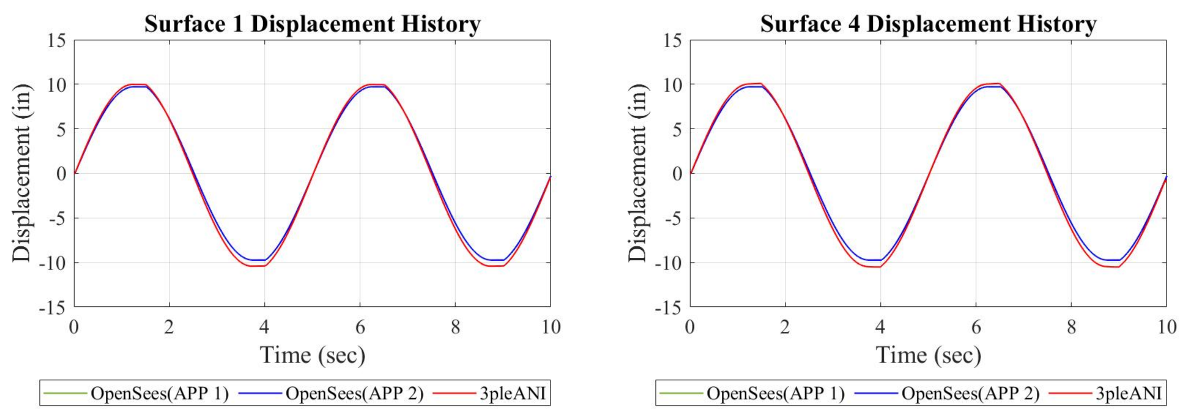

Figure 4-76 Comparison of Displacement Histories on Outer Surfaces (Surfaces 1 and 4)

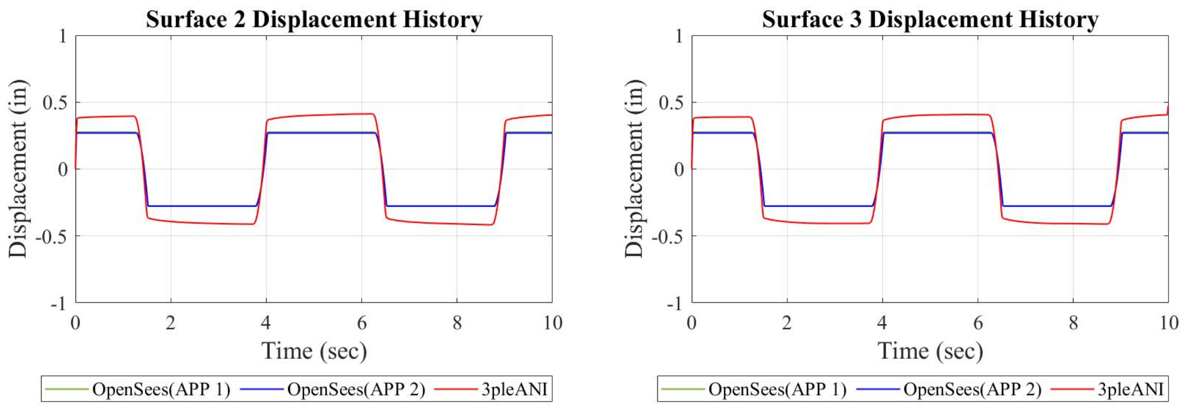

Figure 4-77 Comparison of Displacement Histories on Inner Surfaces (Surfaces 2 and 3)

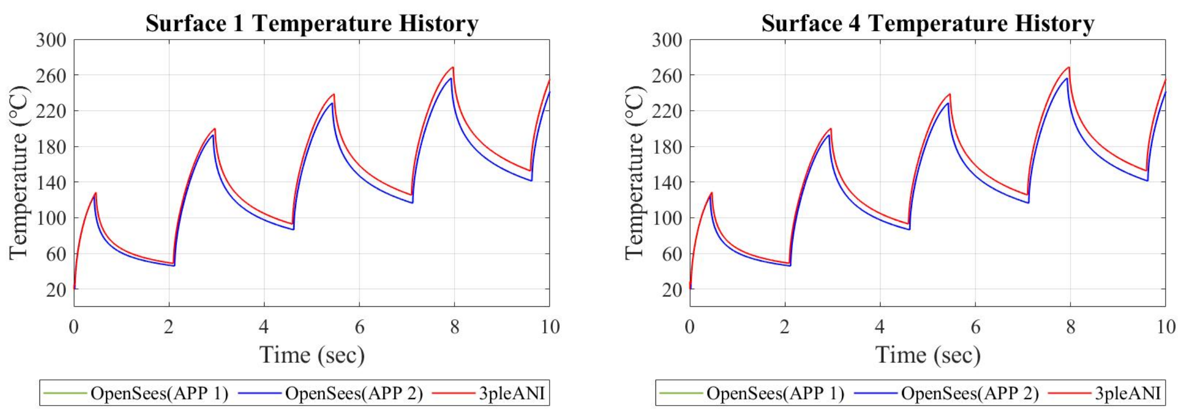

Figure 4-78 Comparison of Temperature Histories on Outer Surfaces (Surfaces 1 and 4)

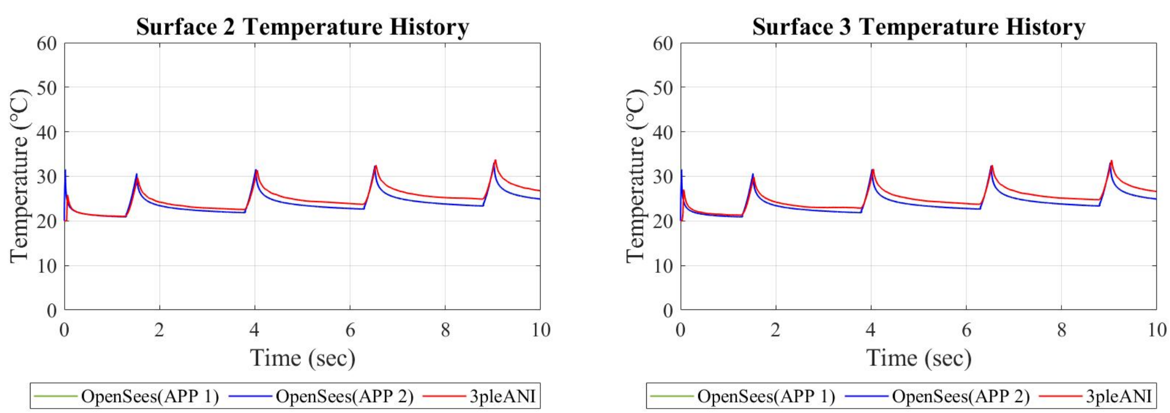

Figure 4-79 Comparison of Temperature Histories on Inner Surfaces (Surfaces 2 and 3)

4.2 Observations and Comments

The following observations are made in the comparison of results in Section 4.

1) The force-displacement loops obtained by the model in program OpenSees and the more advanced model in program 3pleANI are in good agreement.
2) In general, the two models (Approach 1 and Approach 2) in program OpenSees produce nearly identical results for all computed quantities.
3) In general, the two models in program OpenSees produce results on the displacement, velocity and temperature of the main surfaces 1 and 4 that are in good agreement with those produced by the more advanced model in program 3pleANI.
4) In general, the two models in program OpenSees produce results on the displacement, velocity and temperature of the inner surfaces 2 and 3 that differ from those produced by the more advanced model in program 3pleANI. The temperature is underpredicted by the models in program OpenSees. However, the motion and temperature in the inner surfaces are significantly smaller than those of the main surfaces 1 and 4 (e.g., the temperature rise in the outer surfaces is an order of magnitude larger than that in the inner surfaces) so that the effect on the behavior of the bearing is insignificant.

SECTION 5
VERIFICATION EXAMPLES FOR PRESCRIBED BEARING MOTION AND VARIABLE FRICTION

This section presents verification examples when the friction coefficients are temperature-dependent. Dependencies on velocity and pressure are not considered in this section. The geometric properties of the Triple FP bearings are same as those used in Section 4 (Table 4-1) with the exemption that friction is not constant. In the examples of this section, the values of friction coefficient in Table 4-1 represent the reference values, that is, the values at high speed of motion, and at the initiation of motion prior to any increase in temperature of the sliding interfaces. Values of parameters used in the analysis in addition to those below are presented in Appendix A. Moreover, the values of thermal diffusivity and conductivity listed in Table 2-2 are used.

5.1 Examples of Displacement Control Analysis with Temperature-Dependent Friction Coefficient

In program OpenSees, the dependency of the friction coefficients on velocity, pressure and temperature is described by equation (2-7). Parameters k_p and k_v are set equal to unity so that pressure and velocity effects are excluded. The remaining equation describes the dependency of friction on only temperature:

$$\mu_i(T) = \mu_{ref,i} * 0.79 * (0.7^{0.02T_i} + 0.40) \qquad (5-1)$$

In this equation, μ_{ref} is the reference high speed coefficient of friction at the initial (time t=0) temperature $T_0 = 20°\mathrm{C}$ at surface i, and T_i is temperature rise.

In program 3pleANI, the dependency of the friction coefficients on temperature is given by the following exponential form:

$$\mu_i(T) = \mu_{min,i} + (\mu_{max,i} - \mu_{min,i})e^{-h(T_i - T_0)} \qquad (5-2)$$

In this equation, μ_i is friction coefficient at surface i, h is the heating rate parameter, T_i is temperature rise, T_0 is initial temperature, $\mu_{max,i}$ is the friction coefficient at initial temperature, $\mu_{min,i}$ is minimum value of friction coefficient at a large temperature. For the examples of this section, $\mu_{min,i} = \mu_{max,i}/2$ and parameter h=0.01/°C are used.

Moreover, the values of the coefficient of friction in the Sarlis and Constantinou (2013, 2016) model differ from those of the Fenz and Constantinou (2008a-d) model which is used in program OpenSees. In general, the two values are identical when the sliding interfaces have infinitely large radii of curvature. Otherwise, they are related through the geometry of the sliding surfaces by the following equations:

$$\mu_{ref,2} = \mu_{max,2} \frac{R_2}{R_{eff2}} \qquad (5-3)$$

$$\mu_{ref,1} = \frac{\mu_{max,1} R_1 - \mu_{max,2} R_2}{R_{eff1} - R_{eff2}} \qquad (5-4)$$

$$\mu_{ref,4} = \frac{\mu_{max,4} R_4 - \mu_{max,2} R_2}{R_{eff1} - R_{eff2}} \qquad (5-5)$$

In these equations, $\mu_{ref,i}$ is the friction coefficient used in OpenSees, $\mu_{max,i}$ is the friction coefficient used in 3pleANI, R_i is the radius of curvature, R_{effi} is effective radius of curvature which is equal to $R_{effi} = R_i - h_i$, and subscript i indicates sliding surface i=1 to 4. Based on the geometric parameters of the Triple FP bearing configuration A listed in Table 4-1, the values of the friction coefficients, $\mu_{ref,i}$ and $\mu_{max,i}$, are listed in Table 5-1 and plotted in Figure 5-1. Note that for comparison of the two models of friction-temperature dependency, the values of the Sarlis and Constantinou (2013, 2016) were adjusted per equations (5-3) to (5-5) and shown in Figure 5-1 for an initial temperature of 20ºC.

Table 5-1 Friction Coefficients used in OpenSees and 3pleANI

Friction Coefficient	Value of $\mu_{ref,i}$ in OpenSees	Value of $\mu_{max,i}$ in 3pleANI
$\boldsymbol{\mu_{ref1}}$	0.04	0.03484
$\boldsymbol{\mu_{ref4}}$	0.08	0.06869
$\boldsymbol{\mu_{ref2} = \mu_{ref3}}$	0.01	0.00705

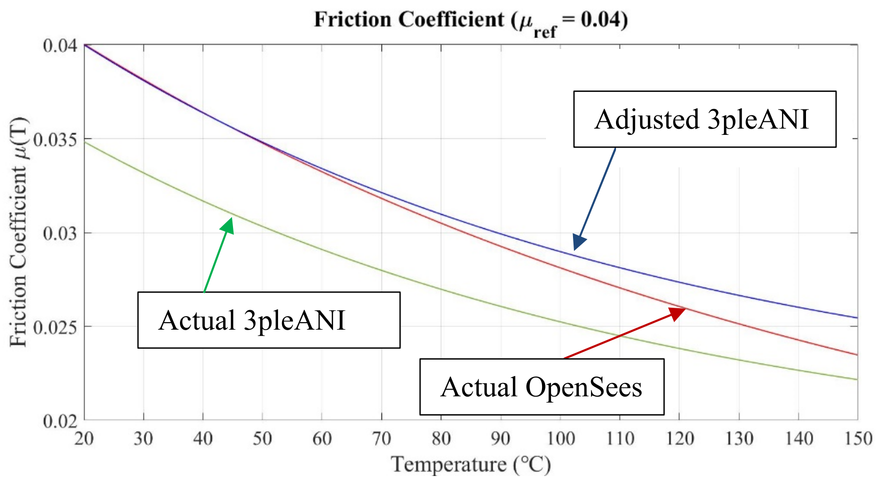

Figure 5-1 Friction-Temperature Dependency in OpenSees and 3pleANI

The two friction models differ but the differences are small in the range of 20℃ to about 100℃ so results of the two programs in this range of temperatures should be comparable.

Results by the two programs are presented and compared for prescribed conditions of motion of the top of the bearing. Approach 1 has been used in program OpenSees. These results include force-displacement loops, and displacement, velocity and temperature histories at the four sliding interfaces. Also, results are presented in the form of histories of the coefficient of friction. In the figures that follow, results of program OpenSees are in color blue and results of program 3pleANI are in color red. Note that in the comparison of histories of the friction coefficient, the two programs produce comparable results but the values differ based on the interpretation provided above and demonstrated in the results of Table 5-1 and Figure 5-1.

5.1.1 Harmonic Motion: Amplitude of 20in and Period of 20sec

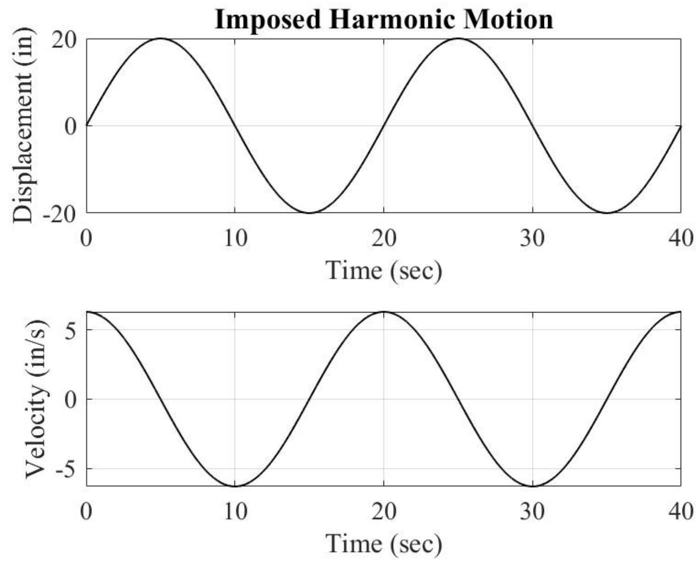

Figure 5-2 Imposed Harmonic Motion (Amplitude: 20in, Period: 20sec)

A) Configuration A

a. Case 1: Different Coefficient of Friction for Surfaces 1 and 4

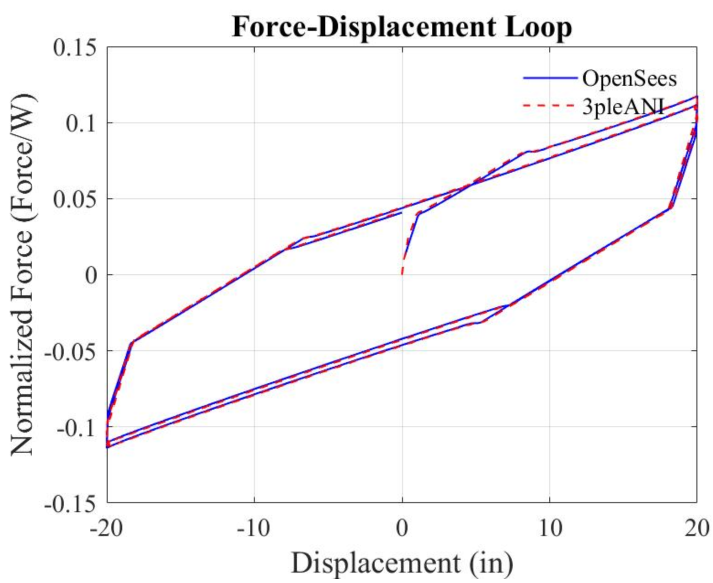

Figure 5-3 Comparison of Force-Displacement Loops

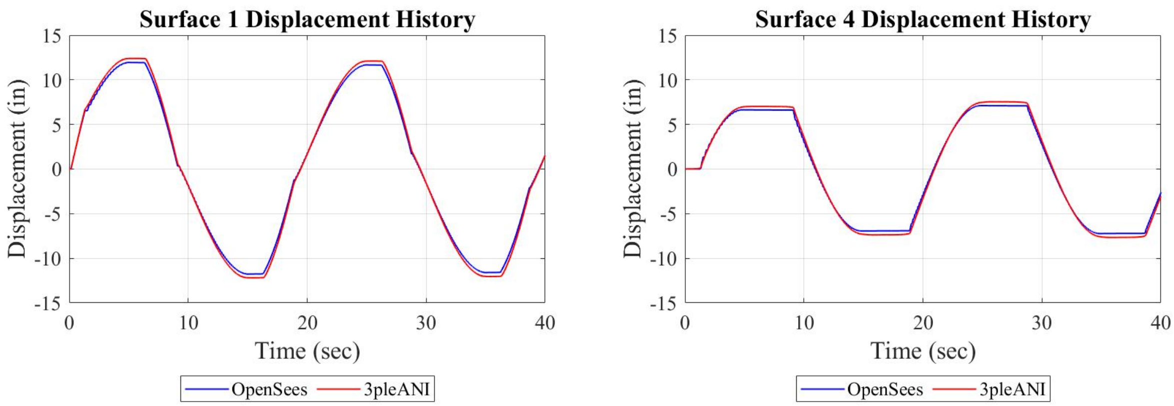

Figure 5-4 Comparison of Displacement Histories on Outer Surfaces (Surfaces 1 and 4)

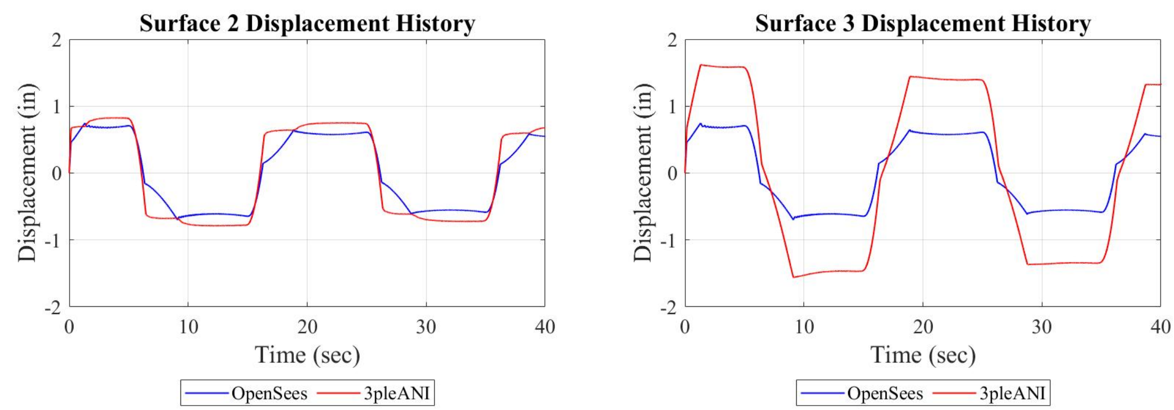

Figure 5-5 Comparison of Displacement Histories on Inner Surfaces (Surfaces 2 and 3)

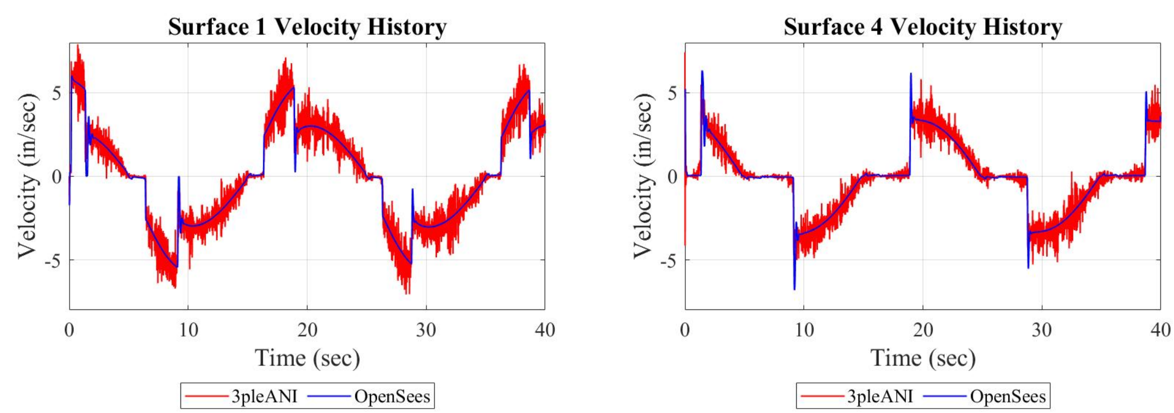

Figure 5-6 Comparison of Velocity Histories on Outer Surfaces (Surfaces 1 and 4)

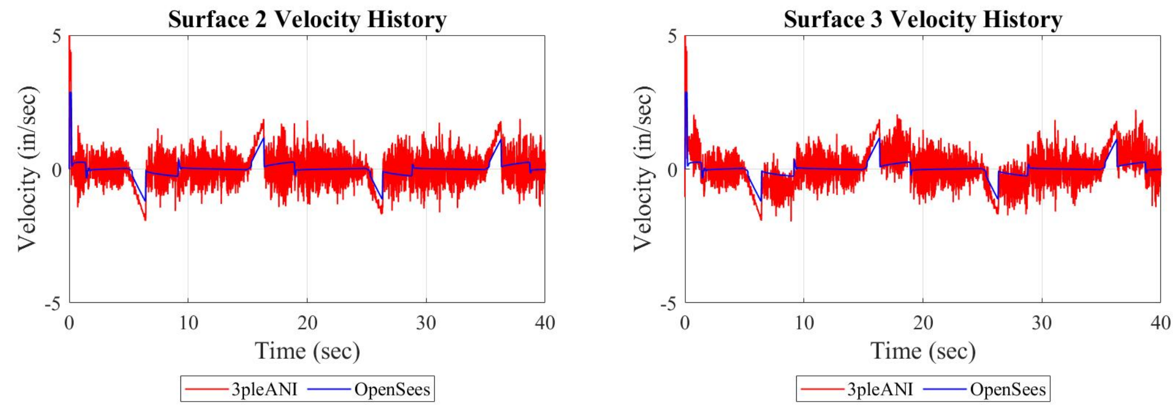

Figure 5-7 Comparison of Velocity Histories on Inner Surfaces (Surfaces 2 and 3)

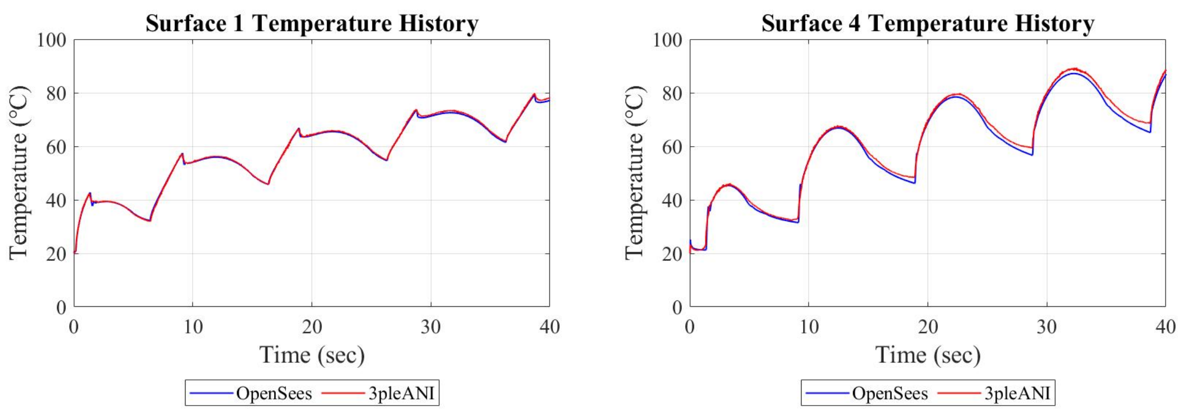

Figure 5-8 Comparison of Temperature Histories on Outer Surfaces (Surfaces 1 and 4)

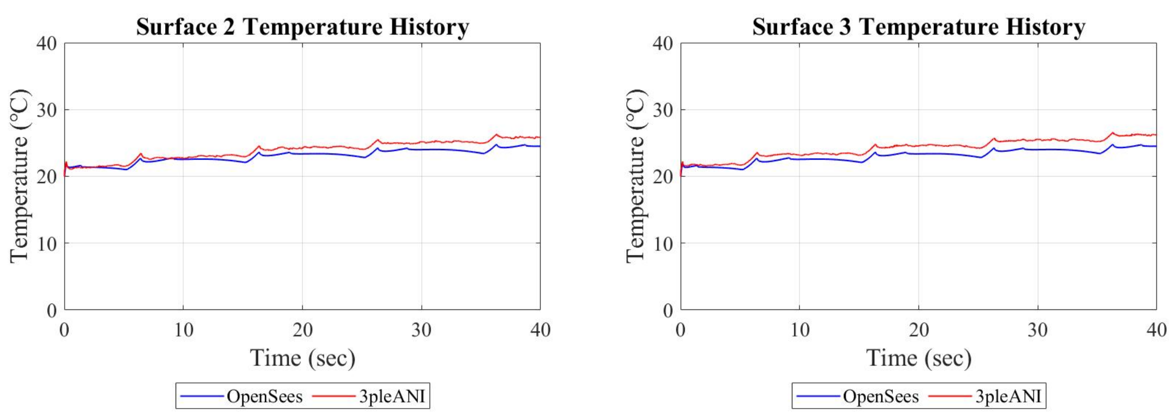

Figure 5-9 Comparison of Temperature Histories on Inner Surfaces (Surfaces 2 and 3)

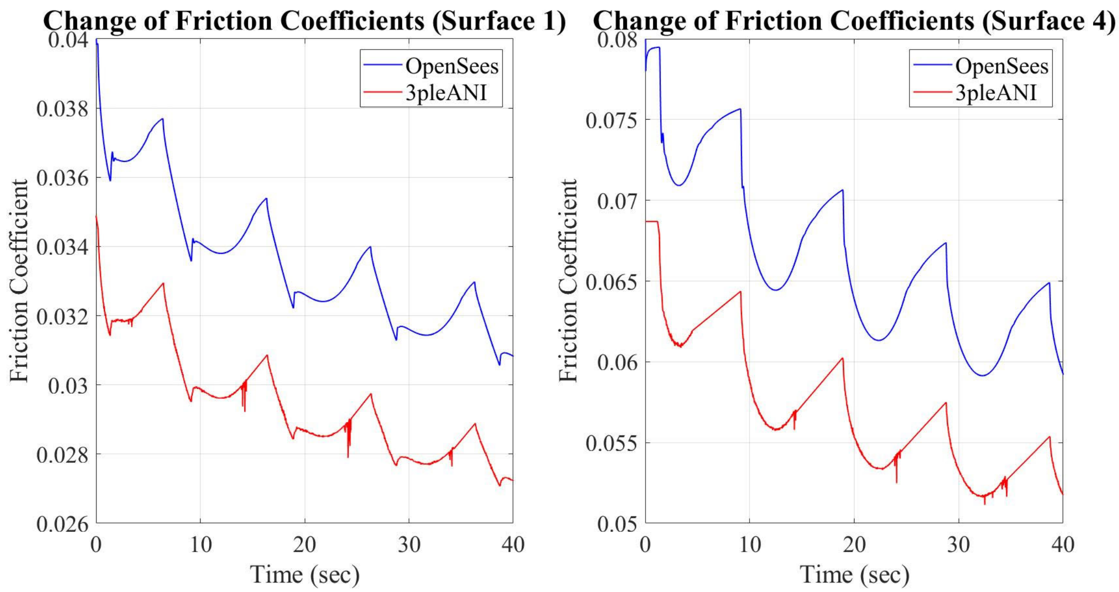

Figure 5-10 Histories of Friction Coefficients on Outer Surfaces (note that the friction coefficient values are not the same but related through equations 5-3 to 5-5)

b. Case 2: Same Coefficient of Friction for Surfaces 1 and 4

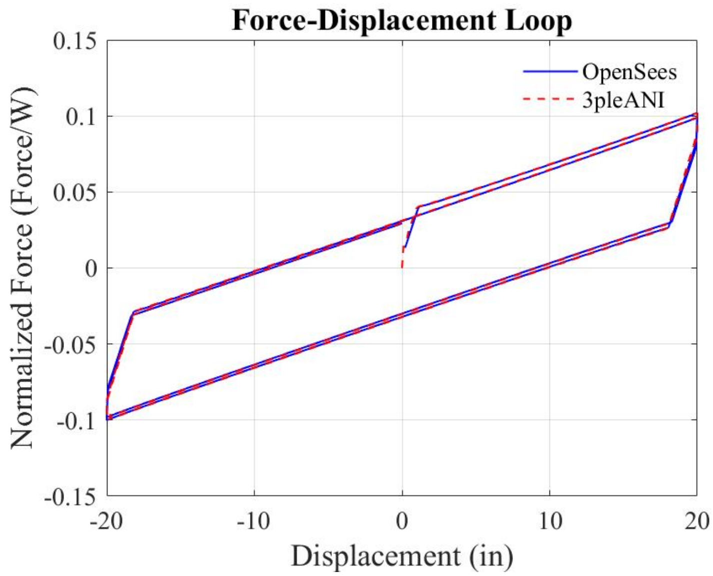

Figure 5-11 Comparison of Force-Displacement Loops

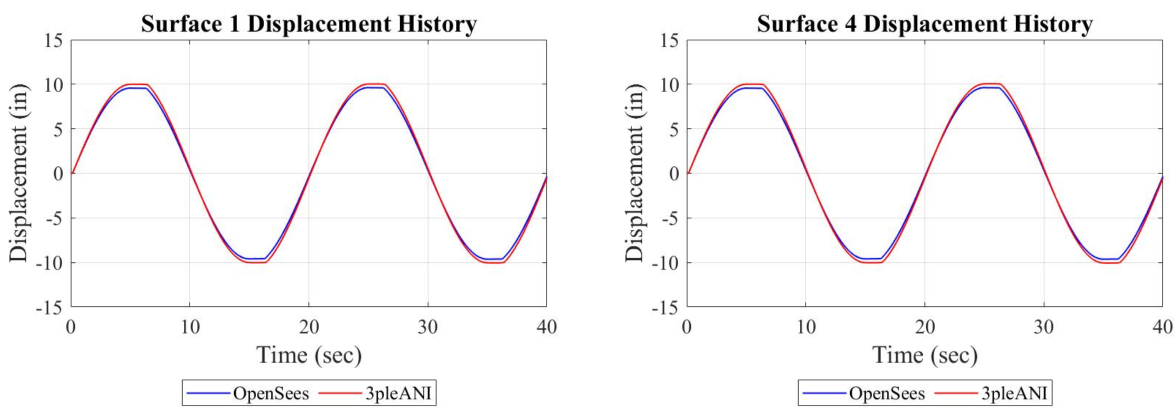

Figure 5-12 Comparison of Displacement Histories on Outer Surfaces (Surfaces 1 and 4)

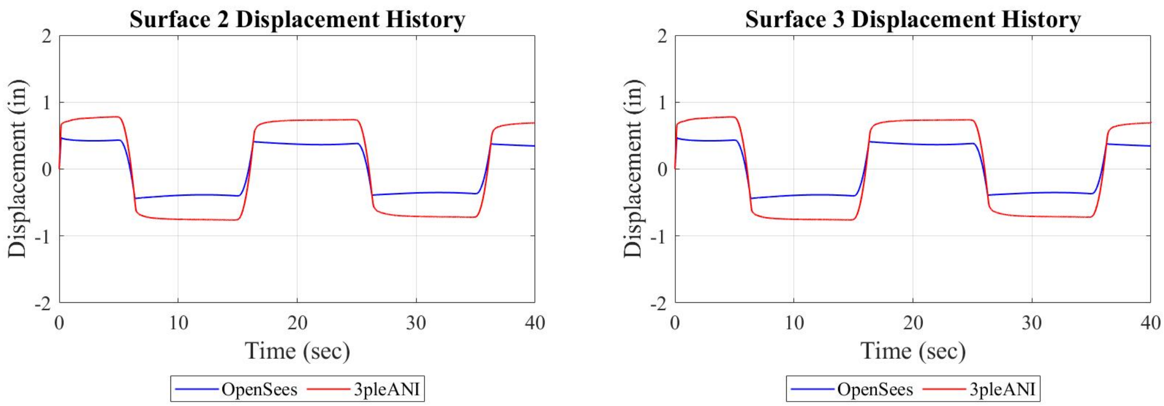

Figure 5-13 Comparison of Displacement Histories on Inner Surfaces (Surfaces 2 and 3)

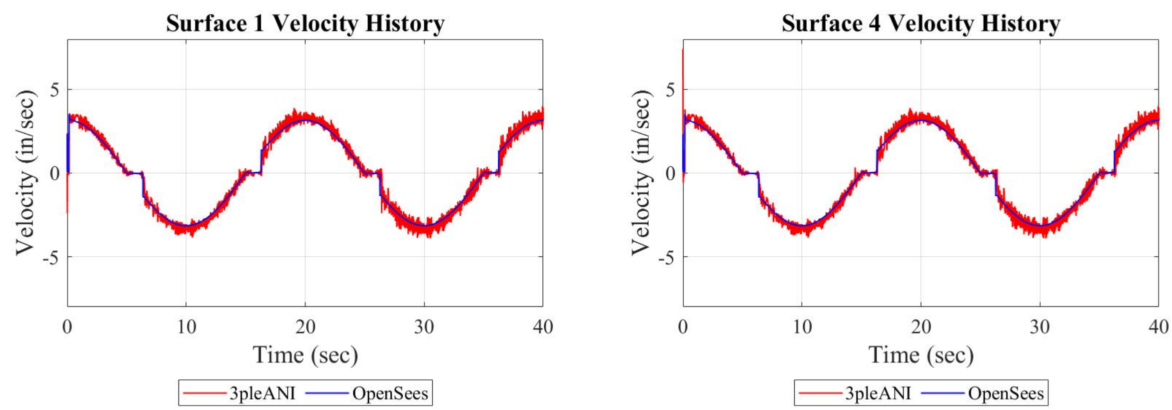

Figure 5-14 Comparison of Velocity Histories on Outer Surfaces (Surfaces 1 and 4)

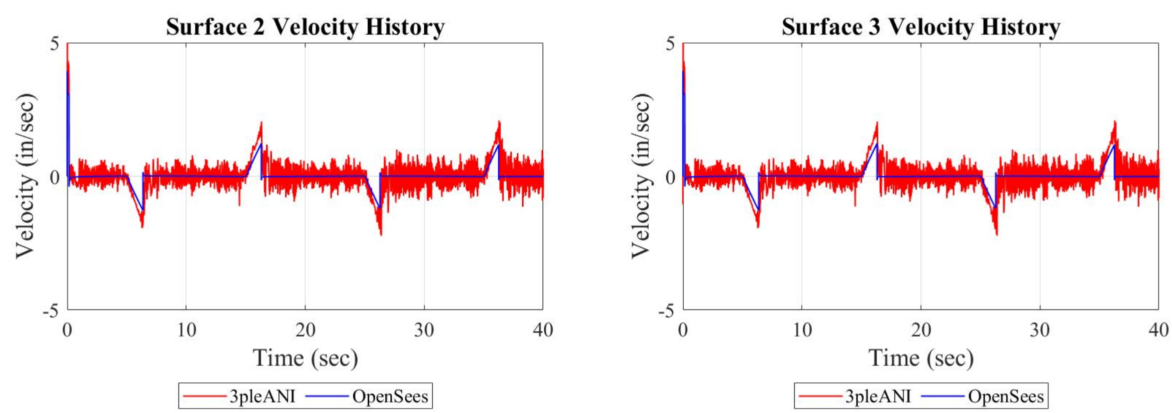

Figure 5-15 Comparison of Velocity Histories on Inner Surfaces (Surface 2 and 3)

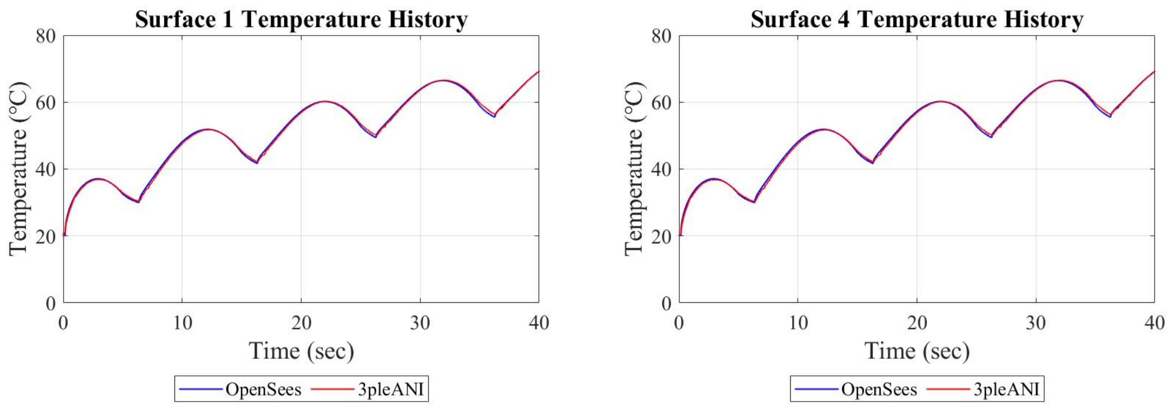

Figure 5-16 Comparison of Temperature Histories on Outer Surfaces (Surfaces 1 and 4)

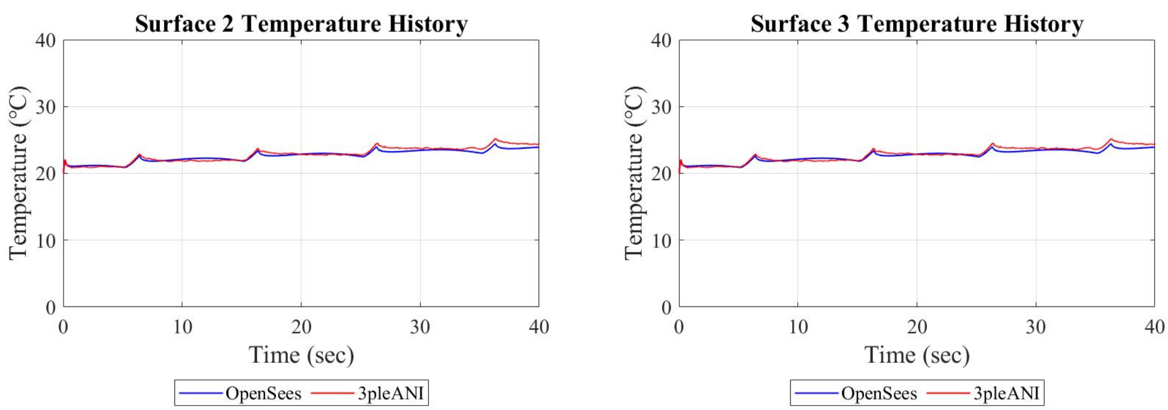

Figure 5-17 Comparison of Temperature Histories on Inner Surfaces (Surfaces 2 and 3)

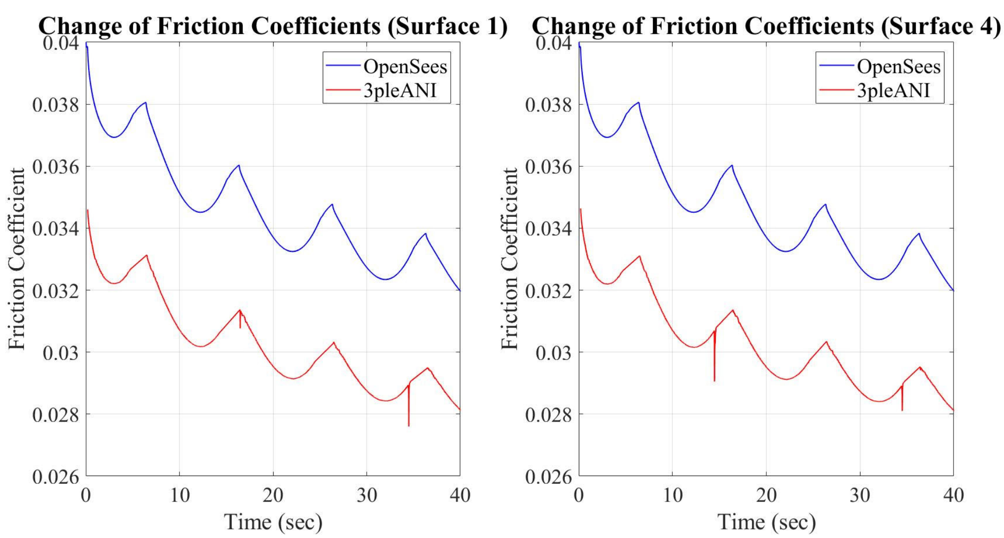

Figure 5-18 Histories of Friction Coefficients on Outer Surfaces (note that the friction coefficient values are not the same but related through equations 5-3 to 5-5)

B) Configuration B

a. Case 1: Different Coefficient of Friction for Surfaces 1 and 4

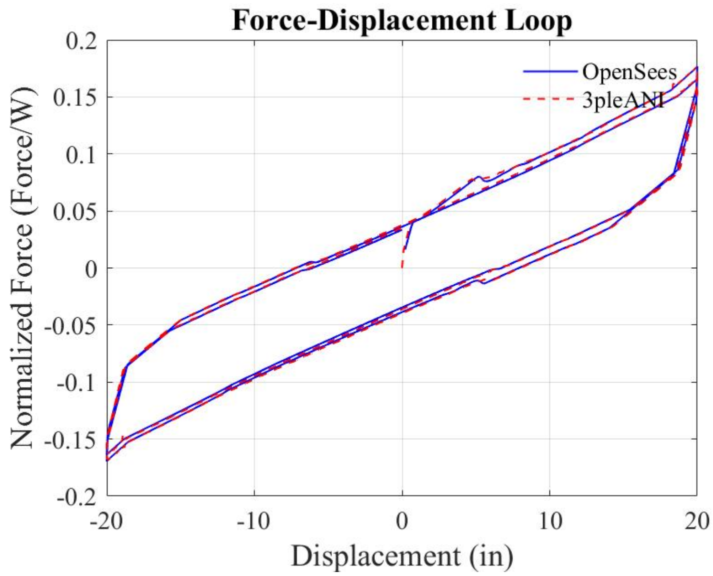

Figure 5-19 Comparison of Force-Displacement Loops

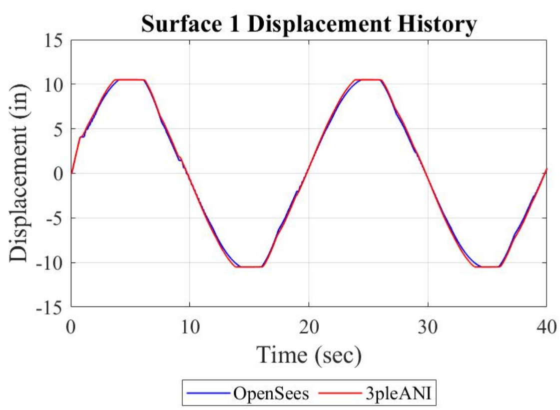

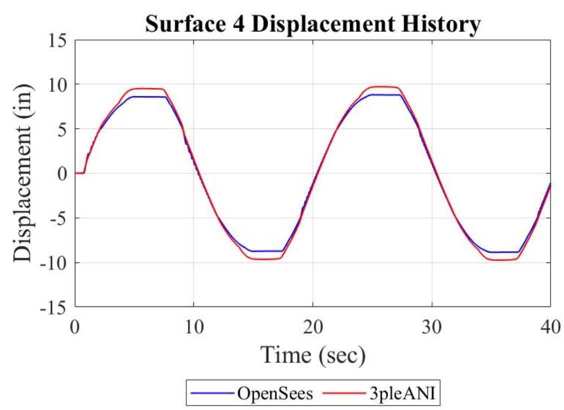

Figure 5-20 Comparison of Displacement Histories on Outer Surfaces (Surfaces 1 and 4)

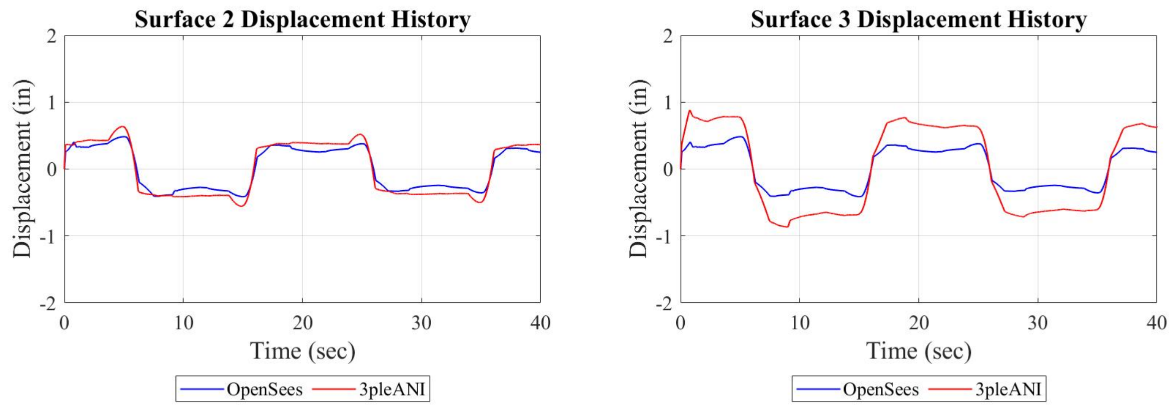

Figure 5-21 Comparison of Displacement Histories on Inner Surfaces (Surfaces 2 and 3)

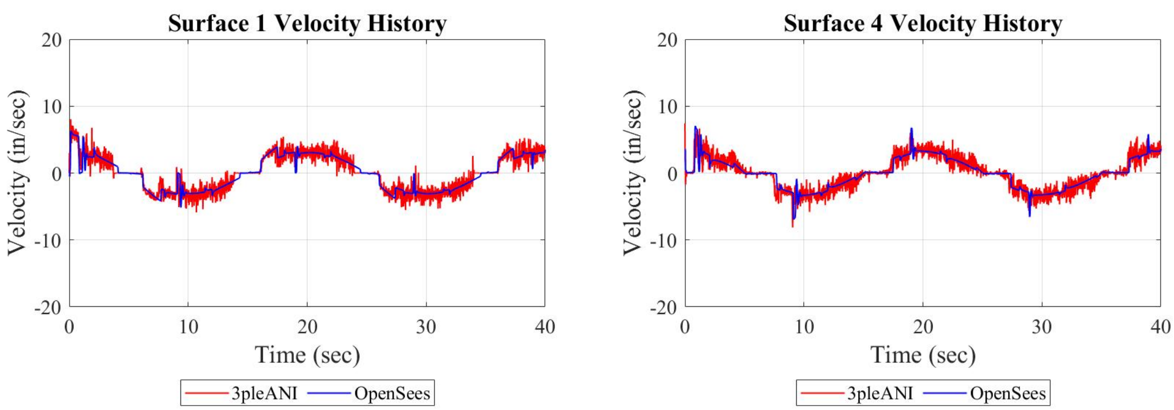

Figure 5-22 Comparison of Velocity Histories on Outer Surfaces (Surfaces 1 and 4)

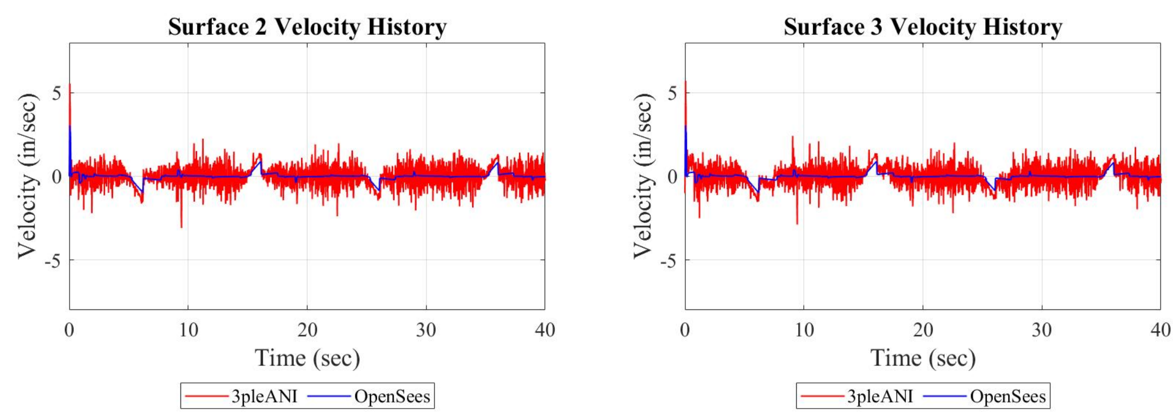

Figure 5-23 Comparison of Velocity Histories on Inner Surfaces (Surfaces 2 and 3)

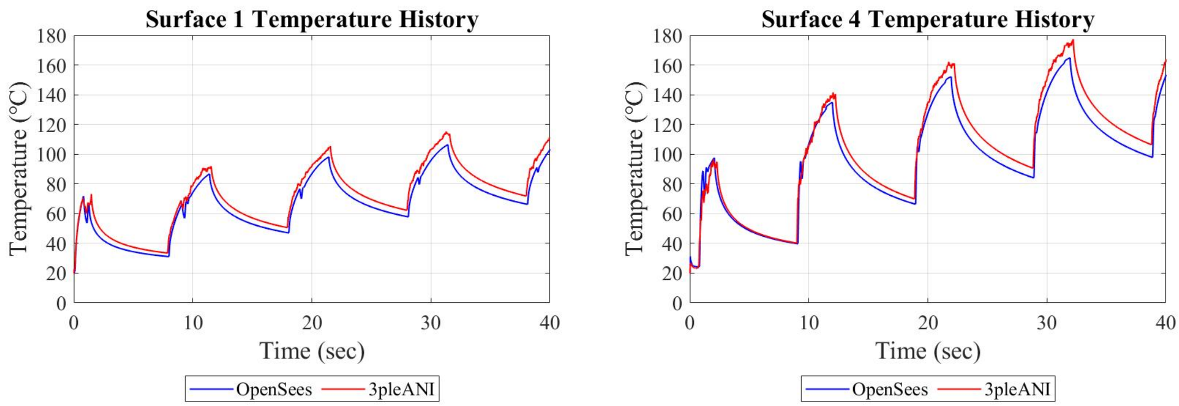

Figure 5-24 Comparison of Temperature Histories on Outer Surfaces (Surfaces 1 and 4)

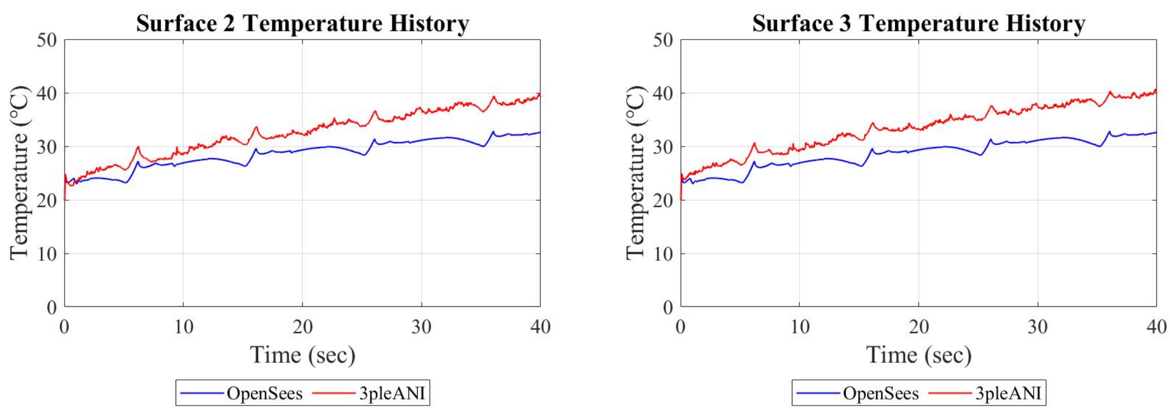

Figure 5-25 Comparison of Temperature Histories on Inner Surfaces (Surfaces 2 and 3)

b. Case 2: Same Coefficient of Friction for Surfaces 1 and 4

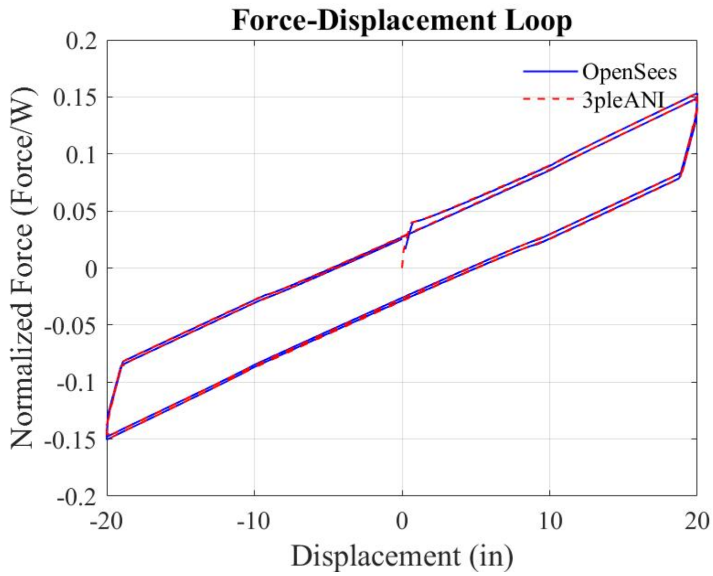

Figure 5-26 Comparison of Force-Displacement Loops

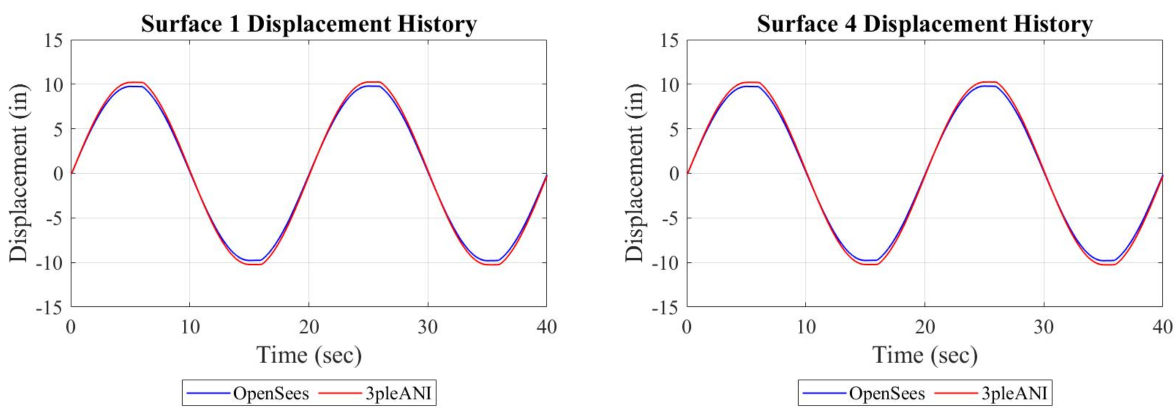

Figure 5-27 Comparison of Displacement Histories on Outer Surfaces (Surfaces 1 and 4)

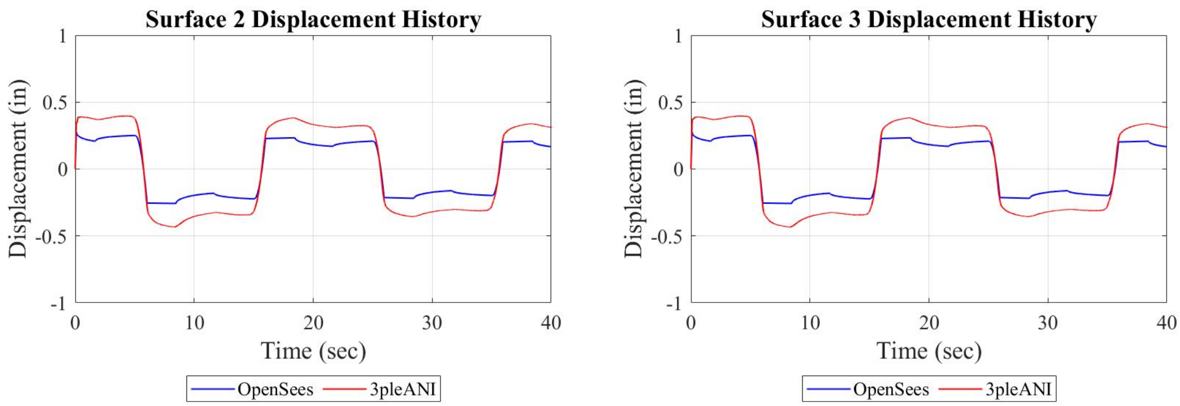

Figure 5-28 Comparison of Displacement Histories on Inner Surfaces (Surfaces 2 and 3)

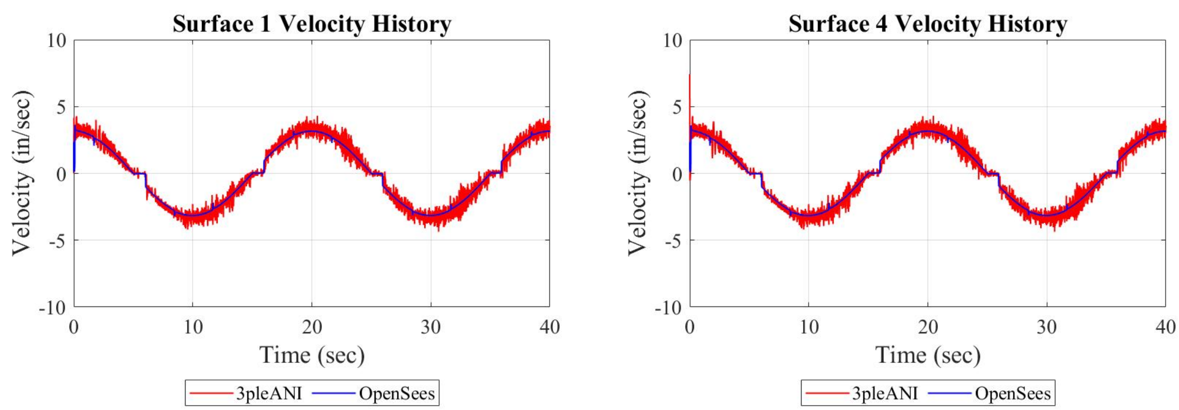

Figure 5-29 Comparison of Velocity Histories on Outer Surfaces (Surfaces 1 and 4)

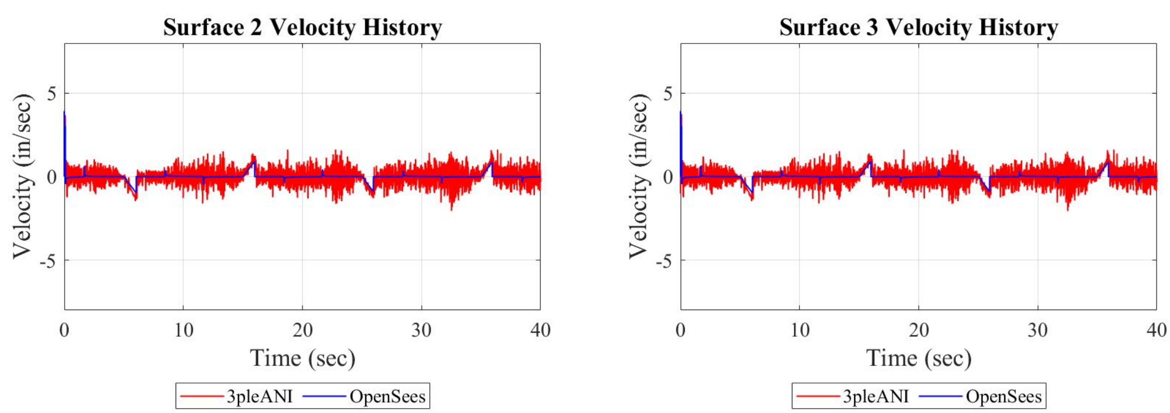

Figure 5-30 Comparison of Velocity Histories on Inner Surfaces (Surfaces 2 and 3)

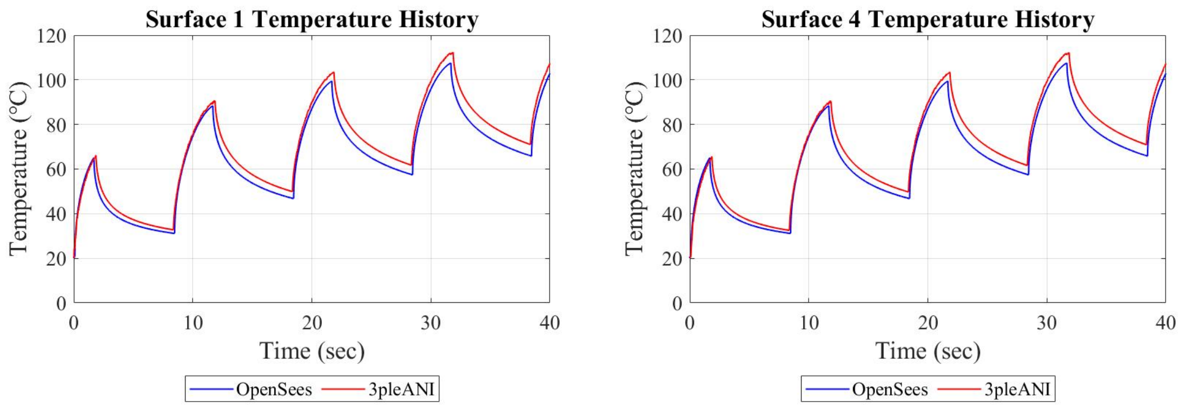

Figure 5-31 Comparison of Temperature Histories on Outer Surfaces (Surfaces 1 and 4)

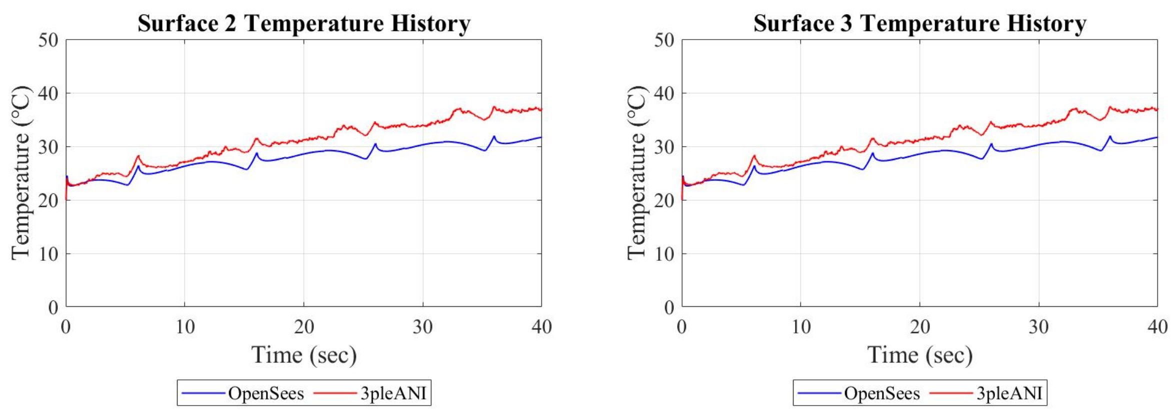

Figure 5-32 Comparison of Temperature Histories on Inner Surfaces (Surfaces 2 and 3)

5.1.2 Harmonic Motion: Amplitude of 22in and Period of 10sec

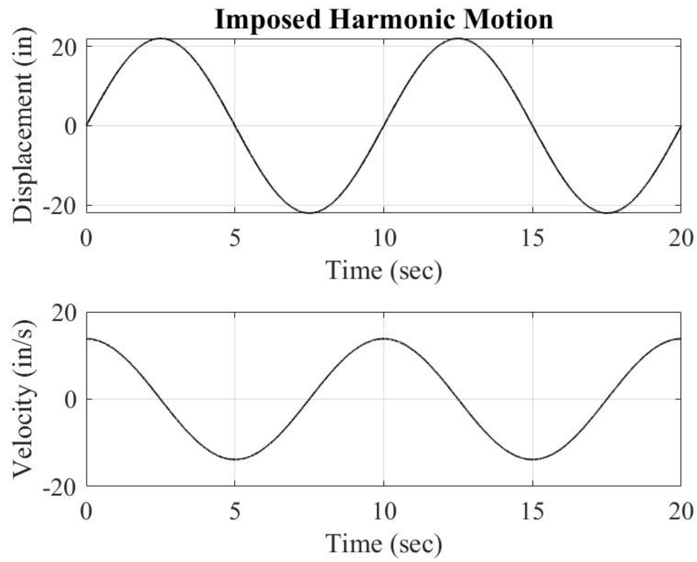

Figure 5-33 Imposed Harmonic Motion (Amplitude: 22in, Period: 10sec)

A) Configuration A

a. Case 1: Different Coefficient of Friction for Surfaces 1 and 4

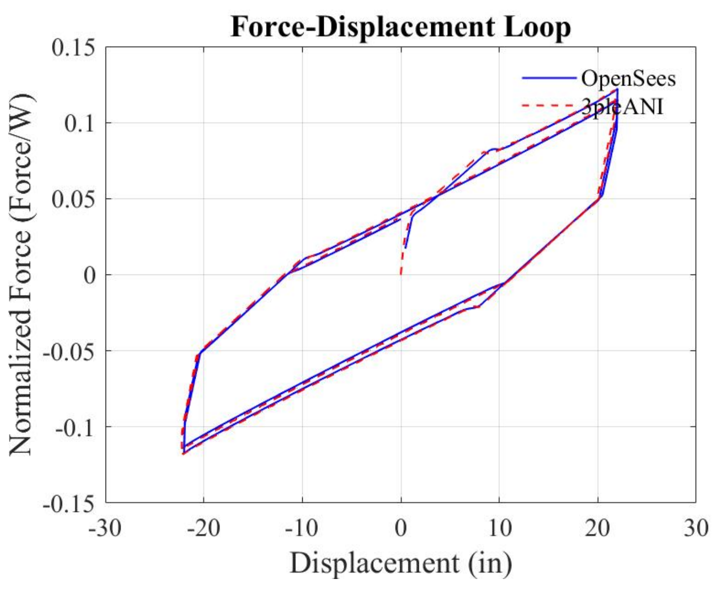

Figure 5-34 Comparison of Force-Displacement Loops

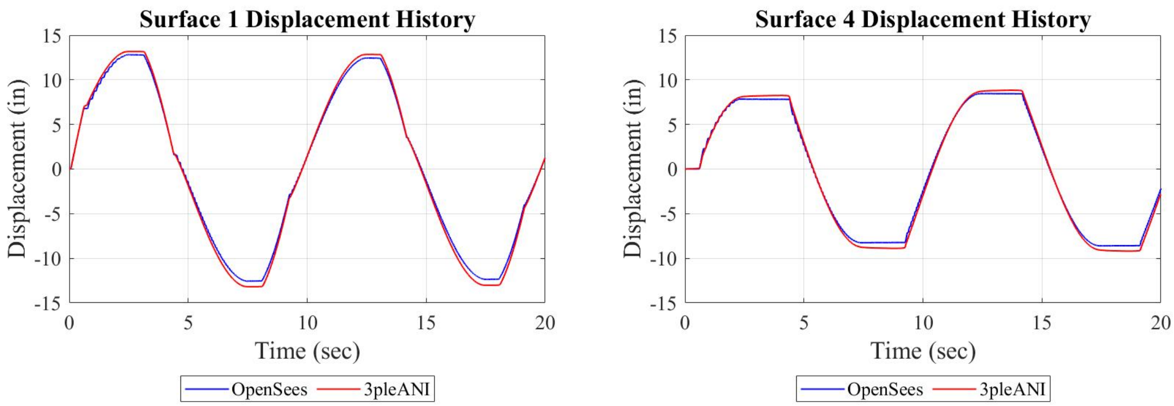

Figure 5-35 Comparison of Displacement Histories on Outer Surfaces (Surfaces 1 and 4)

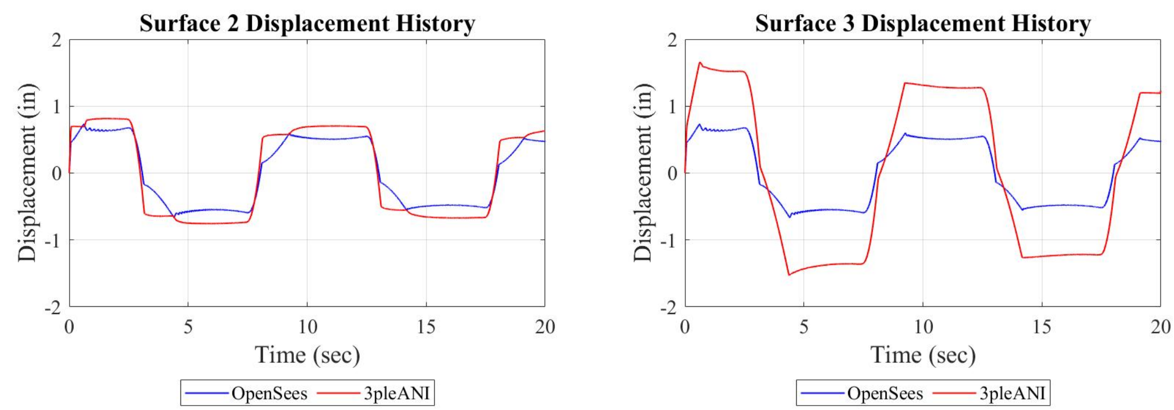

Figure 5-36 Comparison of Displacement Histories on Inner Surfaces (Surfaces 2 and 3)

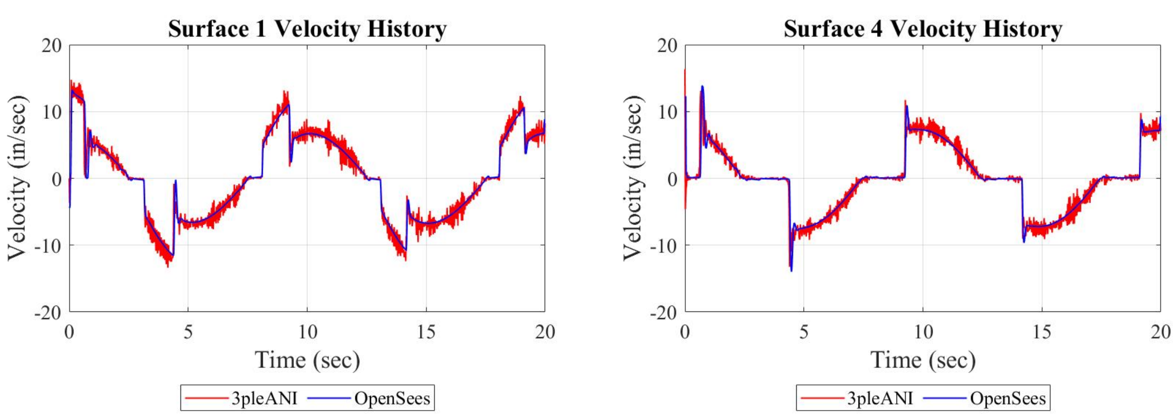

Figure 5-37 Comparison of Velocity Histories on Outer Surfaces (Surfaces 1 and 4)

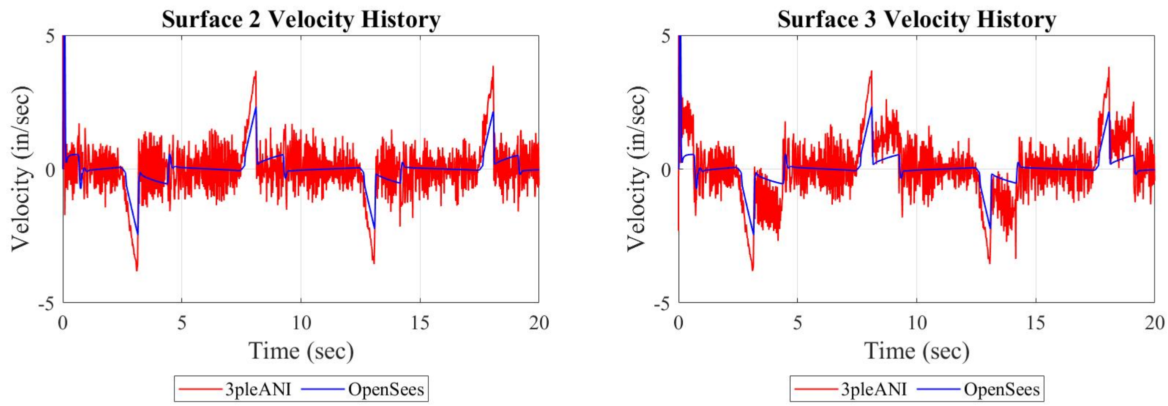

Figure 5-38 Comparison of Velocity Histories on Inner Surfaces (Surfaces 2 and 3)

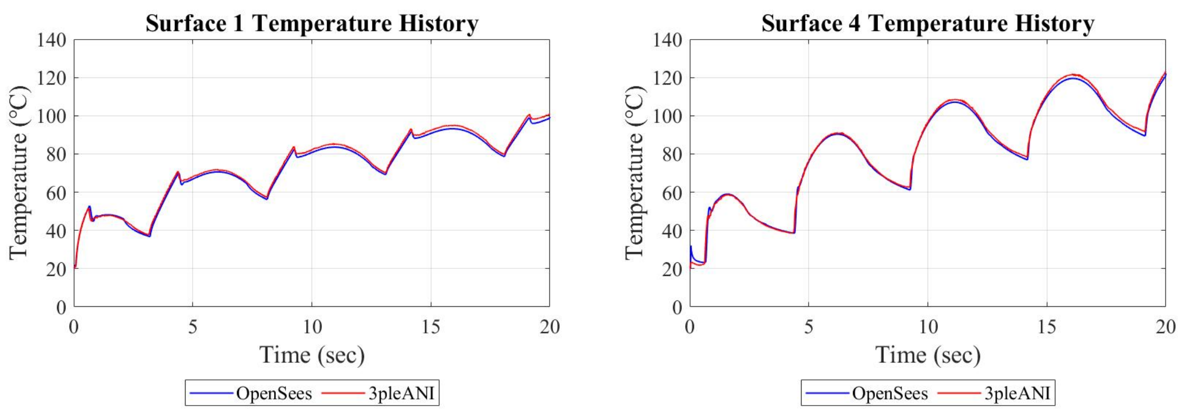

Figure 5-39 Comparison of Temperature Histories on Outer Surfaces (Surfaces 1 and 4)

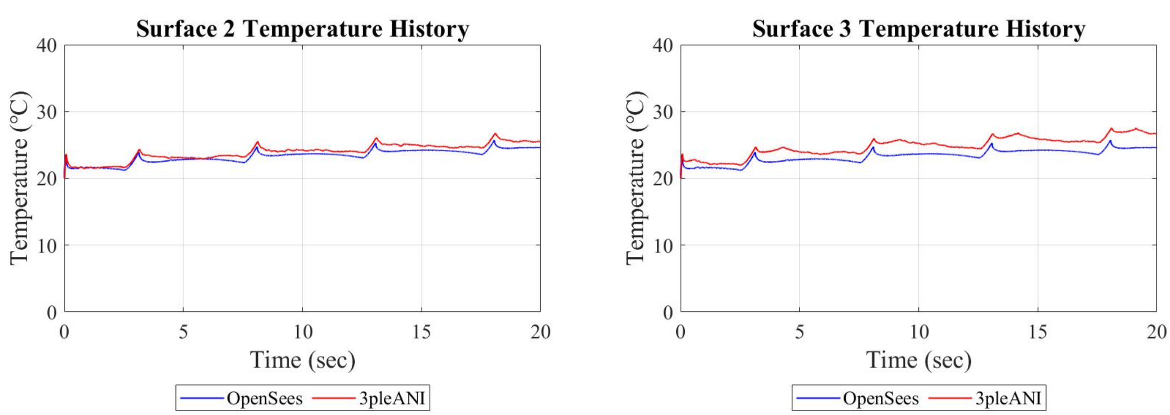

Figure 5-40 Comparison of Temperature Histories on Inner Surfaces (Surfaces 2 and 3)

b. **Case 2: Same Coefficient of Friction for Surfaces 1 and 4**

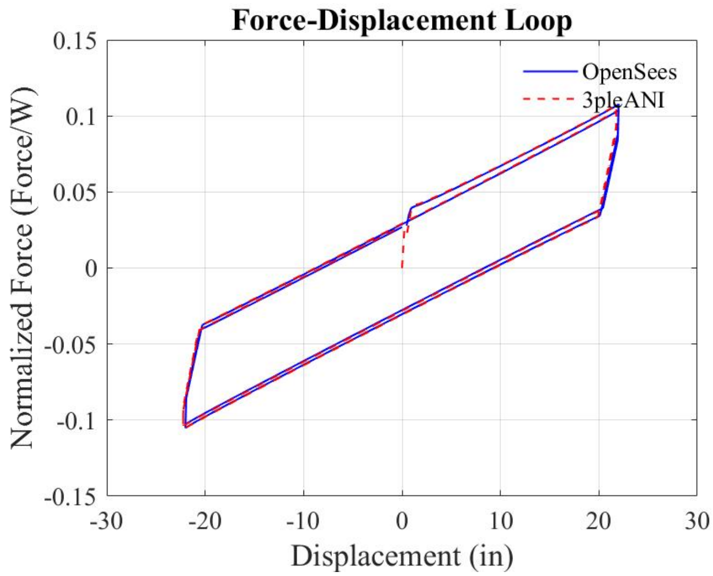

Figure 5-41 Comparison of Force-Displacement Loops

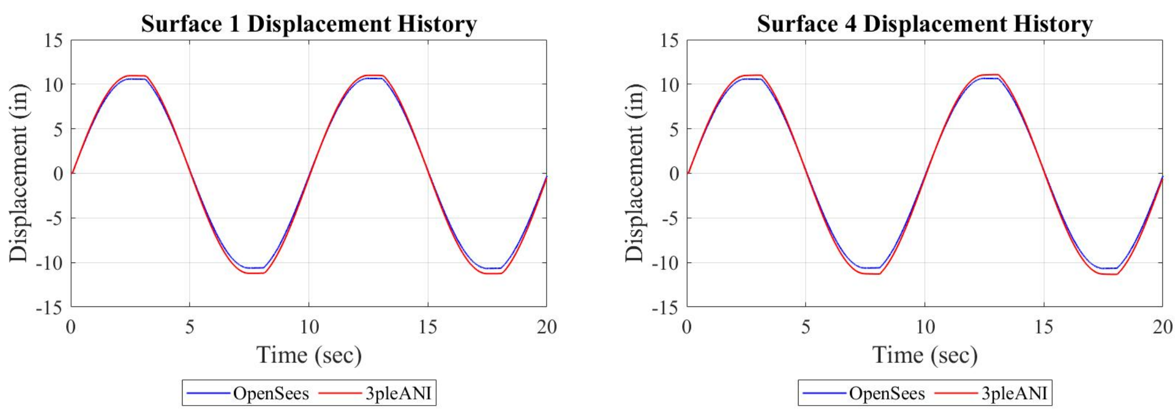

Figure 5-42 Comparison of Displacement Histories on Outer Surfaces (Surface 1 and 4)

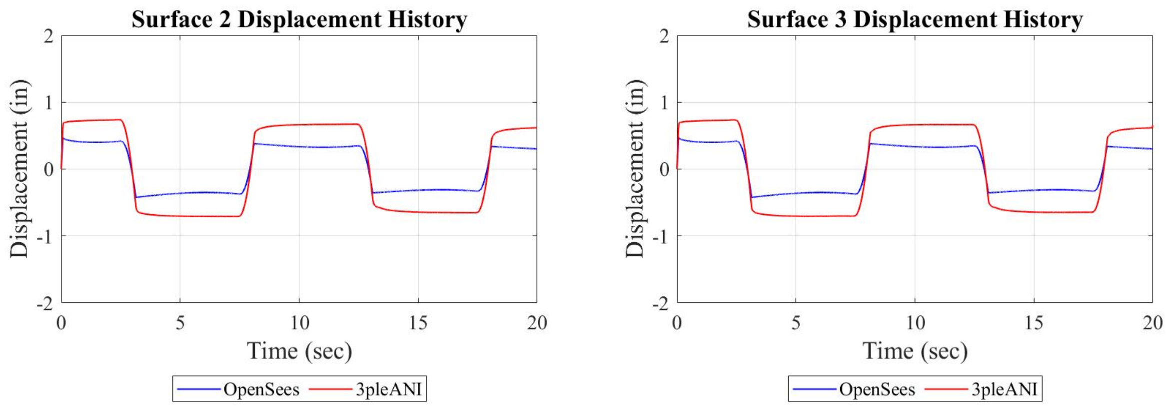

Figure 5-43 Comparison of Displacement Histories on Inner Surfaces (Surface 2 and 3)

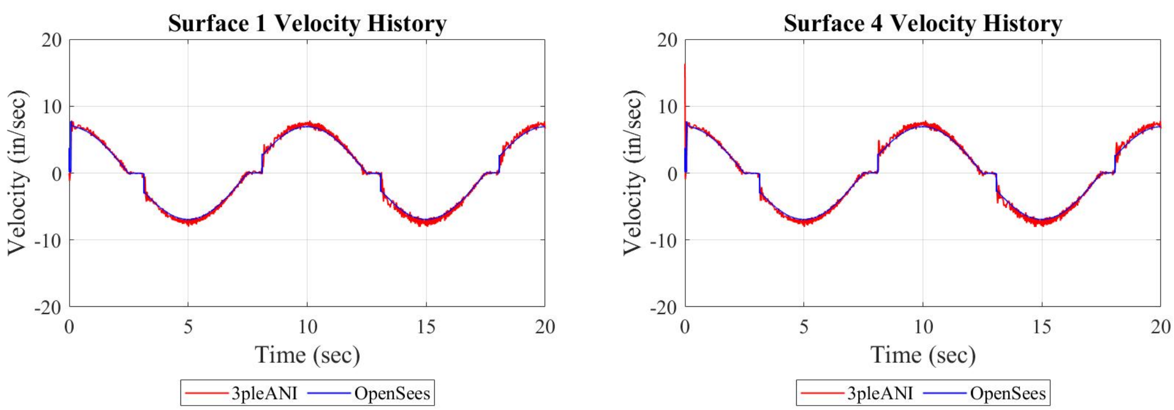

Figure 5-44 Comparison of Velocity Histories on Outer Surfaces (Surface 1 and 4)

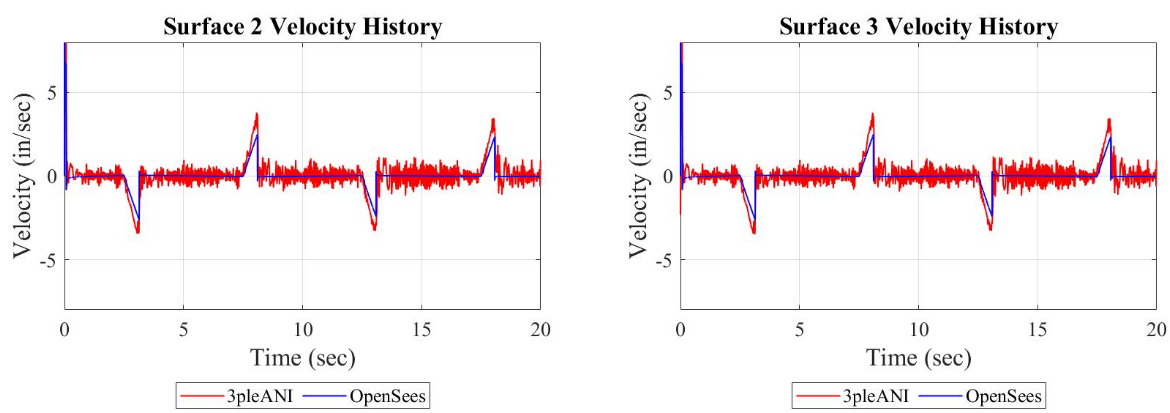

Figure 5-45 Comparison of Velocity Histories on Inner Surfaces (Surfaces 2 and 3)

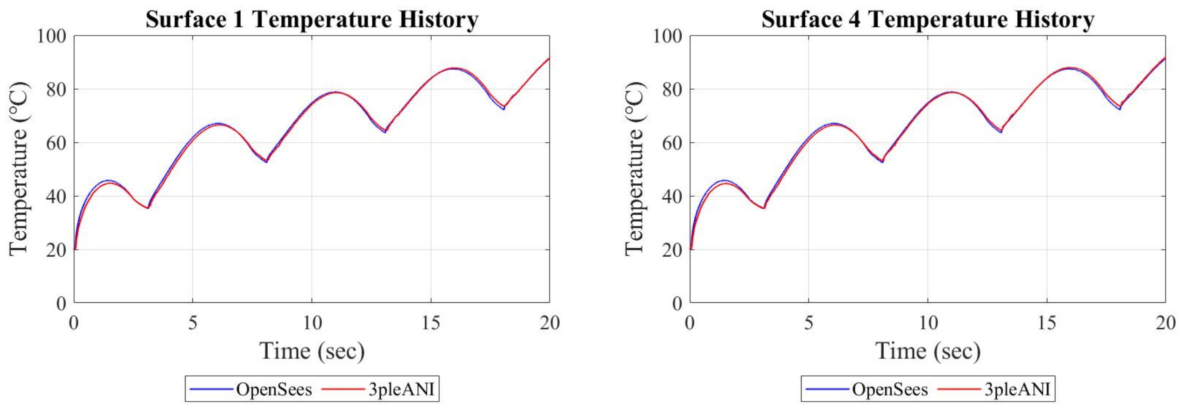

Figure 5-46 Comparison of Temperature Histories on Outer Surfaces (Surfaces 1 and 4)

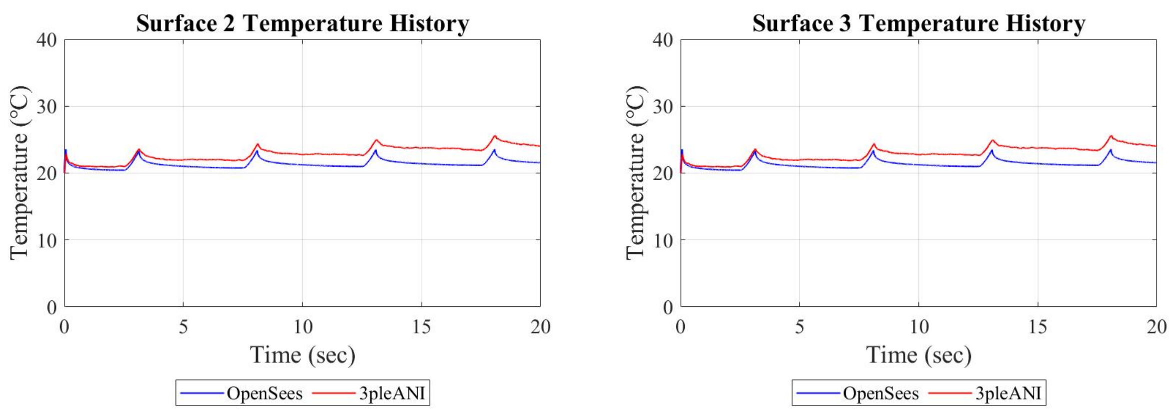

Figure 5-47 Comparison of Temperature Histories on Inner Surfaces (Surfaces 2 and 3)

B) Configuration B

a. Case 1: Different Coefficient of Friction for Surface 1 and 4

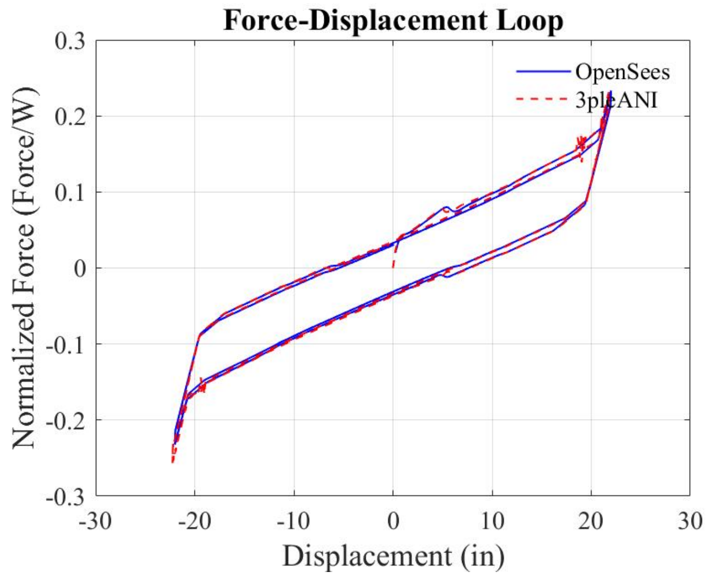

Figure 5-48 Comparison of Force-Displacement Loops

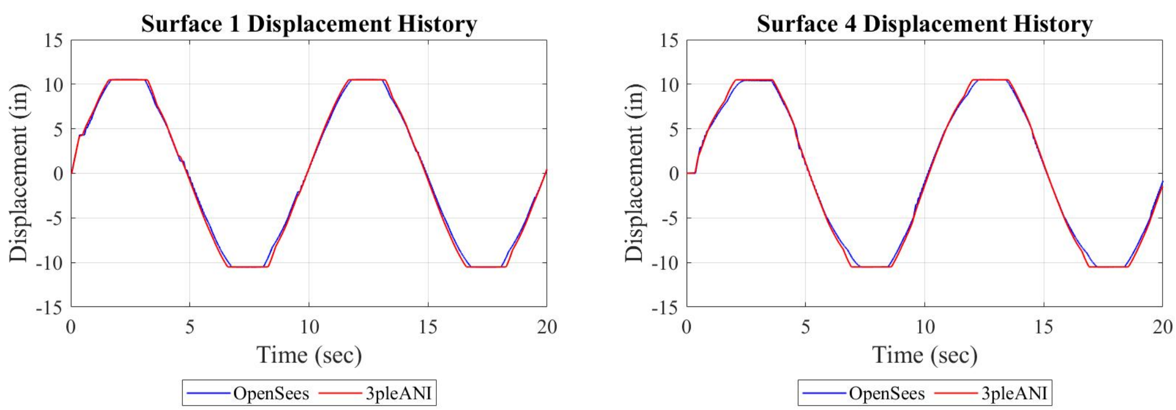

Figure 5-49 Comparison of Displacement Histories on Outer Surfaces (Surfaces 1 and 4)

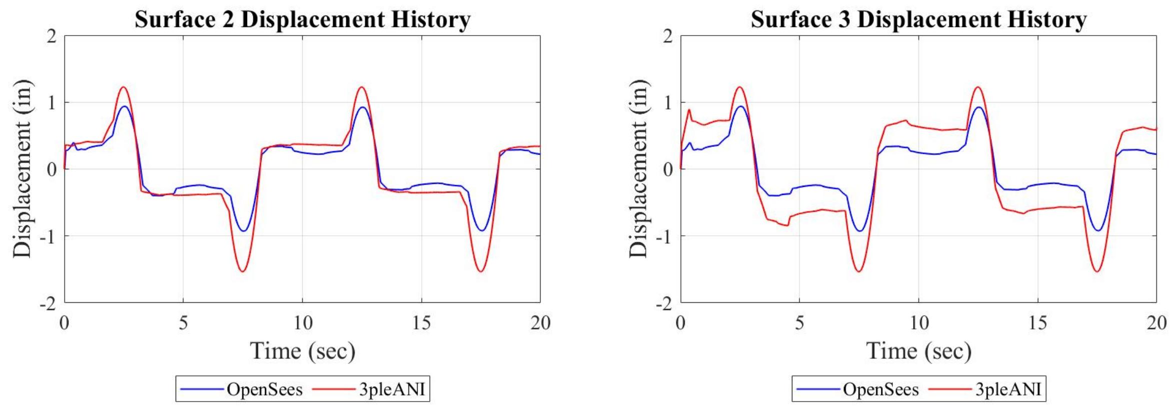

Figure 5-50 Comparison of Displacement Histories on Inner Surfaces (Surfaces 2 and 3)

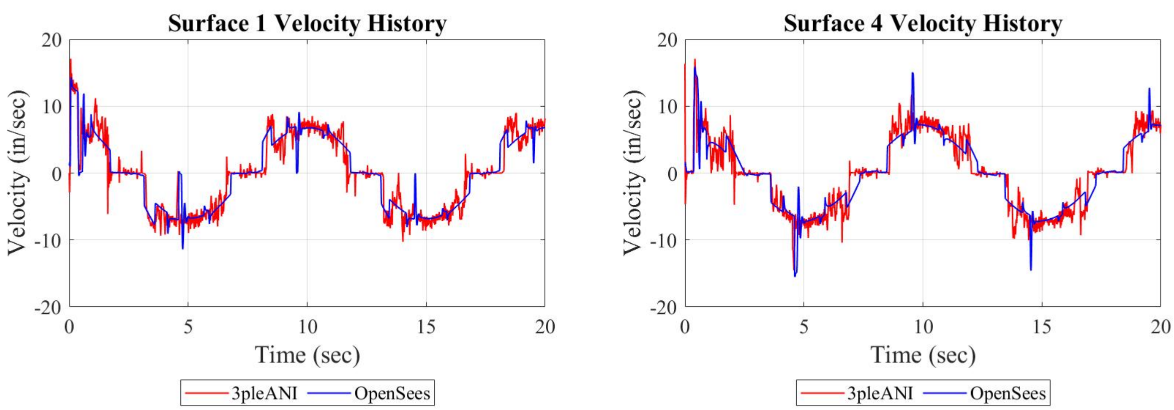

Figure 5-51 Comparison of Velocity Histories on Outer Surfaces (Surfaces 1 and 4)

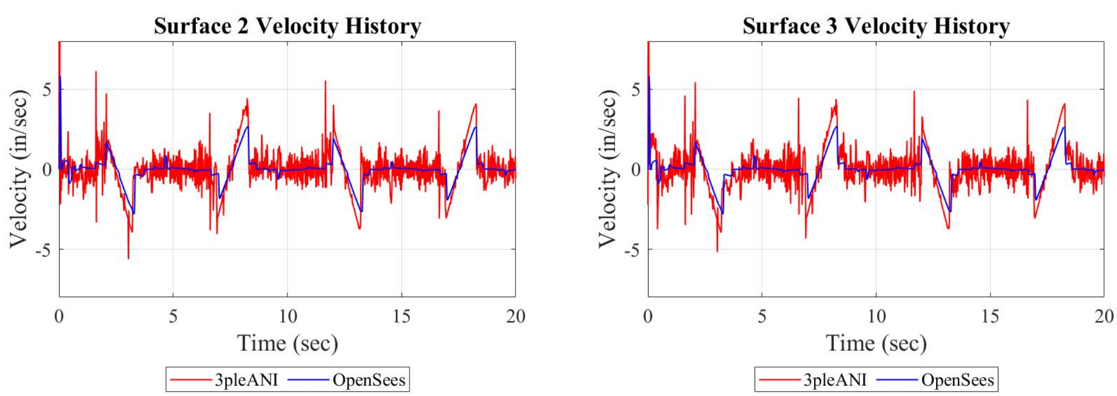

Figure 5-52 Comparison of Velocity Histories on Inner Surfaces (Surfaces 2 and 3)

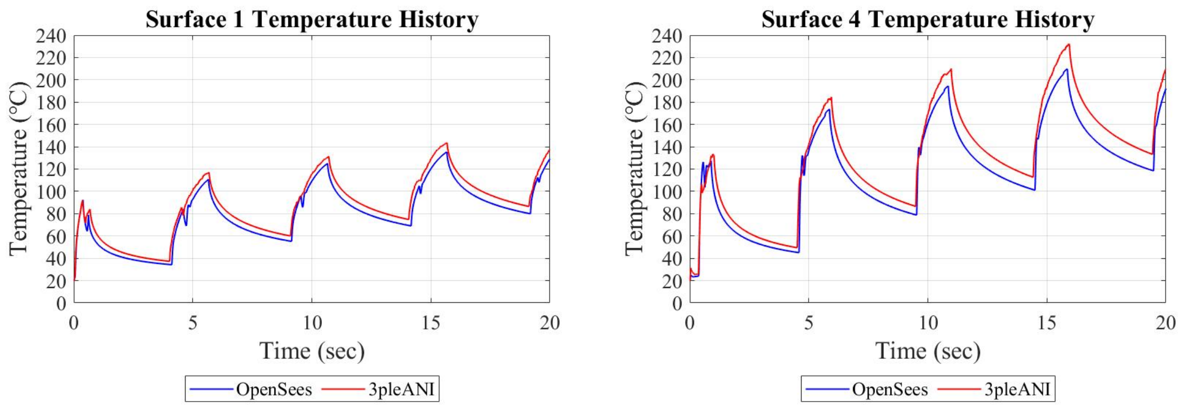

Figure 5-53 Comparison of Temperature Histories on Outer Surfaces (Surfaces 1 and 4)

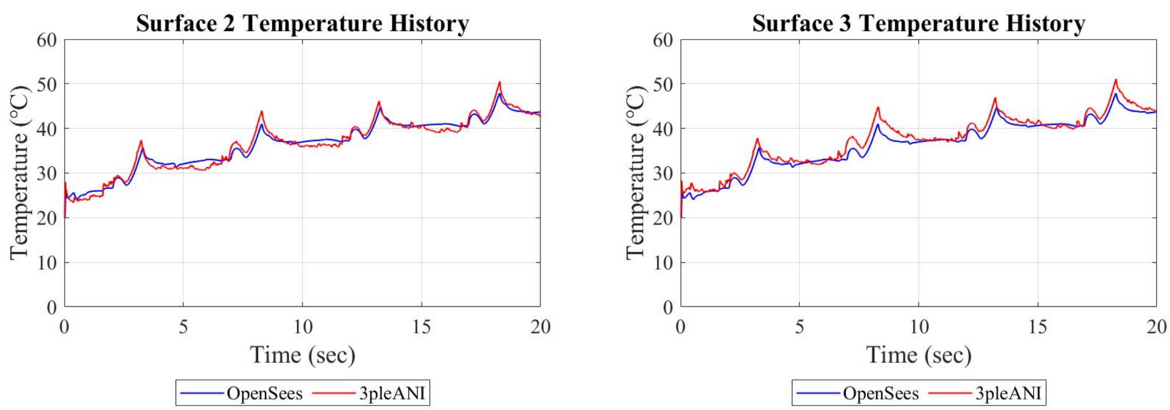

Figure 5-54 Comparison of Temperature Histories on Inner Surfaces (Surfaces 2 and 3)

b. Case 2: Same Coefficient of Friction for Surface 1 and 4

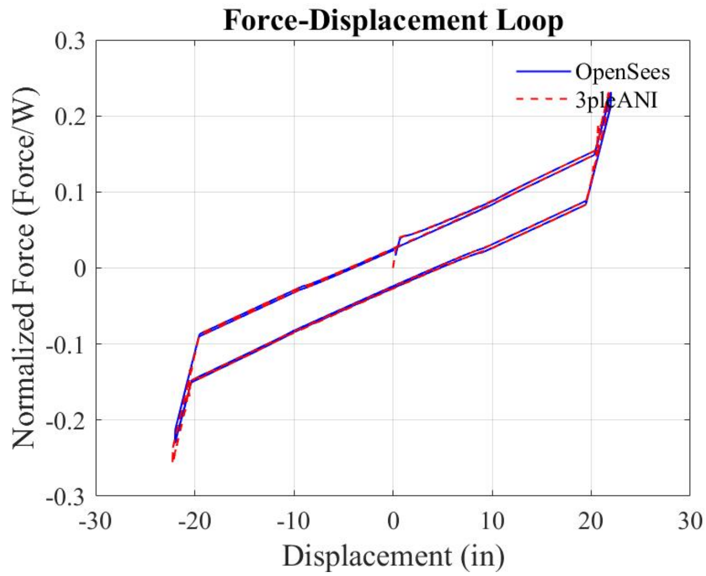

Figure 5-55 Comparison of Force-Displacement Loops

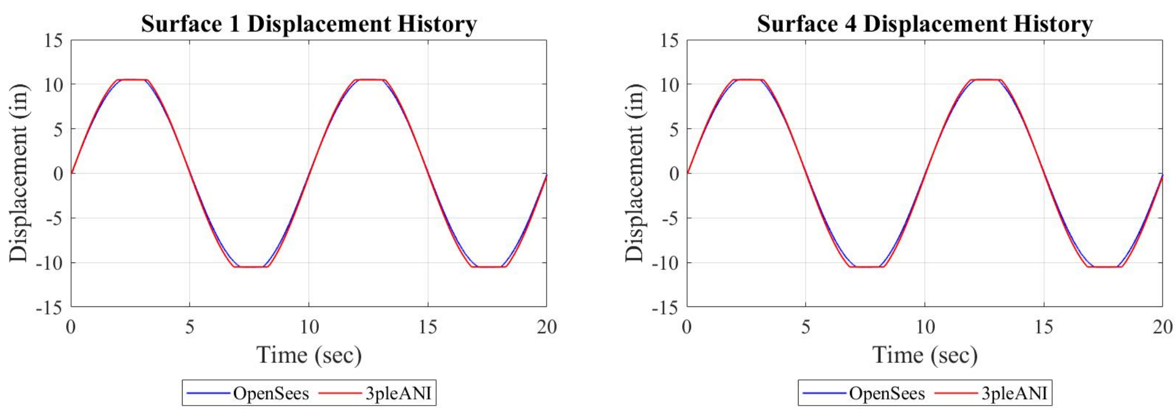

Figure 5-56 Comparison of Displacement Histories on Outer Surfaces (Surfaces 1 and 4)

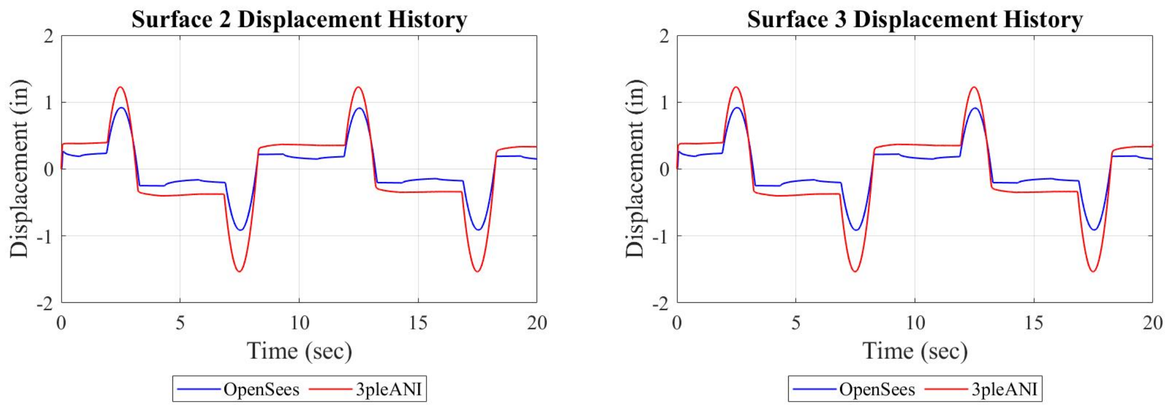

Figure 5-57 Comparison of Displacement Histories on Inner Surfaces (Surfaces 2 and 3)

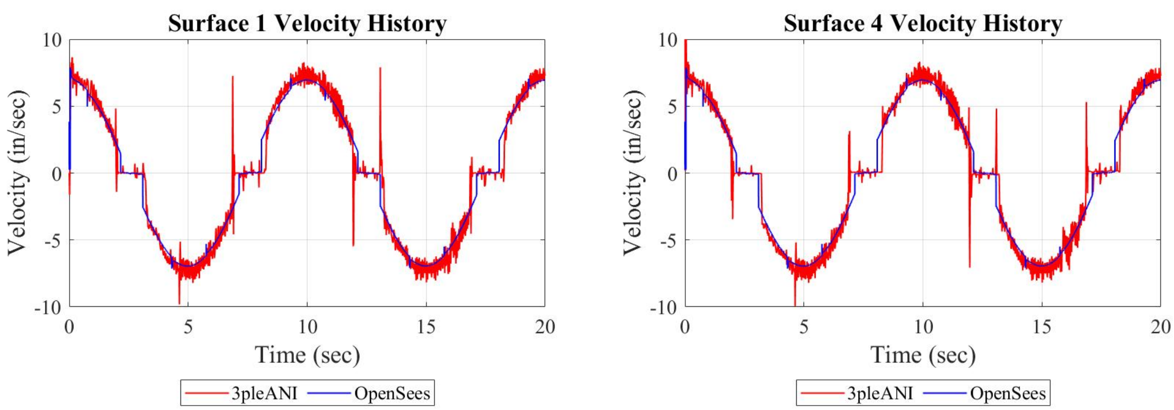

Figure 5-58 Comparison of Velocity Histories on Outer Surfaces (Surfaces 1 and 4)

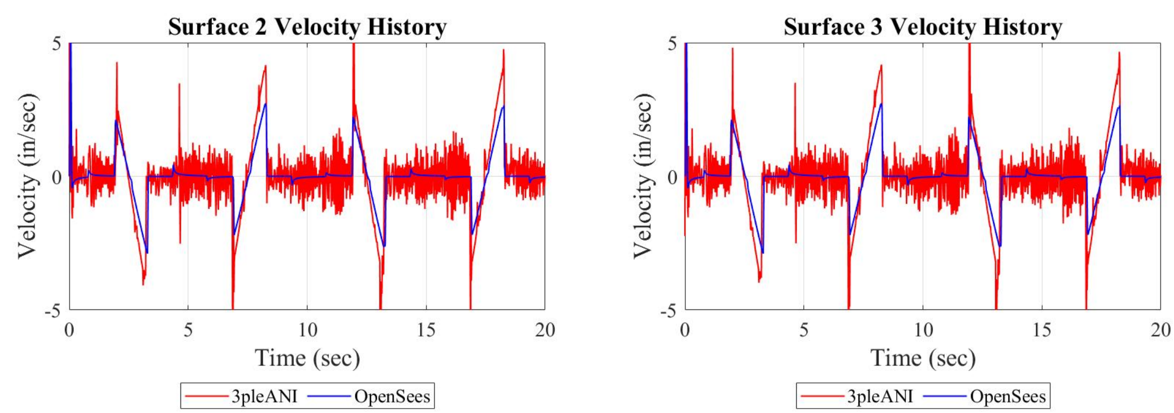

Figure 5-59 Comparison of Velocity Histories on Inner Surfaces (Surfaces 2 and 3)

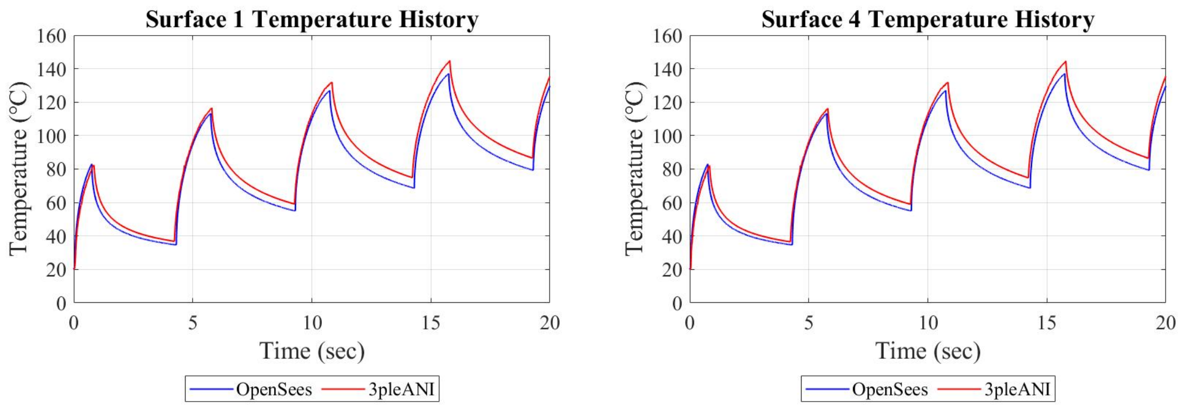

Figure 5-60 Comparison of Temperature Histories on Outer Surfaces (Surfaces 1 and 4)

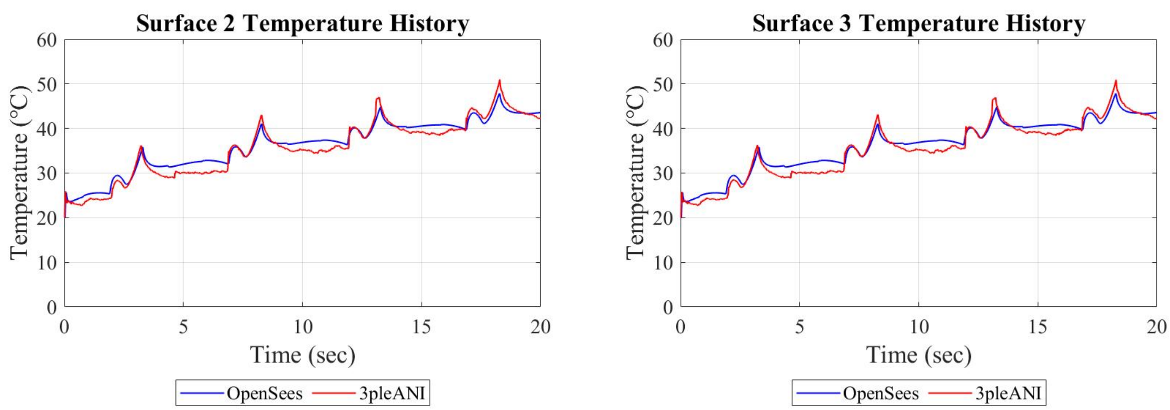

Figure 5-61 Comparison of Temperature Histories on Inner Surfaces (Surfaces 2 and 3)

5.1.3 Harmonic Motion: Amplitude of 20in and Period of 5sec

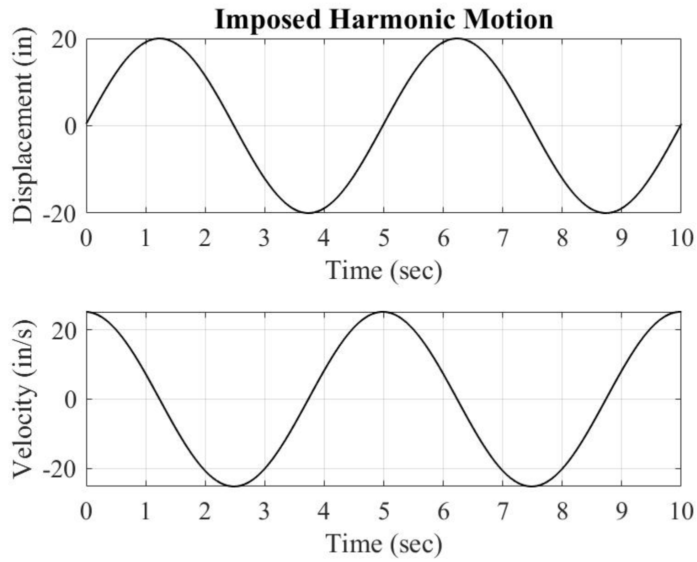

Figure 5-62 Imposed Harmonic Motion (Amplitude: 20in, Period: 5sec)

A) Configuration A

a. Case 1: Different Coefficient of Friction for Surfaces 1 and 4

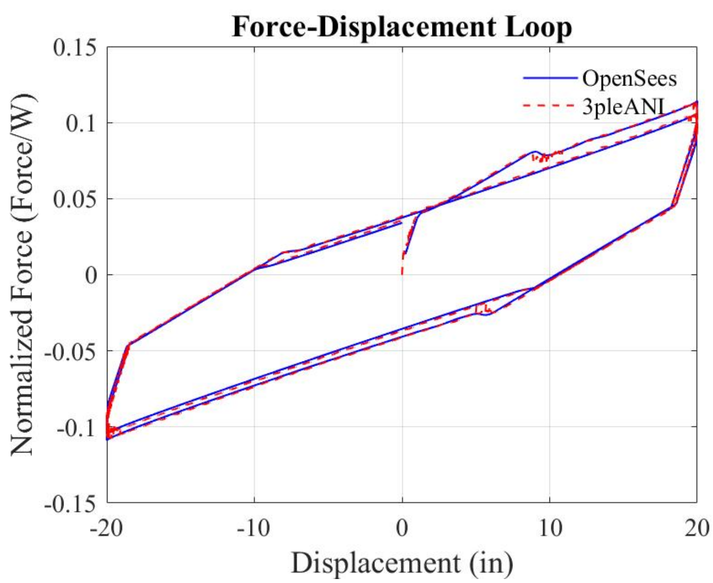

Figure 5-63 Comparison of Force-Displacement Loops

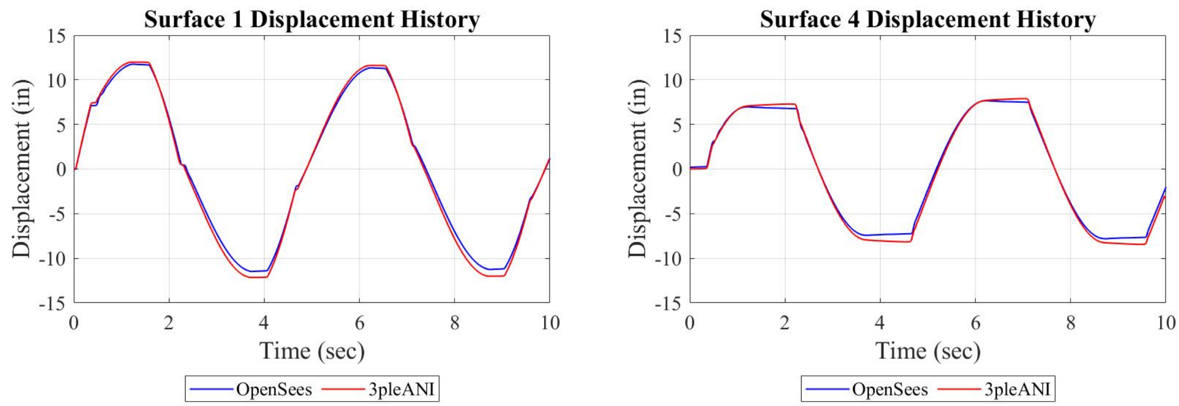

Figure 5-64 Comparison of Displacement Histories on Outer Surfaces (Surfaces 1 and 4)

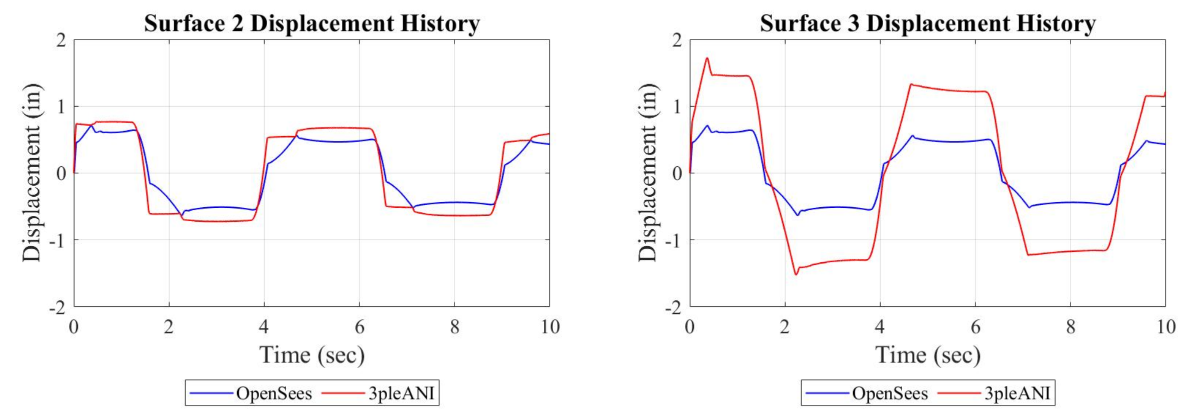

Figure 5-65 Comparison of Displacement Histories on Inner Surfaces (Surfaces 2 and 3)

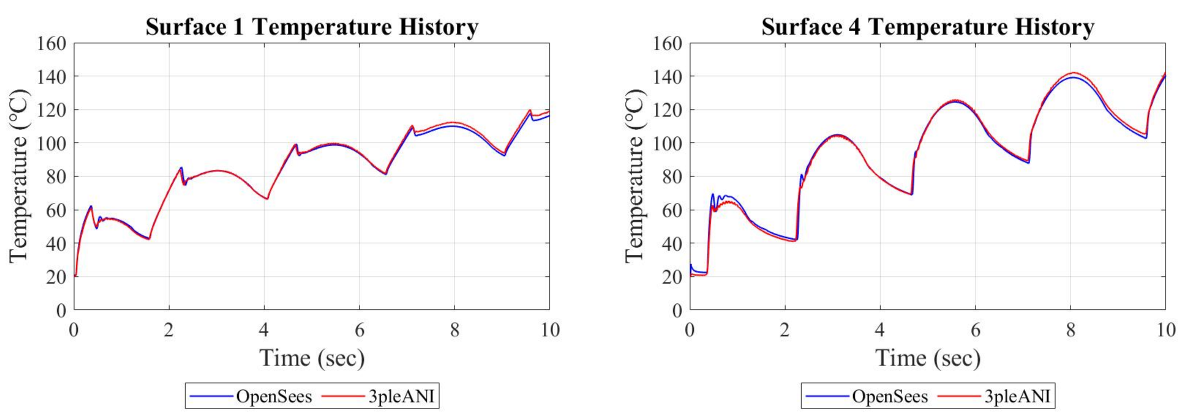

Figure 5-66 Comparison of Temperature Histories on Outer Surfaces (Surfaces 1 and 4)

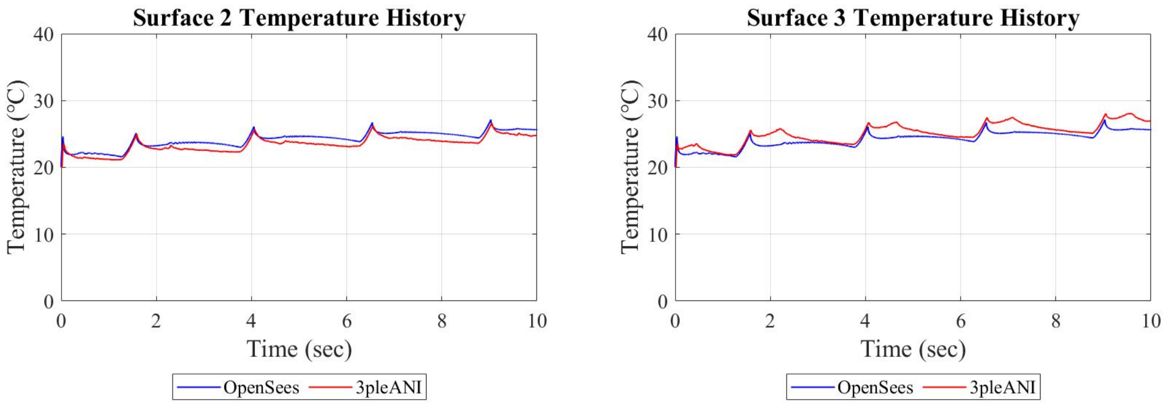

Figure 5-67 Comparison of Temperature Histories on Inner Surfaces (Surfaces 2 and 3)

b. **Case 2: Same Coefficient of Friction for Surfaces 1 and 4**

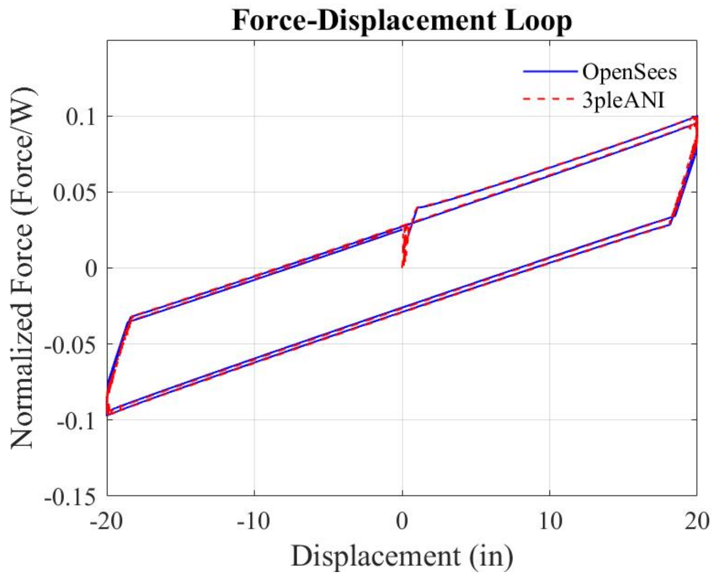

Figure 5-68 Comparison of Force-Displacement Loops

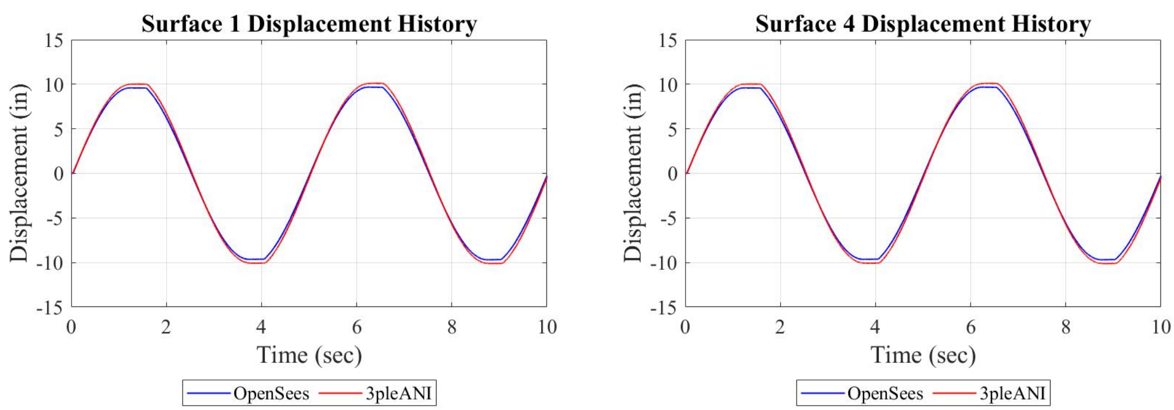

Figure 5-69 Comparison of Displacement Histories on Outer Surfaces (Surface 1 and 4)

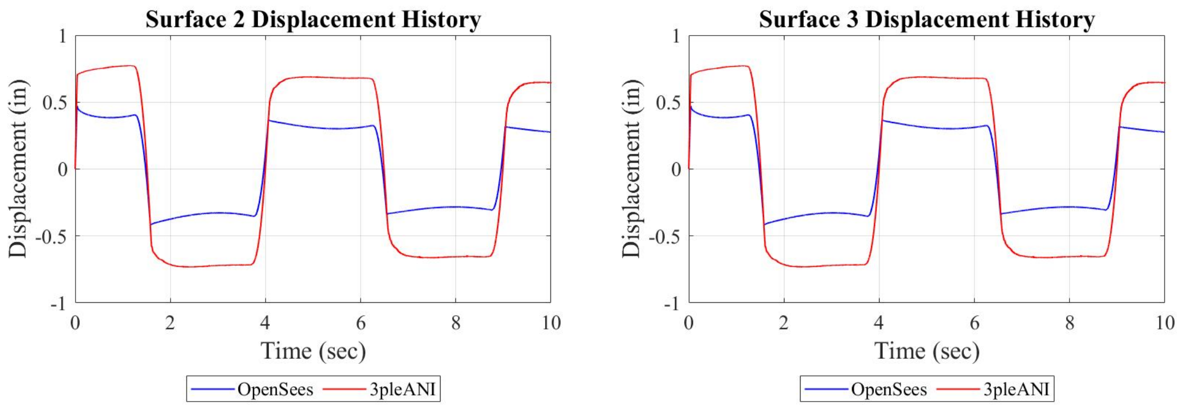

Figure 5-70 Comparison of Displacement Histories on Inner Surfaces (Surface 2 and 3)

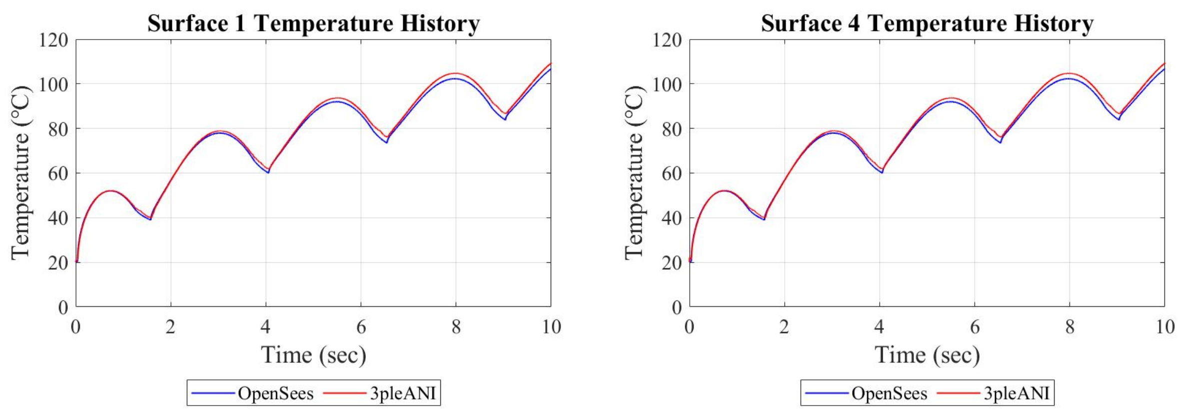

Figure 5-71 Comparison of Temperature Histories on Outer Surfaces (Surfaces 1 and 4)

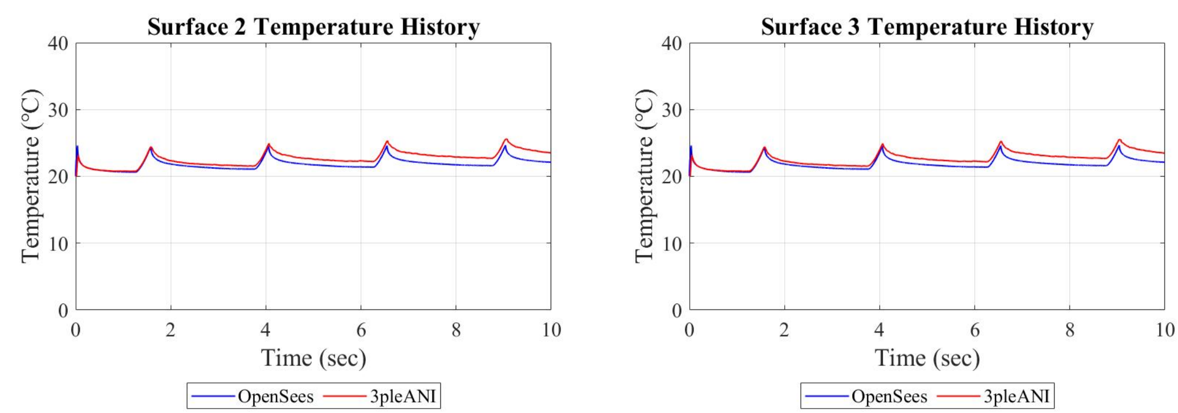

Figure 5-72 Comparison of Temperature Histories on Inner Surfaces (Surfaces 2 and 3)

B) Configuration B

a. Case 1: Different Coefficient of Friction for Surface 1 and 4

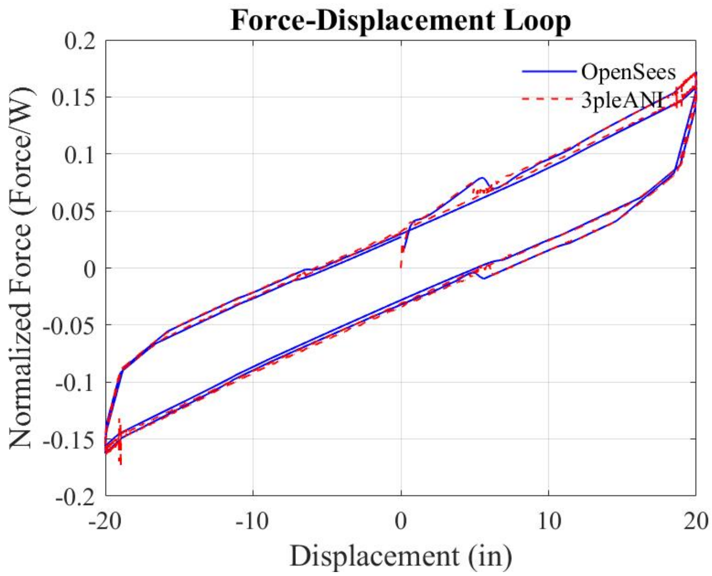

Figure 5-73 Comparison of Force-Displacement Loops

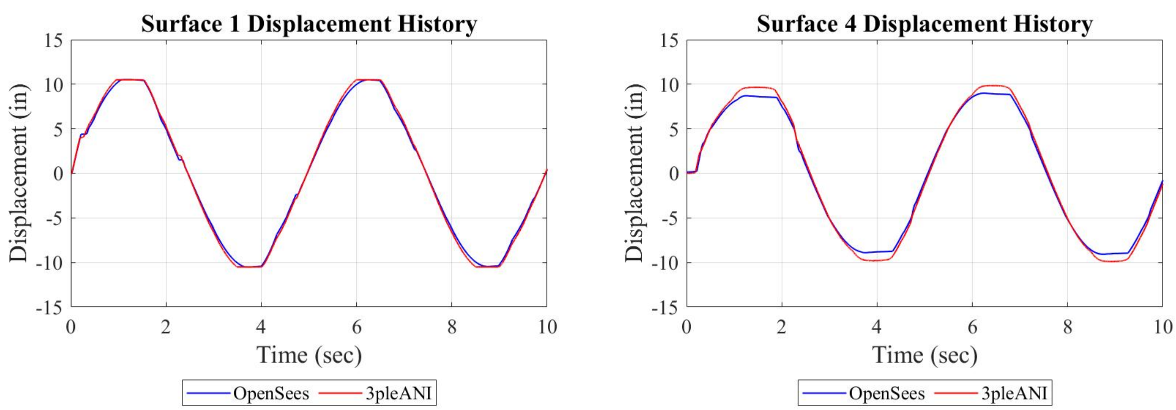

Figure 5-74 Comparison of Displacement Histories on Outer Surfaces (Surfaces 1 and 4)

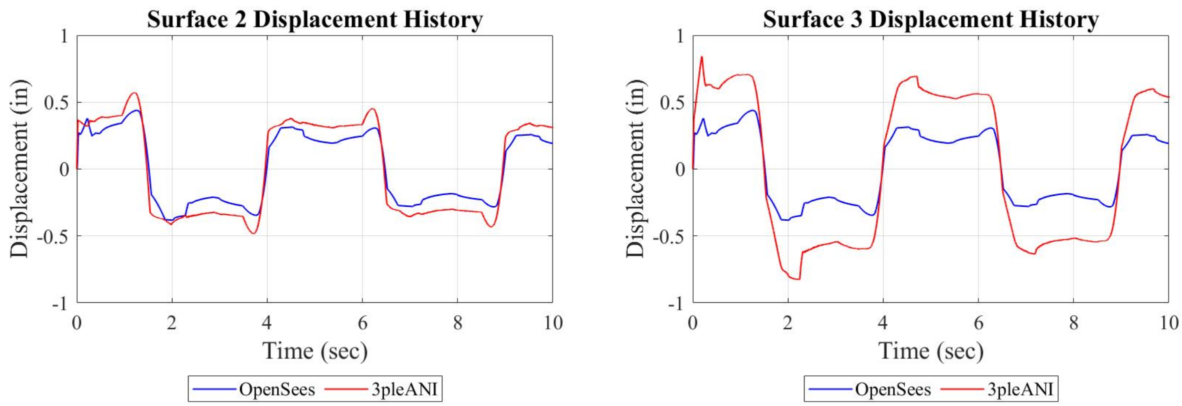

Figure 5-75 Comparison of Displacement Histories on Inner Surfaces (Surfaces 2 and 3)

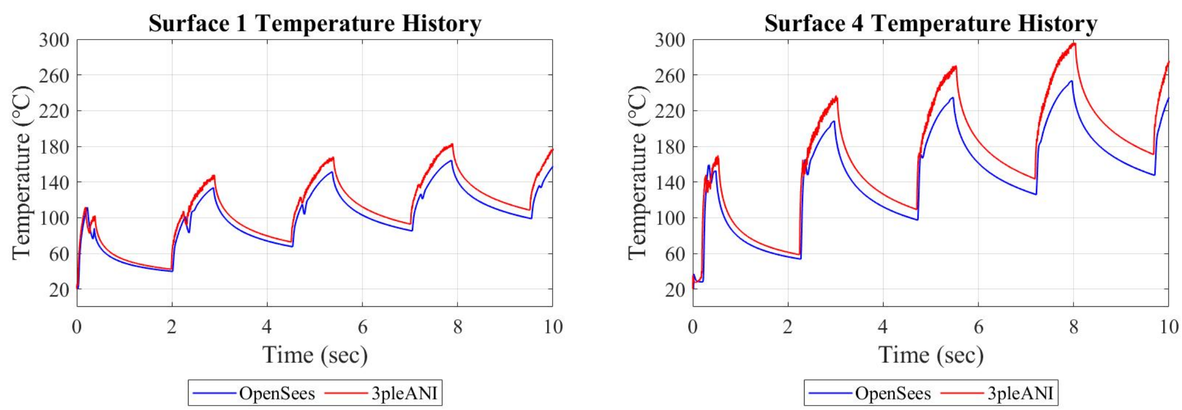

Figure 5-76 Comparison of Temperature Histories on Outer Surfaces (Surfaces 1 and 4)

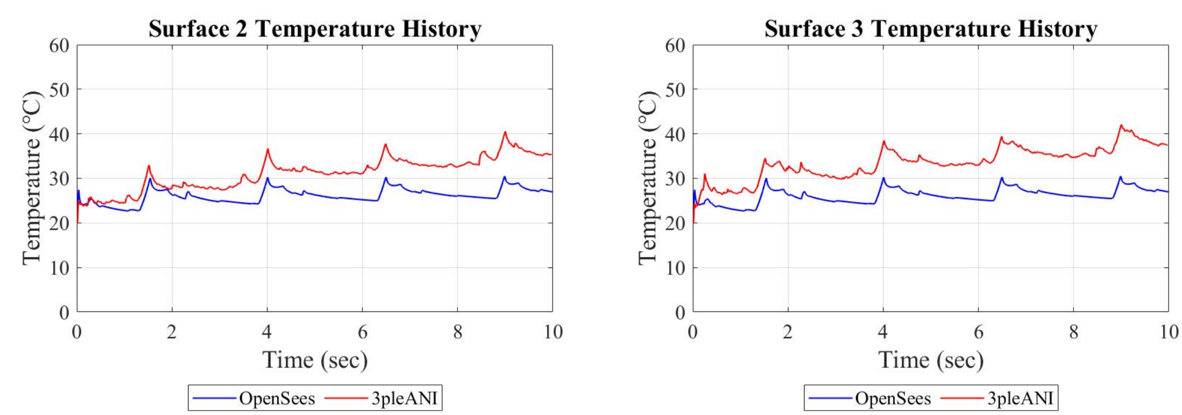

Figure 5-77 Comparison of Temperature Histories on Inner Surfaces (Surfaces 2 and 3)

b. Case 2: Same Coefficient of Friction for Surface 1 and 4

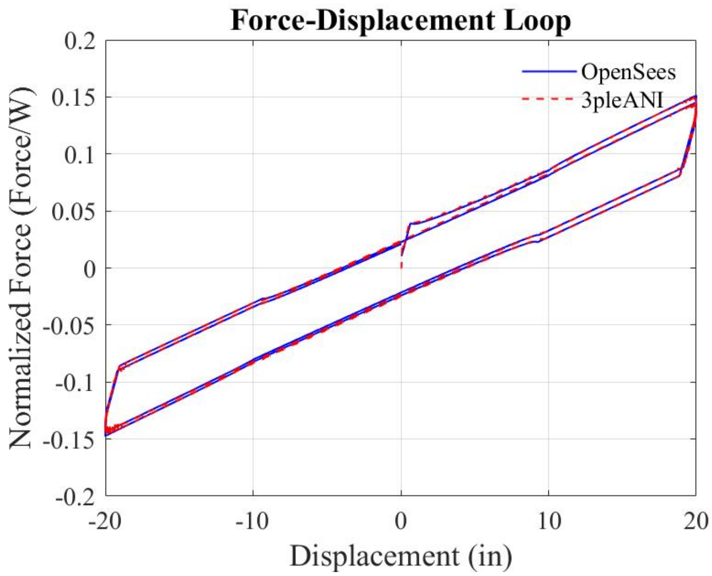

Figure 5-78 Comparison of Force-Displacement Loops

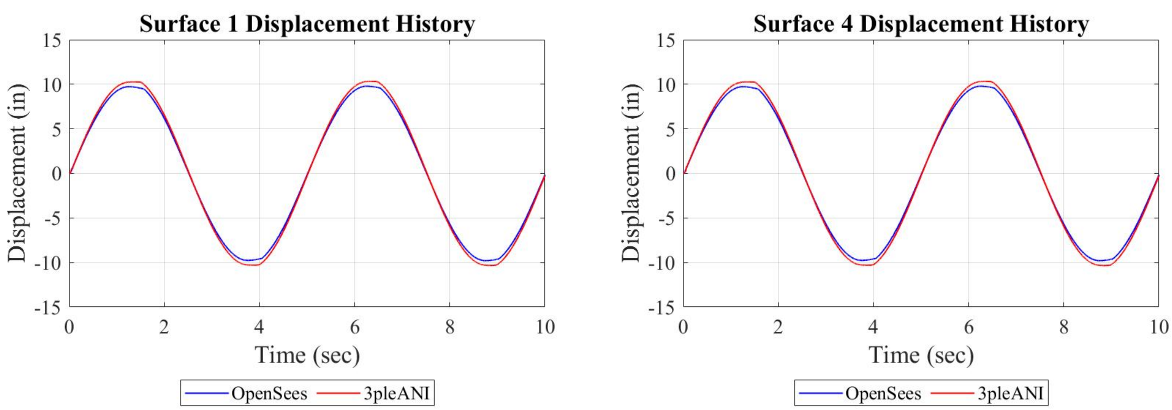

Figure 5-79 Comparison of Displacement Histories on Outer Surfaces (Surfaces 1 and 4)

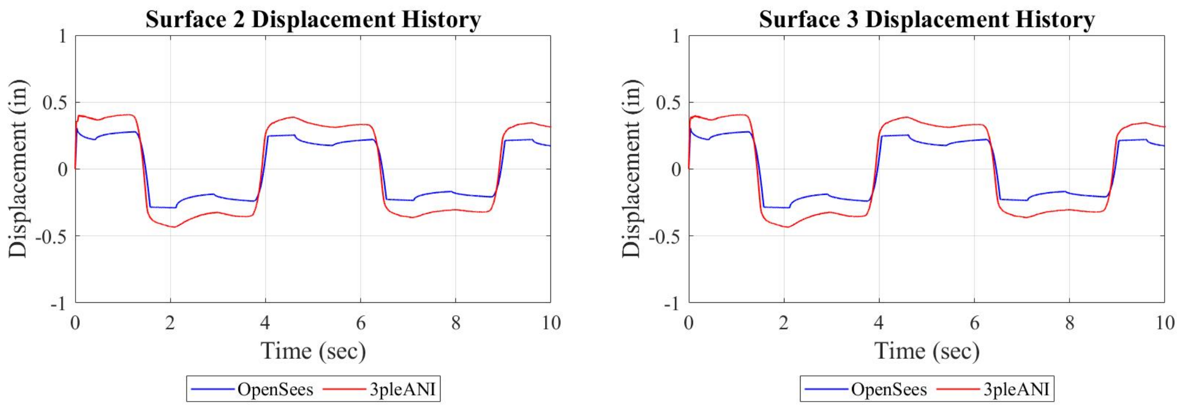

Figure 5-80 Comparison of Displacement Histories on Inner Surfaces (Surfaces 2 and 3)

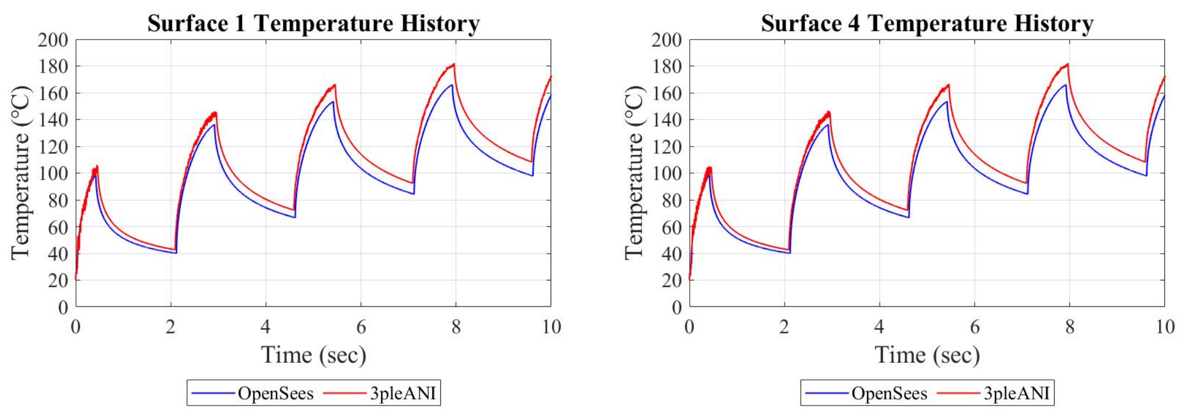

Figure 5-81 Comparison of Temperature Histories on Outer Surfaces (Surfaces 1 and 4)

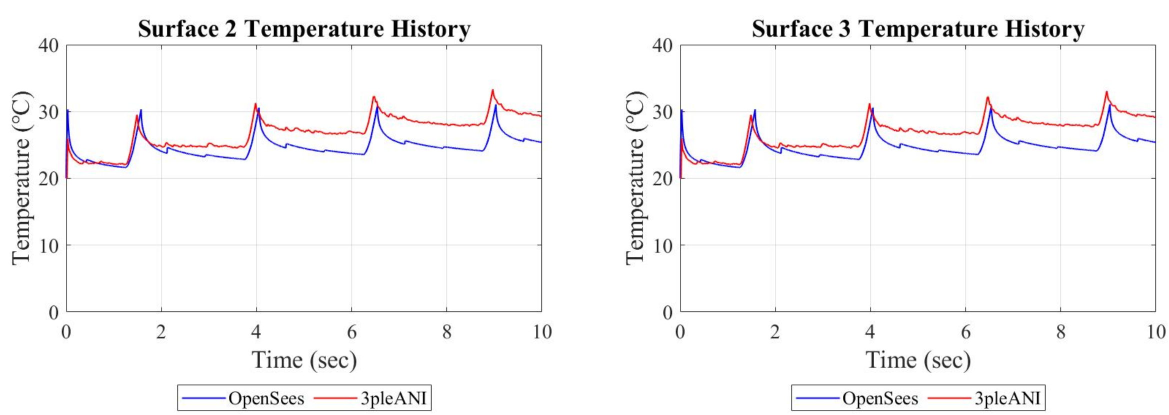

Figure 5-82 Comparison of Temperature Histories on Inner Surfaces (Surfaces 2 and 3)

5.2 Observations and Comments

The observations made in the comparison of results when friction is temperature independent in Section 4 (presented in subsection 4.1.3) are valid for the case of friction that is temperature dependent. Specifically:

1) The force-displacement loops obtained by the model in program OpenSees and the more advanced model in program 3pleANI are in good agreement.
2) In general, the two models in program OpenSees produce results on the displacement, velocity and temperature of the main surfaces 1 and 4 that are in good agreement with those produced by the more advanced model in program 3pleANI.
3) In general, the two models in program OpenSees produce results on the displacement, velocity and temperature of the inner surfaces 2 and 3 that differ from those produced by the more advanced model in program 3pleANI. Nevertheless, the motion and temperature in the inner surfaces are significantly smaller than those of the main surfaces 1 and 4 (e.g., the temperature rise in the outer surfaces is an order of magnitude larger than that in the inner surfaces) so that effect on the behavior of the bearing is insignificant.

It is also observed that in examples where there is large increase in the temperature at the sliding surfaces, the two models in OpenSees and 3pleANI have predictions of temperature histories that differ more than that observed in examples with smaller temperature increases. This is best seen in comparing the results of Figure 5-24 (temperatures reaching about 110^{o}C) and Figure 5-81 (temperatures reaching about 180^{o}C)- both are for the same configurations (B with same friction coefficients on surfaces 1 and 4) and subjected to the same amplitude motion but with period of 20sec in the case of Figure 5-24 and period of 5sec in the case of Figure 5-81. This is due to differences in the temperature-dependency of the friction coefficient in the models in programs OpenSees and 3pleANI, as explained in Section 5.1 (see also Figure 5-1).

SECTION 6
RESPONSE HISTORY ANALYSIS OF BUILDINGS WITH TRIPLE FP BEARINGS

6.1 Example: Response History Analysis of a Rigid Structure

A rigid structure supported on triple FP isolators is subjected to ground motion in bidirectional horizontal and in the vertical directions. Results produced by programs OpenSees and 3pleANI on isolation system force-displacement loops, and the histories of isolator displacement, structural acceleration and temperature at the sliding surfaces are compared. In the analysis, only one isolator of Configuration B and two cases of friction (different and equal at the two main sliding interfaces-see Table 4-1) is utilized. The weight of the structure carried by the single isolator is W=2225kN (W=500kip). Analyses were performed with only temperature-dependent friction for comparison to results of program 3pleANI, which is limited to only this option. Additional results of program OpenSees with temperature, velocity and pressure-dependent friction are presented and evaluated. The parameters used in the analysis when friction is temperature-dependent are listed in Table 6-1. Also, values of parameters used in the analysis other than those in Section 4 and below are presented in Appendix A.

Table 6-1 Parameters for accounting for dependency of friction coefficient on temperature

Parameter	Unit	Value
Thermal Diffusivity	m^2/sec	$0.444 * 10^{-5}$
Thermal Conductivity	$W/(m°\mathrm{C})$	18
Initial Temperature	°C	20

When analyzing with only temperature-dependent friction, equations (2-7) to (2-10) are used but with parameters k_v and k_p set equal to unity. When analyzing with pressure and velocity-dependent friction, equations (2-8) and (2-9) are used with the following values for the initial pressure p_o, and velocity parameter.

Table 6-2 Values in equations 2-8 and 2-9 to account for dependency of friction on pressure and velocity

Parameter	Unit	Value
Axial Load on Isolator	kN	2225
Initial Pressure at Surfaces 2 and 3	MPa	73.7

Initial Pressure at Surface 1	MPa	36.4
Initial Pressure at Surface 4	MPa	36.4
Velocity Rate Parameter	sec/m	100 (2.54sec/inch)

The ground motion used in analysis consists of the fault-normal (FN), fault-parallel (FP), and vertical (V) components of the ground motion recorded at the Kaminoyama station in the 2011 Tohoku earthquake, scaled in amplitude by factor of 8.0. The ground motion data were obtained from the K-NET (Kyoshin Network) operated by the National Research Institute for Earth Science and Disaster Resilience (NIED) in Japan. This motion is of long duration having a D_{s5-75} duration (Chandramohan et al., 2016) equal to 85.9sec for the FN component, 81.0sec for the FP component, and 82.4sec for the vertical component. Figures 6-1 to 6-3 present histories of the ground acceleration of the three components, after scaling by factor of 8 as used in the analyses, and their normalized Arias intensity histories in order to identify the sections of the D_{s5-75} duration.

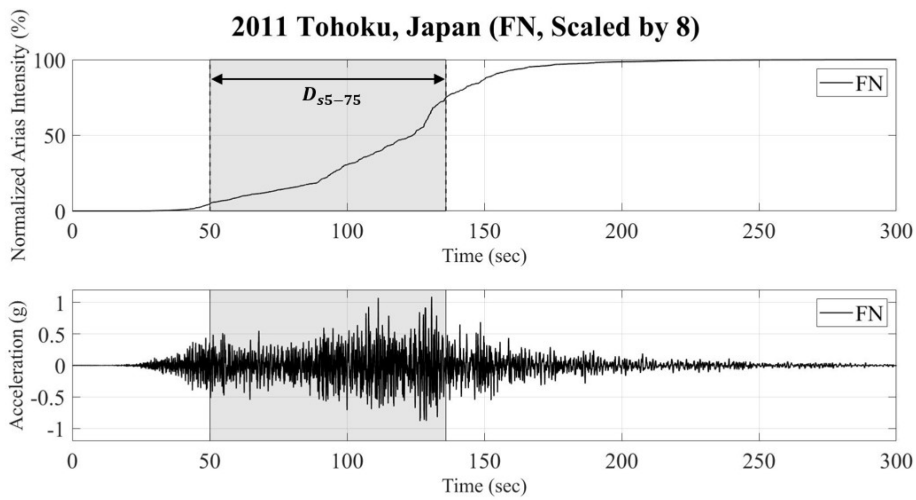

Figure 6-1 Scaled 2011 Tohoku Motion at Kaminoyama (FN) and Normalized Arias Intensity

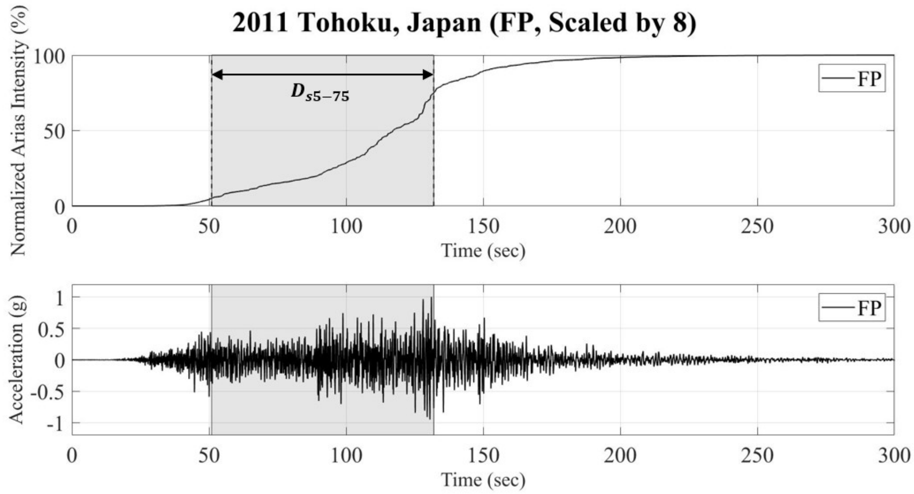

Figure 6-2 Scaled 2011 Tohoku Motion at Kaminoyama (FP) and Normalized Arias Intensity

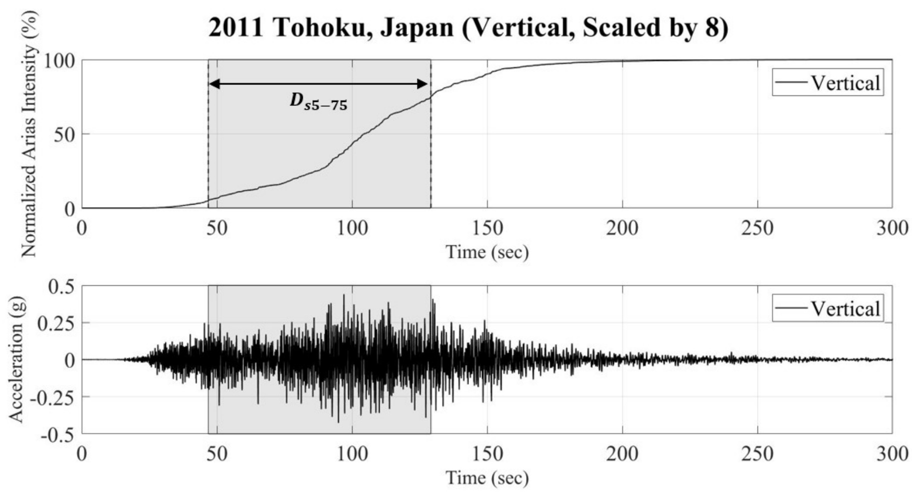

Figure 6-3 Scaled 2011 Tohoku Motion at Kaminoyama (V) and Normalized Arias Intensity

Results are presented for the following four cases:

1) Analysis using only the fault-normal (FN) component of the ground motion and with only temperature-dependent-friction for the two cases of friction of isolator of configuration B. The results of program OpenSees are compared to those of program 3pleANI.
2) Analysis using the fault-normal (FN) and vertical components of ground motion and with only temperature-dependent-friction and then again with temperature and pressure-dependent friction and then again with temperature, velocity and pressure-dependent friction. Results produced by program OpenSees are presented and evaluated.

3) Analysis using triaxial ground motions and with constant friction and with only temperature-dependent-friction, and then again with temperature, velocity and pressure-dependent friction. Results produced by program OpenSees are presented and evaluated.
4) Analysis using triaxial ground motions and with constant friction. Results produced by the two different triple FP bearing elements "TripleFrictionPendulum" and "TripleFrictionPendulumX" in program OpenSees are presented and evaluated.

6.1.1 Analysis with Temperature-Dependent Friction and Horizontal Ground Motion

Results produced by program OpenSees and 3pleANI are compared for the case of only temperature-dependent friction. The scale factor for the FN component is 8.

A) Different Friction Coefficients ($\mu_1 = 0.04, \mu_4 = 0.08,\ \mu_2 = \mu_3 = 0.01$)

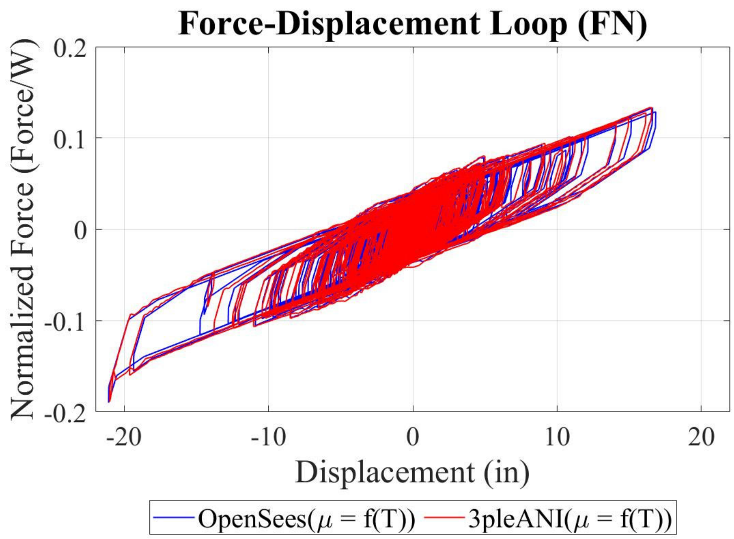

Figure 6-4 Comparison of Force-Displacement Loops (W=500kip)

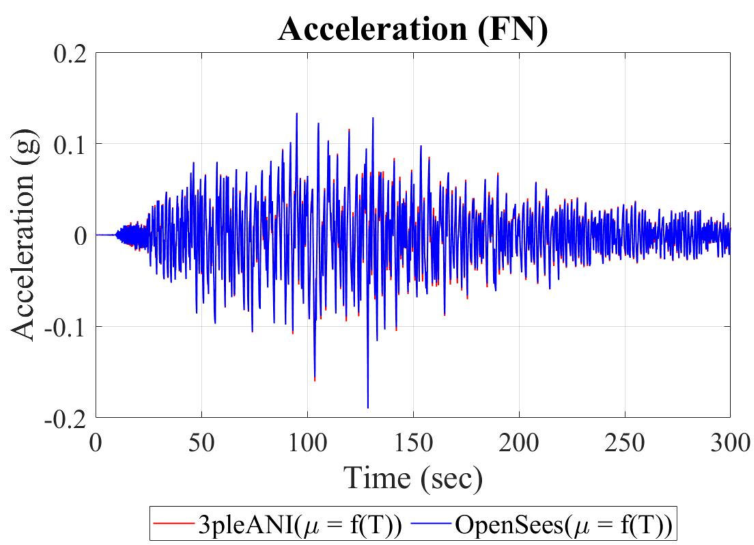

Figure 6-5 Comparison of Horizontal Acceleration Histories

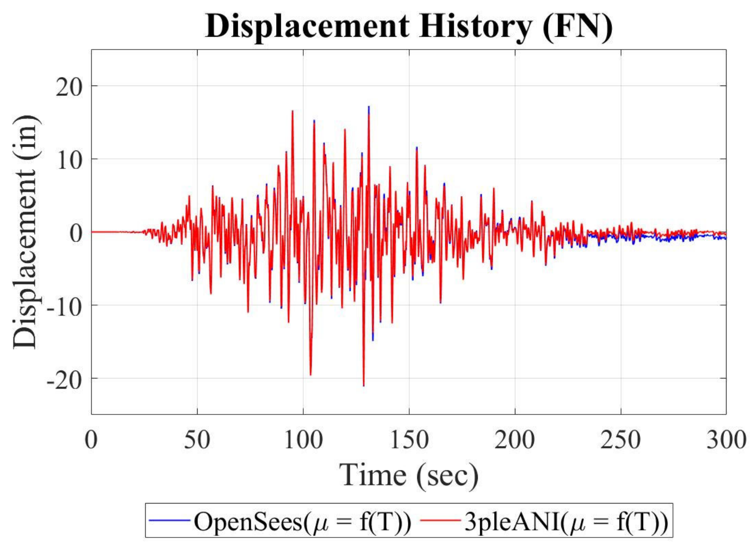

Figure 6-6 Comparison of Isolator Displacement Histories

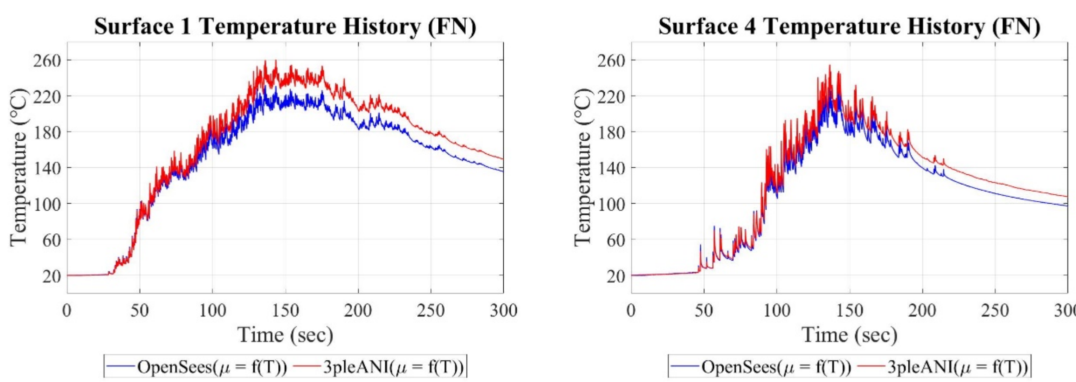

Figure 6-7 Comparison of Temperature Histories on Outer Surfaces (Surfaces 1 and 4)

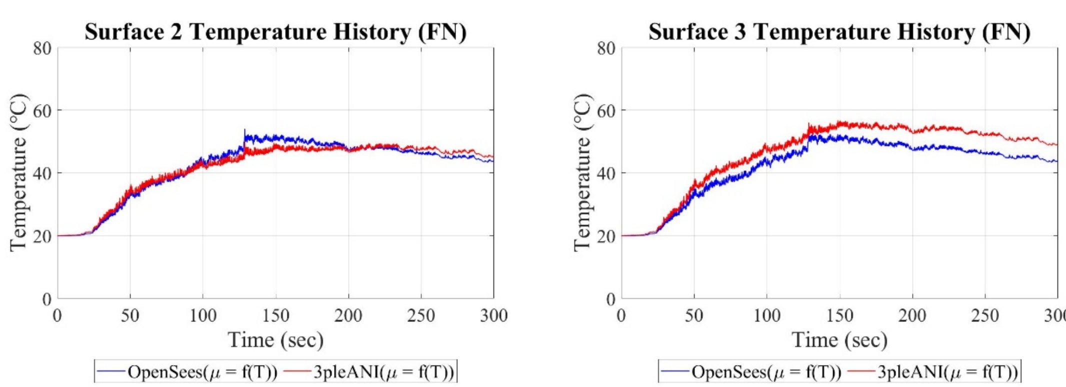

Figure 6-8 Comparison of Temperature Histories on Inner Surfaces (Surfaces 2 and 3)

B) Same Friction Coefficients ($\mu_1 = \mu_4 = 0.04,\ \mu_2 = \mu_3 = 0.01$)

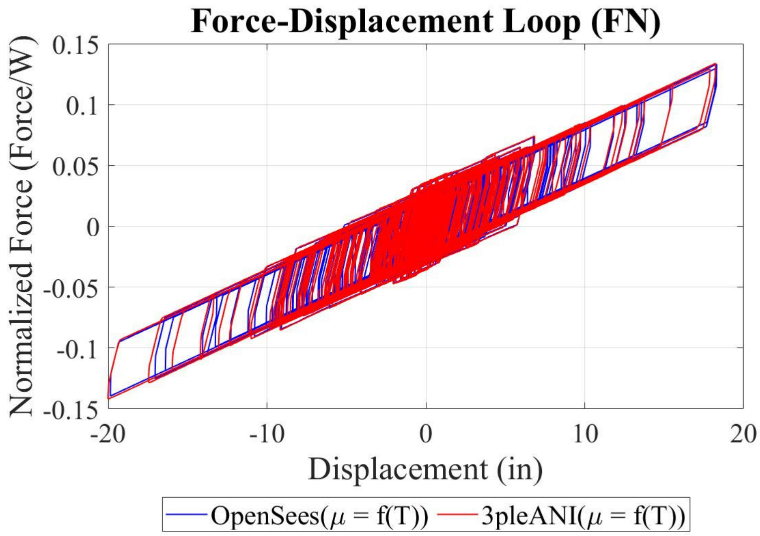

Figure 6-9 Comparison of Force-Displacement Loops (W=500kip)

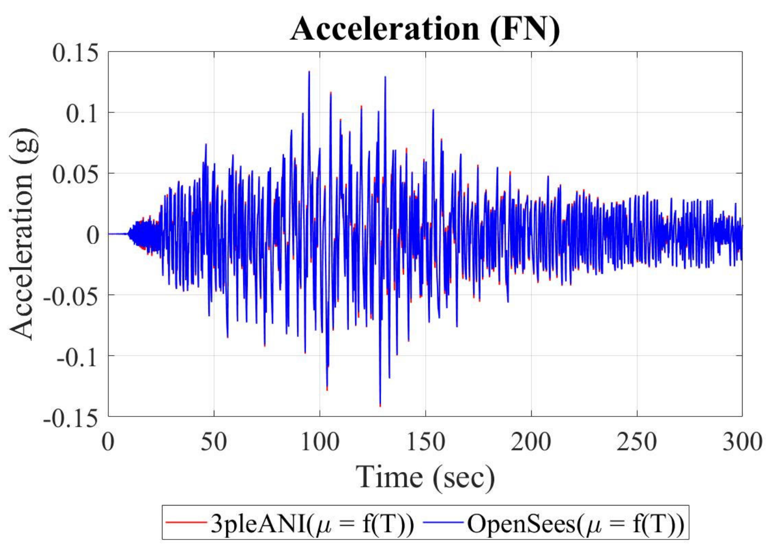

Figure 6-10 Comparison of Horizontal Acceleration Histories

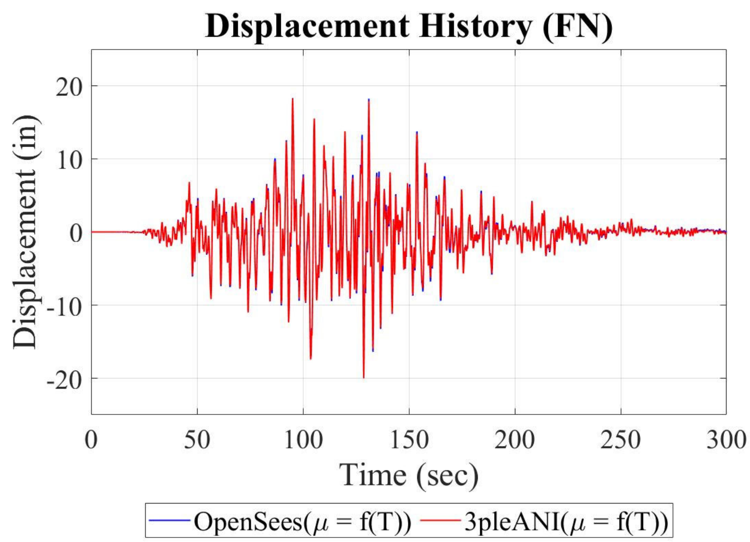

Figure 6-11 Comparison of Isolator Displacement History

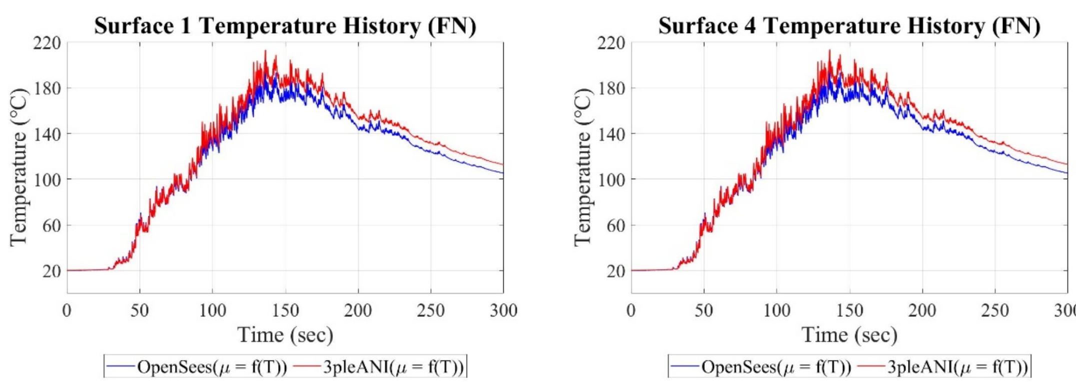

Figure 6-12 Comparison of Temperature Histories on Outer Surfaces (Surfaces 1 and 4)

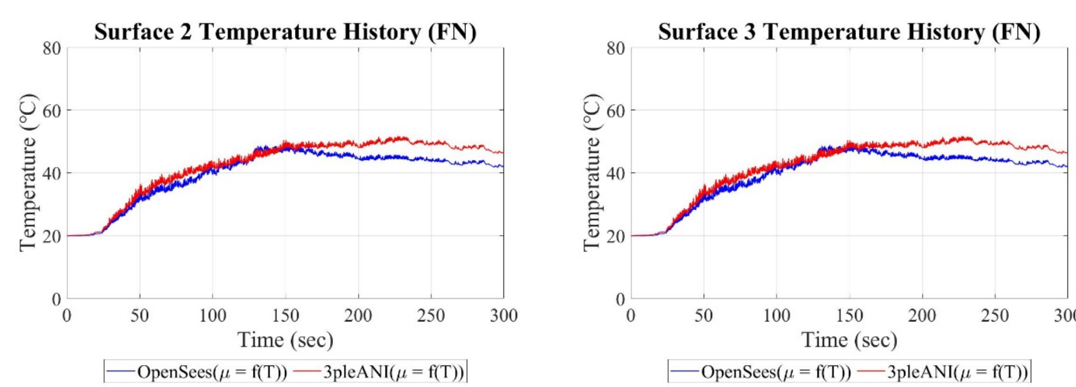

Figure 6-13 Comparison of Temperature Histories on Inner Surfaces (Surfaces 2 and 3)

6.1.2 Observations and Comments

For the case of only temperature-dependent friction, the observations made in Section 5 are valid as programs OpenSees and 3pleANI produce results on force-displacement loops, acceleration and displacement histories that are in very good agreement. The histories of temperature on surfaces 1 and 4 differ a little when temperatures are large but that has been explained by the differences in the model of the differences in the friction-temperature relationships in the two programs (see Figure 5-1). Also, there are some differences in the computed histories of temperature on surfaces 2 and 3 which are of the same order as those observed in the analyses in Section 5. These differences have apparently insignificant effects on the important force-displacement loops and the histories of isolator displacement and acceleration.

6.1.3 Analysis with Pressure and Temperature-Dependent Friction and Combined Horizontal-Vertical Ground Motion

Results produced by program OpenSees are compared for the two cases of combined pressure and temperature-dependent friction and only temperature-dependent friction ($\mu(P,T)$ versus $\mu(T)$ in the graphs that follow). The scale factor for FN and V components is 8.

A) **Different Friction Coefficients ($\mu_1 = 0.04, \mu_4 = 0.08,\ \mu_2 = \mu_3 = 0.01$)**

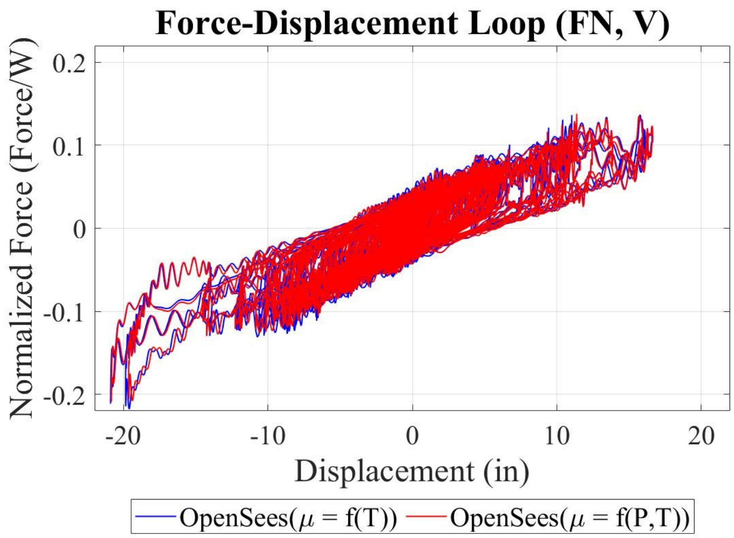

Figure 6-14 Comparison of Force-Displacement Loops (W=500kip)

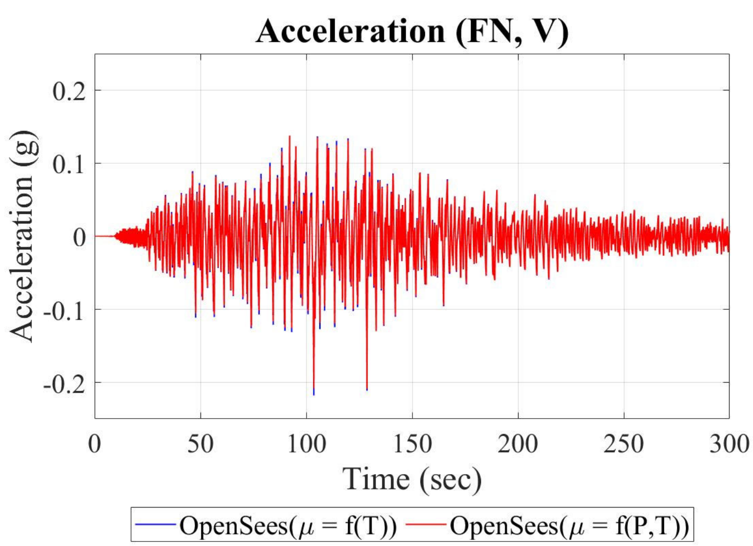

Figure 6-15 Comparison of Horizontal Acceleration Histories

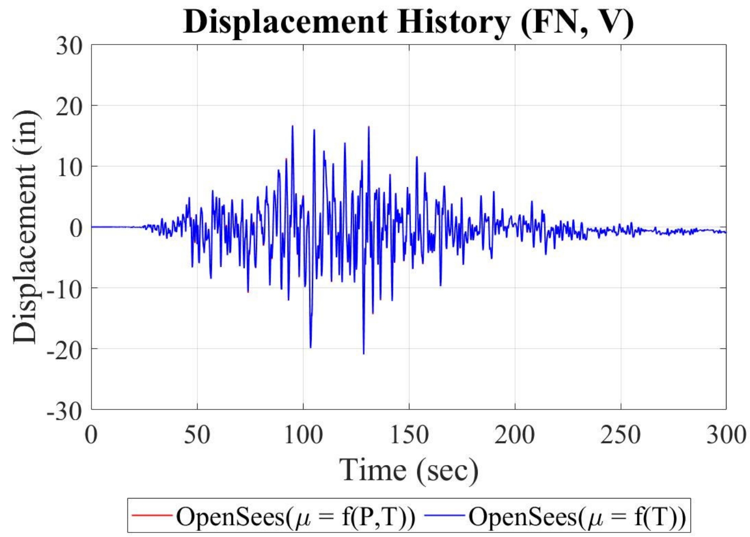

Figure 6-16 Comparison of Isolator Displacement Histories

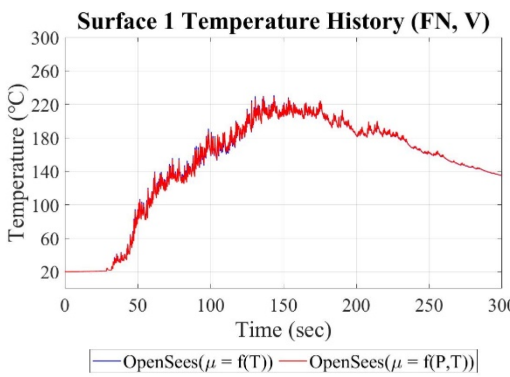

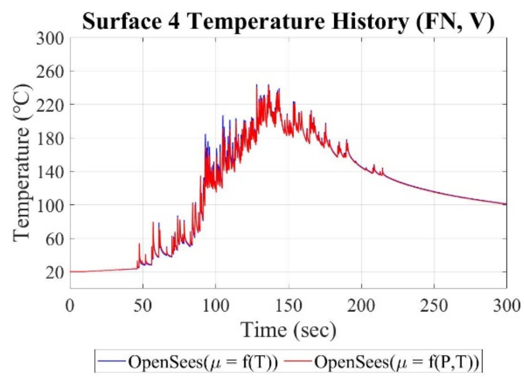

Figure 6-17 Comparison of Temperature Histories on Outer Surfaces (Surfaces 1 and 4)

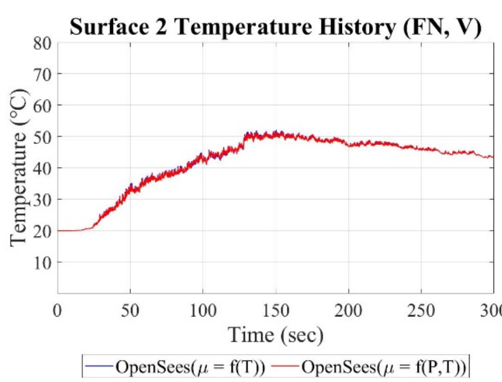

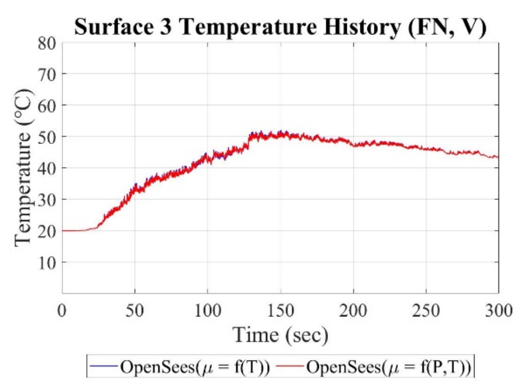

Figure 6-18 Comparison of Temperature Histories on Inner Surfaces (Surfaces 2 and 3)

B) Same Friction Coefficients ($\mu_1 = \mu_4 = 0.04,\ \mu_2 = \mu_3 = 0.01$)

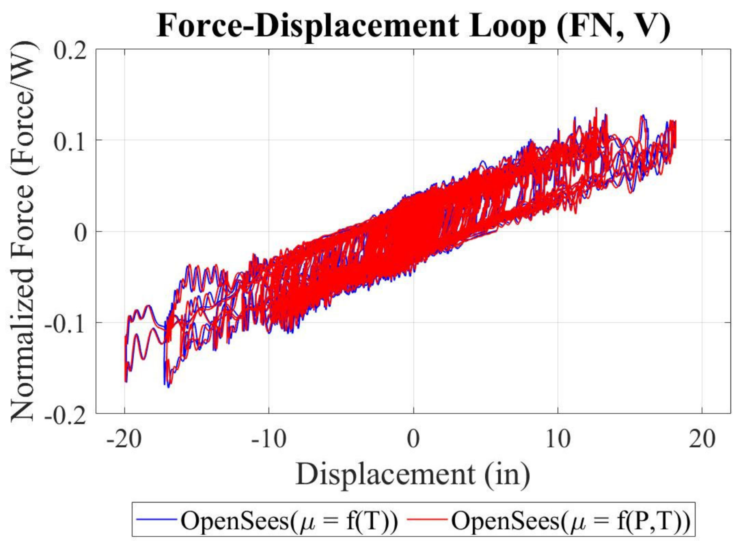

Figure 6-19 Comparison of Force-Displacement Loops (W=500kip)

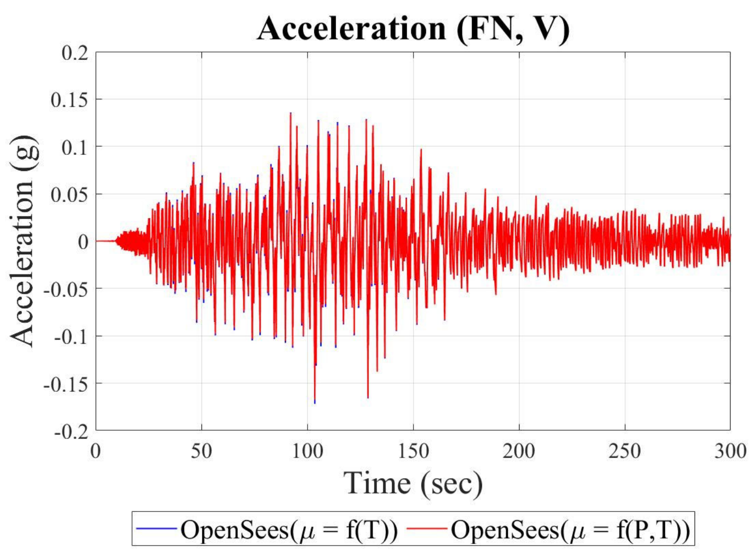

Figure 6-20 Comparison of Horizontal Acceleration Histories

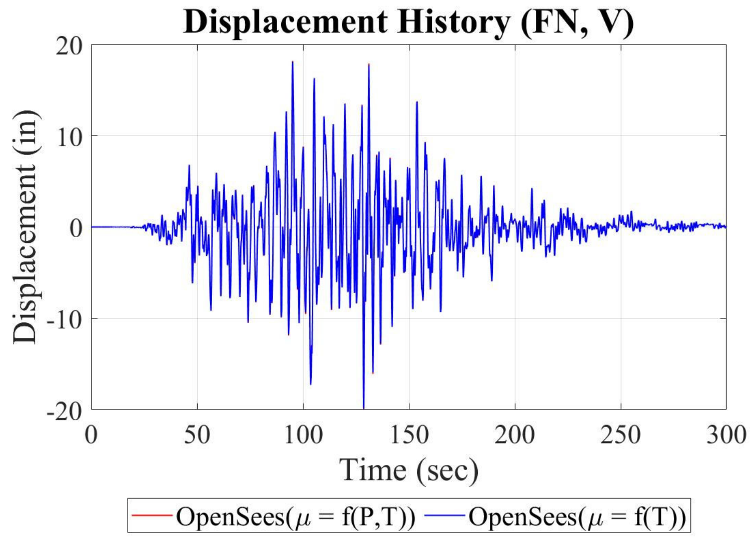

Figure 6-21 Comparison of Isolator Displacement Histories

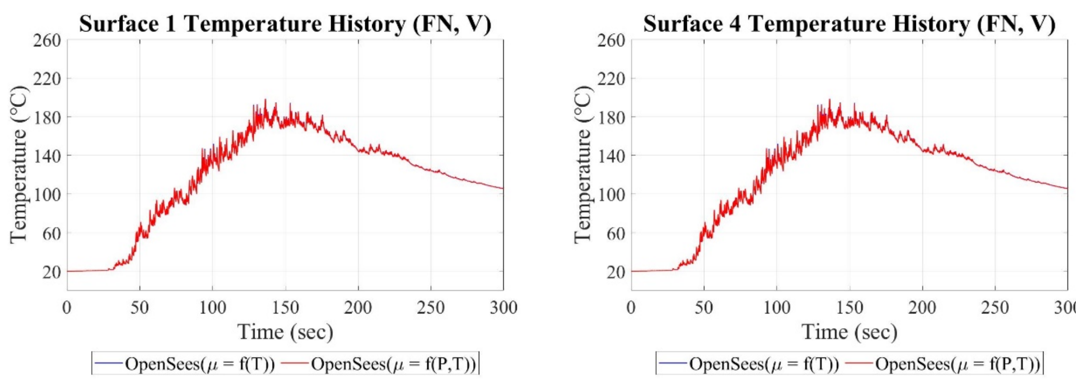

Figure 6-22 Comparison of Temperature Histories on Outer Surfaces (Surfaces 1 and 4)

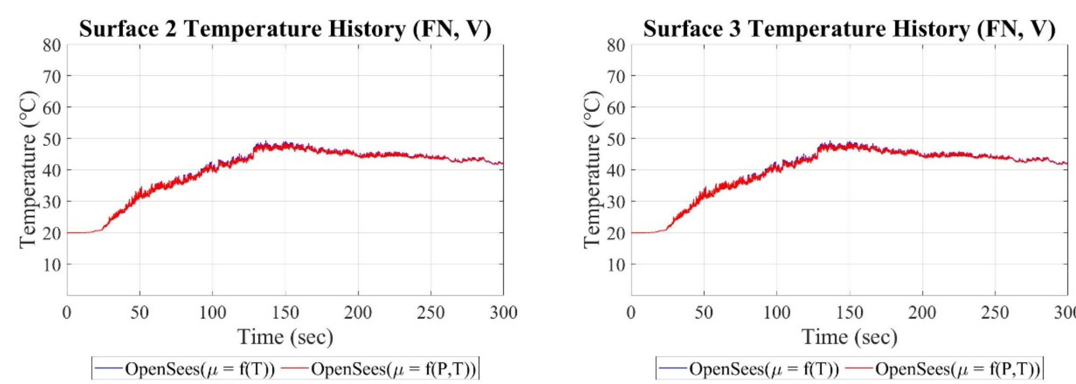

Figure 6-23 Comparison of Temperature Histories on Inner Surfaces (Surfaces 2 and 3)

6.1.4 Observations and Comments

There are insignificant differences in the computed response by program OpenSees when temperature-dependent only and when combined pressure and temperature-dependent friction are considered. The fluctuating vertical load, and thus fluctuating pressure, are not large enough to cause a significant change in behavior. Rather, temperature is important in modifying friction and has an effect on response.

6.1.5 Analysis with Pressure, Velocity and Temperature-Dependent Friction and Combined Horizontal-Vertical Ground Motion

Results produced by program OpenSees are compared for the two cases of combined pressure, velocity and temperature-dependent friction and only temperature-dependent friction ($\mu(P,T,V)$ versus $\mu(T)$ in the graphs that follow). The scale factor for FN and V components is 8.

A) Different Friction Coefficients ($\mu_1 = 0.04, \mu_4 = 0.08,\ \mu_2 = \mu_3 = 0.01$)

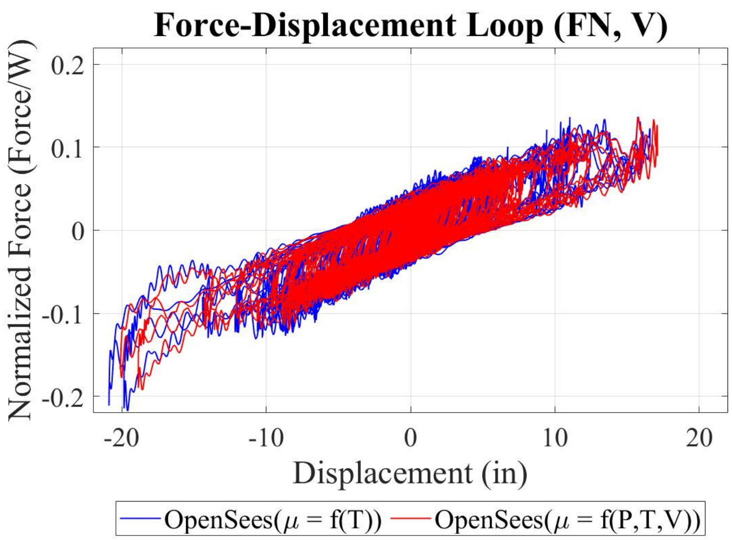

Figure 6-24 Comparison of Force-Displacement Loops (W = 500kip)

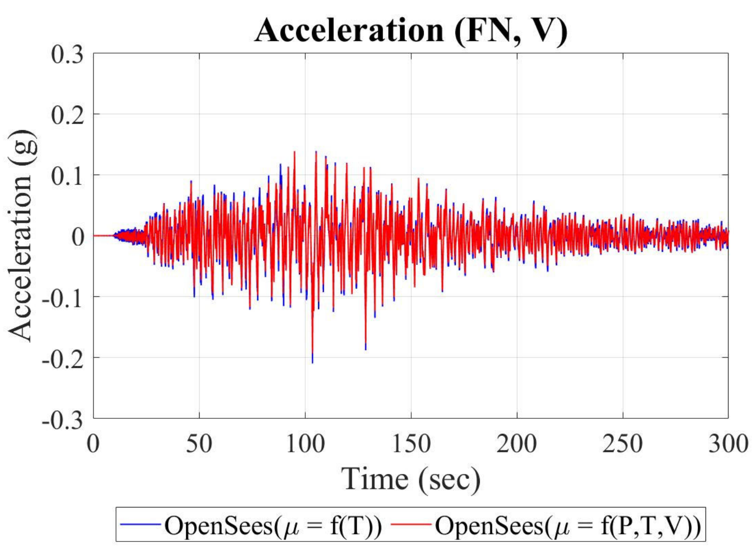

Figure 6-25 Comparison of Horizontal Acceleration Histories

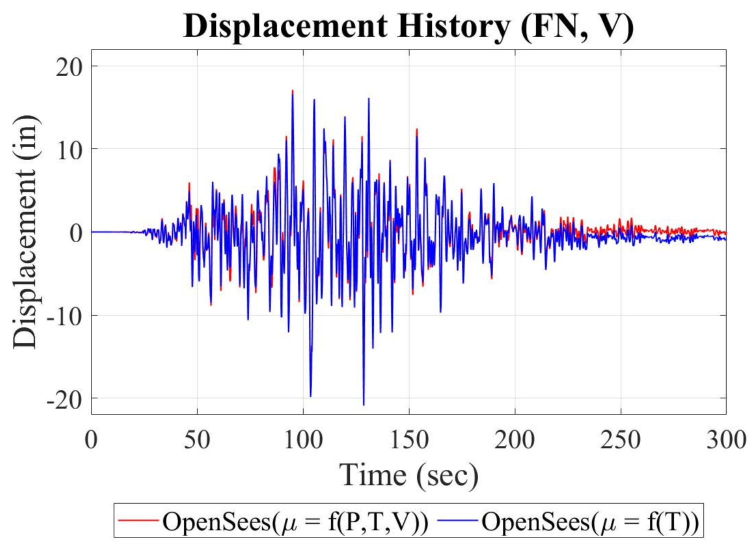

Figure 6-26 Comparison of Isolator Displacement Histories

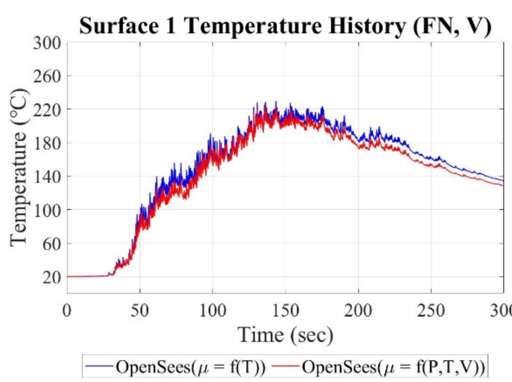

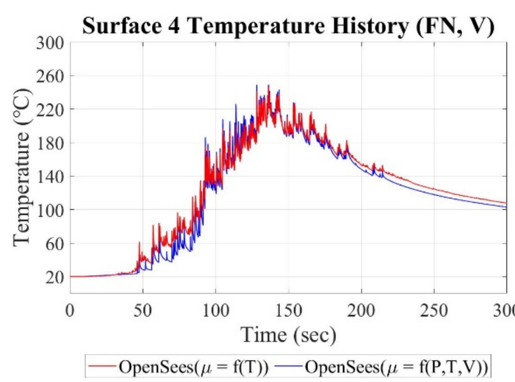

Figure 6-27 Comparison of Temperature Histories on Outer Surfaces (Surfaces 1 and 4)

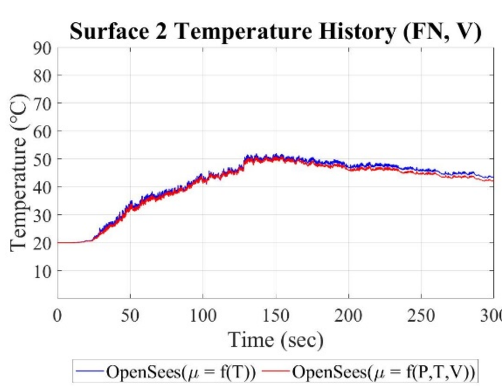

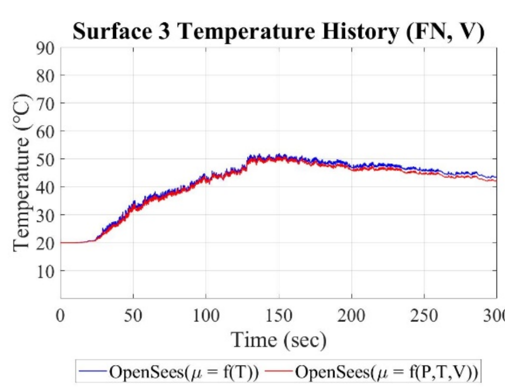

Figure 6-28 Comparison of Temperature Histories on Inner Surfaces (Surfaces 2 and 3)

B) Same Friction Coefficients ($\mu_1 = \mu_4 = 0.04,\ \mu_2 = \mu_3 = 0.01$)

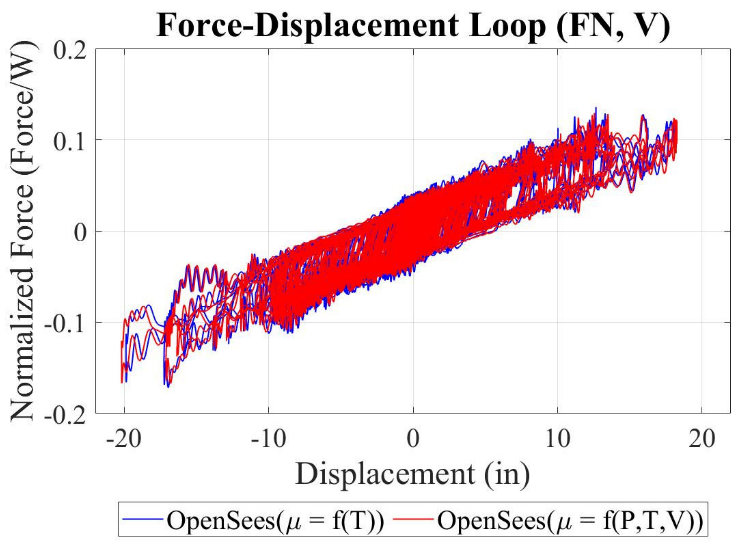

Figure 6-29 Comparison of Force-Displacement Loops (W= 500kip)

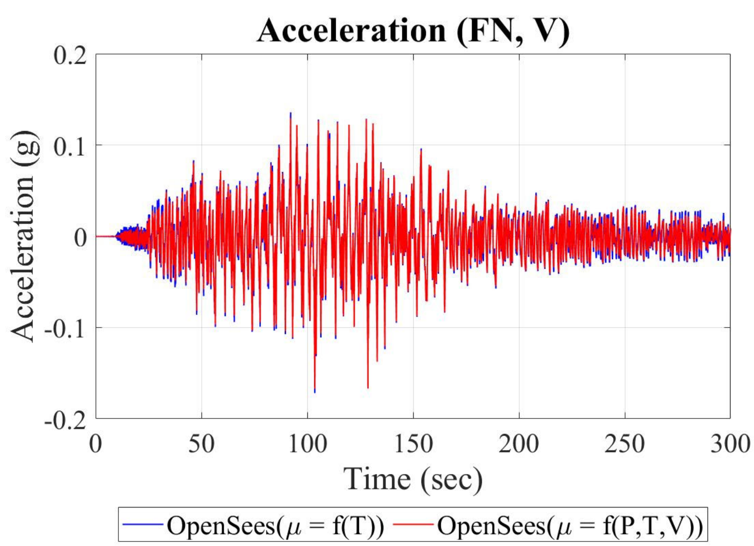

Figure 6-30 Comparison of Horizontal Acceleration Histories

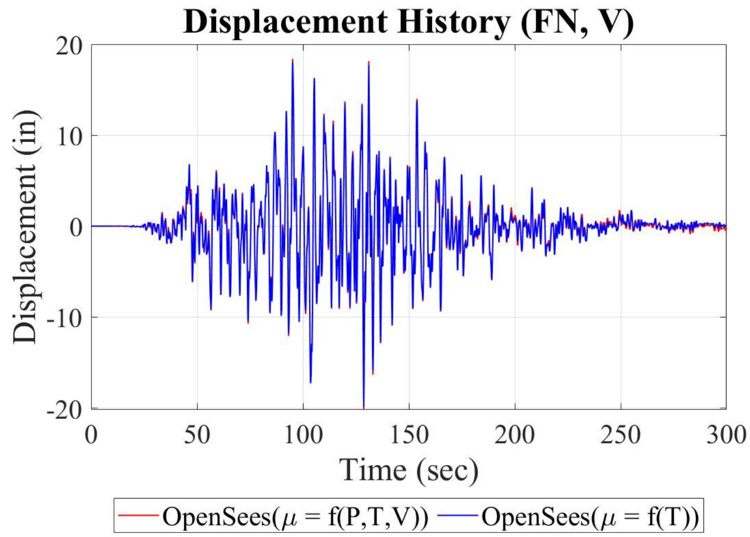

Figure 6-31 Comparison of Isolator Displacement Histories

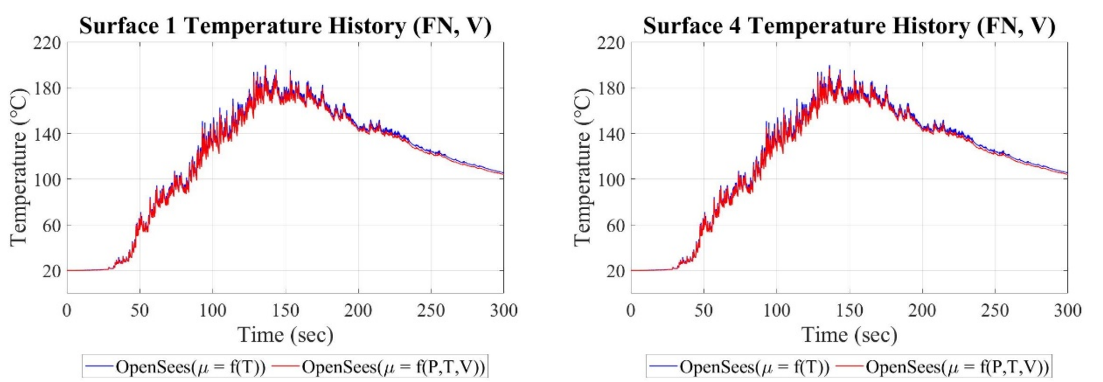

Figure 6-32 Comparison of Temperature Histories on Outer Surfaces (Surfaces 1 and 4)

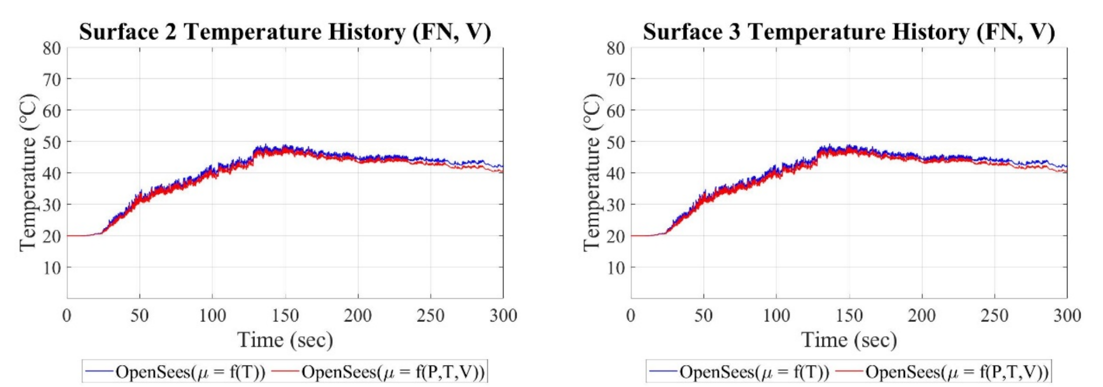

Figure 6-33 Comparison of Temperature Histories on Inner Surfaces (Surfaces 2 and 3)

6.1.6 Observations and Comments

Including the velocity dependence in the model of friction did not have any important change in the computed response for the analyzed rigid structure (it could have for the accelerations in a flexible multi-degree-of-freedom structure). The only important observation has to do with permanent displacements which are less when velocity-dependent friction is utilized. This is illustrated for the case of $\mu_1 \neq \mu_4$ for which the force-displacement loop and displacement history of the isolator are shown in Figures 6-24 and 6-26, respectively. Figure 6-34 below compares the displacement histories for surfaces 1 and 4 (unlike Figure 6-26 which shows the displacement of the top of the bearing with respect to its bottom). For surface 1 of friction coefficient equal to 0.04, there is insignificant permanent offset computed with both models. However, for surface 4 of higher friction (=0.08) there is permanent offset when the velocity dependence of friction is ignored.

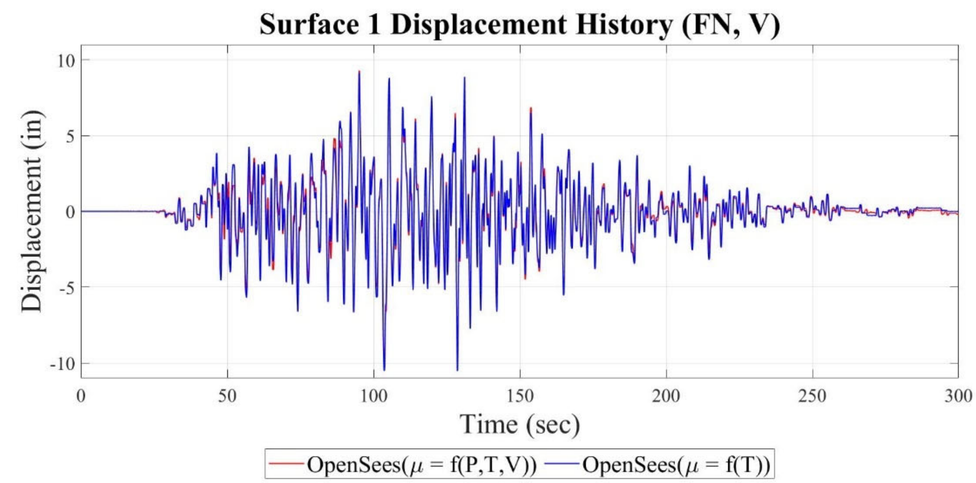

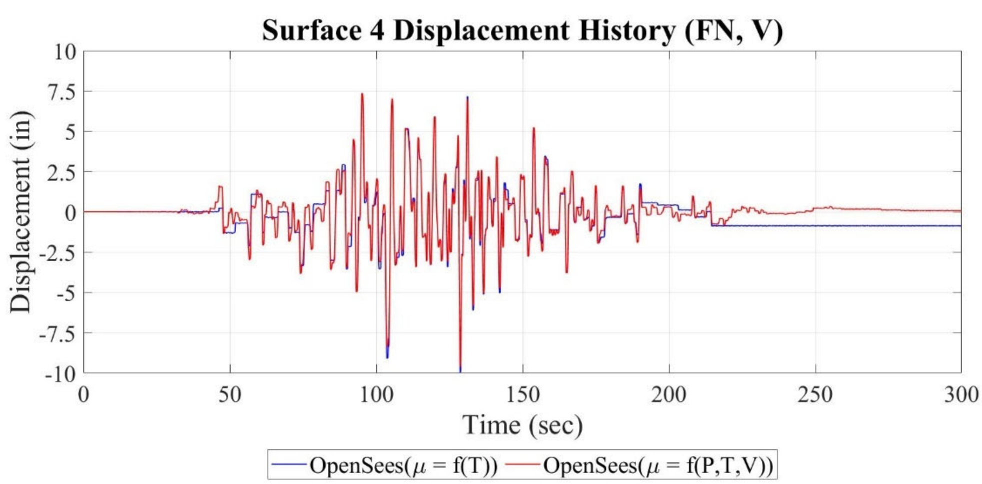

Figure 6-34 Displacement History on Surface 1 and 4 in case of unequal friction $\mu_1 \neq \mu_4$

It is interesting to observe the instantaneous values of friction computed during the analysis by the two models and shown in Figure 6-35. In the $\mu(P,T,V)$ model, there is a rapid fluctuation of the friction coefficient value between the lower and upper limits as the sliding velocity varies from zero to its maximum value in every cycle of motion. In the $\mu(T)$ model, the friction coefficient varies much less and smoothly with temperature. Evidently, consideration of the velocity dependence of friction is important when permanent offsets are assessed.

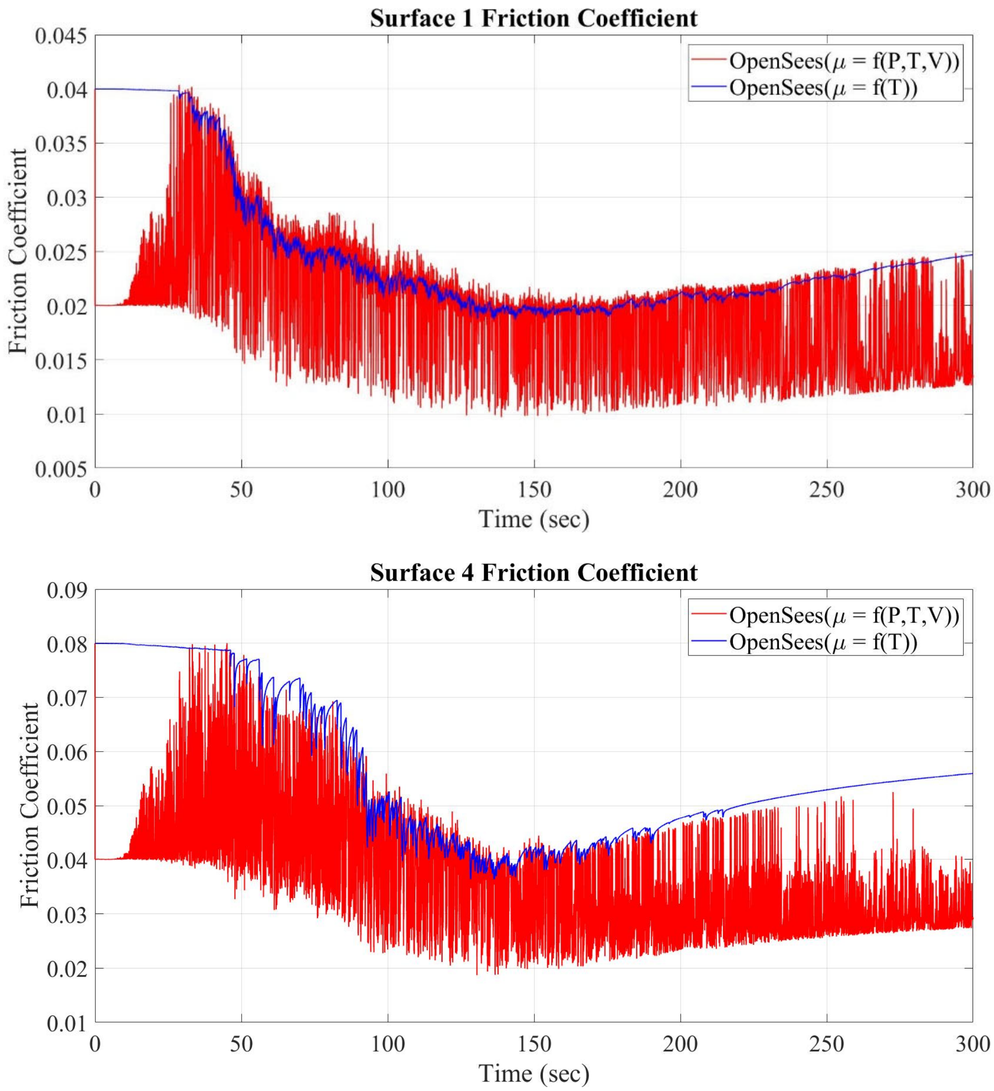

Figure 6-35 Friction Coefficient on Surface 1 and 4 in case of unequal friction $\mu_1 \neq \mu_4$

6.1.7 Analysis with Pressure, Velocity and Temperature-Dependent Friction and Triaxial Ground Motion

Results produced by program OpenSees are compared for the three cases of combined pressure, velocity and temperature-dependent friction, only temperature-dependent friction, and Coulomb friction ($\mu(P,T,V)$ versus $\mu(T)$ versus $\mu = Coulomb$ in the graphs that follow). In the analysis, the FN and FP components are used in X and Y directions, respectively. The scale factor for the FN, FP, and V components is 7. Moreover, the isolators are assumed to be without an interior ring or displacement restrainer so that the total displacement capacity is increased by $b_2/2$ and u_{limit}=26.2in. (see Table 2-1).

A) Different Friction Coefficients ($\mu_1 = 0.04, \mu_4 = 0.08,\ \mu_2 = \mu_3 = 0.01$)

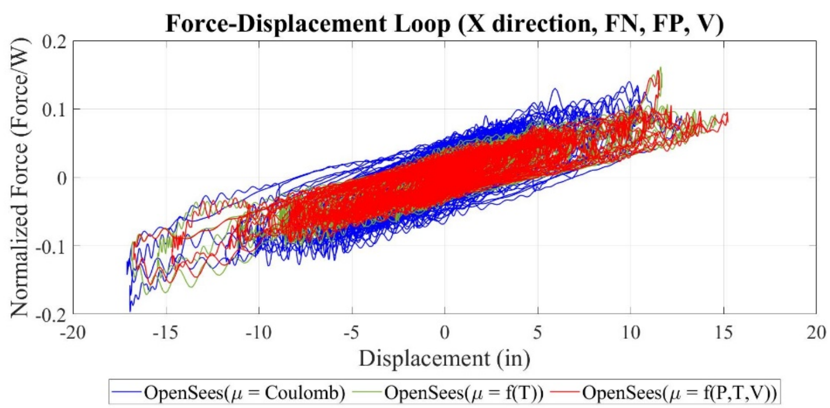

Figure 6-36 Comparison of Force-Displacement Loops in X direction for Three Cases of Friction (W = 500kip)

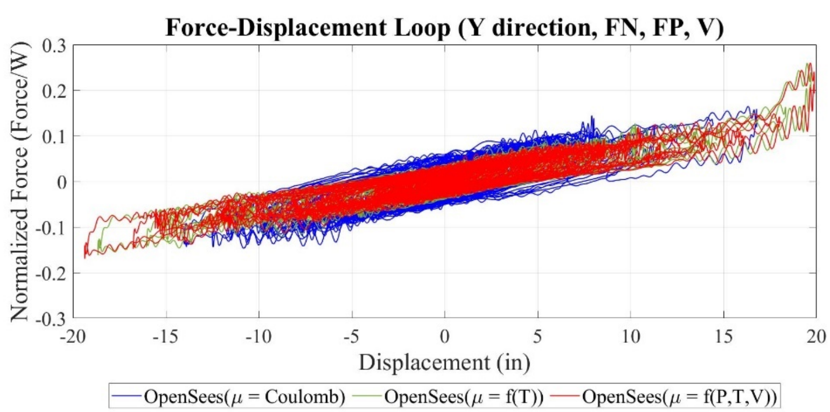

Figure 6-37 Comparison of Force-Displacement Loops in Y direction for Three Cases of Friction (W = 500kip)

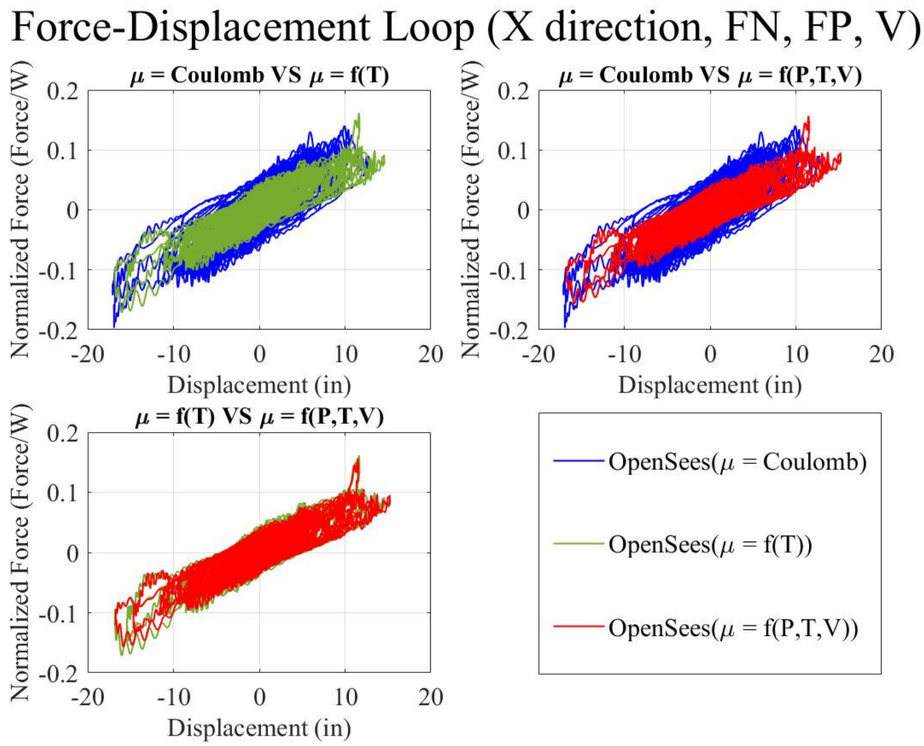

Figure 6-38 Comparison of Force-Displacement Loops in X direction (W = 500kip)

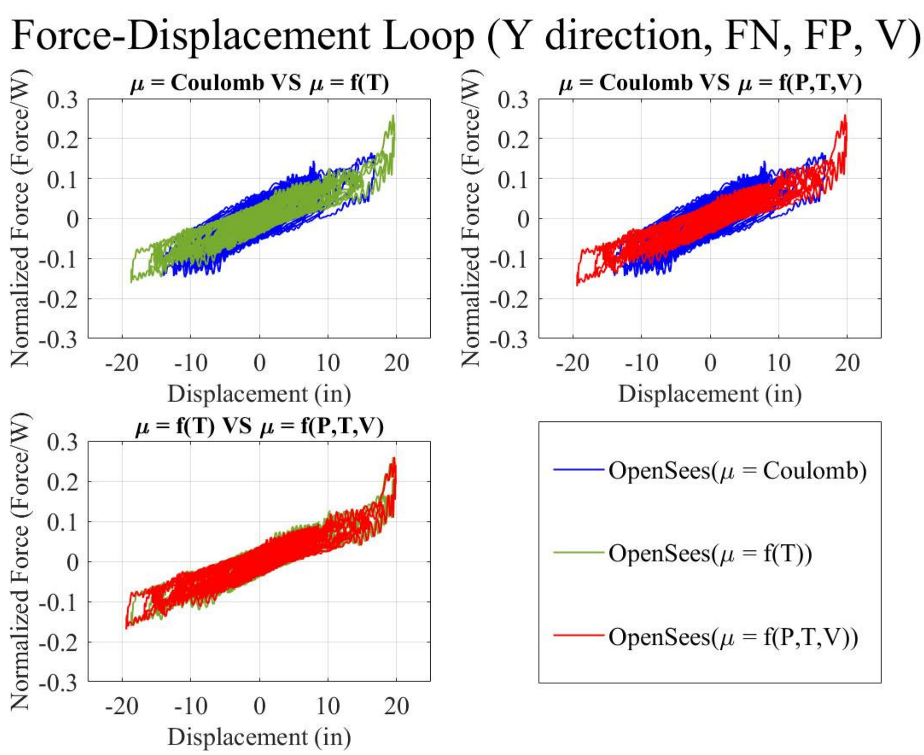

Figure 6-39 Comparison of Force-Displacement Loops in Y direction (W = 500kip)

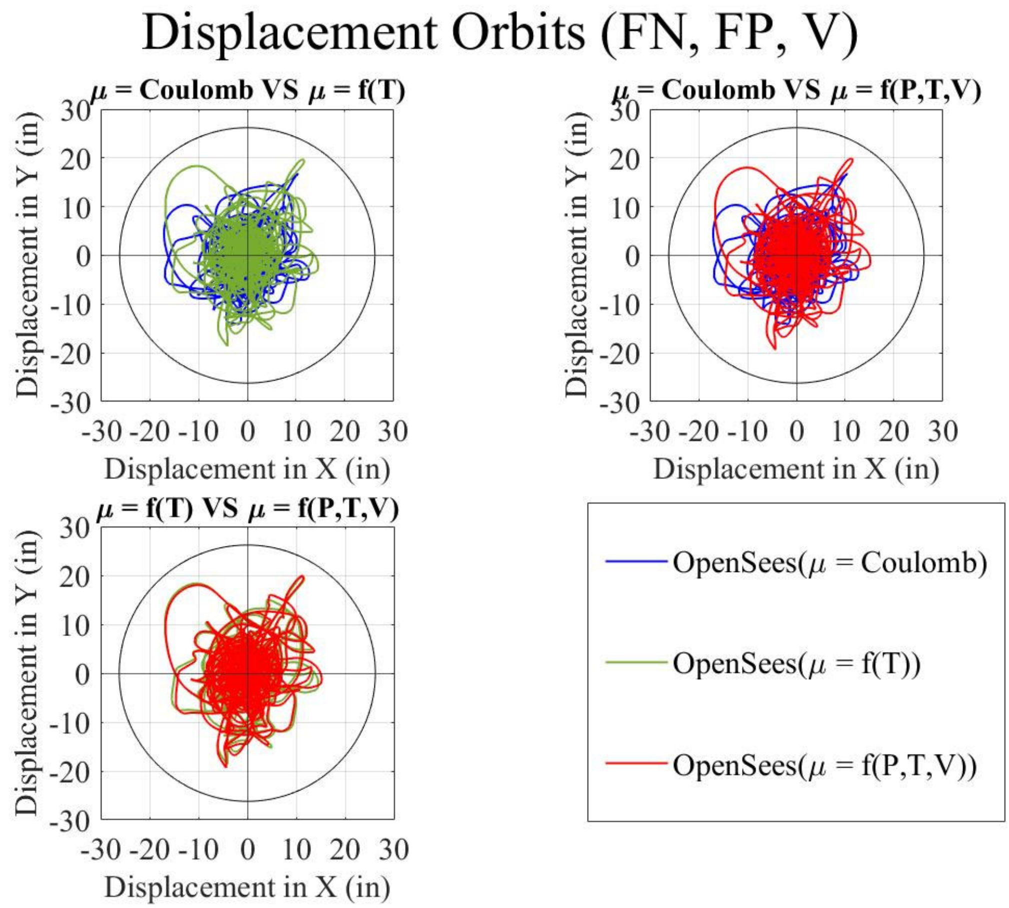

Figure 6-40 Comparison of Isolator Displacement Orbits (Circle shows u_{limit}=26.2in)

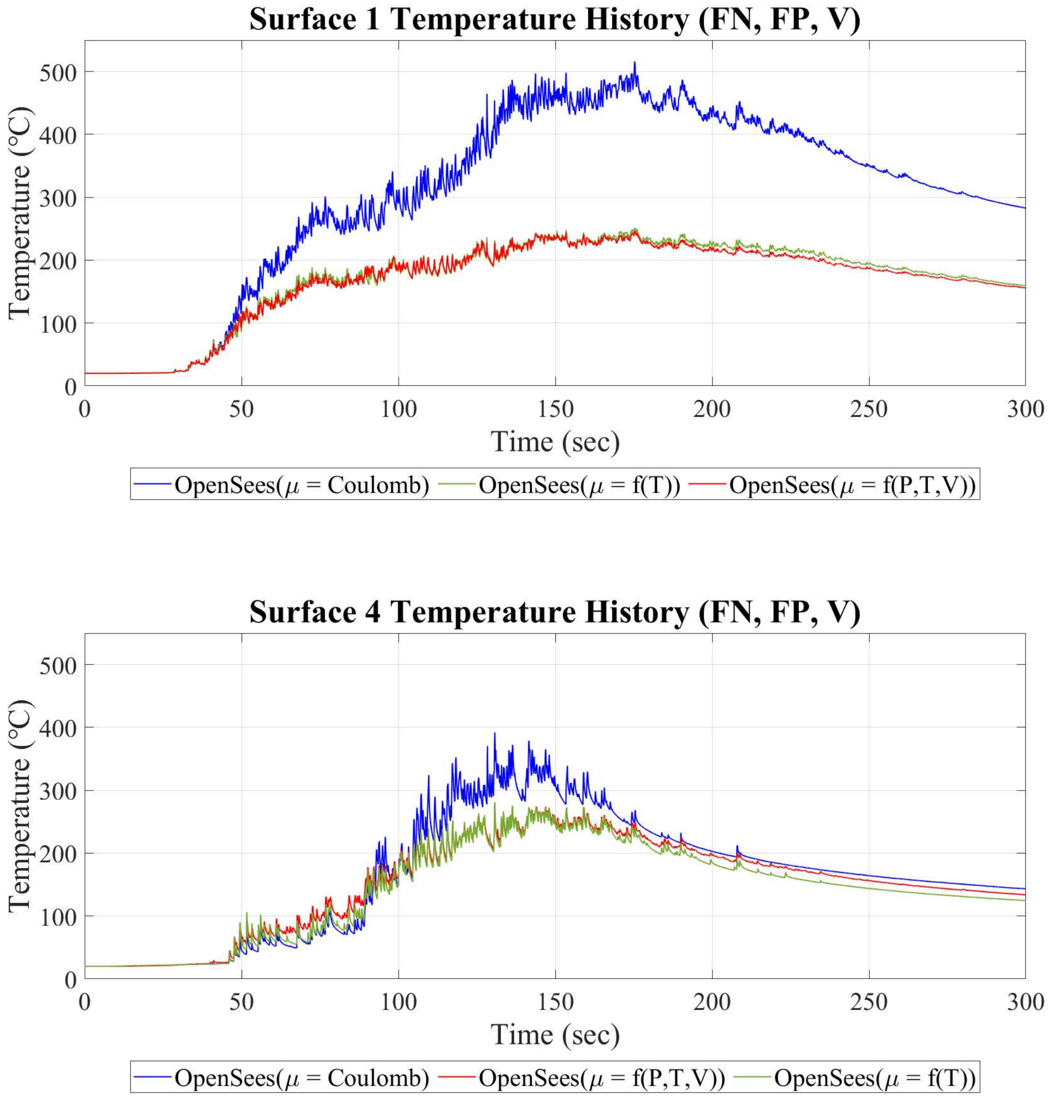

Figure 6-41 Comparison of Temperature Histories on Outer Surfaces (Surfaces 1 and 4)

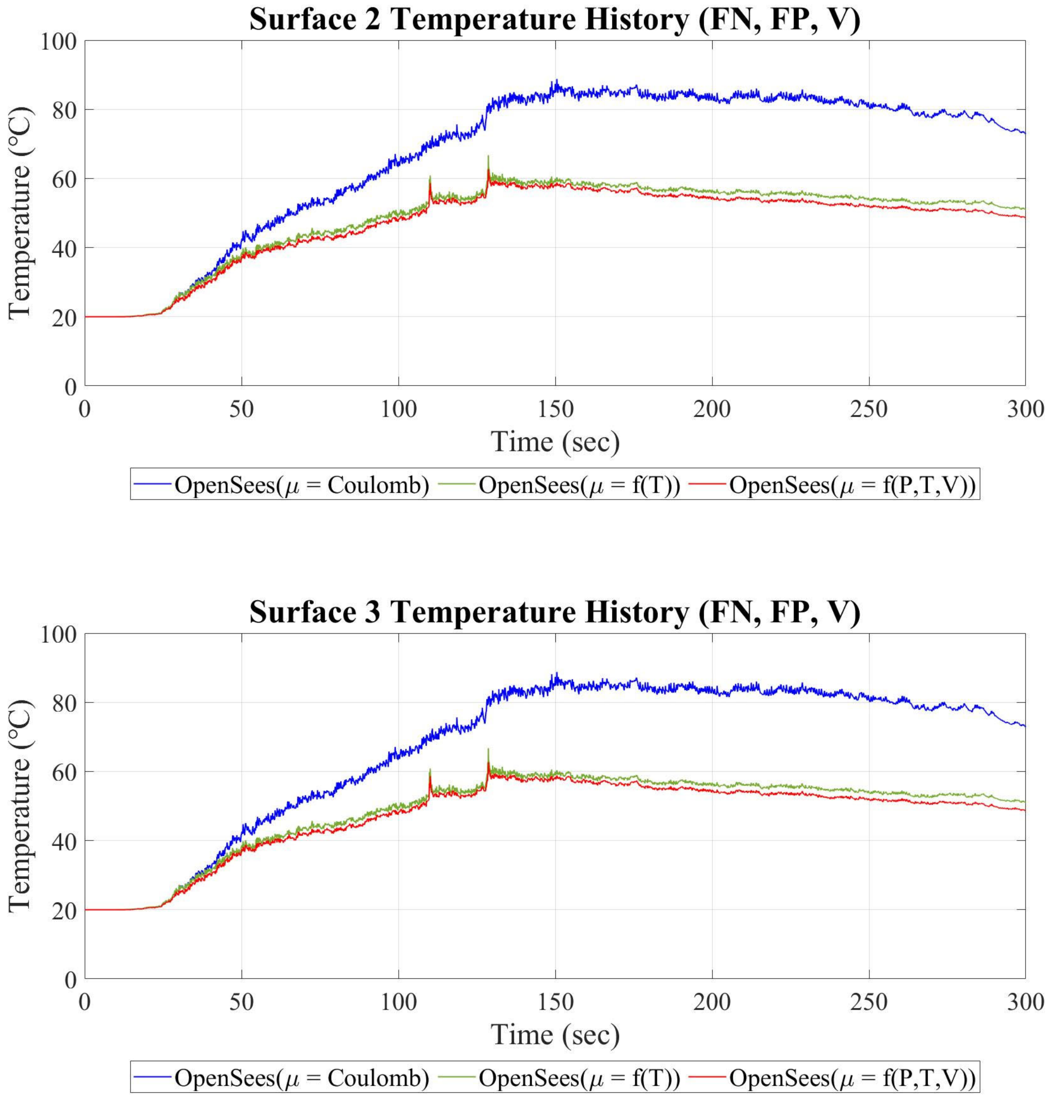

Figure 6-42 Comparison of Temperature Histories on Inner Surfaces (Surfaces 2 and 3)

B) Same Friction Coefficients ($\mu_1 = \mu_4 = 0.04,\ \mu_2 = \mu_3 = 0.01$)

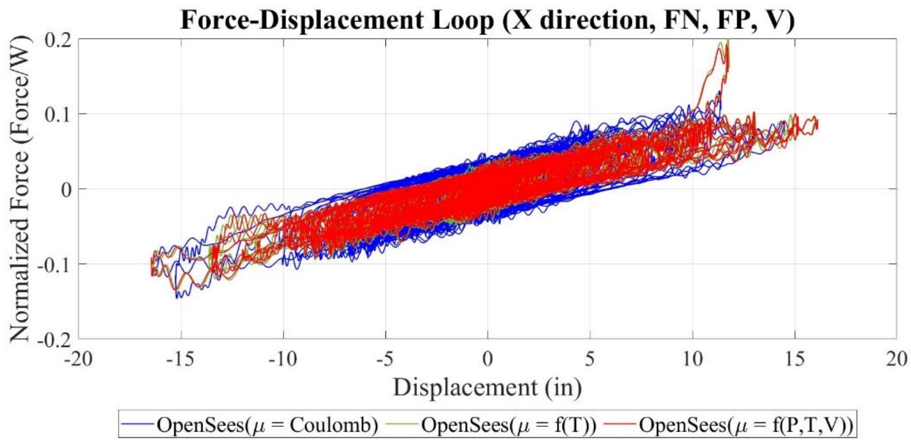

Figure 6-43 Comparison of Force-Displacement Loops in X direction for Three Cases of Friction (W = 500kip)

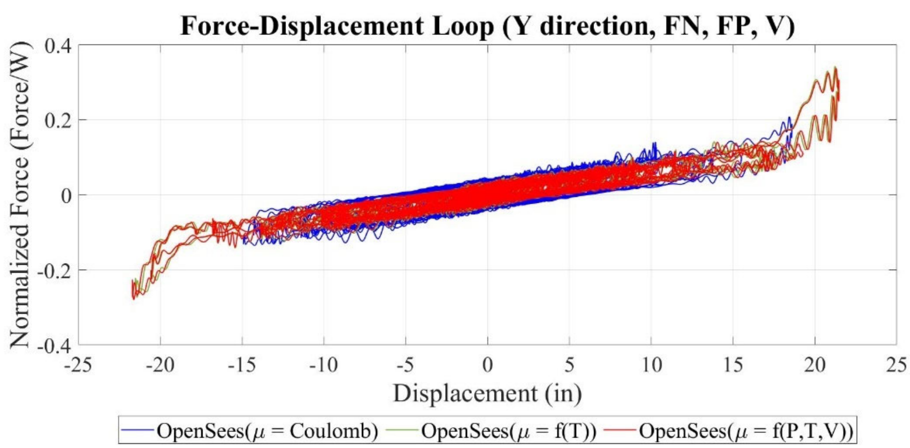

Figure 6-44 Comparison of Force-Displacement Loops in Y direction for Three Cases of Friction (W = 500kip)

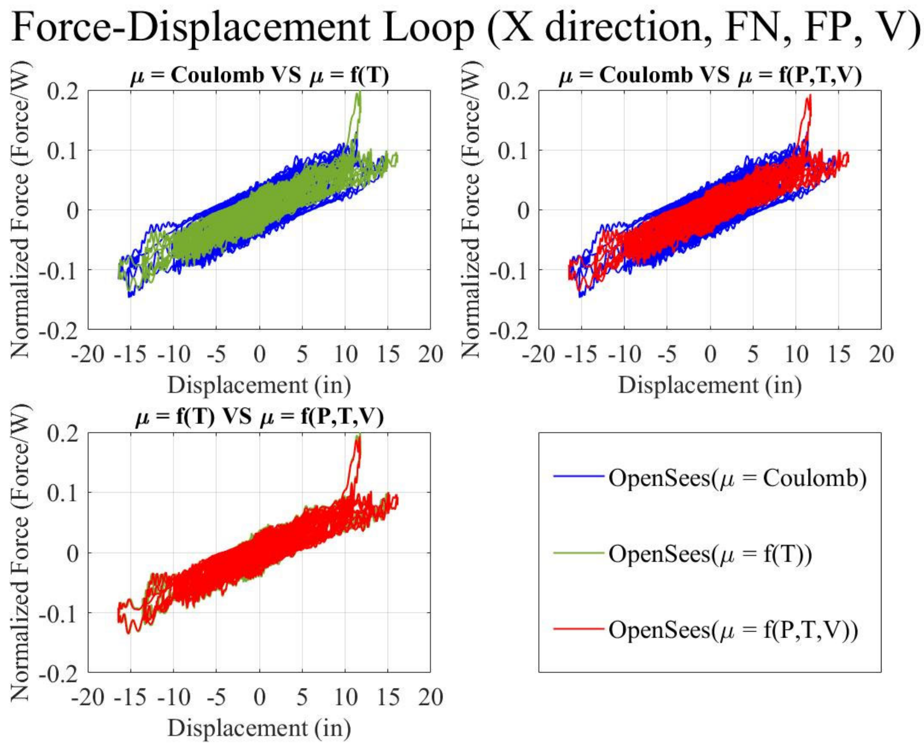

Figure 6-45 Comparison of Force-Displacement Loops in X direction (W = 500kip)

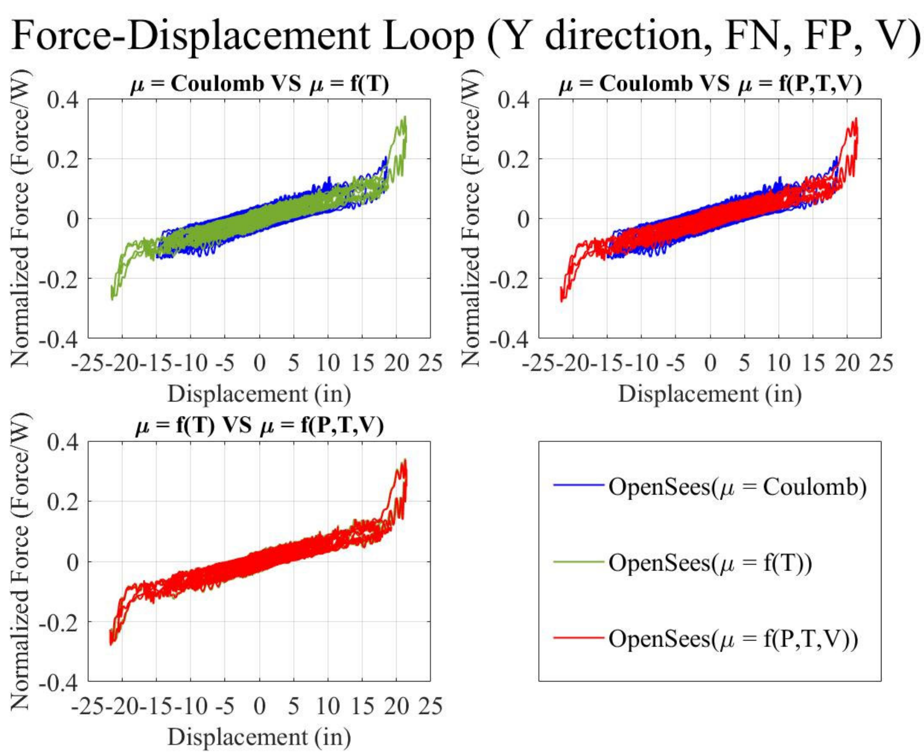

Figure 6-46 Comparison of Force-Displacement Loops in Y direction (W = 500kip)

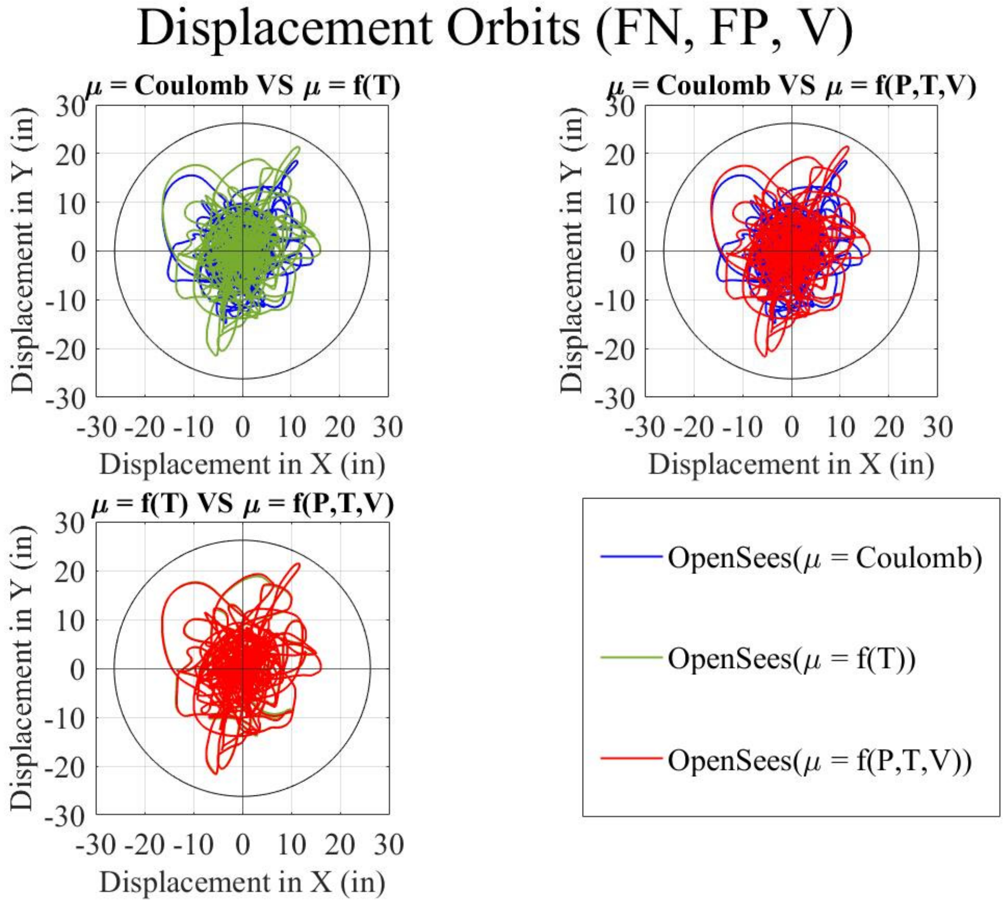

Figure 6-47 Comparison of Isolator Displacement Orbits (Circle shows u_{limit}=26.2in)

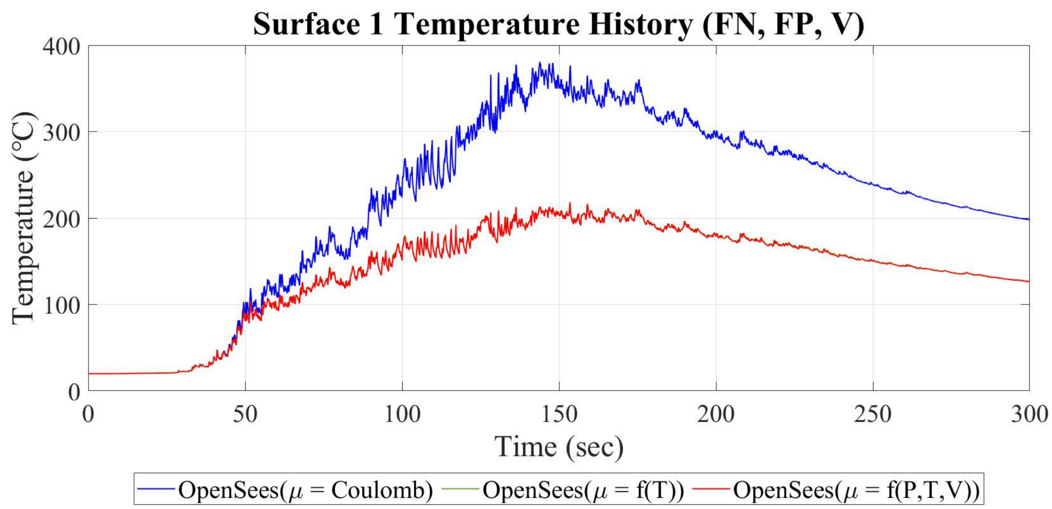

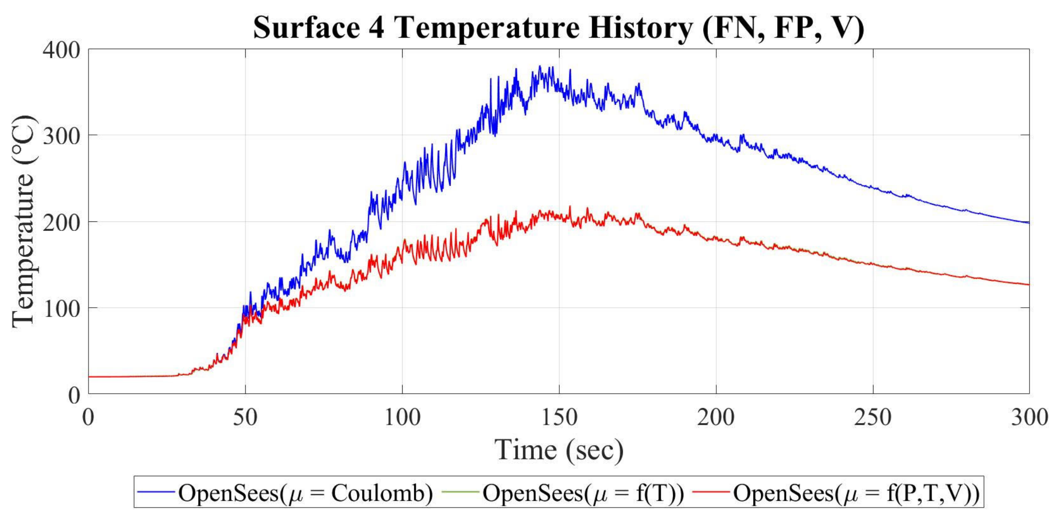

Figure 6-48 Comparison of Temperature Histories on Outer Surfaces (Surfaces 1 and 4)

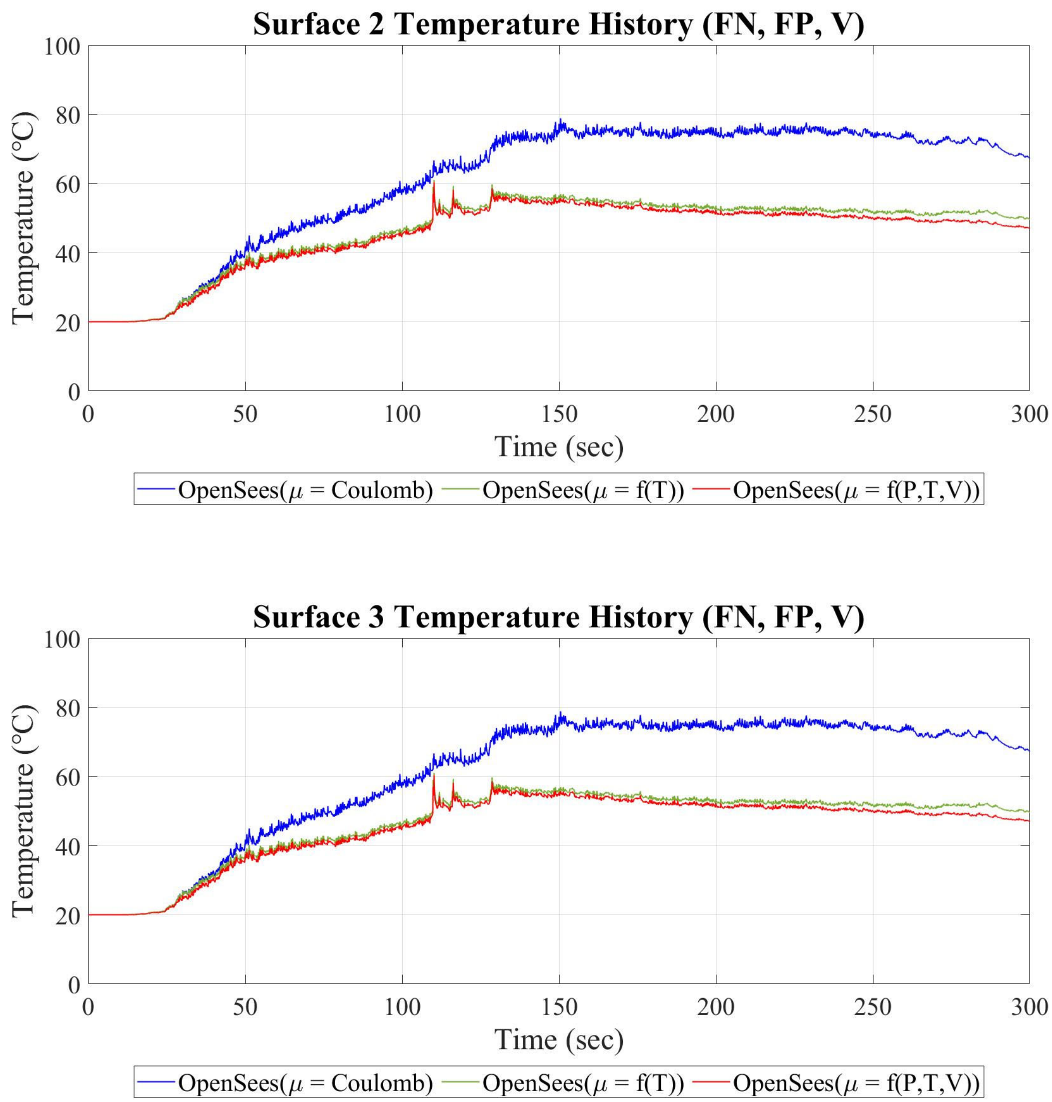

Figure 6-49 Comparison of Temperature Histories on Inner Surfaces (Surfaces 2 and 3)

6.1.8 Observations and Comments

Overall, observations and comments made in subsection 6.1.6 are still valid. The most important parameter that affects the response is the temperature dependence of the coefficient of friction, whereas the pressure and velocity effects are minor. As expected, the triaxial ground motion results in increases in the isolator response in terms of displacements and temperature at the sliding interfaces. The increase in displacement demand results in the isolators entering regime V (high stiffness) so that the shear force is significantly increased.

6.1.9 Comparison of Results Produced by Elements TripleFrictionPendulum and TripleFrictionPendulumX in OpenSees

Results for triaxial ground motion produced by TripleFrictionPendulum and TripleFrictionPendulumX elements in program OpenSees are compared in the case of constant friction coefficients when the two elements should produce identical results. In the analysis, the FN and FP components are used in X and Y directions, respectively. The temperature is calculated only by element TripleFrictionPendulumX and its histories are presented. The scale factor for FN, FP, and V components is 7.

A) **Different Friction Coefficients ($\mu_1 = 0.04, \mu_4 = 0.08,\ \mu_2 = \mu_3 = 0.01$)**

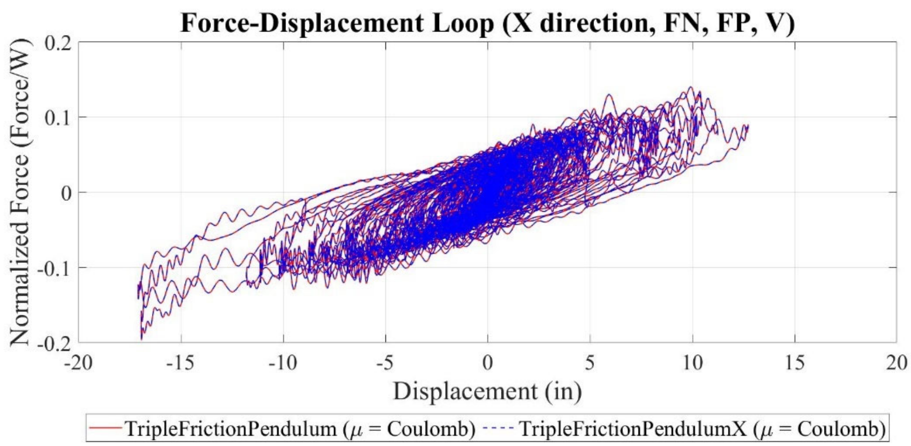

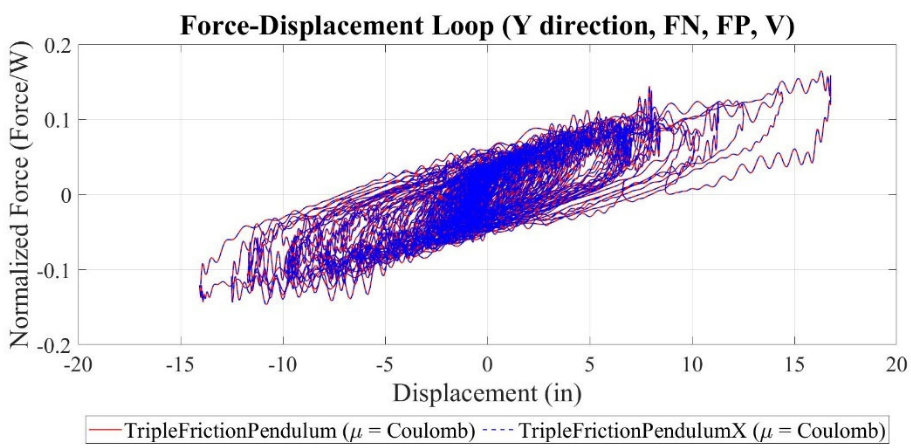

Figure 6-50 Comparison of Force-Displacement Loops (W = 500kip)

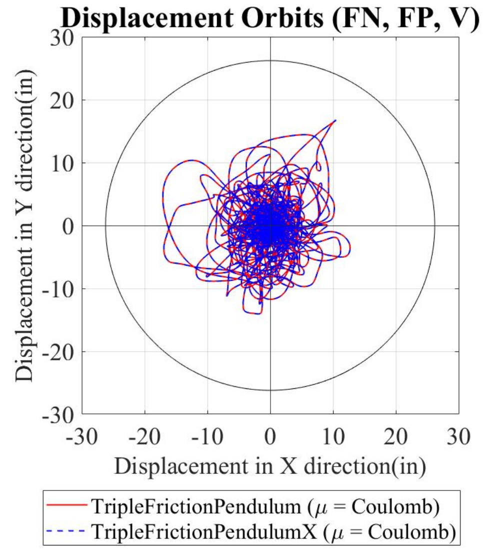

Figure 6-51 Comparison of Isolator Displacement Orbits (Circle shows u_{limit}=26.2in)

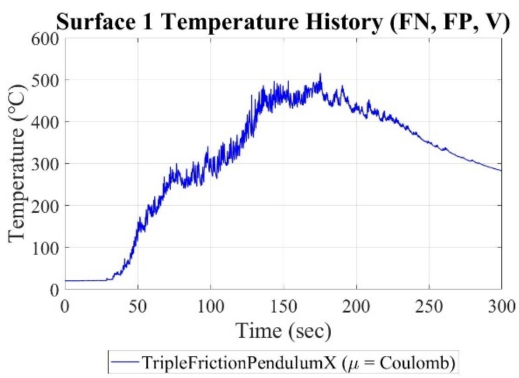

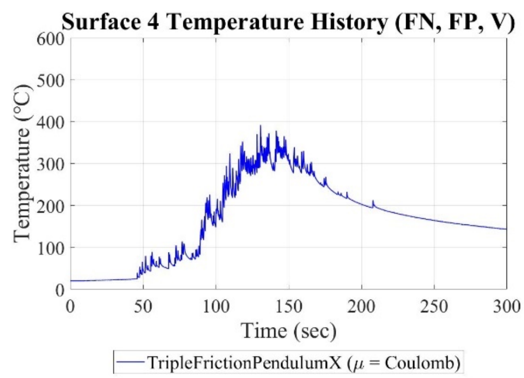

Figure 6-52 Comparison of Temperature Histories on Outer Surfaces (Surfaces 1 and 4)

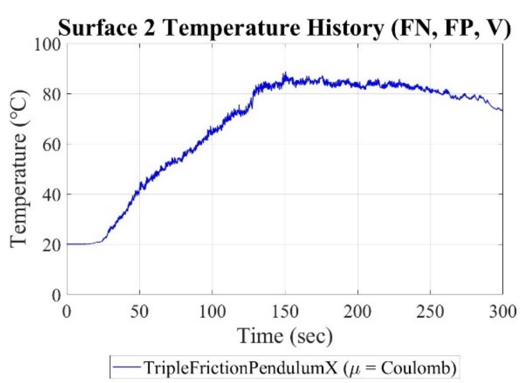

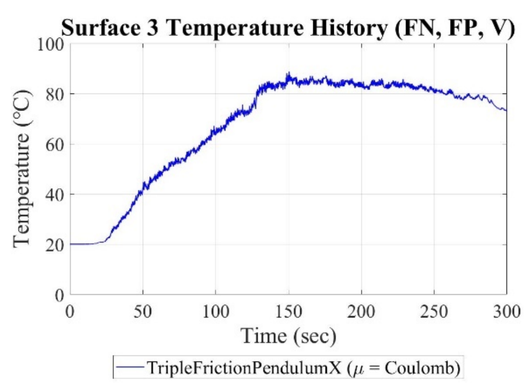

Figure 6-53 Comparison of Temperature Histories on Inner Surfaces (Surfaces 2 and 3)

A) Same Friction Coefficients ($\mu_1 = \mu_4 = 0.04,\ \mu_2 = \mu_3 = 0.01$)

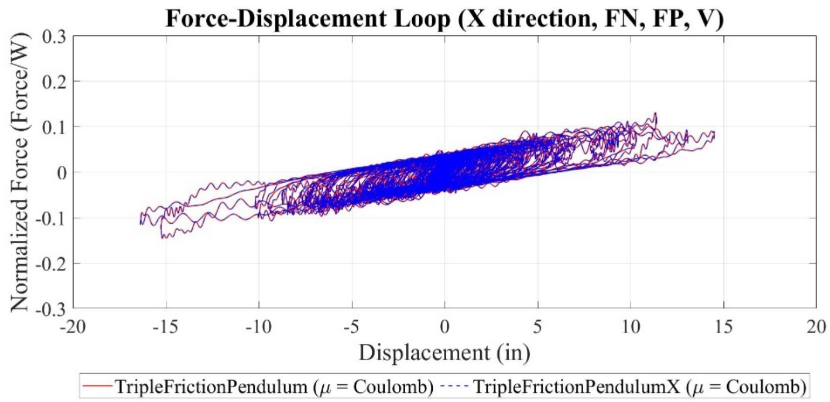

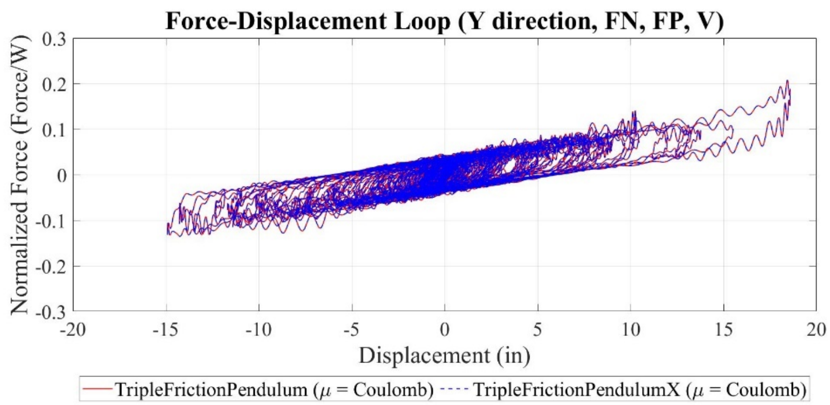

Figure 6-54 Comparison of Force-Displacement Loops (W= 500kip)

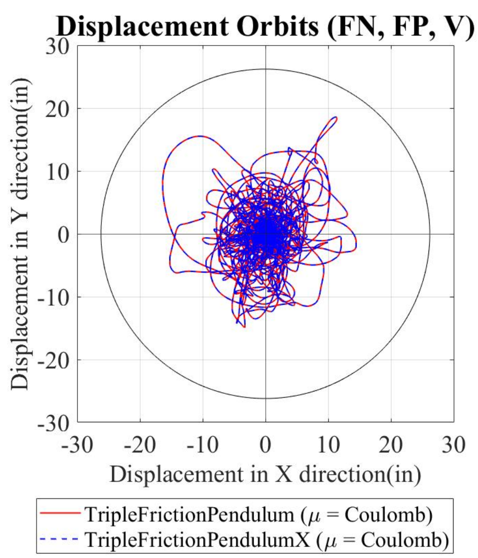

Figure 6-55 Comparison of Isolator Displacement Orbits (Circle shows u_{limit}=26.2in)

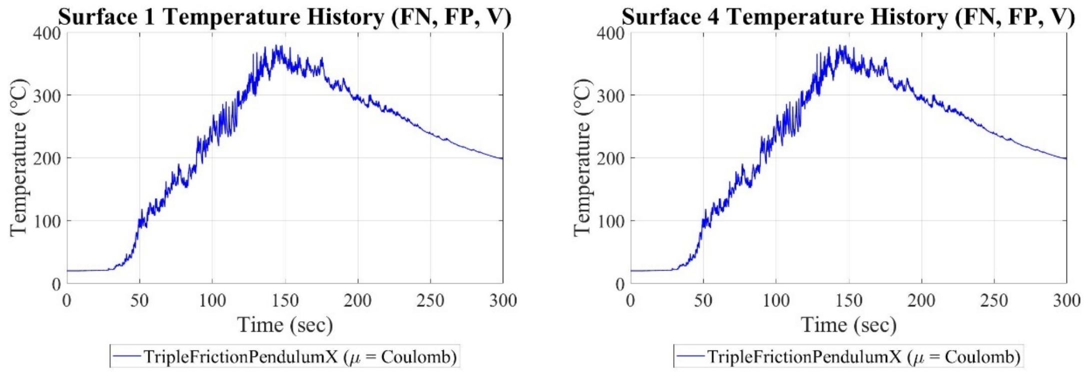

Figure 6-56 Comparison of Temperature Histories on Outer Surfaces (Surfaces 1 and 4)

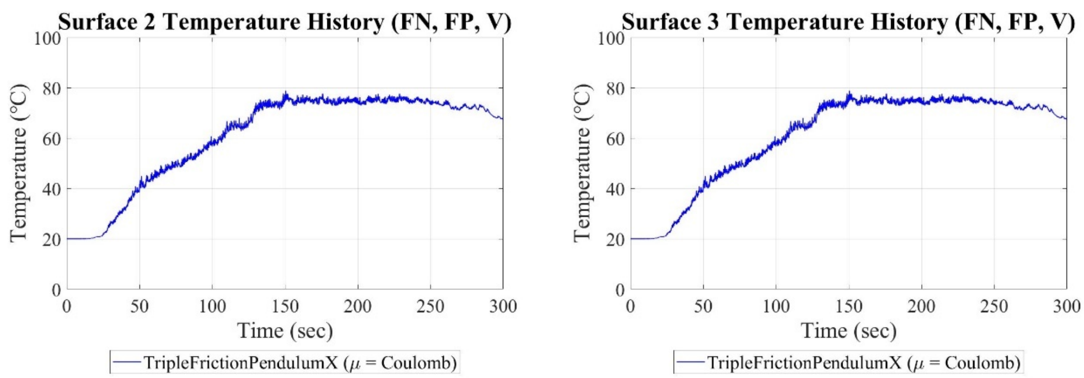

Figure 6-57 Comparison of Temperature Histories on Inner Surfaces (Surfaces 2 and 3)

6.1.10 Observations and Comments

Elements TripleFrictionPendulum and TripleFrictionPendulumX in program OpenSees produce identical results in the case of constant friction coefficients.

SECTION 7
IMPLEMENTING NEW TRIPLE FP BEARING ELEMENT IN PROGRAM OPENSEES

Element TripleFrictionPendulumX has not been implemented in program OpenSees for direct use. Rather, interested users need to obtain the source code of program OpenSees and attach to it the source code for element TripleFrictionPendulumX. Details on how to do this and the source code for element TripleFrictionPendulumX are provided in a digital appendix entitled IMPLEMENTING "TRIPLEFRICTIONPENDULUMX" ELEMENT IN OPENSEES which can be obtained from the authors.

SECTION 8
SUMMARY AND CONCLUSIONS

This report presented an enhancement of the theory for the Triple FP isolators presented by Fenz et al (2018a, b, c, d, 2019) which was used in the implementation of a Triple FP element in program OpenSees (Dao et al., 2013). The enhanced theory computes the displacement and velocity histories at each of the four sliding interfaces of the isolator which are then used to introduce dependence of the coefficient of friction on axial pressure, sliding velocity, and temperature. The Dao et al. (2013) element in program OpenSees has been modified to introduce dependencies on pressure, velocity and temperature. The dependency on temperature is a new development, whereas the dependency on velocity is direct and based on the actual sliding velocities rather than based on the partitioning of velocity of the Fenz et al. (2008a, b, c, d, 2019) model.

Several examples have been presented in which results obtained by this model in program OpenSees were compared with results obtained by a much more complex and advanced model implemented in program 3pleANI (Sarlis et al., 2013, 2016). There is good agreement in the results in terms of displacement, velocity and temperature histories at the four sliding interfaces, and of force-displacement loops. Furthermore, the enhanced Triple FP element in OpenSees has been verified.

SECTION 9
REFERENCES

1. Burden, R. L. and Faires, J. D. (1989). "Numerical Analysis", 4th edn (Boston: PWS-Kent).
2. Chandramohan, R., Baker, J. W. and Deierlein, G. G. (2016). "Quantifying the influence of ground motion duration on structural collapse capacity using spectrally equivalent records", Earthquake Spectra, 32(2), 927-950.
3. Computers and Structures, Inc. (2011). "SAP 2000—Integrated Software for Structural Analysis and Design".
4. Constantinou, M. C., Whittaker, A. S., Kalpakidis, Y., Fenz, D. M. and Warn, G. P. (2007). "Performance of seismic isolation hardware under service and seismic loading", Report No. MCEER-07-0012, Multidisciplinary Center for Earthquake Engineering Research, Buffalo, NY.
5. Constantinou, M. C., Kalpakidis, I., Filiatrault, A., and Ecker Lay, R. A. (2011). "LRFD-Based Analysis and Design Procedures for Bridge Bearings and Seismic Isolators", Report No. MCEER-11-0004, Multidisciplinary Center for Earthquake Engineering Research, Buffalo, NY.
6. Dao, N. D., Ryan, K. L., Sato, E. and Sasaki, T. (2013). "Predicting the displacement of triple pendulum bearings in a full-scale shaking experiment using a three-dimensional element", Earthquake engineering and structural dynamics, 42(11), 1677-1695.
7. Fenz, D. M. and Constantinou, M. C. (2008a), "Spherical sliding isolation bearings with adaptive behavior: Theory", Earthquake Engineering and Structural Dynamics, Vol. 37, No. 2, 163-183.
8. Fenz, D. M. and Constantinou, M. C. (2008b), "Spherical sliding isolation bearings with adaptive behavior: Experimental verification", Earthquake Engineering and Structural Dynamics, Vol. 37, No. 2, 185-205.
9. Fenz, D. M. and Constantinou, M. C. (2008c). "Mechanical behavior of multi-spherical sliding bearings", Report No. MCEER 08-0007, Multidisciplinary Center for Earthquake Engineering Research, Buffalo, NY.
10. Fenz, D. M. and Constantinou, M. C. (2008d), "Development, implementation and verification of dynamic analysis models for multi-spherical sliding bearings", Report No. MCEER-08-0018, Multidisciplinary Center for Earthquake Engineering Research, Buffalo, NY.
11. Fenz, D. M. and Constantinou, M. C. (2009), "Modelling Triple Friction Pendulum bearings for response-history analysis", Earthquake Spectra, Vol. 24, No. 4, 1011-1028.
12. Kumar, M., Whittaker, A. S. and Constantinou, M. C. (2015). "Seismic isolation of nuclear power plants using sliding bearings", Report MCEER-15-0006, Multidisciplinary Center for Earthquake Engineering Research, Buffalo, NY.

13. McKenna, F., Scott, M. H. and Fenves, G. L. (2010). “Nonlinear finite-element analysis software architecture using object composition”, Journal of Computing in Civil Engineering, 24(1), 95-107.
14. National Research Institute for Earth Science and Disaster Resilience (2019). “NIED K-NET, KiK-net”.
15. Sarlis, A. A. and Constantinou, M. C. (2010), “Modeling Triple Friction Pendulum Isolators in Program SAP2000”, document distributed to the engineering community together with example files, University at Buffalo.
16. Sarlis, A. A. and Constantinou, M. C. (2013). ”Model of Triple Friction Pendulum bearing for general geometric and frictional parameters and for uplift conditions”, Report No. MCEER-13-0010, Multidisciplinary Center for Earthquake Engineering Research, State University of New York at Buffalo, Buffalo, NY.
17. Sarlis, A. A. and Constantinou, M. C. (2016). “A model of Triple Friction Pendulum Bearing for general geometric and frictional parameters”, Earthquake Engineering & Structural Dynamics, 45(11), 1837-1853.
18. Tsopelas, P. C., Roussis, P. C., Constantinou, M. C, Buchanan, R. and Reinhorn, A. M. (2005), “3D-BASIS-ME-MB: Computer program for nonlinear dynamic analysis of seismically isolated structures”, Report No. MCEER-05-0009, Multidisciplinary Center for Earthquake Engineering Research, Buffalo, NY.

APPENDIX A

PARAMETERS USED IN ANALYSIS IN PROGRAM OPENSEES

Table A-1 presents values of the parameters used in each example presented in Sections 4, 5 and 6. All parameters are defined in the report except for the following: Y is yield displacement in the friction model; dt_{load} is loading time step; dt is analysis time step; Tol is a convergence tolerance parameter utilized by the Newton-Raphson method that is used in the numerical solution; a is friction velocity rate parameter (see equation 2-3).

Table A-1 Parameters Used in Analysis

Section	Model	Motion	Isolator Configuration	Model Parameters
4.1.1	Constant μ	Amplitude = 20in Period = 20sec	Configuration A ($\mu_1 = 0.04$, $\mu_4 = 0.08$, $\mu_2 = \mu_3 = 0.01$)	Y = 0.04in, dt_{load} = 0.001sec, dt = 0.001sec, Tol = 10^{-5}
			Configuration A ($\mu_1 = \mu_4 = 0.04$, $\mu_2 = \mu_3 = 0.01$)	Y = 0.04in, dt_{load} = 0.001sec, dt = 0.001sec, Tol = 10^{-5}
			Configuration B ($\mu_1 = 0.04$, $\mu_4 = 0.08$, $\mu_2 = \mu_3 = 0.01$)	Y = 0.04in dt_{load} = 0.001sec, dt = 0.001sec, Tol = 10^{-5}
			Configuration B ($\mu_1 = \mu_4 = 0.04$, $\mu_2 = \mu_3 = 0.01$)	Y = 0.04in dt_{load} = 0.001sec, dt = 0.001sec, Tol = 10^{-5}
4.1.2	Constant μ	Amplitude = 22in Period = 10sec	Configuration A ($\mu_1 = 0.04$, $\mu_4 = 0.08$, $\mu_2 = \mu_3 = 0.01$)	Y = 0.04in, dt_{load} = 0.001sec, dt = 0.001sec, Tol = 10^{-5}
			Configuration A ($\mu_1 = \mu_4 = 0.04$, $\mu_2 = \mu_3 = 0.01$)	Y = 0.04in, dt_{load} = 0.001sec, dt = 0.001sec, Tol = 10^{-5}
			Configuration B ($\mu_1 = 0.04$, $\mu_4 = 0.08$, $\mu_2 = \mu_3 = 0.01$)	Y = 0.04in, dt_{load} = 0.001sec, dt = 0.001sec, Tol = 10^{-5}
			Configuration B ($\mu_1 = \mu_4 = 0.04$, $\mu_2 = \mu_3 = 0.01$)	Y = 0.04in, dt_{load} = 0.001sec, dt = 0.001sec, Tol = 10^{-5}

4.1.3	Constant μ	Amplitude = 20in Period = 5sec	Configuration A ($\mu_1 = 0.04$, $\mu_4 = 0.08$, $\mu_2 = \mu_3 = 0.01$)	Y = 0.04in, dt_{load} = 0.001sec, dt = 0.001sec, Tol = 10^{-5}
			Configuration A ($\mu_1 = \mu_4 = 0.04$, $\mu_2 = \mu_3 = 0.01$)	Y = 0.04in, dt_{load} = 0.001sec, dt = 0.001sec, Tol = 10^{-5}
			Configuration B ($\mu_1 = 0.04$, $\mu_4 = 0.08$, $\mu_2 = \mu_3 = 0.01$)	Y = 0.04in, dt_{load} = 0.001sec, dt = 0.001sec, Tol = 10^{-5}
			Configuration B ($\mu_1 = \mu_4 = 0.04$, $\mu_2 = \mu_3 = 0.01$)	Y = 0.04in, dt_{load} = 0.001sec, dt = 0.001sec, Tol = 10^{-5}
5.1.1	$\mu(T)$	Amplitude = 20in Period = 20sec	Configuration A ($\mu_1 = 0.04$, $\mu_4 = 0.08$, $\mu_2 = \mu_3 = 0.01$)	Y = 0.04in, dt_{load} = 0.0167sec, dt = 0.0167sec, Tol = 10^{-5}
			Configuration A ($\mu_1 = \mu_4 = 0.04$, $\mu_2 = \mu_3 = 0.01$)	Y = 0.04in, dt_{load} = 0.0167sec, dt = 0.0167sec, Tol = 10^{-5}
			Configuration B ($\mu_1 = 0.04$, $\mu_4 = 0.08$, $\mu_2 = \mu_3 = 0.01$)	Y = 0.04in, dt_{load} = 0.0167sec, dt = 0.0167sec, Tol = 10^{-5}
			Configuration B ($\mu_1 = \mu_4 = 0.04$, $\mu_2 = \mu_3 = 0.01$)	Y = 0.04in, dt_{load} = 0.0167sec, dt = 0.0167sec, Tol = 10^{-5}
5.1.2	$\mu(T)$	Amplitude = 22in Period = 10sec	Configuration A ($\mu_1 = 0.04$, $\mu_4 = 0.08$, $\mu_2 = \mu_3 = 0.01$)	Y = 0.04in, dt_{load} = 0.0167sec, dt = 0.0167sec, Tol = 10^{-5}
			Configuration A ($\mu_1 = \mu_4 = 0.04$, $\mu_2 = \mu_3 = 0.01$)	Y = 0.04in, dt_{load} = 0.0167sec, dt = 0.0167sec, Tol = 10^{-5}
			Configuration B ($\mu_1 = 0.04$, $\mu_4 = 0.08$, $\mu_2 = \mu_3 = 0.01$)	Y = 0.04in, dt_{load} = 0.001sec, dt = 0.0167sec, Tol = 10^{-5}
			Configuration B ($\mu_1 = \mu_4 = 0.04$, $\mu_2 = \mu_3 = 0.01$)	Y = 0.04in, dt_{load} = 0.001sec, dt = 0.0167sec, Tol = 10^{-5}
5.1.3	$\mu(T)$	Amplitude = 20in Period = 5sec	Configuration A ($\mu_1 = 0.04$, $\mu_4 = 0.08$, $\mu_2 = \mu_3 = 0.01$)	Y = 0.04in, dt_{load} = 0.001sec, dt = 0.008sec, Tol = 10^{-5}

			Configuration A ($\mu_1 = \mu_4 = 0.04$, $\mu_2 = \mu_3 = 0.01$)	Y = 0.04in, dt_{load} = 0.001sec, dt = 0.001sec, Tol = 10^{-5}
			Configuration B ($\mu_1 = 0.04$, $\mu_4 = 0.08$, $\mu_2 = \mu_3 = 0.01$)	Y = 0.04in, dt_{load} = 0.001sec, dt = 0.008sec, Tol = 10^{-5}
			Configuration B ($\mu_1 = \mu_4 = 0.04$, $\mu_2 = \mu_3 = 0.01$)	Y = 0.04in, dt_{load} = 0.001sec, dt = 0.001sec, Tol = 10^{-5}
6.1.1	$\mu(T)$	2011 Tohoku Earthquake at Kaminoyama station (FN, Scaled by 8)	Configuration B ($\mu_1 = 0.04$, $\mu_4 = 0.08$, $\mu_2 = \mu_3 = 0.01$)	Y = 0.01in, dt_{load} = 0.001sec, dt = 0.0016sec, Tol = 10^{-3}
			Configuration B ($\mu_1 = \mu_4 = 0.04$, $\mu_2 = \mu_3 = 0.01$)	Y = 0.01in, dt_{load} = 0.001sec, dt = 0.0016sec, Tol = 10^{-3}
6.1.3	$\mu(T)$ and $\mu(P,T)$	2011 Tohoku Earthquake at Kaminoyama station (FN and V, Scaled by 8)	Configuration B ($\mu_1 = 0.04$, $\mu_4 = 0.08$, $\mu_2 = \mu_3 = 0.01$)	Y = 0.01in, dt_{load} = 0.001sec, dt = 0.004sec, Tol = 10^{-3}
			Configuration B ($\mu_1 = \mu_4 = 0.04$, $\mu_2 = \mu_3 = 0.01$)	Y = 0.01in, dt_{load} = 0.001sec, dt = 0.004sec, Tol = 10^{-3}
6.1.5	$\mu(T)$ and $\mu(P,T,V)$	2011 Tohoku Earthquake at Kaminoyama station (FN and V, Scaled by 8)	Configuration B ($\mu_1 = 0.04$, $\mu_4 = 0.08$, $\mu_2 = \mu_3 = 0.01$)	Y = 0.01in, dt_{load} = 0.001sec, a = 2.54sec/inch (100sec/m) dt = 0.006sec, Tol = 10^{-3}
			Configuration B ($\mu_1 = \mu_4 = 0.04$, $\mu_2 = \mu_3 = 0.01$)	Y = 0.01in, dt_{load} = 0.001sec, a = 2.54sec/inch (100sec/m) dt = 0.004sec, Tol = 10^{-3}
6.1.7	Constant μ and $\mu(T)$ and $\mu(P,T,V)$	2011 Tohoku Earthquake at Kaminoyama station (FN, FP, and V, Scaled by 7)	Configuration B ($\mu_1 = 0.04$, $\mu_4 = 0.08$, $\mu_2 = \mu_3 = 0.01$)	Y = 0.01in, dt_{load} = 0.001sec, a = 2.54sec/inch (100sec/m) dt = 0.006sec, Tol = 10^{-3}
			Configuration B ($\mu_1 = \mu_4 = 0.04$, $\mu_2 = \mu_3 = 0.01$)	Y = 0.01in, dt_{load} = 0.001sec, a = 2.54sec/inch (100sec/m) dt = 0.004sec, Tol = 10^{-3}

6.1.9	Constant μ	2011 Tohoku Earthquake at Kaminoyama station (FN, FP, and V, Scaled by 7)	Configuration B ($\mu_1 = 0.04$, $\mu_4 = 0.08$, $\mu_2 = \mu_3 = 0.01$)	Y = 0.01in, dt_{load} = 0.001sec, a = 2.54sec/inch (100sec/m) dt = 0.001sec, Tol = 10^{-3}
			Configuration B ($\mu_1 = \mu_4 = 0.04$, $\mu_2 = \mu_3 = 0.01$)	Y = 0.01in, dt_{load} = 0.001sec, a = 2.54sec/inch (100sec/m) dt = 0.001sec, Tol = 10^{-3}

MCEER Technical Reports

MCEER publishes technical reports on a variety of subjects written by authors funded through MCEER. These reports can be downloaded from the MCEER website at http://www.buffalo.edu/mceer. They can also be requested through NTIS, P.O. Box 1425, Springfield, Virginia 22151. NTIS accession numbers are shown in parenthesis, if available.

NCEER-87-0001 "First-Year Program in Research, Education and Technology Transfer," 3/5/87, (PB88-134275, A04, MF-A01).

NCEER-87-0002 "Experimental Evaluation of Instantaneous Optimal Algorithms for Structural Control," by R.C. Lin, T.T. Soong and A.M. Reinhorn, 4/20/87, (PB88-134341, A04, MF-A01).

NCEER-87-0003 "Experimentation Using the Earthquake Simulation Facilities at University at Buffalo," by A.M. Reinhorn and R.L. Ketter, not available.

NCEER-87-0004 "The System Characteristics and Performance of a Shaking Table," by J.S. Hwang, K.C. Chang and G.C. Lee, 6/1/87, (PB88-134259, A03, MF-A01). This report is available only through NTIS (see address given above).

NCEER-87-0005 "A Finite Element Formulation for Nonlinear Viscoplastic Material Using a Q Model," by O. Gyebi and G. Dasgupta, 11/2/87, (PB88-213764, A08, MF-A01).

NCEER-87-0006 "Symbolic Manipulation Program (SMP) - Algebraic Codes for Two and Three Dimensional Finite Element Formulations," by X. Lee and G. Dasgupta, 11/9/87, (PB88-218522, A05, MF-A01).

NCEER-87-0007 "Instantaneous Optimal Control Laws for Tall Buildings Under Seismic Excitations," by J.N. Yang, A. Akbarpour and P. Ghaemmaghami, 6/10/87, (PB88-134333, A06, MF-A01). This report is only available through NTIS (see address given above).

NCEER-87-0008 "IDARC: Inelastic Damage Analysis of Reinforced Concrete Frame - Shear-Wall Structures," by Y.J. Park, A.M. Reinhorn and S.K. Kunnath, 7/20/87, (PB88-134325, A09, MF-A01). This report is only available through NTIS (see address given above).

NCEER-87-0009 "Liquefaction Potential for New York State: A Preliminary Report on Sites in Manhattan and Buffalo," by M. Budhu, V. Vijayakumar, R.F. Giese and L. Baumgras, 8/31/87, (PB88-163704, A03, MF-A01). This report is available only through NTIS (see address given above).

NCEER-87-0010 "Vertical and Torsional Vibration of Foundations in Inhomogeneous Media," by A.S. Veletsos and K.W. Dotson, 6/1/87, (PB88-134291, A03, MF-A01). This report is only available through NTIS (see address given above).

NCEER-87-0011 "Seismic Probabilistic Risk Assessment and Seismic Margins Studies for Nuclear Power Plants," by Howard H.M. Hwang, 6/15/87, (PB88-134267, A03, MF-A01). This report is only available through NTIS (see address given above).

NCEER-87-0012 "Parametric Studies of Frequency Response of Secondary Systems Under Ground-Acceleration Excitations," by Y. Yong and Y.K. Lin, 6/10/87, (PB88-134309, A03, MF-A01). This report is only available through NTIS (see address given above).

NCEER-87-0013 "Frequency Response of Secondary Systems Under Seismic Excitation," by J.A. HoLung, J. Cai and Y.K. Lin, 7/31/87, (PB88-134317, A05, MF-A01). This report is only available through NTIS (see address given above).

NCEER-87-0014 "Modelling Earthquake Ground Motions in Seismically Active Regions Using Parametric Time Series Methods," by G.W. Ellis and A.S. Cakmak, 8/25/87, (PB88-134283, A08, MF-A01). This report is only available through NTIS (see address given above).

NCEER-87-0015 "Detection and Assessment of Seismic Structural Damage," by E. DiPasquale and A.S. Cakmak, 8/25/87, (PB88-163712, A05, MF-A01). This report is only available through NTIS (see address given above).

NCEER-87-0016 "Pipeline Experiment at Parkfield, California," by J. Isenberg and E. Richardson, 9/15/87, (PB88-163720, A03, MF-A01). This report is available only through NTIS (see address given above).

NCEER-87-0017 "Digital Simulation of Seismic Ground Motion," by M. Shinozuka, G. Deodatis and T. Harada, 8/31/87, (PB88-155197, A04, MF-A01). This report is available only through NTIS (see address given above).

NCEER-87-0018 "Practical Considerations for Structural Control: System Uncertainty, System Time Delay and Truncation of Small Control Forces," J.N. Yang and A. Akbarpour, 8/10/87, (PB88-163738, A08, MF-A01). This report is only available through NTIS (see address given above).

NCEER-87-0019 "Modal Analysis of Nonclassically Damped Structural Systems Using Canonical Transformation," by J.N. Yang, S. Sarkani and F.X. Long, 9/27/87, (PB88-187851, A04, MF-A01).

NCEER-87-0020 "A Nonstationary Solution in Random Vibration Theory," by J.R. Red-Horse and P.D. Spanos, 11/3/87, (PB88-163746, A03, MF-A01).

NCEER-87-0021 "Horizontal Impedances for Radially Inhomogeneous Viscoelastic Soil Layers," by A.S. Veletsos and K.W. Dotson, 10/15/87, (PB88-150859, A04, MF-A01).

NCEER-87-0022 "Seismic Damage Assessment of Reinforced Concrete Members," by Y.S. Chung, C. Meyer and M. Shinozuka, 10/9/87, (PB88-150867, A05, MF-A01). This report is available only through NTIS (see address given above).

NCEER-87-0023 "Active Structural Control in Civil Engineering," by T.T. Soong, 11/11/87, (PB88-187778, A03, MF-A01).

NCEER-87-0024 "Vertical and Torsional Impedances for Radially Inhomogeneous Viscoelastic Soil Layers," by K.W. Dotson and A.S. Veletsos, 12/87, (PB88-187786, A03, MF-A01).

NCEER-87-0025 "Proceedings from the Symposium on Seismic Hazards, Ground Motions, Soil-Liquefaction and Engineering Practice in Eastern North America," October 20-22, 1987, edited by K.H. Jacob, 12/87, (PB88-188115, A23, MF-A01). This report is available only through NTIS (see address given above).

NCEER-87-0026 "Report on the Whittier-Narrows, California, Earthquake of October 1, 1987," by J. Pantelic and A. Reinhorn, 11/87, (PB88-187752, A03, MF-A01). This report is available only through NTIS (see address given above).

NCEER-87-0027 "Design of a Modular Program for Transient Nonlinear Analysis of Large 3-D Building Structures," by S. Srivastav and J.F. Abel, 12/30/87, (PB88-187950, A05, MF-A01). This report is only available through NTIS (see address given above).

NCEER-87-0028 "Second-Year Program in Research, Education and Technology Transfer," 3/8/88, (PB88-219480, A04, MF-A01).

NCEER-88-0001 "Workshop on Seismic Computer Analysis and Design of Buildings With Interactive Graphics," by W. McGuire, J.F. Abel and C.H. Conley, 1/18/88, (PB88-187760, A03, MF-A01). This report is only available through NTIS (see address given above).

NCEER-88-0002 "Optimal Control of Nonlinear Flexible Structures," by J.N. Yang, F.X. Long and D. Wong, 1/22/88, (PB88-213772, A06, MF-A01).

NCEER-88-0003 "Substructuring Techniques in the Time Domain for Primary-Secondary Structural Systems," by G.D. Manolis and G. Juhn, 2/10/88, (PB88-213780, A04, MF-A01).

NCEER-88-0004 "Iterative Seismic Analysis of Primary-Secondary Systems," by A. Singhal, L.D. Lutes and P.D. Spanos, 2/23/88, (PB88-213798, A04, MF-A01).

NCEER-88-0005 "Stochastic Finite Element Expansion for Random Media," by P.D. Spanos and R. Ghanem, 3/14/88, (PB88-213806, A03, MF-A01).

NCEER-88-0006 "Combining Structural Optimization and Structural Control," by F.Y. Cheng and C.P. Pantelides, 1/10/88, (PB88-213814, A05, MF-A01).

NCEER-88-0007 "Seismic Performance Assessment of Code-Designed Structures," by H.H-M. Hwang, J-W. Jaw and H-J. Shau, 3/20/88, (PB88-219423, A04, MF-A01). This report is only available through NTIS (see address given above).

NCEER-88-0008 "Reliability Analysis of Code-Designed Structures Under Natural Hazards," by H.H-M. Hwang, H. Ushiba and M. Shinozuka, 2/29/88, (PB88-229471, A07, MF-A01). This report is only available through NTIS (see address given above).

NCEER-88-0009 "Seismic Fragility Analysis of Shear Wall Structures," by J-W Jaw and H.H-M. Hwang, 4/30/88, (PB89-102867, A04, MF-A01).

NCEER-88-0010 "Base Isolation of a Multi-Story Building Under a Harmonic Ground Motion - A Comparison of Performances of Various Systems," by F-G Fan, G. Ahmadi and I.G. Tadjbakhsh, 5/18/88, (PB89-122238, A06, MF-A01). This report is only available through NTIS (see address given above).

NCEER-88-0011 "Seismic Floor Response Spectra for a Combined System by Green's Functions," by F.M. Lavelle, L.A. Bergman and P.D. Spanos, 5/1/88, (PB89-102875, A03, MF-A01).

NCEER-88-0012 "A New Solution Technique for Randomly Excited Hysteretic Structures," by G.Q. Cai and Y.K. Lin, 5/16/88, (PB89-102883, A03, MF-A01).

NCEER-88-0013 "A Study of Radiation Damping and Soil-Structure Interaction Effects in the Centrifuge," by K. Weissman, supervised by J.H. Prevost, 5/24/88, (PB89-144703, A06, MF-A01).

NCEER-88-0014 "Parameter Identification and Implementation of a Kinematic Plasticity Model for Frictional Soils," by J.H. Prevost and D.V. Griffiths, not available.

NCEER-88-0015 "Two- and Three- Dimensional Dynamic Finite Element Analyses of the Long Valley Dam," by D.V. Griffiths and J.H. Prevost, 6/17/88, (PB89-144711, A04, MF-A01).

NCEER-88-0016 "Damage Assessment of Reinforced Concrete Structures in Eastern United States," by A.M. Reinhorn, M.J. Seidel, S.K. Kunnath and Y.J. Park, 6/15/88, (PB89-122220, A04, MF-A01). This report is only available through NTIS (see address given above).

NCEER-88-0017 "Dynamic Compliance of Vertically Loaded Strip Foundations in Multilayered Viscoelastic Soils," by S. Ahmad and A.S.M. Israil, 6/17/88, (PB89-102891, A04, MF-A01).

NCEER-88-0018 "An Experimental Study of Seismic Structural Response With Added Viscoelastic Dampers," by R.C. Lin, Z. Liang, T.T. Soong and R.H. Zhang, 6/30/88, (PB89-122212, A05, MF-A01). This report is available only through NTIS (see address given above).

NCEER-88-0019 "Experimental Investigation of Primary - Secondary System Interaction," by G.D. Manolis, G. Juhn and A.M. Reinhorn, 5/27/88, (PB89-122204, A04, MF-A01).

NCEER-88-0020 "A Response Spectrum Approach For Analysis of Nonclassically Damped Structures," by J.N. Yang, S. Sarkani and F.X. Long, 4/22/88, (PB89-102909, A04, MF-A01).

NCEER-88-0021 "Seismic Interaction of Structures and Soils: Stochastic Approach," by A.S. Veletsos and A.M. Prasad, 7/21/88, (PB89-122196, A04, MF-A01). This report is only available through NTIS (see address given above).

NCEER-88-0022 "Identification of the Serviceability Limit State and Detection of Seismic Structural Damage," by E. DiPasquale and A.S. Cakmak, 6/15/88, (PB89-122188, A05, MF-A01). This report is available only through NTIS (see address given above).

NCEER-88-0023 "Multi-Hazard Risk Analysis: Case of a Simple Offshore Structure," by B.K. Bhartia and E.H. Vanmarcke, 7/21/88, (PB89-145213, A05, MF-A01).

NCEER-88-0024 "Automated Seismic Design of Reinforced Concrete Buildings," by Y.S. Chung, C. Meyer and M. Shinozuka, 7/5/88, (PB89-122170, A06, MF-A01). This report is available only through NTIS (see address given above).

NCEER-88-0025 "Experimental Study of Active Control of MDOF Structures Under Seismic Excitations," by L.L. Chung, R.C. Lin, T.T. Soong and A.M. Reinhorn, 7/10/88, (PB89-122600, A04, MF-A01).

NCEER-88-0026 "Earthquake Simulation Tests of a Low-Rise Metal Structure," by J.S. Hwang, K.C. Chang, G.C. Lee and R.L. Ketter, 8/1/88, (PB89-102917, A04, MF-A01).

NCEER-88-0027 "Systems Study of Urban Response and Reconstruction Due to Catastrophic Earthquakes," by F. Kozin and H.K. Zhou, 9/22/88, (PB90-162348, A04, MF-A01).

NCEER-88-0028 "Seismic Fragility Analysis of Plane Frame Structures," by H.H-M. Hwang and Y.K. Low, 7/31/88, (PB89-131445, A06, MF-A01).

NCEER-88-0029 "Response Analysis of Stochastic Structures," by A. Kardara, C. Bucher and M. Shinozuka, 9/22/88, (PB89-174429, A04, MF-A01).

NCEER-88-0030 "Nonnormal Accelerations Due to Yielding in a Primary Structure," by D.C.K. Chen and L.D. Lutes, 9/19/88, (PB89-131437, A04, MF-A01).

NCEER-88-0031 "Design Approaches for Soil-Structure Interaction," by A.S. Veletsos, A.M. Prasad and Y. Tang, 12/30/88, (PB89-174437, A03, MF-A01). This report is available only through NTIS (see address given above).

NCEER-88-0032 "A Re-evaluation of Design Spectra for Seismic Damage Control," by C.J. Turkstra and A.G. Tallin, 11/7/88, (PB89-145221, A05, MF-A01).

NCEER-88-0033 "The Behavior and Design of Noncontact Lap Splices Subjected to Repeated Inelastic Tensile Loading," by V.E. Sagan, P. Gergely and R.N. White, 12/8/88, (PB89-163737, A08, MF-A01).

NCEER-88-0034 "Seismic Response of Pile Foundations," by S.M. Mamoon, P.K. Banerjee and S. Ahmad, 11/1/88, (PB89-145239, A04, MF-A01).

NCEER-88-0035 "Modeling of R/C Building Structures With Flexible Floor Diaphragms (IDARC2)," by A.M. Reinhorn, S.K. Kunnath and N. Panahshahi, 9/7/88, (PB89-207153, A07, MF-A01).

NCEER-88-0036 "Solution of the Dam-Reservoir Interaction Problem Using a Combination of FEM, BEM with Particular Integrals, Modal Analysis, and Substructuring," by C-S. Tsai, G.C. Lee and R.L. Ketter, 12/31/88, (PB89-207146, A04, MF-A01).

NCEER-88-0037 "Optimal Placement of Actuators for Structural Control," by F.Y. Cheng and C.P. Pantelides, 8/15/88, (PB89-162846, A05, MF-A01).

NCEER-88-0038 "Teflon Bearings in Aseismic Base Isolation: Experimental Studies and Mathematical Modeling," by A. Mokha, M.C. Constantinou and A.M. Reinhorn, 12/5/88, (PB89-218457, A10, MF-A01). This report is available only through NTIS (see address given above).

NCEER-88-0039 "Seismic Behavior of Flat Slab High-Rise Buildings in the New York City Area," by P. Weidlinger and M. Ettouney, 10/15/88, (PB90-145681, A04, MF-A01).

NCEER-88-0040 "Evaluation of the Earthquake Resistance of Existing Buildings in New York City," by P. Weidlinger and M. Ettouney, 10/15/88, not available.

NCEER-88-0041 "Small-Scale Modeling Techniques for Reinforced Concrete Structures Subjected to Seismic Loads," by W. Kim, A. El-Attar and R.N. White, 11/22/88, (PB89-189625, A05, MF-A01).

NCEER-88-0042 "Modeling Strong Ground Motion from Multiple Event Earthquakes," by G.W. Ellis and A.S. Cakmak, 10/15/88, (PB89-174445, A03, MF-A01).

NCEER-88-0043 "Nonstationary Models of Seismic Ground Acceleration," by M. Grigoriu, S.E. Ruiz and E. Rosenblueth, 7/15/88, (PB89-189617, A04, MF-A01).

NCEER-88-0044 "SARCF User's Guide: Seismic Analysis of Reinforced Concrete Frames," by Y.S. Chung, C. Meyer and M. Shinozuka, 11/9/88, (PB89-174452, A08, MF-A01).

NCEER-88-0045 "First Expert Panel Meeting on Disaster Research and Planning," edited by J. Pantelic and J. Stoyle, 9/15/88, (PB89-174460, A05, MF-A01).

NCEER-88-0046 "Preliminary Studies of the Effect of Degrading Infill Walls on the Nonlinear Seismic Response of Steel Frames," by C.Z. Chrysostomou, P. Gergely and J.F. Abel, 12/19/88, (PB89-208383, A05, MF-A01).

NCEER-88-0047 "Reinforced Concrete Frame Component Testing Facility - Design, Construction, Instrumentation and Operation," by S.P. Pessiki, C. Conley, T. Bond, P. Gergely and R.N. White, 12/16/88, (PB89-174478, A04, MF-A01).

NCEER-89-0001 "Effects of Protective Cushion and Soil Compliancy on the Response of Equipment Within a Seismically Excited Building," by J.A. HoLung, 2/16/89, (PB89-207179, A04, MF-A01).

NCEER-89-0002 "Statistical Evaluation of Response Modification Factors for Reinforced Concrete Structures," by H.H-M. Hwang and J-W. Jaw, 2/17/89, (PB89-207187, A05, MF-A01).

NCEER-89-0003 "Hysteretic Columns Under Random Excitation," by G-Q. Cai and Y.K. Lin, 1/9/89, (PB89-196513, A03, MF-A01).

NCEER-89-0004 "Experimental Study of `Elephant Foot Bulge' Instability of Thin-Walled Metal Tanks," by Z-H. Jia and R.L. Ketter, 2/22/89, (PB89-207195, A03, MF-A01).

NCEER-89-0005 "Experiment on Performance of Buried Pipelines Across San Andreas Fault," by J. Isenberg, E. Richardson and T.D. O'Rourke, 3/10/89, (PB89-218440, A04, MF-A01). This report is available only through NTIS (see address given above).

NCEER-89-0006 "A Knowledge-Based Approach to Structural Design of Earthquake-Resistant Buildings," by M. Subramani, P. Gergely, C.H. Conley, J.F. Abel and A.H. Zaghw, 1/15/89, (PB89-218465, A06, MF-A01).

NCEER-89-0007 "Liquefaction Hazards and Their Effects on Buried Pipelines," by T.D. O'Rourke and P.A. Lane, 2/1/89, (PB89-218481, A09, MF-A01).

NCEER-89-0008 "Fundamentals of System Identification in Structural Dynamics," by H. Imai, C-B. Yun, O. Maruyama and M. Shinozuka, 1/26/89, (PB89-207211, A04, MF-A01).

NCEER-89-0009 "Effects of the 1985 Michoacan Earthquake on Water Systems and Other Buried Lifelines in Mexico," by A.G. Ayala and M.J. O'Rourke, 3/8/89, (PB89-207229, A06, MF-A01).

NCEER-89-R010 "NCEER Bibliography of Earthquake Education Materials," by K.E.K. Ross, Second Revision, 9/1/89, (PB90-125352, A05, MF-A01). This report is replaced by NCEER-92-0018.

NCEER-89-0011 "Inelastic Three-Dimensional Response Analysis of Reinforced Concrete Building Structures (IDARC-3D), Part I - Modeling," by S.K. Kunnath and A.M. Reinhorn, 4/17/89, (PB90-114612, A07, MF-A01). This report is available only through NTIS (see address given above).

NCEER-89-0012 "Recommended Modifications to ATC-14," by C.D. Poland and J.O. Malley, 4/12/89, (PB90-108648, A15, MF-A01).

NCEER-89-0013 "Repair and Strengthening of Beam-to-Column Connections Subjected to Earthquake Loading," by M. Corazao and A.J. Durrani, 2/28/89, (PB90-109885, A06, MF-A01).

NCEER-89-0014 "Program EXKAL2 for Identification of Structural Dynamic Systems," by O. Maruyama, C-B. Yun, M. Hoshiya and M. Shinozuka, 5/19/89, (PB90-109877, A09, MF-A01).

NCEER-89-0015 "Response of Frames With Bolted Semi-Rigid Connections, Part I - Experimental Study and Analytical Predictions," by P.J. DiCorso, A.M. Reinhorn, J.R. Dickerson, J.B. Radziminski and W.L. Harper, 6/1/89, not available.

NCEER-89-0016 "ARMA Monte Carlo Simulation in Probabilistic Structural Analysis," by P.D. Spanos and M.P. Mignolet, 7/10/89, (PB90-109893, A03, MF-A01).

NCEER-89-P017 "Preliminary Proceedings from the Conference on Disaster Preparedness - The Place of Earthquake Education in Our Schools," Edited by K.E.K. Ross, 6/23/89, (PB90-108606, A03, MF-A01).

NCEER-89-0017 "Proceedings from the Conference on Disaster Preparedness - The Place of Earthquake Education in Our Schools," Edited by K.E.K. Ross, 12/31/89, (PB90-207895, A012, MF-A02). This report is available only through NTIS (see address given above).

NCEER-89-0018 "Multidimensional Models of Hysteretic Material Behavior for Vibration Analysis of Shape Memory Energy Absorbing Devices, by E.J. Graesser and F.A. Cozzarelli, 6/7/89, (PB90-164146, A04, MF-A01).

NCEER-89-0019 "Nonlinear Dynamic Analysis of Three-Dimensional Base Isolated Structures (3D-BASIS)," by S. Nagarajaiah, A.M. Reinhorn and M.C. Constantinou, 8/3/89, (PB90-161936, A06, MF-A01). This report has been replaced by NCEER-93-0011.

NCEER-89-0020 "Structural Control Considering Time-Rate of Control Forces and Control Rate Constraints," by F.Y. Cheng and C.P. Pantelides, 8/3/89, (PB90-120445, A04, MF-A01).

NCEER-89-0021 "Subsurface Conditions of Memphis and Shelby County," by K.W. Ng, T-S. Chang and H-H.M. Hwang, 7/26/89, (PB90-120437, A03, MF-A01).

NCEER-89-0022 "Seismic Wave Propagation Effects on Straight Jointed Buried Pipelines," by K. Elhmadi and M.J. O'Rourke, 8/24/89, (PB90-162322, A10, MF-A02).

NCEER-89-0023 "Workshop on Serviceability Analysis of Water Delivery Systems," edited by M. Grigoriu, 3/6/89, (PB90-127424, A03, MF-A01).

NCEER-89-0024 "Shaking Table Study of a 1/5 Scale Steel Frame Composed of Tapered Members," by K.C. Chang, J.S. Hwang and G.C. Lee, 9/18/89, (PB90-160169, A04, MF-A01).

NCEER-89-0025 "DYNA1D: A Computer Program for Nonlinear Seismic Site Response Analysis - Technical Documentation," by Jean H. Prevost, 9/14/89, (PB90-161944, A07, MF-A01). This report is available only through NTIS (see address given above).

NCEER-89-0026 "1:4 Scale Model Studies of Active Tendon Systems and Active Mass Dampers for Aseismic Protection," by A.M. Reinhorn, T.T. Soong, R.C. Lin, Y.P. Yang, Y. Fukao, H. Abe and M. Nakai, 9/15/89, (PB90-173246, A10, MF-A02). This report is available only through NTIS (see address given above).

NCEER-89-0027 "Scattering of Waves by Inclusions in a Nonhomogeneous Elastic Half Space Solved by Boundary Element Methods," by P.K. Hadley, A. Askar and A.S. Cakmak, 6/15/89, (PB90-145699, A07, MF-A01).

NCEER-89-0028 "Statistical Evaluation of Deflection Amplification Factors for Reinforced Concrete Structures," by H.H.M. Hwang, J-W. Jaw and A.L. Ch'ng, 8/31/89, (PB90-164633, A05, MF-A01).

NCEER-89-0029 "Bedrock Accelerations in Memphis Area Due to Large New Madrid Earthquakes," by H.H.M. Hwang, C.H.S. Chen and G. Yu, 11/7/89, (PB90-162330, A04, MF-A01).

NCEER-89-0030 "Seismic Behavior and Response Sensitivity of Secondary Structural Systems," by Y.Q. Chen and T.T. Soong, 10/23/89, (PB90-164658, A08, MF-A01).

NCEER-89-0031 "Random Vibration and Reliability Analysis of Primary-Secondary Structural Systems," by Y. Ibrahim, M. Grigoriu and T.T. Soong, 11/10/89, (PB90-161951, A04, MF-A01).

NCEER-89-0032 "Proceedings from the Second U.S. - Japan Workshop on Liquefaction, Large Ground Deformation and Their Effects on Lifelines, September 26-29, 1989," Edited by T.D. O'Rourke and M. Hamada, 12/1/89, (PB90-209388, A22, MF-A03).

NCEER-89-0033 "Deterministic Model for Seismic Damage Evaluation of Reinforced Concrete Structures," by J.M. Bracci, A.M. Reinhorn, J.B. Mander and S.K. Kunnath, 9/27/89, (PB91-108803, A06, MF-A01).

NCEER-89-0034 "On the Relation Between Local and Global Damage Indices," by E. DiPasquale and A.S. Cakmak, 8/15/89, (PB90-173865, A05, MF-A01).

NCEER-89-0035 "Cyclic Undrained Behavior of Nonplastic and Low Plasticity Silts," by A.J. Walker and H.E. Stewart, 7/26/89, (PB90-183518, A10, MF-A01).

NCEER-89-0036 "Liquefaction Potential of Surficial Deposits in the City of Buffalo, New York," by M. Budhu, R. Giese and L. Baumgrass, 1/17/89, (PB90-208455, A04, MF-A01).

NCEER-89-0037 "A Deterministic Assessment of Effects of Ground Motion Incoherence," by A.S. Veletsos and Y. Tang, 7/15/89, (PB90-164294, A03, MF-A01).

NCEER-89-0038 "Workshop on Ground Motion Parameters for Seismic Hazard Mapping," July 17-18, 1989, edited by R.V. Whitman, 12/1/89, (PB90-173923, A04, MF-A01).

NCEER-89-0039 "Seismic Effects on Elevated Transit Lines of the New York City Transit Authority," by C.J. Costantino, C.A. Miller and E. Heymsfield, 12/26/89, (PB90-207887, A06, MF-A01).

NCEER-89-0040 "Centrifugal Modeling of Dynamic Soil-Structure Interaction," by K. Weissman, Supervised by J.H. Prevost, 5/10/89, (PB90-207879, A07, MF-A01).

NCEER-89-0041 "Linearized Identification of Buildings With Cores for Seismic Vulnerability Assessment," by I-K. Ho and A.E. Aktan, 11/1/89, (PB90-251943, A07, MF-A01).

NCEER-90-0001 "Geotechnical and Lifeline Aspects of the October 17, 1989 Loma Prieta Earthquake in San Francisco," by T.D. O'Rourke, H.E. Stewart, F.T. Blackburn and T.S. Dickerman, 1/90, (PB90-208596, A05, MF-A01).

NCEER-90-0002 "Nonnormal Secondary Response Due to Yielding in a Primary Structure," by D.C.K. Chen and L.D. Lutes, 2/28/90, (PB90-251976, A07, MF-A01).

NCEER-90-0003 "Earthquake Education Materials for Grades K-12," by K.E.K. Ross, 4/16/90, (PB91-251984, A05, MF-A05). This report has been replaced by NCEER-92-0018.

NCEER-90-0004 "Catalog of Strong Motion Stations in Eastern North America," by R.W. Busby, 4/3/90, (PB90-251984, A05, MF-A01).

NCEER-90-0005 "NCEER Strong-Motion Data Base: A User Manual for the GeoBase Release (Version 1.0 for the Sun3)," by P. Friberg and K. Jacob, 3/31/90 (PB90-258062, A04, MF-A01).

NCEER-90-0006 "Seismic Hazard Along a Crude Oil Pipeline in the Event of an 1811-1812 Type New Madrid Earthquake," by H.H.M. Hwang and C-H.S. Chen, 4/16/90, (PB90-258054, A04, MF-A01).

NCEER-90-0007 "Site-Specific Response Spectra for Memphis Sheahan Pumping Station," by H.H.M. Hwang and C.S. Lee, 5/15/90, (PB91-108811, A05, MF-A01).

NCEER-90-0008 "Pilot Study on Seismic Vulnerability of Crude Oil Transmission Systems," by T. Ariman, R. Dobry, M. Grigoriu, F. Kozin, M. O'Rourke, T. O'Rourke and M. Shinozuka, 5/25/90, (PB91-108837, A06, MF-A01).

NCEER-90-0009 "A Program to Generate Site Dependent Time Histories: EQGEN," by G.W. Ellis, M. Srinivasan and A.S. Cakmak, 1/30/90, (PB91-108829, A04, MF-A01).

NCEER-90-0010 "Active Isolation for Seismic Protection of Operating Rooms," by M.E. Talbott, Supervised by M. Shinozuka, 6/8/9, (PB91-110205, A05, MF-A01).

NCEER-90-0011 "Program LINEARID for Identification of Linear Structural Dynamic Systems," by C-B. Yun and M. Shinozuka, 6/25/90, (PB91-110312, A08, MF-A01).

NCEER-90-0012 "Two-Dimensional Two-Phase Elasto-Plastic Seismic Response of Earth Dams," by A.N. Yiagos, Supervised by J.H. Prevost, 6/20/90, (PB91-110197, A13, MF-A02).

NCEER-90-0013 "Secondary Systems in Base-Isolated Structures: Experimental Investigation, Stochastic Response and Stochastic Sensitivity," by G.D. Manolis, G. Juhn, M.C. Constantinou and A.M. Reinhorn, 7/1/90, (PB91-110320, A08, MF-A01).

NCEER-90-0014 "Seismic Behavior of Lightly-Reinforced Concrete Column and Beam-Column Joint Details," by S.P. Pessiki, C.H. Conley, P. Gergely and R.N. White, 8/22/90, (PB91-108795, A11, MF-A02).

NCEER-90-0015 "Two Hybrid Control Systems for Building Structures Under Strong Earthquakes," by J.N. Yang and A. Danielians, 6/29/90, (PB91-125393, A04, MF-A01).

NCEER-90-0016 "Instantaneous Optimal Control with Acceleration and Velocity Feedback," by J.N. Yang and Z. Li, 6/29/90, (PB91-125401, A03, MF-A01).

NCEER-90-0017 "Reconnaissance Report on the Northern Iran Earthquake of June 21, 1990," by M. Mehrain, 10/4/90, (PB91-125377, A03, MF-A01).

NCEER-90-0018 "Evaluation of Liquefaction Potential in Memphis and Shelby County," by T.S. Chang, P.S. Tang, C.S. Lee and H. Hwang, 8/10/90, (PB91-125427, A09, MF-A01).

NCEER-90-0019 "Experimental and Analytical Study of a Combined Sliding Disc Bearing and Helical Steel Spring Isolation System," by M.C. Constantinou, A.S. Mokha and A.M. Reinhorn, 10/4/90, (PB91-125385, A06, MF-A01). This report is available only through NTIS (see address given above).

NCEER-90-0020 "Experimental Study and Analytical Prediction of Earthquake Response of a Sliding Isolation System with a Spherical Surface," by A.S. Mokha, M.C. Constantinou and A.M. Reinhorn, 10/11/90, (PB91-125419, A05, MF-A01).

NCEER-90-0021 "Dynamic Interaction Factors for Floating Pile Groups," by G. Gazetas, K. Fan, A. Kaynia and E. Kausel, 9/10/90, (PB91-170381, A05, MF-A01).

NCEER-90-0022 "Evaluation of Seismic Damage Indices for Reinforced Concrete Structures," by S. Rodriguez-Gomez and A.S. Cakmak, 9/30/90, PB91-171322, A06, MF-A01).

NCEER-90-0023 "Study of Site Response at a Selected Memphis Site," by H. Desai, S. Ahmad, E.S. Gazetas and M.R. Oh, 10/11/90, (PB91-196857, A03, MF-A01).

NCEER-90-0024 "A User's Guide to Strongmo: Version 1.0 of NCEER's Strong-Motion Data Access Tool for PCs and Terminals," by P.A. Friberg and C.A.T. Susch, 11/15/90, (PB91-171272, A03, MF-A01).

NCEER-90-0025 "A Three-Dimensional Analytical Study of Spatial Variability of Seismic Ground Motions," by L-L. Hong and A.H.-S. Ang, 10/30/90, (PB91-170399, A09, MF-A01).

NCEER-90-0026 "MUMOID User's Guide - A Program for the Identification of Modal Parameters," by S. Rodriguez-Gomez and E. DiPasquale, 9/30/90, (PB91-171298, A04, MF-A01).

NCEER-90-0027 "SARCF-II User's Guide - Seismic Analysis of Reinforced Concrete Frames," by S. Rodriguez-Gomez, Y.S. Chung and C. Meyer, 9/30/90, (PB91-171280, A05, MF-A01).

NCEER-90-0028 "Viscous Dampers: Testing, Modeling and Application in Vibration and Seismic Isolation," by N. Makris and M.C. Constantinou, 12/20/90 (PB91-190561, A06, MF-A01).

NCEER-90-0029 "Soil Effects on Earthquake Ground Motions in the Memphis Area," by H. Hwang, C.S. Lee, K.W. Ng and T.S. Chang, 8/2/90, (PB91-190751, A05, MF-A01).

NCEER-91-0001 "Proceedings from the Third Japan-U.S. Workshop on Earthquake Resistant Design of Lifeline Facilities and Countermeasures for Soil Liquefaction, December 17-19, 1990," edited by T.D. O'Rourke and M. Hamada, 2/1/91, (PB91-179259, A99, MF-A04).

NCEER-91-0002 "Physical Space Solutions of Non-Proportionally Damped Systems," by M. Tong, Z. Liang and G.C. Lee, 1/15/91, (PB91-179242, A04, MF-A01).

NCEER-91-0003 "Seismic Response of Single Piles and Pile Groups," by K. Fan and G. Gazetas, 1/10/91, (PB92-174994, A04, MF-A01).

NCEER-91-0004 "Damping of Structures: Part 1 - Theory of Complex Damping," by Z. Liang and G. Lee, 10/10/91, (PB92-197235, A12, MF-A03).

NCEER-91-0005 "3D-BASIS - Nonlinear Dynamic Analysis of Three Dimensional Base Isolated Structures: Part II," by S. Nagarajaiah, A.M. Reinhorn and M.C. Constantinou, 2/28/91, (PB91-190553, A07, MF-A01). This report has been replaced by NCEER-93-0011.

NCEER-91-0006 "A Multidimensional Hysteretic Model for Plasticity Deforming Metals in Energy Absorbing Devices," by E.J. Graesser and F.A. Cozzarelli, 4/9/91, (PB92-108364, A04, MF-A01).

NCEER-91-0007 "A Framework for Customizable Knowledge-Based Expert Systems with an Application to a KBES for Evaluating the Seismic Resistance of Existing Buildings," by E.G. Ibarra-Anaya and S.J. Fenves, 4/9/91, (PB91-210930, A08, MF-A01).

NCEER-91-0008 "Nonlinear Analysis of Steel Frames with Semi-Rigid Connections Using the Capacity Spectrum Method," by G.G. Deierlein, S-H. Hsieh, Y-J. Shen and J.F. Abel, 7/2/91, (PB92-113828, A05, MF-A01).

NCEER-91-0009 "Earthquake Education Materials for Grades K-12," by K.E.K. Ross, 4/30/91, (PB91-212142, A06, MF-A01). This report has been replaced by NCEER-92-0018.

NCEER-91-0010 "Phase Wave Velocities and Displacement Phase Differences in a Harmonically Oscillating Pile," by N. Makris and G. Gazetas, 7/8/91, (PB92-108356, A04, MF-A01).

NCEER-91-0011 "Dynamic Characteristics of a Full-Size Five-Story Steel Structure and a 2/5 Scale Model," by K.C. Chang, G.C. Yao, G.C. Lee, D.S. Hao and Y.C. Yeh," 7/2/91, (PB93-116648, A06, MF-A02).

NCEER-91-0012 "Seismic Response of a 2/5 Scale Steel Structure with Added Viscoelastic Dampers," by K.C. Chang, T.T. Soong, S-T. Oh and M.L. Lai, 5/17/91, (PB92-110816, A05, MF-A01).

NCEER-91-0013 "Earthquake Response of Retaining Walls; Full-Scale Testing and Computational Modeling," by S. Alampalli and A-W.M. Elgamal, 6/20/91, not available.

NCEER-91-0014 "3D-BASIS-M: Nonlinear Dynamic Analysis of Multiple Building Base Isolated Structures," by P.C. Tsopelas, S. Nagarajaiah, M.C. Constantinou and A.M. Reinhorn, 5/28/91, (PB92-113885, A09, MF-A02).

NCEER-91-0015 "Evaluation of SEAOC Design Requirements for Sliding Isolated Structures," by D. Theodossiou and M.C. Constantinou, 6/10/91, (PB92-114602, A11, MF-A03).

NCEER-91-0016 "Closed-Loop Modal Testing of a 27-Story Reinforced Concrete Flat Plate-Core Building," by H.R. Somaprasad, T. Toksoy, H. Yoshiyuki and A.E. Aktan, 7/15/91, (PB92-129980, A07, MF-A02).

NCEER-91-0017 "Shake Table Test of a 1/6 Scale Two-Story Lightly Reinforced Concrete Building," by A.G. El-Attar, R.N. White and P. Gergely, 2/28/91, (PB92-222447, A06, MF-A02).

NCEER-91-0018 "Shake Table Test of a 1/8 Scale Three-Story Lightly Reinforced Concrete Building," by A.G. El-Attar, R.N. White and P. Gergely, 2/28/91, (PB93-116630, A08, MF-A02).

NCEER-91-0019 "Transfer Functions for Rigid Rectangular Foundations," by A.S. Veletsos, A.M. Prasad and W.H. Wu, 7/31/91, not available.

NCEER-91-0020 "Hybrid Control of Seismic-Excited Nonlinear and Inelastic Structural Systems," by J.N. Yang, Z. Li and A. Danielians, 8/1/91, (PB92-143171, A06, MF-A02).

NCEER-91-0021 "The NCEER-91 Earthquake Catalog: Improved Intensity-Based Magnitudes and Recurrence Relations for U.S. Earthquakes East of New Madrid," by L. Seeber and J.G. Armbruster, 8/28/91, (PB92-176742, A06, MF-A02).

NCEER-91-0022 "Proceedings from the Implementation of Earthquake Planning and Education in Schools: The Need for Change - The Roles of the Changemakers," by K.E.K. Ross and F. Winslow, 7/23/91, (PB92-129998, A12, MF-A03).

NCEER-91-0023 "A Study of Reliability-Based Criteria for Seismic Design of Reinforced Concrete Frame Buildings," by H.H.M. Hwang and H-M. Hsu, 8/10/91, (PB92-140235, A09, MF-A02).

NCEER-91-0024 "Experimental Verification of a Number of Structural System Identification Algorithms," by R.G. Ghanem, H. Gavin and M. Shinozuka, 9/18/91, (PB92-176577, A18, MF-A04).

NCEER-91-0025 "Probabilistic Evaluation of Liquefaction Potential," by H.H.M. Hwang and C.S. Lee," 11/25/91, (PB92-143429, A05, MF-A01).

NCEER-91-0026 "Instantaneous Optimal Control for Linear, Nonlinear and Hysteretic Structures - Stable Controllers," by J.N. Yang and Z. Li, 11/15/91, (PB92-163807, A04, MF-A01).

NCEER-91-0027 "Experimental and Theoretical Study of a Sliding Isolation System for Bridges," by M.C. Constantinou, A. Kartoum, A.M. Reinhorn and P. Bradford, 11/15/91, (PB92-176973, A10, MF-A03).

NCEER-92-0001 "Case Studies of Liquefaction and Lifeline Performance During Past Earthquakes, Volume 1: Japanese Case Studies," Edited by M. Hamada and T. O'Rourke, 2/17/92, (PB92-197243, A18, MF-A04).

NCEER-92-0002 "Case Studies of Liquefaction and Lifeline Performance During Past Earthquakes, Volume 2: United States Case Studies," Edited by T. O'Rourke and M. Hamada, 2/17/92, (PB92-197250, A20, MF-A04).

NCEER-92-0003 "Issues in Earthquake Education," Edited by K. Ross, 2/3/92, (PB92-222389, A07, MF-A02).

NCEER-92-0004 "Proceedings from the First U.S. - Japan Workshop on Earthquake Protective Systems for Bridges," Edited by I.G. Buckle, 2/4/92, (PB94-142239, A99, MF-A06).

NCEER-92-0005 "Seismic Ground Motion from a Haskell-Type Source in a Multiple-Layered Half-Space," A.P. Theoharis, G. Deodatis and M. Shinozuka, 1/2/92, not available.

NCEER-92-0006 "Proceedings from the Site Effects Workshop," Edited by R. Whitman, 2/29/92, (PB92-197201, A04, MF-A01).

NCEER-92-0007 "Engineering Evaluation of Permanent Ground Deformations Due to Seismically-Induced Liquefaction," by M.H. Baziar, R. Dobry and A-W.M. Elgamal, 3/24/92, (PB92-222421, A13, MF-A03).

NCEER-92-0008 "A Procedure for the Seismic Evaluation of Buildings in the Central and Eastern United States," by C.D. Poland and J.O. Malley, 4/2/92, (PB92-222439, A20, MF-A04).

NCEER-92-0009 "Experimental and Analytical Study of a Hybrid Isolation System Using Friction Controllable Sliding Bearings," by M.Q. Feng, S. Fujii and M. Shinozuka, 5/15/92, (PB93-150282, A06, MF-A02).

NCEER-92-0010 "Seismic Resistance of Slab-Column Connections in Existing Non-Ductile Flat-Plate Buildings," by A.J. Durrani and Y. Du, 5/18/92, (PB93-116812, A06, MF-A02).

NCEER-92-0011 "The Hysteretic and Dynamic Behavior of Brick Masonry Walls Upgraded by Ferrocement Coatings Under Cyclic Loading and Strong Simulated Ground Motion," by H. Lee and S.P. Prawel, 5/11/92, not available.

NCEER-92-0012 "Study of Wire Rope Systems for Seismic Protection of Equipment in Buildings," by G.F. Demetriades, M.C. Constantinou and A.M. Reinhorn, 5/20/92, (PB93-116655, A08, MF-A02).

NCEER-92-0013 "Shape Memory Structural Dampers: Material Properties, Design and Seismic Testing," by P.R. Witting and F.A. Cozzarelli, 5/26/92, (PB93-116663, A05, MF-A01).

NCEER-92-0014 "Longitudinal Permanent Ground Deformation Effects on Buried Continuous Pipelines," by M.J. O'Rourke, and C. Nordberg, 6/15/92, (PB93-116671, A08, MF-A02).

NCEER-92-0015 "A Simulation Method for Stationary Gaussian Random Functions Based on the Sampling Theorem," by M. Grigoriu and S. Balopoulou, 6/11/92, (PB93-127496, A05, MF-A01).

NCEER-92-0016 "Gravity-Load-Designed Reinforced Concrete Buildings: Seismic Evaluation of Existing Construction and Detailing Strategies for Improved Seismic Resistance," by G.W. Hoffmann, S.K. Kunnath, A.M. Reinhorn and J.B. Mander, 7/15/92, (PB94-142007, A08, MF-A02).

NCEER-92-0017 "Observations on Water System and Pipeline Performance in the Limón Area of Costa Rica Due to the April 22, 1991 Earthquake," by M. O'Rourke and D. Ballantyne, 6/30/92, (PB93-126811, A06, MF-A02).

NCEER-92-0018 "Fourth Edition of Earthquake Education Materials for Grades K-12," Edited by K.E.K. Ross, 8/10/92, (PB93-114023, A07, MF-A02).

NCEER-92-0019 "Proceedings from the Fourth Japan-U.S. Workshop on Earthquake Resistant Design of Lifeline Facilities and Countermeasures for Soil Liquefaction," Edited by M. Hamada and T.D. O'Rourke, 8/12/92, (PB93-163939, A99, MF-E11).

NCEER-92-0020 "Active Bracing System: A Full Scale Implementation of Active Control," by A.M. Reinhorn, T.T. Soong, R.C. Lin, M.A. Riley, Y.P. Wang, S. Aizawa and M. Higashino, 8/14/92, (PB93-127512, A06, MF-A02).

NCEER-92-0021 "Empirical Analysis of Horizontal Ground Displacement Generated by Liquefaction-Induced Lateral Spreads," by S.F. Bartlett and T.L. Youd, 8/17/92, (PB93-188241, A06, MF-A02).

NCEER-92-0022 "IDARC Version 3.0: Inelastic Damage Analysis of Reinforced Concrete Structures," by S.K. Kunnath, A.M. Reinhorn and R.F. Lobo, 8/31/92, (PB93-227502, A07, MF-A02).

NCEER-92-0023 "A Semi-Empirical Analysis of Strong-Motion Peaks in Terms of Seismic Source, Propagation Path and Local Site Conditions, by M. Kamiyama, M.J. O'Rourke and R. Flores-Berrones, 9/9/92, (PB93-150266, A08, MF-A02).

NCEER-92-0024 "Seismic Behavior of Reinforced Concrete Frame Structures with Nonductile Details, Part I: Summary of Experimental Findings of Full Scale Beam-Column Joint Tests," by A. Beres, R.N. White and P. Gergely, 9/30/92, (PB93-227783, A05, MF-A01).

NCEER-92-0025 "Experimental Results of Repaired and Retrofitted Beam-Column Joint Tests in Lightly Reinforced Concrete Frame Buildings," by A. Beres, S. El-Borgi, R.N. White and P. Gergely, 10/29/92, (PB93-227791, A05, MF-A01).

NCEER-92-0026 "A Generalization of Optimal Control Theory: Linear and Nonlinear Structures," by J.N. Yang, Z. Li and S. Vongchavalitkul, 11/2/92, (PB93-188621, A05, MF-A01).

NCEER-92-0027 "Seismic Resistance of Reinforced Concrete Frame Structures Designed Only for Gravity Loads: Part I - Design and Properties of a One-Third Scale Model Structure," by J.M. Bracci, A.M. Reinhorn and J.B. Mander, 12/1/92, (PB94-104502, A08, MF-A02).

NCEER-92-0028 "Seismic Resistance of Reinforced Concrete Frame Structures Designed Only for Gravity Loads: Part II - Experimental Performance of Subassemblages," by L.E. Aycardi, J.B. Mander and A.M. Reinhorn, 12/1/92, (PB94-104510, A08, MF-A02).

NCEER-92-0029 "Seismic Resistance of Reinforced Concrete Frame Structures Designed Only for Gravity Loads: Part III - Experimental Performance and Analytical Study of a Structural Model," by J.M. Bracci, A.M. Reinhorn and J.B. Mander, 12/1/92, (PB93-227528, A09, MF-A01).

NCEER-92-0030 "Evaluation of Seismic Retrofit of Reinforced Concrete Frame Structures: Part I - Experimental Performance of Retrofitted Subassemblages," by D. Choudhuri, J.B. Mander and A.M. Reinhorn, 12/8/92, (PB93-198307, A07, MF-A02).

NCEER-92-0031 "Evaluation of Seismic Retrofit of Reinforced Concrete Frame Structures: Part II - Experimental Performance and Analytical Study of a Retrofitted Structural Model," by J.M. Bracci, A.M. Reinhorn and J.B. Mander, 12/8/92, (PB93-198315, A09, MF-A03).

NCEER-92-0032 "Experimental and Analytical Investigation of Seismic Response of Structures with Supplemental Fluid Viscous Dampers," by M.C. Constantinou and M.D. Symans, 12/21/92, (PB93-191435, A10, MF-A03). This report is available only through NTIS (see address given above).

NCEER-92-0033 "Reconnaissance Report on the Cairo, Egypt Earthquake of October 12, 1992," by M. Khater, 12/23/92, (PB93-188621, A03, MF-A01).

NCEER-92-0034 "Low-Level Dynamic Characteristics of Four Tall Flat-Plate Buildings in New York City," by H. Gavin, S. Yuan, J. Grossman, E. Pekelis and K. Jacob, 12/28/92, (PB93-188217, A07, MF-A02).

NCEER-93-0001 "An Experimental Study on the Seismic Performance of Brick-Infilled Steel Frames With and Without Retrofit," by J.B. Mander, B. Nair, K. Wojtkowski and J. Ma, 1/29/93, (PB93-227510, A07, MF-A02).

NCEER-93-0002 "Social Accounting for Disaster Preparedness and Recovery Planning," by S. Cole, E. Pantoja and V. Razak, 2/22/93, (PB94-142114, A12, MF-A03).

NCEER-93-0003 "Assessment of 1991 NEHRP Provisions for Nonstructural Components and Recommended Revisions," by T.T. Soong, G. Chen, Z. Wu, R-H. Zhang and M. Grigoriu, 3/1/93, (PB93-188639, A06, MF-A02).

NCEER-93-0004 "Evaluation of Static and Response Spectrum Analysis Procedures of SEAOC/UBC for Seismic Isolated Structures," by C.W. Winters and M.C. Constantinou, 3/23/93, (PB93-198299, A10, MF-A03).

NCEER-93-0005 "Earthquakes in the Northeast - Are We Ignoring the Hazard? A Workshop on Earthquake Science and Safety for Educators," edited by K.E.K. Ross, 4/2/93, (PB94-103066, A09, MF-A02).

NCEER-93-0006 "Inelastic Response of Reinforced Concrete Structures with Viscoelastic Braces," by R.F. Lobo, J.M. Bracci, K.L. Shen, A.M. Reinhorn and T.T. Soong, 4/5/93, (PB93-227486, A05, MF-A02).

NCEER-93-0007 "Seismic Testing of Installation Methods for Computers and Data Processing Equipment," by K. Kosar, T.T. Soong, K.L. Shen, J.A. HoLung and Y.K. Lin, 4/12/93, (PB93-198299, A07, MF-A02).

NCEER-93-0008 "Retrofit of Reinforced Concrete Frames Using Added Dampers," by A. Reinhorn, M. Constantinou and C. Li, not available.

NCEER-93-0009 "Seismic Behavior and Design Guidelines for Steel Frame Structures with Added Viscoelastic Dampers," by K.C. Chang, M.L. Lai, T.T. Soong, D.S. Hao and Y.C. Yeh, 5/1/93, (PB94-141959, A07, MF-A02).

NCEER-93-0010 "Seismic Performance of Shear-Critical Reinforced Concrete Bridge Piers," by J.B. Mander, S.M. Waheed, M.T.A. Chaudhary and S.S. Chen, 5/12/93, (PB93-227494, A08, MF-A02).

NCEER-93-0011 "3D-BASIS-TABS: Computer Program for Nonlinear Dynamic Analysis of Three Dimensional Base Isolated Structures," by S. Nagarajaiah, C. Li, A.M. Reinhorn and M.C. Constantinou, 8/2/93, (PB94-141819, A09, MF-A02).

NCEER-93-0012 "Effects of Hydrocarbon Spills from an Oil Pipeline Break on Ground Water," by O.J. Helweg and H.H.M. Hwang, 8/3/93, (PB94-141942, A06, MF-A02).

NCEER-93-0013 "Simplified Procedures for Seismic Design of Nonstructural Components and Assessment of Current Code Provisions," by M.P. Singh, L.E. Suarez, E.E. Matheu and G.O. Maldonado, 8/4/93, (PB94-141827, A09, MF-A02).

NCEER-93-0014 "An Energy Approach to Seismic Analysis and Design of Secondary Systems," by G. Chen and T.T. Soong, 8/6/93, (PB94-142767, A11, MF-A03).

NCEER-93-0015 "Proceedings from School Sites: Becoming Prepared for Earthquakes - Commemorating the Third Anniversary of the Loma Prieta Earthquake," Edited by F.E. Winslow and K.E.K. Ross, 8/16/93, (PB94-154275, A16, MF-A02).

NCEER-93-0016 "Reconnaissance Report of Damage to Historic Monuments in Cairo, Egypt Following the October 12, 1992 Dahshur Earthquake," by D. Sykora, D. Look, G. Croci, E. Karaesmen and E. Karaesmen, 8/19/93, (PB94-142221, A08, MF-A02).

NCEER-93-0017 "The Island of Guam Earthquake of August 8, 1993," by S.W. Swan and S.K. Harris, 9/30/93, (PB94-141843, A04, MF-A01).

NCEER-93-0018 "Engineering Aspects of the October 12, 1992 Egyptian Earthquake," by A.W. Elgamal, M. Amer, K. Adalier and A. Abul-Fadl, 10/7/93, (PB94-141983, A05, MF-A01).

NCEER-93-0019 "Development of an Earthquake Motion Simulator and its Application in Dynamic Centrifuge Testing," by I. Krstelj, Supervised by J.H. Prevost, 10/23/93, (PB94-181773, A-10, MF-A03).

NCEER-93-0020 "NCEER-Taisei Corporation Research Program on Sliding Seismic Isolation Systems for Bridges: Experimental and Analytical Study of a Friction Pendulum System (FPS)," by M.C. Constantinou, P. Tsopelas, Y-S. Kim and S. Okamoto, 11/1/93, (PB94-142775, A08, MF-A02).

NCEER-93-0021 "Finite Element Modeling of Elastomeric Seismic Isolation Bearings," by L.J. Billings, Supervised by R. Shepherd, 11/8/93, not available.

NCEER-93-0022 "Seismic Vulnerability of Equipment in Critical Facilities: Life-Safety and Operational Consequences," by K. Porter, G.S. Johnson, M.M. Zadeh, C. Scawthorn and S. Eder, 11/24/93, (PB94-181765, A16, MF-A03).

NCEER-93-0023 "Hokkaido Nansei-oki, Japan Earthquake of July 12, 1993, by P.I. Yanev and C.R. Scawthorn, 12/23/93, (PB94-181500, A07, MF-A01).

NCEER-94-0001 "An Evaluation of Seismic Serviceability of Water Supply Networks with Application to the San Francisco Auxiliary Water Supply System," by I. Markov, Supervised by M. Grigoriu and T. O'Rourke, 1/21/94, (PB94-204013, A07, MF-A02).

NCEER-94-0002 "NCEER-Taisei Corporation Research Program on Sliding Seismic Isolation Systems for Bridges: Experimental and Analytical Study of Systems Consisting of Sliding Bearings, Rubber Restoring Force Devices and Fluid Dampers," Volumes I and II, by P. Tsopelas, S. Okamoto, M.C. Constantinou, D. Ozaki and S. Fujii, 2/4/94, (PB94-181740, A09, MF-A02 and PB94-181757, A12, MF-A03).

NCEER-94-0003 "A Markov Model for Local and Global Damage Indices in Seismic Analysis," by S. Rahman and M. Grigoriu, 2/18/94, (PB94-206000, A12, MF-A03).

NCEER-94-0004 "Proceedings from the NCEER Workshop on Seismic Response of Masonry Infills," edited by D.P. Abrams, 3/1/94, (PB94-180783, A07, MF-A02).

NCEER-94-0005 "The Northridge, California Earthquake of January 17, 1994: General Reconnaissance Report," edited by J.D. Goltz, 3/11/94, (PB94-193943, A10, MF-A03).

NCEER-94-0006 "Seismic Energy Based Fatigue Damage Analysis of Bridge Columns: Part I - Evaluation of Seismic Capacity," by G.A. Chang and J.B. Mander, 3/14/94, (PB94-219185, A11, MF-A03).

NCEER-94-0007 "Seismic Isolation of Multi-Story Frame Structures Using Spherical Sliding Isolation Systems," by T.M. Al-Hussaini, V.A. Zayas and M.C. Constantinou, 3/17/94, (PB94-193745, A09, MF-A02).

NCEER-94-0008 "The Northridge, California Earthquake of January 17, 1994: Performance of Highway Bridges," edited by I.G. Buckle, 3/24/94, (PB94-193851, A06, MF-A02).

NCEER-94-0009 "Proceedings of the Third U.S.-Japan Workshop on Earthquake Protective Systems for Bridges," edited by I.G. Buckle and I. Friedland, 3/31/94, (PB94-195815, A99, MF-A06).

NCEER-94-0010 "3D-BASIS-ME: Computer Program for Nonlinear Dynamic Analysis of Seismically Isolated Single and Multiple Structures and Liquid Storage Tanks," by P.C. Tsopelas, M.C. Constantinou and A.M. Reinhorn, 4/12/94, (PB94-204922, A09, MF-A02).

NCEER-94-0011 "The Northridge, California Earthquake of January 17, 1994: Performance of Gas Transmission Pipelines," by T.D. O'Rourke and M.C. Palmer, 5/16/94, (PB94-204989, A05, MF-A01).

NCEER-94-0012 "Feasibility Study of Replacement Procedures and Earthquake Performance Related to Gas Transmission Pipelines," by T.D. O'Rourke and M.C. Palmer, 5/25/94, (PB94-206638, A09, MF-A02).

NCEER-94-0013 "Seismic Energy Based Fatigue Damage Analysis of Bridge Columns: Part II - Evaluation of Seismic Demand," by G.A. Chang and J.B. Mander, 6/1/94, (PB95-18106, A08, MF-A02).

NCEER-94-0014 "NCEER-Taisei Corporation Research Program on Sliding Seismic Isolation Systems for Bridges: Experimental and Analytical Study of a System Consisting of Sliding Bearings and Fluid Restoring Force/Damping Devices," by P. Tsopelas and M.C. Constantinou, 6/13/94, (PB94-219144, A10, MF-A03).

NCEER-94-0015 "Generation of Hazard-Consistent Fragility Curves for Seismic Loss Estimation Studies," by H. Hwang and J-R. Huo, 6/14/94, (PB95-181996, A09, MF-A02).

NCEER-94-0016 "Seismic Study of Building Frames with Added Energy-Absorbing Devices," by W.S. Pong, C.S. Tsai and G.C. Lee, 6/20/94, (PB94-219136, A10, A03).

NCEER-94-0017 "Sliding Mode Control for Seismic-Excited Linear and Nonlinear Civil Engineering Structures," by J. Yang, J. Wu, A. Agrawal and Z. Li, 6/21/94, (PB95-138483, A06, MF-A02).

NCEER-94-0018 "3D-BASIS-TABS Version 2.0: Computer Program for Nonlinear Dynamic Analysis of Three Dimensional Base Isolated Structures," by A.M. Reinhorn, S. Nagarajaiah, M.C. Constantinou, P. Tsopelas and R. Li, 6/22/94, (PB95-182176, A08, MF-A02).

NCEER-94-0019 "Proceedings of the International Workshop on Civil Infrastructure Systems: Application of Intelligent Systems and Advanced Materials on Bridge Systems," Edited by G.C. Lee and K.C. Chang, 7/18/94, (PB95-252474, A20, MF-A04).

NCEER-94-0020 "Study of Seismic Isolation Systems for Computer Floors," by V. Lambrou and M.C. Constantinou, 7/19/94, (PB95-138533, A10, MF-A03).

NCEER-94-0021 "Proceedings of the U.S.-Italian Workshop on Guidelines for Seismic Evaluation and Rehabilitation of Unreinforced Masonry Buildings," Edited by D.P. Abrams and G.M. Calvi, 7/20/94, (PB95-138749, A13, MF-A03).

NCEER-94-0022 "NCEER-Taisei Corporation Research Program on Sliding Seismic Isolation Systems for Bridges: Experimental and Analytical Study of a System Consisting of Lubricated PTFE Sliding Bearings and Mild Steel Dampers," by P. Tsopelas and M.C. Constantinou, 7/22/94, (PB95-182184, A08, MF-A02).

NCEER-94-0023 “Development of Reliability-Based Design Criteria for Buildings Under Seismic Load,” by Y.K. Wen, H. Hwang and M. Shinozuka, 8/1/94, (PB95-211934, A08, MF-A02).

NCEER-94-0024 “Experimental Verification of Acceleration Feedback Control Strategies for an Active Tendon System,” by S.J. Dyke, B.F. Spencer, Jr., P. Quast, M.K. Sain, D.C. Kaspari, Jr. and T.T. Soong, 8/29/94, (PB95-212320, A05, MF-A01).

NCEER-94-0025 “Seismic Retrofitting Manual for Highway Bridges,” Edited by I.G. Buckle and I.F. Friedland, published by the Federal Highway Administration (PB95-212676, A15, MF-A03).

NCEER-94-0026 “Proceedings from the Fifth U.S.-Japan Workshop on Earthquake Resistant Design of Lifeline Facilities and Countermeasures Against Soil Liquefaction,” Edited by T.D. O’Rourke and M. Hamada, 11/7/94, (PB95-220802, A99, MF-E08).

NCEER-95-0001 "Experimental and Analytical Investigation of Seismic Retrofit of Structures with Supplemental Damping: Part 1 - Fluid Viscous Damping Devices," by A.M. Reinhorn, C. Li and M.C. Constantinou, 1/3/95, (PB95-266599, A09, MF-A02).

NCEER-95-0002 "Experimental and Analytical Study of Low-Cycle Fatigue Behavior of Semi-Rigid Top-And-Seat Angle Connections," by G. Pekcan, J.B. Mander and S.S. Chen, 1/5/95, (PB95-220042, A07, MF-A02).

NCEER-95-0003 "NCEER-ATC Joint Study on Fragility of Buildings," by T. Anagnos, C. Rojahn and A.S. Kiremidjian, 1/20/95, (PB95-220026, A06, MF-A02).

NCEER-95-0004 "Nonlinear Control Algorithms for Peak Response Reduction," by Z. Wu, T.T. Soong, V. Gattulli and R.C. Lin, 2/16/95, (PB95-220349, A05, MF-A01).

NCEER-95-0005 "Pipeline Replacement Feasibility Study: A Methodology for Minimizing Seismic and Corrosion Risks to Underground Natural Gas Pipelines," by R.T. Eguchi, H.A. Seligson and D.G. Honegger, 3/2/95, (PB95-252326, A06, MF-A02).

NCEER-95-0006 "Evaluation of Seismic Performance of an 11-Story Frame Building During the 1994 Northridge Earthquake," by F. Naeim, R. DiSulio, K. Benuska, A. Reinhorn and C. Li, not available.

NCEER-95-0007 "Prioritization of Bridges for Seismic Retrofitting," by N. Basöz and A.S. Kiremidjian, 4/24/95, (PB95-252300, A08, MF-A02).

NCEER-95-0008 "Method for Developing Motion Damage Relationships for Reinforced Concrete Frames," by A. Singhal and A.S. Kiremidjian, 5/11/95, (PB95-266607, A06, MF-A02).

NCEER-95-0009 "Experimental and Analytical Investigation of Seismic Retrofit of Structures with Supplemental Damping: Part II - Friction Devices," by C. Li and A.M. Reinhorn, 7/6/95, (PB96-128087, A11, MF-A03).

NCEER-95-0010 "Experimental Performance and Analytical Study of a Non-Ductile Reinforced Concrete Frame Structure Retrofitted with Elastomeric Spring Dampers," by G. Pekcan, J.B. Mander and S.S. Chen, 7/14/95, (PB96-137161, A08, MF-A02).

NCEER-95-0011 "Development and Experimental Study of Semi-Active Fluid Damping Devices for Seismic Protection of Structures," by M.D. Symans and M.C. Constantinou, 8/3/95, (PB96-136940, A23, MF-A04).

NCEER-95-0012 "Real-Time Structural Parameter Modification (RSPM): Development of Innervated Structures," by Z. Liang, M. Tong and G.C. Lee, 4/11/95, (PB96-137153, A06, MF-A01).

NCEER-95-0013 "Experimental and Analytical Investigation of Seismic Retrofit of Structures with Supplemental Damping: Part III - Viscous Damping Walls," by A.M. Reinhorn and C. Li, 10/1/95, (PB96-176409, A11, MF-A03).

NCEER-95-0014 "Seismic Fragility Analysis of Equipment and Structures in a Memphis Electric Substation," by J-R. Huo and H.H.M. Hwang, 8/10/95, (PB96-128087, A09, MF-A02).

NCEER-95-0015 "The Hanshin-Awaji Earthquake of January 17, 1995: Performance of Lifelines," Edited by M. Shinozuka, 11/3/95, (PB96-176383, A15, MF-A03).

NCEER-95-0016 "Highway Culvert Performance During Earthquakes," by T.L. Youd and C.J. Beckman, available as NCEER-96-0015.

NCEER-95-0017 "The Hanshin-Awaji Earthquake of January 17, 1995: Performance of Highway Bridges," Edited by I.G. Buckle, 12/1/95, not available.

NCEER-95-0018 "Modeling of Masonry Infill Panels for Structural Analysis," by A.M. Reinhorn, A. Madan, R.E. Valles, Y. Reichmann and J.B. Mander, 12/8/95, (PB97-110886, MF-A01, A06).

NCEER-95-0019 "Optimal Polynomial Control for Linear and Nonlinear Structures," by A.K. Agrawal and J.N. Yang, 12/11/95, (PB96-168737, A07, MF-A02).

NCEER-95-0020 "Retrofit of Non-Ductile Reinforced Concrete Frames Using Friction Dampers," by R.S. Rao, P. Gergely and R.N. White, 12/22/95, (PB97-133508, A10, MF-A02).

NCEER-95-0021 "Parametric Results for Seismic Response of Pile-Supported Bridge Bents," by G. Mylonakis, A. Nikolaou and G. Gazetas, 12/22/95, (PB97-100242, A12, MF-A03).

NCEER-95-0022 "Kinematic Bending Moments in Seismically Stressed Piles," by A. Nikolaou, G. Mylonakis and G. Gazetas, 12/23/95, (PB97-113914, MF-A03, A13).

NCEER-96-0001 "Dynamic Response of Unreinforced Masonry Buildings with Flexible Diaphragms," by A.C. Costley and D.P. Abrams," 10/10/96, (PB97-133573, MF-A03, A15).

NCEER-96-0002 "State of the Art Review: Foundations and Retaining Structures," by I. Po Lam, not available.

NCEER-96-0003 "Ductility of Rectangular Reinforced Concrete Bridge Columns with Moderate Confinement," by N. Wehbe, M. Saiidi, D. Sanders and B. Douglas, 11/7/96, (PB97-133557, A06, MF-A02).

NCEER-96-0004 "Proceedings of the Long-Span Bridge Seismic Research Workshop," edited by I.G. Buckle and I.M. Friedland, not available.

NCEER-96-0005 "Establish Representative Pier Types for Comprehensive Study: Eastern United States," by J. Kulicki and Z. Prucz, 5/28/96, (PB98-119217, A07, MF-A02).

NCEER-96-0006 "Establish Representative Pier Types for Comprehensive Study: Western United States," by R. Imbsen, R.A. Schamber and T.A. Osterkamp, 5/28/96, (PB98-118607, A07, MF-A02).

NCEER-96-0007 "Nonlinear Control Techniques for Dynamical Systems with Uncertain Parameters," by R.G. Ghanem and M.I. Bujakov, 5/27/96, (PB97-100259, A17, MF-A03).

NCEER-96-0008 "Seismic Evaluation of a 30-Year Old Non-Ductile Highway Bridge Pier and Its Retrofit," by J.B. Mander, B. Mahmoodzadegan, S. Bhadra and S.S. Chen, 5/31/96, (PB97-110902, MF-A03, A10).

NCEER-96-0009 "Seismic Performance of a Model Reinforced Concrete Bridge Pier Before and After Retrofit," by J.B. Mander, J.H. Kim and C.A. Ligozio, 5/31/96, (PB97-110910, MF-A02, A10).

NCEER-96-0010 "IDARC2D Version 4.0: A Computer Program for the Inelastic Damage Analysis of Buildings," by R.E. Valles, A.M. Reinhorn, S.K. Kunnath, C. Li and A. Madan, 6/3/96, (PB97-100234, A17, MF-A03).

NCEER-96-0011 "Estimation of the Economic Impact of Multiple Lifeline Disruption: Memphis Light, Gas and Water Division Case Study," by S.E. Chang, H.A. Seligson and R.T. Eguchi, 8/16/96, (PB97-133490, A11, MF-A03).

NCEER-96-0012 "Proceedings from the Sixth Japan-U.S. Workshop on Earthquake Resistant Design of Lifeline Facilities and Countermeasures Against Soil Liquefaction, Edited by M. Hamada and T. O'Rourke, 9/11/96, (PB97-133581, A99, MF-A06).

NCEER-96-0013 "Chemical Hazards, Mitigation and Preparedness in Areas of High Seismic Risk: A Methodology for Estimating the Risk of Post-Earthquake Hazardous Materials Release," by H.A. Seligson, R.T. Eguchi, K.J. Tierney and K. Richmond, 11/7/96, (PB97-133565, MF-A02, A08).

NCEER-96-0014 "Response of Steel Bridge Bearings to Reversed Cyclic Loading," by J.B. Mander, D-K. Kim, S.S. Chen and G.J. Premus, 11/13/96, (PB97-140735, A12, MF-A03).

NCEER-96-0015 "Highway Culvert Performance During Past Earthquakes," by T.L. Youd and C.J. Beckman, 11/25/96, (PB97-133532, A06, MF-A01).

NCEER-97-0001 "Evaluation, Prevention and Mitigation of Pounding Effects in Building Structures," by R.E. Valles and A.M. Reinhorn, 2/20/97, (PB97-159552, A14, MF-A03).

NCEER-97-0002 "Seismic Design Criteria for Bridges and Other Highway Structures," by C. Rojahn, R. Mayes, D.G. Anderson, J. Clark, J.H. Hom, R.V. Nutt and M.J. O'Rourke, 4/30/97, (PB97-194658, A06, MF-A03).

NCEER-97-0003 “Proceedings of the U.S.-Italian Workshop on Seismic Evaluation and Retrofit,” Edited by D.P. Abrams and G.M. Calvi, 3/19/97, (PB97-194666, A13, MF-A03).

NCEER-97-0004 "Investigation of Seismic Response of Buildings with Linear and Nonlinear Fluid Viscous Dampers," by A.A. Seleemah and M.C. Constantinou, 5/21/97, (PB98-109002, A15, MF-A03).

NCEER-97-0005 "Proceedings of the Workshop on Earthquake Engineering Frontiers in Transportation Facilities," edited by G.C. Lee and I.M. Friedland, 8/29/97, (PB98-128911, A25, MR-A04).

NCEER-97-0006 "Cumulative Seismic Damage of Reinforced Concrete Bridge Piers," by S.K. Kunnath, A. El-Bahy, A. Taylor and W. Stone, 9/2/97, (PB98-108814, A11, MF-A03).

NCEER-97-0007 "Structural Details to Accommodate Seismic Movements of Highway Bridges and Retaining Walls," by R.A. Imbsen, R.A. Schamber, E. Thorkildsen, A. Kartoum, B.T. Martin, T.N. Rosser and J.M. Kulicki, 9/3/97, (PB98-108996, A09, MF-A02).

NCEER-97-0008 "A Method for Earthquake Motion-Damage Relationships with Application to Reinforced Concrete Frames," by A. Singhal and A.S. Kiremidjian, 9/10/97, (PB98-108988, A13, MF-A03).

NCEER-97-0009 "Seismic Analysis and Design of Bridge Abutments Considering Sliding and Rotation," by K. Fishman and R. Richards, Jr., 9/15/97, (PB98-108897, A06, MF-A02).

NCEER-97-0010 "Proceedings of the FHWA/NCEER Workshop on the National Representation of Seismic Ground Motion for New and Existing Highway Facilities," edited by I.M. Friedland, M.S. Power and R.L. Mayes, 9/22/97, (PB98-128903, A21, MF-A04).

NCEER-97-0011 "Seismic Analysis for Design or Retrofit of Gravity Bridge Abutments," by K.L. Fishman, R. Richards, Jr. and R.C. Divito, 10/2/97, (PB98-128937, A08, MF-A02).

NCEER-97-0012 "Evaluation of Simplified Methods of Analysis for Yielding Structures," by P. Tsopelas, M.C. Constantinou, C.A. Kircher and A.S. Whittaker, 10/31/97, (PB98-128929, A10, MF-A03).

NCEER-97-0013 "Seismic Design of Bridge Columns Based on Control and Repairability of Damage," by C-T. Cheng and J.B. Mander, 12/8/97, (PB98-144249, A11, MF-A03).

NCEER-97-0014 "Seismic Resistance of Bridge Piers Based on Damage Avoidance Design," by J.B. Mander and C-T. Cheng, 12/10/97, (PB98-144223, A09, MF-A02).

NCEER-97-0015 “Seismic Response of Nominally Symmetric Systems with Strength Uncertainty,” by S. Balopoulou and M. Grigoriu, 12/23/97, (PB98-153422, A11, MF-A03).

NCEER-97-0016 “Evaluation of Seismic Retrofit Methods for Reinforced Concrete Bridge Columns,” by T.J. Wipf, F.W. Klaiber and F.M. Russo, 12/28/97, (PB98-144215, A12, MF-A03).

NCEER-97-0017 “Seismic Fragility of Existing Conventional Reinforced Concrete Highway Bridges,” by C.L. Mullen and A.S. Cakmak, 12/30/97, (PB98-153406, A08, MF-A02).

NCEER-97-0018 “Loss Asssessment of Memphis Buildings,” edited by D.P. Abrams and M. Shinozuka, 12/31/97, (PB98-144231, A13, MF-A03).

NCEER-97-0019 “Seismic Evaluation of Frames with Infill Walls Using Quasi-static Experiments,” by K.M. Mosalam, R.N. White and P. Gergely, 12/31/97, (PB98-153455, A07, MF-A02).

NCEER-97-0020 “Seismic Evaluation of Frames with Infill Walls Using Pseudo-dynamic Experiments,” by K.M. Mosalam, R.N. White and P. Gergely, 12/31/97, (PB98-153430, A07, MF-A02).

NCEER-97-0021 “Computational Strategies for Frames with Infill Walls: Discrete and Smeared Crack Analyses and Seismic Fragility,” by K.M. Mosalam, R.N. White and P. Gergely, 12/31/97, (PB98-153414, A10, MF-A02).

NCEER-97-0022 "Proceedings of the NCEER Workshop on Evaluation of Liquefaction Resistance of Soils," edited by T.L. Youd and I.M. Idriss, 12/31/97, (PB98-155617, A15, MF-A03).

MCEER-98-0001 "Extraction of Nonlinear Hysteretic Properties of Seismically Isolated Bridges from Quick-Release Field Tests," by Q. Chen, B.M. Douglas, E.M. Maragakis and I.G. Buckle, 5/26/98, (PB99-118838, A06, MF-A01).

MCEER-98-0002 "Methodologies for Evaluating the Importance of Highway Bridges," by A. Thomas, S. Eshenaur and J. Kulicki, 5/29/98, (PB99-118846, A10, MF-A02).

MCEER-98-0003 "Capacity Design of Bridge Piers and the Analysis of Overstrength," by J.B. Mander, A. Dutta and P. Goel, 6/1/98, (PB99-118853, A09, MF-A02).

MCEER-98-0004 "Evaluation of Bridge Damage Data from the Loma Prieta and Northridge, California Earthquakes," by N. Basoz and A. Kiremidjian, 6/2/98, (PB99-118861, A15, MF-A03).

MCEER-98-0005 "Screening Guide for Rapid Assessment of Liquefaction Hazard at Highway Bridge Sites," by T. L. Youd, 6/16/98, (PB99-118879, A06, not available on microfiche).

MCEER-98-0006 "Structural Steel and Steel/Concrete Interface Details for Bridges," by P. Ritchie, N. Kauhl and J. Kulicki, 7/13/98, (PB99-118945, A06, MF-A01).

MCEER-98-0007 "Capacity Design and Fatigue Analysis of Confined Concrete Columns," by A. Dutta and J.B. Mander, 7/14/98, (PB99-118960, A14, MF-A03).

MCEER-98-0008 "Proceedings of the Workshop on Performance Criteria for Telecommunication Services Under Earthquake Conditions," edited by A.J. Schiff, 7/15/98, (PB99-118952, A08, MF-A02).

MCEER-98-0009 "Fatigue Analysis of Unconfined Concrete Columns," by J.B. Mander, A. Dutta and J.H. Kim, 9/12/98, (PB99-123655, A10, MF-A02).

MCEER-98-0010 "Centrifuge Modeling of Cyclic Lateral Response of Pile-Cap Systems and Seat-Type Abutments in Dry Sands," by A.D. Gadre and R. Dobry, 10/2/98, (PB99-123606, A13, MF-A03).

MCEER-98-0011 "IDARC-BRIDGE: A Computational Platform for Seismic Damage Assessment of Bridge Structures," by A.M. Reinhorn, V. Simeonov, G. Mylonakis and Y. Reichman, 10/2/98, (PB99-162919, A15, MF-A03).

MCEER-98-0012 "Experimental Investigation of the Dynamic Response of Two Bridges Before and After Retrofitting with Elastomeric Bearings," by D.A. Wendichansky, S.S. Chen and J.B. Mander, 10/2/98, (PB99-162927, A15, MF-A03).

MCEER-98-0013 "Design Procedures for Hinge Restrainers and Hinge Sear Width for Multiple-Frame Bridges," by R. Des Roches and G.L. Fenves, 11/3/98, (PB99-140477, A13, MF-A03).

MCEER-98-0014 "Response Modification Factors for Seismically Isolated Bridges," by M.C. Constantinou and J.K. Quarshie, 11/3/98, (PB99-140485, A14, MF-A03).

MCEER-98-0015 "Proceedings of the U.S.-Italy Workshop on Seismic Protective Systems for Bridges," edited by I.M. Friedland and M.C. Constantinou, 11/3/98, (PB2000-101711, A22, MF-A04).

MCEER-98-0016 "Appropriate Seismic Reliability for Critical Equipment Systems: Recommendations Based on Regional Analysis of Financial and Life Loss," by K. Porter, C. Scawthorn, C. Taylor and N. Blais, 11/10/98, (PB99-157265, A08, MF-A02).

MCEER-98-0017 "Proceedings of the U.S. Japan Joint Seminar on Civil Infrastructure Systems Research," edited by M. Shinozuka and A. Rose, 11/12/98, (PB99-156713, A16, MF-A03).

MCEER-98-0018 "Modeling of Pile Footings and Drilled Shafts for Seismic Design," by I. PoLam, M. Kapuskar and D. Chaudhuri, 12/21/98, (PB99-157257, A09, MF-A02).

MCEER-99-0001 "Seismic Evaluation of a Masonry Infilled Reinforced Concrete Frame by Pseudodynamic Testing," by S.G. Buonopane and R.N. White, 2/16/99, (PB99-162851, A09, MF-A02).

MCEER-99-0002 "Response History Analysis of Structures with Seismic Isolation and Energy Dissipation Systems: Verification Examples for Program SAP2000," by J. Scheller and M.C. Constantinou, 2/22/99, (PB99-162869, A08, MF-A02).

MCEER-99-0003 "Experimental Study on the Seismic Design and Retrofit of Bridge Columns Including Axial Load Effects," by A. Dutta, T. Kokorina and J.B. Mander, 2/22/99, (PB99-162877, A09, MF-A02).

MCEER-99-0004 "Experimental Study of Bridge Elastomeric and Other Isolation and Energy Dissipation Systems with Emphasis on Uplift Prevention and High Velocity Near-source Seismic Excitation," by A. Kasalanati and M. C. Constantinou, 2/26/99, (PB99-162885, A12, MF-A03).

MCEER-99-0005 "Truss Modeling of Reinforced Concrete Shear-flexure Behavior," by J.H. Kim and J.B. Mander, 3/8/99, (PB99-163693, A12, MF-A03).

MCEER-99-0006 "Experimental Investigation and Computational Modeling of Seismic Response of a 1:4 Scale Model Steel Structure with a Load Balancing Supplemental Damping System," by G. Pekcan, J.B. Mander and S.S. Chen, 4/2/99, (PB99-162893, A11, MF-A03).

MCEER-99-0007 "Effect of Vertical Ground Motions on the Structural Response of Highway Bridges," by M.R. Button, C.J. Cronin and R.L. Mayes, 4/10/99, (PB2000-101411, A10, MF-A03).

MCEER-99-0008 "Seismic Reliability Assessment of Critical Facilities: A Handbook, Supporting Documentation, and Model Code Provisions," by G.S. Johnson, R.E. Sheppard, M.D. Quilici, S.J. Eder and C.R. Scawthorn, 4/12/99, (PB2000-101701, A18, MF-A04).

MCEER-99-0009 "Impact Assessment of Selected MCEER Highway Project Research on the Seismic Design of Highway Structures," by C. Rojahn, R. Mayes, D.G. Anderson, J.H. Clark, D'Appolonia Engineering, S. Gloyd and R.V. Nutt, 4/14/99, (PB99-162901, A10, MF-A02).

MCEER-99-0010 "Site Factors and Site Categories in Seismic Codes," by R. Dobry, R. Ramos and M.S. Power, 7/19/99, (PB2000-101705, A08, MF-A02).

MCEER-99-0011 "Restrainer Design Procedures for Multi-Span Simply-Supported Bridges," by M.J. Randall, M. Saiidi, E. Maragakis and T. Isakovic, 7/20/99, (PB2000-101702, A10, MF-A02).

MCEER-99-0012 "Property Modification Factors for Seismic Isolation Bearings," by M.C. Constantinou, P. Tsopelas, A. Kasalanati and E. Wolff, 7/20/99, (PB2000-103387, A11, MF-A03).

MCEER-99-0013 "Critical Seismic Issues for Existing Steel Bridges," by P. Ritchie, N. Kauhl and J. Kulicki, 7/20/99, (PB2000-101697, A09, MF-A02).

MCEER-99-0014 "Nonstructural Damage Database," by A. Kao, T.T. Soong and A. Vender, 7/24/99, (PB2000-101407, A06, MF-A01).

MCEER-99-0015 "Guide to Remedial Measures for Liquefaction Mitigation at Existing Highway Bridge Sites," by H.G. Cooke and J. K. Mitchell, 7/26/99, (PB2000-101703, A11, MF-A03).

MCEER-99-0016 "Proceedings of the MCEER Workshop on Ground Motion Methodologies for the Eastern United States," edited by N. Abrahamson and A. Becker, 8/11/99, (PB2000-103385, A07, MF-A02).

MCEER-99-0017 "Quindío, Colombia Earthquake of January 25, 1999: Reconnaissance Report," by A.P. Asfura and P.J. Flores, 10/4/99, (PB2000-106893, A06, MF-A01).

MCEER-99-0018 "Hysteretic Models for Cyclic Behavior of Deteriorating Inelastic Structures," by M.V. Sivaselvan and A.M. Reinhorn, 11/5/99, (PB2000-103386, A08, MF-A02).

MCEER-99-0019 "Proceedings of the 7th U.S.- Japan Workshop on Earthquake Resistant Design of Lifeline Facilities and Countermeasures Against Soil Liquefaction," edited by T.D. O'Rourke, J.P. Bardet and M. Hamada, 11/19/99, (PB2000-103354, A99, MF-A06).

MCEER-99-0020 "Development of Measurement Capability for Micro-Vibration Evaluations with Application to Chip Fabrication Facilities," by G.C. Lee, Z. Liang, J.W. Song, J.D. Shen and W.C. Liu, 12/1/99, (PB2000-105993, A08, MF-A02).

MCEER-99-0021 "Design and Retrofit Methodology for Building Structures with Supplemental Energy Dissipating Systems," by G. Pekcan, J.B. Mander and S.S. Chen, 12/31/99, (PB2000-105994, A11, MF-A03).

MCEER-00-0001 "The Marmara, Turkey Earthquake of August 17, 1999: Reconnaissance Report," edited by C. Scawthorn; with major contributions by M. Bruneau, R. Eguchi, T. Holzer, G. Johnson, J. Mander, J. Mitchell, W. Mitchell, A. Papageorgiou, C. Scaethorn, and G. Webb, 3/23/00, (PB2000-106200, A11, MF-A03).

MCEER-00-0002 "Proceedings of the MCEER Workshop for Seismic Hazard Mitigation of Health Care Facilities," edited by G.C. Lee, M. Ettouney, M. Grigoriu, J. Hauer and J. Nigg, 3/29/00, (PB2000-106892, A08, MF-A02).

MCEER-00-0003 "The Chi-Chi, Taiwan Earthquake of September 21, 1999: Reconnaissance Report," edited by G.C. Lee and C.H. Loh, with major contributions by G.C. Lee, M. Bruneau, I.G. Buckle, S.E. Chang, P.J. Flores, T.D. O'Rourke, M. Shinozuka, T.T. Soong, C-H. Loh, K-C. Chang, Z-J. Chen, J-S. Hwang, M-L. Lin, G-Y. Liu, K-C. Tsai, G.C. Yao and C-L. Yen, 4/30/00, (PB2001-100980, A10, MF-A02).

MCEER-00-0004 "Seismic Retrofit of End-Sway Frames of Steel Deck-Truss Bridges with a Supplemental Tendon System: Experimental and Analytical Investigation," by G. Pekcan, J.B. Mander and S.S. Chen, 7/1/00, (PB2001-100982, A10, MF-A02).

MCEER-00-0005 "Sliding Fragility of Unrestrained Equipment in Critical Facilities," by W.H. Chong and T.T. Soong, 7/5/00, (PB2001-100983, A08, MF-A02).

MCEER-00-0006 "Seismic Response of Reinforced Concrete Bridge Pier Walls in the Weak Direction," by N. Abo-Shadi, M. Saiidi and D. Sanders, 7/17/00, (PB2001-100981, A17, MF-A03).

MCEER-00-0007 "Low-Cycle Fatigue Behavior of Longitudinal Reinforcement in Reinforced Concrete Bridge Columns," by J. Brown and S.K. Kunnath, 7/23/00, (PB2001-104392, A08, MF-A02).

MCEER-00-0008 "Soil Structure Interaction of Bridges for Seismic Analysis," I. PoLam and H. Law, 9/25/00, (PB2001-105397, A08, MF-A02).

MCEER-00-0009 "Proceedings of the First MCEER Workshop on Mitigation of Earthquake Disaster by Advanced Technologies (MEDAT-1), edited by M. Shinozuka, D.J. Inman and T.D. O'Rourke, 11/10/00, (PB2001-105399, A14, MF-A03).

MCEER-00-0010 "Development and Evaluation of Simplified Procedures for Analysis and Design of Buildings with Passive Energy Dissipation Systems, Revision 01," by O.M. Ramirez, M.C. Constantinou, C.A. Kircher, A.S. Whittaker, M.W. Johnson, J.D. Gomez and C. Chrysostomou, 11/16/01, (PB2001-105523, A23, MF-A04).

MCEER-00-0011 "Dynamic Soil-Foundation-Structure Interaction Analyses of Large Caissons," by C-Y. Chang, C-M. Mok, Z-L. Wang, R. Settgast, F. Waggoner, M.A. Ketchum, H.M. Gonnermann and C-C. Chin, 12/30/00, (PB2001-104373, A07, MF-A02).

MCEER-00-0012 "Experimental Evaluation of Seismic Performance of Bridge Restrainers," by A.G. Vlassis, E.M. Maragakis and M. Saiid Saiidi, 12/30/00, (PB2001-104354, A09, MF-A02).

MCEER-00-0013 "Effect of Spatial Variation of Ground Motion on Highway Structures," by M. Shinozuka, V. Saxena and G. Deodatis, 12/31/00, (PB2001-108755, A13, MF-A03).

MCEER-00-0014 "A Risk-Based Methodology for Assessing the Seismic Performance of Highway Systems," by S.D. Werner, C.E. Taylor, J.E. Moore, II, J.S. Walton and S. Cho, 12/31/00, (PB2001-108756, A14, MF-A03).

MCEER-01-0001 "Experimental Investigation of P-Delta Effects to Collapse During Earthquakes," by D. Vian and M. Bruneau, 6/25/01, (PB2002-100534, A17, MF-A03).

MCEER-01-0002 "Proceedings of the Second MCEER Workshop on Mitigation of Earthquake Disaster by Advanced Technologies (MEDAT-2)," edited by M. Bruneau and D.J. Inman, 7/23/01, (PB2002-100434, A16, MF-A03).

MCEER-01-0003 "Sensitivity Analysis of Dynamic Systems Subjected to Seismic Loads," by C. Roth and M. Grigoriu, 9/18/01, (PB2003-100884, A12, MF-A03).

MCEER-01-0004 "Overcoming Obstacles to Implementing Earthquake Hazard Mitigation Policies: Stage 1 Report," by D.J. Alesch and W.J. Petak, 12/17/01, (PB2002-107949, A07, MF-A02).

MCEER-01-0005 "Updating Real-Time Earthquake Loss Estimates: Methods, Problems and Insights," by C.E. Taylor, S.E. Chang and R.T. Eguchi, 12/17/01, (PB2002-107948, A05, MF-A01).

MCEER-01-0006 "Experimental Investigation and Retrofit of Steel Pile Foundations and Pile Bents Under Cyclic Lateral Loadings," by A. Shama, J. Mander, B. Blabac and S. Chen, 12/31/01, (PB2002-107950, A13, MF-A03).

MCEER-02-0001 "Assessment of Performance of Bolu Viaduct in the 1999 Duzce Earthquake in Turkey" by P.C. Roussis, M.C. Constantinou, M. Erdik, E. Durukal and M. Dicleli, 5/8/02, (PB2003-100883, A08, MF-A02).

MCEER-02-0002 "Seismic Behavior of Rail Counterweight Systems of Elevators in Buildings," by M.P. Singh, Rildova and L.E. Suarez, 5/27/02. (PB2003-100882, A11, MF-A03).

MCEER-02-0003 "Development of Analysis and Design Procedures for Spread Footings," by G. Mylonakis, G. Gazetas, S. Nikolaou and A. Chauncey, 10/02/02, (PB2004-101636, A13, MF-A03, CD-A13).

MCEER-02-0004 "Bare-Earth Algorithms for Use with SAR and LIDAR Digital Elevation Models," by C.K. Huyck, R.T. Eguchi and B. Houshmand, 10/16/02, (PB2004-101637, A07, CD-A07).

MCEER-02-0005 "Review of Energy Dissipation of Compression Members in Concentrically Braced Frames," by K.Lee and M. Bruneau, 10/18/02, (PB2004-101638, A10, CD-A10).

MCEER-03-0001 "Experimental Investigation of Light-Gauge Steel Plate Shear Walls for the Seismic Retrofit of Buildings" by J. Berman and M. Bruneau, 5/2/03, (PB2004-101622, A10, MF-A03, CD-A10).

MCEER-03-0002 "Statistical Analysis of Fragility Curves," by M. Shinozuka, M.Q. Feng, H. Kim, T. Uzawa and T. Ueda, 6/16/03, (PB2004-101849, A09, CD-A09).

MCEER-03-0003 "Proceedings of the Eighth U.S.-Japan Workshop on Earthquake Resistant Design f Lifeline Facilities and Countermeasures Against Liquefaction," edited by M. Hamada, J.P. Bardet and T.D. O'Rourke, 6/30/03, (PB2004-104386, A99, CD-A99).

MCEER-03-0004 "Proceedings of the PRC-US Workshop on Seismic Analysis and Design of Special Bridges," edited by L.C. Fan and G.C. Lee, 7/15/03, (PB2004-104387, A14, CD-A14).

MCEER-03-0005 "Urban Disaster Recovery: A Framework and Simulation Model," by S.B. Miles and S.E. Chang, 7/25/03, (PB2004-104388, A07, CD-A07).

MCEER-03-0006 "Behavior of Underground Piping Joints Due to Static and Dynamic Loading," by R.D. Meis, M. Maragakis and R. Siddharthan, 11/17/03, (PB2005-102194, A13, MF-A03, CD-A00).

MCEER-04-0001 "Experimental Study of Seismic Isolation Systems with Emphasis on Secondary System Response and Verification of Accuracy of Dynamic Response History Analysis Methods," by E. Wolff and M. Constantinou, 1/16/04 (PB2005-102195, A99, MF-E08, CD-A00).

MCEER-04-0002 "Tension, Compression and Cyclic Testing of Engineered Cementitious Composite Materials," by K. Kesner and S.L. Billington, 3/1/04, (PB2005-102196, A08, CD-A08).

MCEER-04-0003 "Cyclic Testing of Braces Laterally Restrained by Steel Studs to Enhance Performance During Earthquakes," by O.C. Celik, J.W. Berman and M. Bruneau, 3/16/04, (PB2005-102197, A13, MF-A03, CD-A00).

MCEER-04-0004 "Methodologies for Post Earthquake Building Damage Detection Using SAR and Optical Remote Sensing: Application to the August 17, 1999 Marmara, Turkey Earthquake," by C.K. Huyck, B.J. Adams, S. Cho, R.T. Eguchi, B. Mansouri and B. Houshmand, 6/15/04, (PB2005-104888, A10, CD-A00).

MCEER-04-0005 "Nonlinear Structural Analysis Towards Collapse Simulation: A Dynamical Systems Approach," by M.V. Sivaselvan and A.M. Reinhorn, 6/16/04, (PB2005-104889, A11, MF-A03, CD-A00).

MCEER-04-0006 "Proceedings of the Second PRC-US Workshop on Seismic Analysis and Design of Special Bridges," edited by G.C. Lee and L.C. Fan, 6/25/04, (PB2005-104890, A16, CD-A00).

MCEER-04-0007 "Seismic Vulnerability Evaluation of Axially Loaded Steel Built-up Laced Members," by K. Lee and M. Bruneau, 6/30/04, (PB2005-104891, A16, CD-A00).

MCEER-04-0008 "Evaluation of Accuracy of Simplified Methods of Analysis and Design of Buildings with Damping Systems for Near-Fault and for Soft-Soil Seismic Motions," by E.A. Pavlou and M.C. Constantinou, 8/16/04, (PB2005-104892, A08, MF-A02, CD-A00).

MCEER-04-0009 "Assessment of Geotechnical Issues in Acute Care Facilities in California," by M. Lew, T.D. O'Rourke, R. Dobry and M. Koch, 9/15/04, (PB2005-104893, A08, CD-A00).

MCEER-04-0010 "Scissor-Jack-Damper Energy Dissipation System," by A.N. Sigaher-Boyle and M.C. Constantinou, 12/1/04 (PB2005-108221).

MCEER-04-0011 "Seismic Retrofit of Bridge Steel Truss Piers Using a Controlled Rocking Approach," by M. Pollino and M. Bruneau, 12/20/04 (PB2006-105795).

MCEER-05-0001 "Experimental and Analytical Studies of Structures Seismically Isolated with an Uplift-Restraint Isolation System," by P.C. Roussis and M.C. Constantinou, 1/10/05 (PB2005-108222).

MCEER-05-0002 "A Versatile Experimentation Model for Study of Structures Near Collapse Applied to Seismic Evaluation of Irregular Structures," by D. Kusumastuti, A.M. Reinhorn and A. Rutenberg, 3/31/05 (PB2006-101523).

MCEER-05-0003 "Proceedings of the Third PRC-US Workshop on Seismic Analysis and Design of Special Bridges," edited by L.C. Fan and G.C. Lee, 4/20/05, (PB2006-105796).

MCEER-05-0004 "Approaches for the Seismic Retrofit of Braced Steel Bridge Piers and Proof-of-Concept Testing of an Eccentrically Braced Frame with Tubular Link," by J.W. Berman and M. Bruneau, 4/21/05 (PB2006-101524).

MCEER-05-0005 "Simulation of Strong Ground Motions for Seismic Fragility Evaluation of Nonstructural Components in Hospitals," by A. Wanitkorkul and A. Filiatrault, 5/26/05 (PB2006-500027).

MCEER-05-0006 "Seismic Safety in California Hospitals: Assessing an Attempt to Accelerate the Replacement or Seismic Retrofit of Older Hospital Facilities," by D.J. Alesch, L.A. Arendt and W.J. Petak, 6/6/05 (PB2006-105794).

MCEER-05-0007 "Development of Seismic Strengthening and Retrofit Strategies for Critical Facilities Using Engineered Cementitious Composite Materials," by K. Kesner and S.L. Billington, 8/29/05 (PB2006-111701).

MCEER-05-0008 "Experimental and Analytical Studies of Base Isolation Systems for Seismic Protection of Power Transformers," by N. Murota, M.Q. Feng and G-Y. Liu, 9/30/05 (PB2006-111702).

MCEER-05-0009 "3D-BASIS-ME-MB: Computer Program for Nonlinear Dynamic Analysis of Seismically Isolated Structures," by P.C. Tsopelas, P.C. Roussis, M.C. Constantinou, R. Buchanan and A.M. Reinhorn, 10/3/05 (PB2006-111703).

MCEER-05-0010 "Steel Plate Shear Walls for Seismic Design and Retrofit of Building Structures," by D. Vian and M. Bruneau, 12/15/05 (PB2006-111704).

MCEER-05-0011 "The Performance-Based Design Paradigm," by M.J. Astrella and A. Whittaker, 12/15/05 (PB2006-111705).

MCEER-06-0001 "Seismic Fragility of Suspended Ceiling Systems," H. Badillo-Almaraz, A.S. Whittaker, A.M. Reinhorn and G.P. Cimellaro, 2/4/06 (PB2006-111706).

MCEER-06-0002 "Multi-Dimensional Fragility of Structures," by G.P. Cimellaro, A.M. Reinhorn and M. Bruneau, 3/1/06 (PB2007-106974, A09, MF-A02, CD A00).

MCEER-06-0003 "Built-Up Shear Links as Energy Dissipators for Seismic Protection of Bridges," by P. Dusicka, A.M. Itani and I.G. Buckle, 3/15/06 (PB2006-111708).

MCEER-06-0004 "Analytical Investigation of the Structural Fuse Concept," by R.E. Vargas and M. Bruneau, 3/16/06 (PB2006-111709).

MCEER-06-0005 "Experimental Investigation of the Structural Fuse Concept," by R.E. Vargas and M. Bruneau, 3/17/06 (PB2006-111710).

MCEER-06-0006 "Further Development of Tubular Eccentrically Braced Frame Links for the Seismic Retrofit of Braced Steel Truss Bridge Piers," by J.W. Berman and M. Bruneau, 3/27/06 (PB2007-105147).

MCEER-06-0007 "REDARS Validation Report," by S. Cho, C.K. Huyck, S. Ghosh and R.T. Eguchi, 8/8/06 (PB2007-106983).

MCEER-06-0008 "Review of Current NDE Technologies for Post-Earthquake Assessment of Retrofitted Bridge Columns," by J.W. Song, Z. Liang and G.C. Lee, 8/21/06 (PB2007-106984).

MCEER-06-0009 "Liquefaction Remediation in Silty Soils Using Dynamic Compaction and Stone Columns," by S. Thevanayagam, G.R. Martin, R. Nashed, T. Shenthan, T. Kanagalingam and N. Ecemis, 8/28/06 (PB2007-106985).

MCEER-06-0010 "Conceptual Design and Experimental Investigation of Polymer Matrix Composite Infill Panels for Seismic Retrofitting," by W. Jung, M. Chiewanichakorn and A.J. Aref, 9/21/06 (PB2007-106986).

MCEER-06-0011 "A Study of the Coupled Horizontal-Vertical Behavior of Elastomeric and Lead-Rubber Seismic Isolation Bearings," by G.P. Warn and A.S. Whittaker, 9/22/06 (PB2007-108679).

MCEER-06-0012 "Proceedings of the Fourth PRC-US Workshop on Seismic Analysis and Design of Special Bridges: Advancing Bridge Technologies in Research, Design, Construction and Preservation," Edited by L.C. Fan, G.C. Lee and L. Ziang, 10/12/06 (PB2007-109042).

MCEER-06-0013 "Cyclic Response and Low Cycle Fatigue Characteristics of Plate Steels," by P. Dusicka, A.M. Itani and I.G. Buckle, 11/1/06 06 (PB2007-106987).

MCEER-06-0014 "Proceedings of the Second US-Taiwan Bridge Engineering Workshop," edited by W.P. Yen, J. Shen, J-Y. Chen and M. Wang, 11/15/06 (PB2008-500041).

MCEER-06-0015 "User Manual and Technical Documentation for the REDARS™ Import Wizard," by S. Cho, S. Ghosh, C.K. Huyck and S.D. Werner, 11/30/06 (PB2007-114766).

MCEER-06-0016 "Hazard Mitigation Strategy and Monitoring Technologies for Urban and Infrastructure Public Buildings: Proceedings of the China-US Workshops," edited by X.Y. Zhou, A.L. Zhang, G.C. Lee and M. Tong, 12/12/06 (PB2008-500018).

MCEER-07-0001 "Static and Kinetic Coefficients of Friction for Rigid Blocks," by C. Kafali, S. Fathali, M. Grigoriu and A.S. Whittaker, 3/20/07 (PB2007-114767).

MCEER-07-0002 "Hazard Mitigation Investment Decision Making: Organizational Response to Legislative Mandate," by L.A. Arendt, D.J. Alesch and W.J. Petak, 4/9/07 (PB2007-114768).

MCEER-07-0003 "Seismic Behavior of Bidirectional-Resistant Ductile End Diaphragms with Unbonded Braces in Straight or Skewed Steel Bridges," by O. Celik and M. Bruneau, 4/11/07 (PB2008-105141).

MCEER-07-0004 "Modeling Pile Behavior in Large Pile Groups Under Lateral Loading," by A.M. Dodds and G.R. Martin, 4/16/07(PB2008-105142).

MCEER-07-0005 "Experimental Investigation of Blast Performance of Seismically Resistant Concrete-Filled Steel Tube Bridge Piers," by S. Fujikura, M. Bruneau and D. Lopez-Garcia, 4/20/07 (PB2008-105143).

MCEER-07-0006 "Seismic Analysis of Conventional and Isolated Liquefied Natural Gas Tanks Using Mechanical Analogs," by I.P. Christovasilis and A.S. Whittaker, 5/1/07, not available.

MCEER-07-0007 "Experimental Seismic Performance Evaluation of Isolation/Restraint Systems for Mechanical Equipment – Part 1: Heavy Equipment Study," by S. Fathali and A. Filiatrault, 6/6/07 (PB2008-105144).

MCEER-07-0008 "Seismic Vulnerability of Timber Bridges and Timber Substructures," by A.A. Sharma, J.B. Mander, I.M. Friedland and D.R. Allicock, 6/7/07 (PB2008-105145).

MCEER-07-0009 "Experimental and Analytical Study of the XY-Friction Pendulum (XY-FP) Bearing for Bridge Applications," by C.C. Marin-Artieda, A.S. Whittaker and M.C. Constantinou, 6/7/07 (PB2008-105191).

MCEER-07-0010 "Proceedings of the PRC-US Earthquake Engineering Forum for Young Researchers," Edited by G.C. Lee and X.Z. Qi, 6/8/07 (PB2008-500058).

MCEER-07-0011 "Design Recommendations for Perforated Steel Plate Shear Walls," by R. Purba and M. Bruneau, 6/18/07, (PB2008-105192).

MCEER-07-0012 "Performance of Seismic Isolation Hardware Under Service and Seismic Loading," by M.C. Constantinou, A.S. Whittaker, Y. Kalpakidis, D.M. Fenz and G.P. Warn, 8/27/07, (PB2008-105193).

MCEER-07-0013 "Experimental Evaluation of the Seismic Performance of Hospital Piping Subassemblies," by E.R. Goodwin, E. Maragakis and A.M. Itani, 9/4/07, (PB2008-105194).

MCEER-07-0014 "A Simulation Model of Urban Disaster Recovery and Resilience: Implementation for the 1994 Northridge Earthquake," by S. Miles and S.E. Chang, 9/7/07, (PB2008-106426).

MCEER-07-0015 "Statistical and Mechanistic Fragility Analysis of Concrete Bridges," by M. Shinozuka, S. Banerjee and S-H. Kim, 9/10/07, (PB2008-106427).

MCEER-07-0016 "Three-Dimensional Modeling of Inelastic Buckling in Frame Structures," by M. Schachter and AM. Reinhorn, 9/13/07, (PB2008-108125).

MCEER-07-0017 "Modeling of Seismic Wave Scattering on Pile Groups and Caissons," by I. Po Lam, H. Law and C.T. Yang, 9/17/07 (PB2008-108150).

MCEER-07-0018 "Bridge Foundations: Modeling Large Pile Groups and Caissons for Seismic Design," by I. Po Lam, H. Law and G.R. Martin (Coordinating Author), 12/1/07 (PB2008-111190).

MCEER-07-0019 "Principles and Performance of Roller Seismic Isolation Bearings for Highway Bridges," by G.C. Lee, Y.C. Ou, Z. Liang, T.C. Niu and J. Song, 12/10/07 (PB2009-110466).

MCEER-07-0020 "Centrifuge Modeling of Permeability and Pinning Reinforcement Effects on Pile Response to Lateral Spreading," by L.L Gonzalez-Lagos, T. Abdoun and R. Dobry, 12/10/07 (PB2008-111191).

MCEER-07-0021 "Damage to the Highway System from the Pisco, Perú Earthquake of August 15, 2007," by J.S. O'Connor, L. Mesa and M. Nykamp, 12/10/07, (PB2008-108126).

MCEER-07-0022 "Experimental Seismic Performance Evaluation of Isolation/Restraint Systems for Mechanical Equipment – Part 2: Light Equipment Study," by S. Fathali and A. Filiatrault, 12/13/07 (PB2008-111192).

MCEER-07-0023 "Fragility Considerations in Highway Bridge Design," by M. Shinozuka, S. Banerjee and S.H. Kim, 12/14/07 (PB2008-111193).

MCEER-07-0024 "Performance Estimates for Seismically Isolated Bridges," by G.P. Warn and A.S. Whittaker, 12/30/07 (PB2008-112230).

MCEER-08-0001 "Seismic Performance of Steel Girder Bridge Superstructures with Conventional Cross Frames," by L.P. Carden, A.M. Itani and I.G. Buckle, 1/7/08, (PB2008-112231).

MCEER-08-0002 "Seismic Performance of Steel Girder Bridge Superstructures with Ductile End Cross Frames with Seismic Isolators," by L.P. Carden, A.M. Itani and I.G. Buckle, 1/7/08 (PB2008-112232).

MCEER-08-0003 "Analytical and Experimental Investigation of a Controlled Rocking Approach for Seismic Protection of Bridge Steel Truss Piers," by M. Pollino and M. Bruneau, 1/21/08 (PB2008-112233).

MCEER-08-0004 "Linking Lifeline Infrastructure Performance and Community Disaster Resilience: Models and Multi-Stakeholder Processes," by S.E. Chang, C. Pasion, K. Tatebe and R. Ahmad, 3/3/08 (PB2008-112234).

MCEER-08-0005 "Modal Analysis of Generally Damped Linear Structures Subjected to Seismic Excitations," by J. Song, Y-L. Chu, Z. Liang and G.C. Lee, 3/4/08 (PB2009-102311).

MCEER-08-0006 "System Performance Under Multi-Hazard Environments," by C. Kafali and M. Grigoriu, 3/4/08 (PB2008-112235).

MCEER-08-0007 "Mechanical Behavior of Multi-Spherical Sliding Bearings," by D.M. Fenz and M.C. Constantinou, 3/6/08 (PB2008-112236).

MCEER-08-0008 "Post-Earthquake Restoration of the Los Angeles Water Supply System," by T.H.P. Tabucchi and R.A. Davidson, 3/7/08 (PB2008-112237).

MCEER-08-0009 "Fragility Analysis of Water Supply Systems," by A. Jacobson and M. Grigoriu, 3/10/08 (PB2009-105545).

MCEER-08-0010 "Experimental Investigation of Full-Scale Two-Story Steel Plate Shear Walls with Reduced Beam Section Connections," by B. Qu, M. Bruneau, C-H. Lin and K-C. Tsai, 3/17/08 (PB2009-106368).

MCEER-08-0011 "Seismic Evaluation and Rehabilitation of Critical Components of Electrical Power Systems," S. Ersoy, B. Feizi, A. Ashrafi and M. Ala Saadeghvaziri, 3/17/08 (PB2009-105546).

MCEER-08-0012 "Seismic Behavior and Design of Boundary Frame Members of Steel Plate Shear Walls," by B. Qu and M. Bruneau, 4/26/08 . (PB2009-106744).

MCEER-08-0013 "Development and Appraisal of a Numerical Cyclic Loading Protocol for Quantifying Building System Performance," by A. Filiatrault, A. Wanitkorkul and M. Constantinou, 4/27/08 (PB2009-107906).

MCEER-08-0014 "Structural and Nonstructural Earthquake Design: The Challenge of Integrating Specialty Areas in Designing Complex, Critical Facilities," by W.J. Petak and D.J. Alesch, 4/30/08 (PB2009-107907).

MCEER-08-0015 "Seismic Performance Evaluation of Water Systems," by Y. Wang and T.D. O'Rourke, 5/5/08 (PB2009-107908).

MCEER-08-0016 "Seismic Response Modeling of Water Supply Systems," by P. Shi and T.D. O'Rourke, 5/5/08 (PB2009-107910).

MCEER-08-0017 "Numerical and Experimental Studies of Self-Centering Post-Tensioned Steel Frames," by D. Wang and A. Filiatrault, 5/12/08 (PB2009-110479).

MCEER-08-0018 "Development, Implementation and Verification of Dynamic Analysis Models for Multi-Spherical Sliding Bearings," by D.M. Fenz and M.C. Constantinou, 8/15/08 (PB2009-107911).

MCEER-08-0019 "Performance Assessment of Conventional and Base Isolated Nuclear Power Plants for Earthquake Blast Loadings," by Y.N. Huang, A.S. Whittaker and N. Luco, 10/28/08 (PB2009-107912).

MCEER-08-0020 "Remote Sensing for Resilient Multi-Hazard Disaster Response – Volume I: Introduction to Damage Assessment Methodologies," by B.J. Adams and R.T. Eguchi, 11/17/08 (PB2010-102695).

MCEER-08-0021 "Remote Sensing for Resilient Multi-Hazard Disaster Response – Volume II: Counting the Number of Collapsed Buildings Using an Object-Oriented Analysis: Case Study of the 2003 Bam Earthquake," by L. Gusella, C.K. Huyck and B.J. Adams, 11/17/08 (PB2010-100925).

MCEER-08-0022 "Remote Sensing for Resilient Multi-Hazard Disaster Response – Volume III: Multi-Sensor Image Fusion Techniques for Robust Neighborhood-Scale Urban Damage Assessment," by B.J. Adams and A. McMillan, 11/17/08 (PB2010-100926).

MCEER-08-0023 "Remote Sensing for Resilient Multi-Hazard Disaster Response – Volume IV: A Study of Multi-Temporal and Multi-Resolution SAR Imagery for Post-Katrina Flood Monitoring in New Orleans," by A. McMillan, J.G. Morley, B.J. Adams and S. Chesworth, 11/17/08 (PB2010-100927).

MCEER-08-0024 "Remote Sensing for Resilient Multi-Hazard Disaster Response – Volume V: Integration of Remote Sensing Imagery and VIEWS™ Field Data for Post-Hurricane Charley Building Damage Assessment," by J.A. Womble, K. Mehta and B.J. Adams, 11/17/08 (PB2009-115532).

MCEER-08-0025 "Building Inventory Compilation for Disaster Management: Application of Remote Sensing and Statistical Modeling," by P. Sarabandi, A.S. Kiremidjian, R.T. Eguchi and B. J. Adams, 11/20/08 (PB2009-110484).

MCEER-08-0026 "New Experimental Capabilities and Loading Protocols for Seismic Qualification and Fragility Assessment of Nonstructural Systems," by R. Retamales, G. Mosqueda, A. Filiatrault and A. Reinhorn, 11/24/08 (PB2009-110485).

MCEER-08-0027 "Effects of Heating and Load History on the Behavior of Lead-Rubber Bearings," by I.V. Kalpakidis and M.C. Constantinou, 12/1/08 (PB2009-115533).

MCEER-08-0028 "Experimental and Analytical Investigation of Blast Performance of Seismically Resistant Bridge Piers," by S.Fujikura and M. Bruneau, 12/8/08 (PB2009-115534).

MCEER-08-0029 "Evolutionary Methodology for Aseismic Decision Support," by Y. Hu and G. Dargush, 12/15/08.

MCEER-08-0030 "Development of a Steel Plate Shear Wall Bridge Pier System Conceived from a Multi-Hazard Perspective," by D. Keller and M. Bruneau, 12/19/08 (PB2010-102696).

MCEER-09-0001 "Modal Analysis of Arbitrarily Damped Three-Dimensional Linear Structures Subjected to Seismic Excitations," by Y.L. Chu, J. Song and G.C. Lee, 1/31/09 (PB2010-100922).

MCEER-09-0002 "Air-Blast Effects on Structural Shapes," by G. Ballantyne, A.S. Whittaker, A.J. Aref and G.F. Dargush, 2/2/09 (PB2010-102697).

MCEER-09-0003 "Water Supply Performance During Earthquakes and Extreme Events," by A.L. Bonneau and T.D. O'Rourke, 2/16/09 (PB2010-100923).

MCEER-09-0004 "Generalized Linear (Mixed) Models of Post-Earthquake Ignitions," by R.A. Davidson, 7/20/09 (PB2010-102698).

MCEER-09-0005 "Seismic Testing of a Full-Scale Two-Story Light-Frame Wood Building: NEESWood Benchmark Test," by I.P. Christovasilis, A. Filiatrault and A. Wanitkorkul, 7/22/09 (PB2012-102401).

MCEER-09-0006 "IDARC2D Version 7.0: A Program for the Inelastic Damage Analysis of Structures," by A.M. Reinhorn, H. Roh, M. Sivaselvan, S.K. Kunnath, R.E. Valles, A. Madan, C. Li, R. Lobo and Y.J. Park, 7/28/09 (PB2010-103199).

MCEER-09-0007 "Enhancements to Hospital Resiliency: Improving Emergency Planning for and Response to Hurricanes," by D.B. Hess and L.A. Arendt, 7/30/09 (PB2010-100924).

MCEER-09-0008 "Assessment of Base-Isolated Nuclear Structures for Design and Beyond-Design Basis Earthquake Shaking," by Y.N. Huang, A.S. Whittaker, R.P. Kennedy and R.L. Mayes, 8/20/09 (PB2010-102699).

MCEER-09-0009 "Quantification of Disaster Resilience of Health Care Facilities," by G.P. Cimellaro, C. Fumo, A.M Reinhorn and M. Bruneau, 9/14/09 (PB2010-105384).

MCEER-09-0010 "Performance-Based Assessment and Design of Squat Reinforced Concrete Shear Walls," by C.K. Gulec and A.S. Whittaker, 9/15/09 (PB2010-102700).

MCEER-09-0011 "Proceedings of the Fourth US-Taiwan Bridge Engineering Workshop," edited by W.P. Yen, J.J. Shen, T.M. Lee and R.B. Zheng, 10/27/09 (PB2010-500009).

MCEER-09-0012 "Proceedings of the Special International Workshop on Seismic Connection Details for Segmental Bridge Construction," edited by W. Phillip Yen and George C. Lee, 12/21/09 (PB2012-102402).

MCEER-10-0001 "Direct Displacement Procedure for Performance-Based Seismic Design of Multistory Woodframe Structures," by W. Pang and D. Rosowsky, 4/26/10 (PB2012-102403).

MCEER-10-0002 "Simplified Direct Displacement Design of Six-Story NEESWood Capstone Building and Pre-Test Seismic Performance Assessment," by W. Pang, D. Rosowsky, J. van de Lindt and S. Pei, 5/28/10 (PB2012-102404).

MCEER-10-0003 "Integration of Seismic Protection Systems in Performance-Based Seismic Design of Woodframed Structures," by J.K. Shinde and M.D. Symans, 6/18/10 (PB2012-102405).

MCEER-10-0004 "Modeling and Seismic Evaluation of Nonstructural Components: Testing Frame for Experimental Evaluation of Suspended Ceiling Systems," by A.M. Reinhorn, K.P. Ryu and G. Maddaloni, 6/30/10 (PB2012-102406).

MCEER-10-0005 "Analytical Development and Experimental Validation of a Structural-Fuse Bridge Pier Concept," by S. El-Bahey and M. Bruneau, 10/1/10 (PB2012-102407).

MCEER-10-0006 "A Framework for Defining and Measuring Resilience at the Community Scale: The PEOPLES Resilience Framework," by C.S. Renschler, A.E. Frazier, L.A. Arendt, G.P. Cimellaro, A.M. Reinhorn and M. Bruneau, 10/8/10 (PB2012-102408).

MCEER-10-0007 "Impact of Horizontal Boundary Elements Design on Seismic Behavior of Steel Plate Shear Walls," by R. Purba and M. Bruneau, 11/14/10 (PB2012-102409).

MCEER-10-0008 "Seismic Testing of a Full-Scale Mid-Rise Building: The NEESWood Capstone Test," by S. Pei, J.W. van de Lindt, S.E. Pryor, H. Shimizu, H. Isoda and D.R. Rammer, 12/1/10 (PB2012-102410).

MCEER-10-0009 "Modeling the Effects of Detonations of High Explosives to Inform Blast-Resistant Design," by P. Sherkar, A.S. Whittaker and A.J. Aref, 12/1/10 (PB2012-102411).

MCEER-10-0010 "L'Aquila Earthquake of April 6, 2009 in Italy: Rebuilding a Resilient City to Withstand Multiple Hazards," by G.P. Cimellaro, I.P. Christovasilis, A.M. Reinhorn, A. De Stefano and T. Kirova, 12/29/10.

MCEER-11-0001 "Numerical and Experimental Investigation of the Seismic Response of Light-Frame Wood Structures," by I.P. Christovasilis and A. Filiatrault, 8/8/11 (PB2012-102412).

MCEER-11-0002 "Seismic Design and Analysis of a Precast Segmental Concrete Bridge Model," by M. Anagnostopoulou, A. Filiatrault and A. Aref, 9/15/11.

MCEER-11-0003 'Proceedings of the Workshop on Improving Earthquake Response of Substation Equipment," Edited by A.M. Reinhorn, 9/19/11 (PB2012-102413).

MCEER-11-0004 "LRFD-Based Analysis and Design Procedures for Bridge Bearings and Seismic Isolators," by M.C. Constantinou, I. Kalpakidis, A. Filiatrault and R.A. Ecker Lay, 9/26/11.

MCEER-11-0005 "Experimental Seismic Evaluation, Model Parameterization, and Effects of Cold-Formed Steel-Framed Gypsum Partition Walls on the Seismic Performance of an Essential Facility," by R. Davies, R. Retamales, G. Mosqueda and A. Filiatrault, 10/12/11.

MCEER-11-0006 "Modeling and Seismic Performance Evaluation of High Voltage Transformers and Bushings," by A.M. Reinhorn, K. Oikonomou, H. Roh, A. Schiff and L. Kempner, Jr., 10/3/11.

MCEER-11-0007 "Extreme Load Combinations: A Survey of State Bridge Engineers," by G.C. Lee, Z. Liang, J.J. Shen and J.S. O'Connor, 10/14/11.

MCEER-12-0001 "Simplified Analysis Procedures in Support of Performance Based Seismic Design," by Y.N. Huang and A.S. Whittaker.

MCEER-12-0002 "Seismic Protection of Electrical Transformer Bushing Systems by Stiffening Techniques," by M. Koliou, A. Filiatrault, A.M. Reinhorn and N. Oliveto, 6/1/12.

MCEER-12-0003 "Post-Earthquake Bridge Inspection Guidelines," by J.S. O'Connor and S. Alampalli, 6/8/12.

MCEER-12-0004 "Integrated Design Methodology for Isolated Floor Systems in Single-Degree-of-Freedom Structural Fuse Systems," by S. Cui, M. Bruneau and M.C. Constantinou, 6/13/12.

MCEER-12-0005 "Characterizing the Rotational Components of Earthquake Ground Motion," by D. Basu, A.S. Whittaker and M.C. Constantinou, 6/15/12.

MCEER-12-0006 "Bayesian Fragility for Nonstructural Systems," by C.H. Lee and M.D. Grigoriu, 9/12/12.

MCEER-12-0007 "A Numerical Model for Capturing the In-Plane Seismic Response of Interior Metal Stud Partition Walls," by R.L. Wood and T.C. Hutchinson, 9/12/12.

MCEER-12-0008 "Assessment of Floor Accelerations in Yielding Buildings," by J.D. Wieser, G. Pekcan, A.E. Zaghi, A.M. Itani and E. Maragakis, 10/5/12.

MCEER-13-0001 "Experimental Seismic Study of Pressurized Fire Sprinkler Piping Systems," by Y. Tian, A. Filiatrault and G. Mosqueda, 4/8/13.

MCEER-13-0002 "Enhancing Resource Coordination for Multi-Modal Evacuation Planning," by D.B. Hess, B.W. Conley and C.M. Farrell, 2/8/13.

MCEER-13-0003 "Seismic Response of Base Isolated Buildings Considering Pounding to Moat Walls," by A. Masroor and G. Mosqueda, 2/26/13.

MCEER-13-0004 "Seismic Response Control of Structures Using a Novel Adaptive Passive Negative Stiffness Device," by D.T.R. Pasala, A.A. Sarlis, S. Nagarajaiah, A.M. Reinhorn, M.C. Constantinou and D.P. Taylor, 6/10/13.

MCEER-13-0005 "Negative Stiffness Device for Seismic Protection of Structures," by A.A. Sarlis, D.T.R. Pasala, M.C. Constantinou, A.M. Reinhorn, S. Nagarajaiah and D.P. Taylor, 6/12/13.

MCEER-13-0006 "Emilia Earthquake of May 20, 2012 in Northern Italy: Rebuilding a Resilient Community to Withstand Multiple Hazards," by G.P. Cimellaro, M. Chiriatti, A.M. Reinhorn and L. Tirca, June 30, 2013.

MCEER-13-0007 "Precast Concrete Segmental Components and Systems for Accelerated Bridge Construction in Seismic Regions," by A.J. Aref, G.C. Lee, Y.C. Ou and P. Sideris, with contributions from K.C. Chang, S. Chen, A. Filiatrault and Y. Zhou, June 13, 2013.

MCEER-13-0008 "A Study of U.S. Bridge Failures (1980-2012)," by G.C. Lee, S.B. Mohan, C. Huang and B.N. Fard, June 15, 2013.

MCEER-13-0009 "Development of a Database Framework for Modeling Damaged Bridges," by G.C. Lee, J.C. Qi and C. Huang, June 16, 2013.

MCEER-13-0010 "Model of Triple Friction Pendulum Bearing for General Geometric and Frictional Parameters and for Uplift Conditions," by A.A. Sarlis and M.C. Constantinou, July 1, 2013.

MCEER-13-0011 "Shake Table Testing of Triple Friction Pendulum Isolators under Extreme Conditions," by A.A. Sarlis, M.C. Constantinou and A.M. Reinhorn, July 2, 2013.

MCEER-13-0012 "Theoretical Framework for the Development of MH-LRFD," by G.C. Lee (coordinating author), H.A Capers, Jr., C. Huang, J.M. Kulicki, Z. Liang, T. Murphy, J.J.D. Shen, M. Shinozuka and P.W.H. Yen, July 31, 2013.

MCEER-13-0013 "Seismic Protection of Highway Bridges with Negative Stiffness Devices," by N.K.A. Attary, M.D. Symans, S. Nagarajaiah, A.M. Reinhorn, M.C. Constantinou, A.A. Sarlis, D.T.R. Pasala, and D.P. Taylor, September 3, 2014.

MCEER-14-0001 "Simplified Seismic Collapse Capacity-Based Evaluation and Design of Frame Buildings with and without Supplemental Damping Systems," by M. Hamidia, A. Filiatrault, and A. Aref, May 19, 2014.

MCEER-14-0002 "Comprehensive Analytical Seismic Fragility of Fire Sprinkler Piping Systems," by Siavash Soroushian, Emmanuel "Manos" Maragakis, Arash E. Zaghi, Alicia Echevarria, Yuan Tian and Andre Filiatrault, August 26, 2014.

MCEER-14-0003 "Hybrid Simulation of the Seismic Response of a Steel Moment Frame Building Structure through Collapse," by M. Del Carpio Ramos, G. Mosqueda and D.G. Lignos, October 30, 2014.

MCEER-14-0004 "Blast and Seismic Resistant Concrete-Filled Double Skin Tubes and Modified Steel Jacketed Bridge Columns," by P.P. Fouche and M. Bruneau, June 30, 2015.

MCEER-14-0005 "Seismic Performance of Steel Plate Shear Walls Considering Various Design Approaches," by R. Purba and M. Bruneau, October 31, 2014.

MCEER-14-0006 "Air-Blast Effects on Civil Structures," by Jinwon Shin, Andrew S. Whittaker, Amjad J. Aref and David Cormie, October 30, 2014.

MCEER-14-0007 "Seismic Performance Evaluation of Precast Girders with Field-Cast Ultra High Performance Concrete (UHPC) Connections," by G.C. Lee, C. Huang, J. Song, and J. S. O'Connor, July 31, 2014.

MCEER-14-0008 "Post-Earthquake Fire Resistance of Ductile Concrete-Filled Double-Skin Tube Columns," by Reza Imani, Gilberto Mosqueda and Michel Bruneau, December 1, 2014.

MCEER-14-0009 "Cyclic Inelastic Behavior of Concrete Filled Sandwich Panel Walls Subjected to In-Plane Flexure," by Y. Alzeni and M. Bruneau, December 19, 2014.

MCEER-14-0010 "Analytical and Experimental Investigation of Self-Centering Steel Plate Shear Walls," by D.M. Dowden and M. Bruneau, December 19, 2014.

MCEER-15-0001 "Seismic Analysis of Multi-story Unreinforced Masonry Buildings with Flexible Diaphragms," by J. Aleman, G. Mosqueda and A.S. Whittaker, June 12, 2015.

MCEER-15-0002 "Site Response, Soil-Structure Interaction and Structure-Soil-Structure Interaction for Performance Assessment of Buildings and Nuclear Structures," by C. Bolisetti and A.S. Whittaker, June 15, 2015.

MCEER-15-0003 "Stress Wave Attenuation in Solids for Mitigating Impulsive Loadings," by R. Rafiee-Dehkharghani, A.J. Aref and G. Dargush, August 15, 2015.

MCEER-15-0004 "Computational, Analytical, and Experimental Modeling of Masonry Structures," by K.M. Dolatshahi and A.J. Aref, November 16, 2015.

MCEER-15-0005 "Property Modification Factors for Seismic Isolators: Design Guidance for Buildings," by W.J. McVitty and M.C. Constantinou, June 30, 2015.

MCEER-15-0006 "Seismic Isolation of Nuclear Power Plants using Sliding Bearings," by Manish Kumar, Andrew S. Whittaker and Michael C. Constantinou, December 27, 2015.

MCEER-15-0007 "Quintuple Friction Pendulum Isolator Behavior, Modeling and Validation," by Donghun Lee and Michael C. Constantinou, December 28, 2015.

MCEER-15-0008 "Seismic Isolation of Nuclear Power Plants using Elastomeric Bearings," by Manish Kumar, Andrew S. Whittaker and Michael C. Constantinou, December 29, 2015.

MCEER-16-0001 "Experimental, Numerical and Analytical Studies on the Seismic Response of Steel-Plate Concrete (SC) Composite Shear Walls," by Siamak Epackachi and Andrew S. Whittaker, June 15, 2016.

MCEER-16-0002 "Seismic Demand in Columns of Steel Frames," by Lisa Shrestha and Michel Bruneau, June 17, 2016.

MCEER-16-0003 "Development and Evaluation of Procedures for Analysis and Design of Buildings with Fluidic Self-Centering Systems" by Shoma Kitayama and Michael C. Constantinou, July 21, 2016.

MCEER-16-0004 "Real Time Control of Shake Tables for Nonlinear Hysteretic Systems," by Ki Pung Ryu and Andrei M. Reinhorn, October 22, 2016.

MCEER-16-0006 "Seismic Isolation of High Voltage Electrical Power Transformers," by Kostis Oikonomou, Michael C. Constantinou, Andrei M. Reinhorn and Leon Kemper, Jr., November 2, 2016.

MCEER-16-0007 "Open Space Damping System Theory and Experimental Validation," by Erkan Polat and Michael C. Constantinou, December 13, 2016.

MCEER-16-0008 "Seismic Response of Low Aspect Ratio Reinforced Concrete Walls for Buildings and Safety-Related Nuclear Applications," by Bismarck N. Luna and Andrew S. Whittaker.

MCEER-16-0009 "Buckling Restrained Braces Applications for Superstructure and Substructure Protection in Bridges," by Xiaone Wei and Michel Bruneau, December 28, 2016.

MCEER-16-0010 "Procedures and Results of Assessment of Seismic Performance of Seismically Isolated Electrical Transformers with Due Consideration for Vertical Isolation and Vertical Ground Motion Effects," by Shoma Kitayama, Michael C. Constantinou and Donghun Lee, December 31, 2016.

MCEER-17-0001 "Diagonal Tension Field Inclination Angle in Steel Plate Shear Walls," by Yushan Fu, Fangbo Wang and Michel Bruneau, February 10, 2017.

MCEER-17-0002 "Behavior of Steel Plate Shear Walls Subjected to Long Duration Earthquakes," by Ramla Qureshi and Michel Bruneau, September 1, 2017.

MCEER-17-0003 "Response of Steel-plate Concrete (SC) Wall Piers to Combined In-plane and Out-of-plane Seismic Loadings," by Brian Terranova, Andrew S. Whittaker, Siamak Epackachi and Nebojsa Orbovic, July 17, 2017.

MCEER-17-0004 "Design of Reinforced Concrete Panels for Wind-borne Missile Impact," by Brian Terranova, Andrew S. Whittaker and Len Schwer, July 18, 2017.

MCEER-17-0005 "A Simple Strategy for Dynamic Substructuring and its Application to Soil-Foundation-Structure Interaction," by Aikaterini Stefanaki and Metttupalayam V. Sivaselvan, December 15, 2017.

MCEER-17-0006 "Dynamics of Cable Structures: Modeling and Applications," by Nicholas D. Oliveto and Mettupalayam V. Sivaselvan, December 1, 2017.

MCEER-17-0007 "Development and Validation of a Combined Horizontal-Vertical Seismic Isolation System for High-Voltage-Power Transformers," by Donghun Lee and Michael C. Constantinou, November 3, 2017.

MCEER-18-0001 "Reduction of Seismic Acceleration Parameters for Temporary Bridge Design," by Conor Stucki and Michel Bruneau, March 22, 2018.

MCEER-18-0002 "Seismic Response of Low Aspect Ratio Reinforced Concrete Walls," by Bismarck N. Luna, Jonathan P. Rivera, Siamak Epackachi and Andrew S. Whittaker, April 21, 2018.

MCEER-18-0003 "Seismic Damage Assessment of Low Aspect Ratio Reinforced Concrete Shear Walls," by Jonathan P. Rivera, Bismarck N. Luna and Andrew S. Whittaker, April 16, 2018.

MCEER-18-0004 "Seismic Performance Assessment of Seismically Isolated Buildings Designed by the Procedures of ASCE/SEI 7," by Shoma Kitayama and Michael C. Constantinou, April 14, 2018.

MCEER-19-0001 MCEER-19-0001 "Development and Validation of a Seismic Isolation System for Lightweight Residential Construction," by Huseyin Cisalar and Michael C. Constantinou, March 24, 2019.

MCEER-20-0001 "A Multiscale Study of Reinforced Concrete Shear Walls Subjected to Elevated Temperatures," by Alok Deshpande and Andrew S. Whittaker, June 26, 2020.

MCEER-20-0002 "Further Results on the Assessment of Performance of Seismically Isolated Electrical Transformers," by Shoma Kitayama and Michael C. Constantinou, June 30, 2020.

MCEER-20-0003 "Analytical and Numerical Studies of Seismic Fluid-Structure Interaction in Liquid-Filled Vessels," by Ching-Ching Yu and Andrew S. Whittaker, August 1, 2020.

MCEER-22-0001 "Modeling Triple Friction Pendulum Bearings in Program OpenSees Including Frictional Heating Effects," by Hyun-Myung Kim and Michael C. Constantinou, April 18, 2022.

University at Buffalo
at Buffalo
The State University of New York

MCEER: Earthquake Engineering to Extreme Events

University at Buffalo, The State University of New York
133A Ketter Hall | Buffalo, NY 14260
mceer@buffalo.edu; buffalo.edu/mceer

ISSN 1520-295X